



2018

DEVELOPMENT OF A DECISION SUPPORT SYSTEM FOR CAPACITY PLANNING FROM GRAIN HARVEST TO STORAGE

Aaron P. Turner

University of Kentucky, turner.aaronp@gmail.com

Author ORCID Identifier:

 <https://orcid.org/0000-0003-2938-6800>

Digital Object Identifier: <https://doi.org/10.13023/etd.2018.376>

[Click here to let us know how access to this document benefits you.](#)

Recommended Citation

Turner, Aaron P., "DEVELOPMENT OF A DECISION SUPPORT SYSTEM FOR CAPACITY PLANNING FROM GRAIN HARVEST TO STORAGE" (2018). *Theses and Dissertations--Biosystems and Agricultural Engineering*. 58.
https://uknowledge.uky.edu/bae_etds/58

This Doctoral Dissertation is brought to you for free and open access by the Biosystems and Agricultural Engineering at UKnowledge. It has been accepted for inclusion in Theses and Dissertations--Biosystems and Agricultural Engineering by an authorized administrator of UKnowledge. For more information, please contact UKnowledge@lsv.uky.edu.

STUDENT AGREEMENT:

I represent that my thesis or dissertation and abstract are my original work. Proper attribution has been given to all outside sources. I understand that I am solely responsible for obtaining any needed copyright permissions. I have obtained needed written permission statement(s) from the owner(s) of each third-party copyrighted matter to be included in my work, allowing electronic distribution (if such use is not permitted by the fair use doctrine) which will be submitted to UKnowledge as Additional File.

I hereby grant to The University of Kentucky and its agents the irrevocable, non-exclusive, and royalty-free license to archive and make accessible my work in whole or in part in all forms of media, now or hereafter known. I agree that the document mentioned above may be made available immediately for worldwide access unless an embargo applies.

I retain all other ownership rights to the copyright of my work. I also retain the right to use in future works (such as articles or books) all or part of my work. I understand that I am free to register the copyright to my work.

REVIEW, APPROVAL AND ACCEPTANCE

The document mentioned above has been reviewed and accepted by the student's advisor, on behalf of the advisory committee, and by the Director of Graduate Studies (DGS), on behalf of the program; we verify that this is the final, approved version of the student's thesis including all changes required by the advisory committee. The undersigned agree to abide by the statements above.

Aaron P. Turner, Student

Dr. Michael D. Montross, Major Professor

Dr. Donald G. Colliver, Director of Graduate Studies

DEVELOPMENT OF A DECISION SUPPORT SYSTEM FOR CAPACITY
PLANNING FROM GRAIN HARVEST TO STORAGE

DISSERTATION

A dissertation submitted in partial fulfillment of the
requirements for the degree of Doctor of Philosophy in the
Colleges of Agriculture and Engineering
at the University of Kentucky

By

Aaron P. Turner

Lexington, Kentucky

Co-Directors: Dr. Michael Montross, Professor of Biosystems & Agricultural
Engineering
and Dr. Michael Sama, Assistant Professor of Biosystems & Agricultural Engineering

Lexington, Kentucky

2018

Copyright © Aaron P. Turner 2018

ABSTRACT OF DISSERTATION

DEVELOPMENT OF A DECISION SUPPORT SYSTEM FOR CAPACITY PLANNING FROM GRAIN HARVEST TO STORAGE

This dissertation investigated issues surrounding grain harvest and transportation logistics. A discrete event simulation model of grain transportation from the field to an on-farm storage facility was developed to evaluate how truck and driver resource constraints impact material flow efficiency, resource utilization, and system throughput. Harvest rate and in-field transportation were represented as a stochastic entity generation process, and service times associated with various material handling steps were represented by a combination of deterministic times and statistical distributions. The model was applied to data collected for three distinct harvest scenarios (18 total days). The observed number of deliveries was within ± 2 standard deviations of the simulation mean for 15 of the 18 input conditions examined, and on a daily basis, the median error between the simulated and observed deliveries was -4.1%.

The model was expanded to simulate the whole harvest season and include temporary wet storage capacity and grain drying. Moisture content changes due to field dry down was modeled using weather data and grain equilibrium moisture content relationships and resulted in an RMSE of 0.73 pts. Dryer capacity and performance were accounted for by adjusting the specified dryer performance to the observed level of moisture removal and drying temperature. Dryer capacity was generally underpredicted, and large variations were found in the observed data. The expanded model matched the observed cumulative mass of grain delivered well and estimated the harvest would take one partial day longer than was observed.

Usefulness of the model to evaluate both costs and system performance was demonstrated by conducting a sensitivity analysis and examining system changes for a hypothetical operation. A dry year and a slow drying crop had the largest impact on the system's operating and drying costs (12.7% decrease and 10.8% increase, respectively). The impact of reducing the drying temperature to maintain quality in drying white corn had no impact on the combined drying and operating cost, but harvest took six days longer. The reduced drying capacity at lower temperatures resulted in more field drying which counteracted the reduced drying efficiency and increased field time. The

sensitivity analysis demonstrated varied benefits of increased drying and transportation capacity based on how often these systems created a bottleneck in the operation. For some combinations of longer transportation times and higher harvest rates, increasing hauling and drying capacity could shorten the harvest window by a week or more at an increase in costs of less than \$12 ha⁻¹.

An additional field study was conducted to examine corn harvest losses in Kentucky. Total losses for cooperated combines were found to be between 0.8%-2.4% of total yield (86 to 222 kg ha⁻¹). On average, the combine head accounted for 66% of the measured losses, and the total losses were highly variable, with coefficients of variation ranging from 21.7% to 77.2%. Yield and harvest losses were monitored in a single field as the grain dried from 33.9% to 14.6%. There was no significant difference in the potential yield at any moisture level, and the observed yield and losses displayed little variation for moisture levels from 33.9% to 19.8%, with total losses less than 1% (82 to 130 kg dry matter ha⁻¹). Large amounts of lodging occurred while the grain dried from 19.8% to 14.6%, which resulted in an 18.9% reduction in yield, and harvest losses in excess of 9%. Allowing the grain to field dry generally improved test weight and reduced mechanical damage, however, there was a trend of increased mold and other damage in prolonged field drying.

KEYWORDS: Machinery management, Harvest logistics, Grain transportation, Grain drying, Yield loss, Discrete event simulation

Aaron P. Turner

September 14, 2018

DEVELOPMENT OF A DECISION SUPPORT SYSTEM FOR CAPACITY
PLANNING FROM GRAIN HARVEST TO STORAGE

By

Aaron P. Turner

Dr. Michael D. Montross

Co-Director of Dissertation

Dr. Michael P. Sama

Co-Director of Dissertation

Dr. Donald G. Colliver

Director of Graduate Studies

September 14, 2018

ACKNOWLEDGMENTS

This work was made possible through the support and guidance of my dissertation committee and through funding provided by the USDA*. First and foremost, I would like to thank my advisor, Dr. Mike Montross, for sharing in countless hot days in the field and cold beverages in hotel rooms at night. His support, advice, and mentorship over my time at the University of Kentucky have been invaluable. Thanks to Dr. Michael Sama for his support, encouragement, and for being a great personal and professional role model. Dr. Sam McNeill's contagious enthusiasm and encouragement greatly contributed to this project. Dr. Joe Dvorak and Dr. Tyler Mark round out my committee and their ideas, input, and feedback has greatly improved my research.

Thanks to the entire Biosystems & Agricultural Engineering Department for making my time at UK memorable. Special thanks to Shawn O'Neal, Donnie Stamper, and Ben Martin for their assistance in collecting field data for this project. Thanks to Ali Hamidisepehr for being a fantastic office mate for the last few years.

Additionally, I would like to thank the producers who were kind enough to allow me to observe their operation and pick up corn kernels out of their fields. Specifically, thanks to Miles Farms, Back 40 Farms, Evan McCord, Shaffner Brothers Farms, and to Shannon and the farm crew at the UK farm.

Finally, I'd like to thank my family for all their love and support. Mom and Dad, thank you for instilling the desire to learn and explore the world around me from a young age. My wife Allie provided constant love and support and carried the lion's share of the responsibilities throughout the dissertation process.

* Agriculture and Food Research Initiative Foundational Program [grant no. 2016-67022-25124] from the USDA National Institute of Food and Agriculture

TABLE OF CONTENTS

Acknowledgments.....	iii
Table of Contents.....	iv
List of Figures.....	xi
List of Tables.....	xiv
List of Equations.....	xv
Chapter 1. Introduction.....	1
1.1 Project Goals.....	4
1.2 Organization of Dissertation.....	5
1.3 References.....	5
Chapter 2. A Discrete Event Simulation Model for Analysis of Farm Scale Grain Transportation Systems.....	7
2.1 Summary.....	7
2.2 Introduction.....	7
2.2.1 Overview.....	7
2.2.2 Literature Review.....	9
2.2.3 Motivation.....	11
2.3 Materials and Methods.....	12
2.3.1 Model Implementation.....	12
2.3.1.1 Description.....	12
2.3.1.2 Simulation.....	14
2.3.1.3 Model Structure.....	17
2.3.1.4 Analysis.....	20
2.3.2 Case Studies.....	24
2.3.2.1 Operation 1—Data Collection.....	24

2.3.2.2	Operation 2—Data Collection	26
2.3.2.3	Data Analysis	27
2.4	Results and Discussion	27
2.4.1	Example Operation System Characteristics.....	27
2.4.1.1	Operation Summary	27
2.4.1.2	Harvest Trends	30
2.4.2	Distributions for Stochastic Elements.....	33
2.4.3	Model Application and Validation.....	39
2.4.3.1	Overall Performance	39
2.4.3.2	Example Performance	44
2.5	Conclusions.....	51
2.6	References.....	52
Chapter 3.	Variability in Corn Harvest Losses in Kentucky	55
3.1	Summary	55
3.2	Introduction.....	55
3.2.1	Machine Losses.....	55
3.2.2	Losses Associated with Harvest Timing.....	57
3.2.3	Motivation.....	58
3.3	Materials and Methods.....	59
3.3.1	Measurement Locations:.....	59
3.3.2	Field Procedure	61
3.3.3	Tracking Yield Changes with Time	65
3.3.4	Laboratory Procedure.....	66
3.4	Results and Discussion	67
3.4.1	Cooperator Locations.....	67

3.4.2	Woodford County Location	69
3.4.3	Quality Changes.....	74
3.5	Conclusions.....	76
3.6	References.....	77
Chapter 4.	Discrete Event Simulation of Grain Transportation and Drying	82
4.1	Summary	82
4.2	Introduction.....	82
4.2.1	Overview.....	82
4.2.2	Wet Holding.....	84
4.2.3	Drying	84
4.2.4	Harvest System Models	86
4.2.5	Motivation.....	89
4.3	Materials and Methods.....	90
4.3.1	Dryer Capacity	92
4.3.2	Modeling Incoming Grain Moisture	95
4.3.3	Daily Model Implementation	96
4.3.3.1	Analysis.....	98
4.3.4	Whole Season Simulation.....	101
4.3.5	Model Application	103
4.4	Results and Discussion	104
4.4.1	Relative Dryer Capacity.....	104
4.4.2	Weather Impacts and Grain Moisture Content	109
4.4.3	Example Operation System Characteristics.....	110
4.4.3.1	Example Single Day Simulation	112
4.4.3.2	Whole Season Simulation	117

4.5	Conclusions.....	121
4.6	References.....	121
Chapter 5.	Sensitivity Analysis of Grain Transportation and Drying Systems	127
5.1	Summary	127
5.2	Introduction.....	127
5.2.1	Overview.....	127
5.2.2	Drying Efficiency.....	130
5.2.3	Motivation.....	131
5.3	Materials and Methods.....	132
5.3.1	Model Application	132
5.3.2	System Configurations.....	133
5.3.3	Harvest Costs	138
5.3.4	Drying Energy Use and Cost	142
5.3.5	Labor and Equipment Cost Estimation.....	144
5.3.6	Evaluation	148
5.4	Results and Discussion	149
5.4.1	Simulation Overview	149
5.4.2	Seasonal Impacts.....	152
5.4.3	Drying Temperature.....	156
5.4.4	Operating Characteristics.....	158
5.4.5	Sensitivity Analysis	160
5.4.6	Assumptions and Limitations	174
5.5	Conclusions.....	175
5.6	References.....	176
Chapter 6.	Summary, Conclusions, and Future Work.....	179

6.1	Summary and Conclusions	179
6.2	Future Work	183
APPENDICES		185
Appendix A. Simulink Model Details.....		185
	Whole Model Diagram	185
	Harvest Time Out Subsystem	186
	Harvest Gate Control Logic	186
	HarvestCtrl1 Logic for Gate to Control Loading Partial Trucks	187
	Pit Control Gate Logic	187
	Restart Harvest Subsystem	188
	Entity Generation Block Code	188
	Example Timestamp Between Processes & Priority Setting	190
	Example Service Time Selection	190
	Entity Generation Block to Fill Wet Holding at the Start of the Daily Simulation	191
Appendix B. Sample code for DES Transportation Model.....		192
	Script to Create PDF Objects	192
	Script to Run the Simulation Model	198
	Script to Analyze Simulation Output.....	200
Appendix C. Sample Code for Whole Season Simulation.....		207
	Main Function.....	207
	Main Function Initialization for Whole Season Validation Conditions	213
	Fieldwork and Moisture Content Estimation	215
	Energy Use in Drying Estimation	217
	Drying Capacity Adjustment	219

Processes Simulation Data—Flow and Utilization.....	220
Processes Simulation Data—Delays and Final Status	226
Clean Simulink Utilization Output Data.....	228
Main Function for Sensitivity Analysis	230
Define System for Sensitivity Analysis	231
Appendix D. Yield Loss Measurement	234
Appendix E. Supplemental Information for DES Transportation Model	235
Operating Characteristics.....	235
Pit Wait Times	236
Flow Time Efficiency	238
Loads Delivered.....	240
Appendix F. Supplemental Information for Whole Season Application	244
Daily Simulation Overview	244
Driver Utilization.....	246
Truck Utilization.....	249
Dryer Utilization.....	252
Flow Time.....	255
Wait Time	258
Appendix G. Supplemental Information from Sensitivity Analysis	261
Daily Simulation Overview	261
Example Harvest Length from Sensitivity Analysis.....	266
Example Labor Requirements from Sensitivity Analysis.....	267
Appendix H. Trends in Weather and Yield.....	268
Kentucky Yield Trends 2008-2017.....	268
Estimated Corn Field Drying for Bowling Green, KY	268

Weather Data for Bowling Green, Ky	269
REFERENCES	272
VITA.....	281

LIST OF FIGURES

Figure 1-1: Typical flow of grain from the field to storage.....	2
Figure 2-1: Simplified model structure.....	14
Figure 2-2: Simulink model flow diagram.....	18
Figure 2-3: Trends over the harvest window.	31
Figure 2-4: Grain moisture content plotted against the grain cart interarrival rate	32
Figure 2-5: Grain cart interarrival time.....	36
Figure 2-6: Pit service time.....	37
Figure 2-7: Loading service time	38
Figure 2-8: Observed versus simulated daily deliveries.....	40
Figure 2-9: Example simulation output for all simulations (n=500) for a single day (08/27) for Operation 1 corn.....	46
Figure 2-10: Example simulation output for all simulations (n=500) for a single day (06/09) for Operation 1 wheat.....	48
Figure 2-11: Example simulation output for all simulations (n=500) for a single day in Operation 2.....	50
Figure 3-1: Overview of loss component measurement locations.....	62
Figure 3-2: Example staked out area to collect loose kernels.....	62
Figure 3-3: Plot sampling layout. Each block was sampled once per measurement date.	65
Figure 3-4: Approximate breakdown of loss components at cooperators other measurement locations.....	69
Figure 3-5: Change in yield as grain was allowed to dry in the field.	70
Figure 3-6: Lodged and wind damaged corn observed during 12/01 loss measurement..	71
Figure 3-7: Approximate breakdown of loss components as the grain field dried at the Woodford County location.	73
Figure 3-8: Percentage of kernels damaged, on a mass basis, as grain was allowed to dry in the field.	75
Figure 3-9: Test weight of samples harvested at various field moistures.....	76
Figure 4-1: Combined on-farm and off-farm storage for 2017.....	83
Figure 4-2: Simplified diagram of the DES model.....	97

Figure 4-3: Whole season flow diagram.....	102
Figure 4-4: Plot of relative drying capacity estimated from Thompson et al. (1994) plotted against the estimated ratio from equation (4-4).....	105
Figure 4-5: Relative drying capacity estimated for various moisture removal levels and temperature reductions. All ratios are relative to 5 points of moisture removal at 104°C.....	106
Figure 4-6 Change in harvest moisture content over season.....	110
Figure 4-7 Overview of material flow through the harvest system on Aug-27.....	113
Figure 4-8 Resource utilization over the course of an example day (Aug-27).....	115
Figure 4-9 Overview of wait time and material flow efficiency for an example day of the simulation (Aug-27).....	117
Figure 4-10 Observed and simulated cumulative mass of grain delivered, dry t. Simulation data was based on average input conditions.....	120
Figure 5-1: Change in field capacity utilization over the course of the simulated harvest season.....	150
Figure 5-2: Change in field time over the course of the harvest season.....	151
Figure 5-3: Change in drying energy usage over the course of the harvest season.....	152
Figure 5-4: Whole season field equipment area capacity utilization as a function of transportation distance and harvest rate. Shown for the baseline configuration..	162
Figure 5-5: Comparison of fieldwork delays due to a downstream bottleneck for the base configuration and an increased harvest rate of 4.5 ha hr ⁻¹	163
Figure 5-6: Whole season field equipment area capacity utilization as a function of transportation distance and harvest rate. Shown for the minimally-equipped configuration.....	164
Figure 5-7: Whole season field equipment area capacity utilization as a function of transportation time and harvest rate. Shown for the baseline configuration with doubled drying capacity.....	165
Figure 5-8: Whole season field equipment area capacity utilization as a function of transportation time and harvest rate. Shown for the baseline configuration with doubled drying capacity and an additional driver.....	166

Figure 5-9: Per area costs of harvesting, transporting, and drying grain as a function of transportation time and harvest rate. Shown for the baseline configuration..... 167

Figure 5-10: Per area costs of harvesting, transporting, and drying grain as a function of transportation time and harvest rate. Shown for the baseline configuration with doubled drying capacity. Value includes the annual cost of ownership for the large dryer upgrade. 168

Figure 5-11: Per area costs of harvesting, transporting, and drying grain as a function of transportation time and harvest rate. Shown for baseline configuration with doubled drying capacity and an additional driver..... 170

Figure 5-12: Change in harvest length with doubled drying capacity and three drivers 172

Figure 5-13: Change in harvest costs with doubled drying capacity and three drivers .. 174

LIST OF TABLES

Table 2-1: Model Variable Nomenclature	16
Table 2-2: Operation Characteristics	29
Table 2-3: Input Parameters and Associated Distribution for Model Validation	34
Table 2-4: Simulation Results: Resource Utilization and Cumulative Deliveries.....	41
Table 2-5: Simulated Results: Flow Time Efficiency and Wait Times	43
Table 3-1: Overview of Measurement Locations and Equipment	60
Table 3-2: Summary of Cooperator Combine Measurements	68
Table 3-3: Yield Loss Breakdown for the Measurements Taken at the 14.6% Moisture Level (12/01).....	71
Table 3-4: Summary Measurements at Woodford County Location	72
Table 4-1: Model Variable Nomenclature	91
Table 4-2 Comparison of Estimated Drying Capacity to Producer Drying Log	107
Table 4-3 Summary of Weather Data from the Midwestern Regional Climate Center (2018) for Bowling Green, KY	108
Table 4-4: Parameters Used for the Example Simulation	111
Table 4-5 Whole Season Overview of Simulated Resource Utilization and Material Flow	118
Table 4-6 Summary of Grain Entering and Leaving the System.....	120
Table 5-1: System Characteristics for Baseline System	134
Table 5-2: System Variations Explored.....	136
Table 5-3: Labor and Equipment Cost Estimates	140
Table 5-4: Seasonal Impacts on System Performance.....	154
Table 5-5: Impacts of Switching Reduced Drying Temperature	157
Table 5-6: Impacts of Additional Equipment	159

LIST OF EQUATIONS

Equation (2-1)	21
Equation (2-2)	21
Equation (2-3)	21
Equation (2-4)	22
Equation (2-5)	22
Equation (2-6)	23
Equation (2-7)	23
Equation (2-8)	24
Equation (2-9)	24
Equation (2-10)	25
Equation (3-1)	64
Equation (3-2)	64
Equation (3-3)	64
Equation (3-4)	64
Equation (3-5)	64
Equation (4-1)	93
Equation (4-2)	93
Equation (4-3)	94
Equation (4-4)	94
Equation (4-5)	94
Equation (4-6)	95
Equation (4-7)	99
Equation (4-8)	99
Equation (4-9)	99
Equation (4-10)	100
Equation (4-11)	101
Equation (4-12)	103
Equation (5-1)	133
Equation (5-2)	142
Equation (5-3)	143

Equation (5-4)	143
Equation (5-5)	143
Equation (5-6)	144
Equation (5-7)	144
Equation (5-8)	144
Equation (5-9)	144
Equation (5-10)	145
Equation (5-11)	145
Equation (5-12)	145
Equation (5-13)	146
Equation (5-14)	146
Equation (5-15)	147
Equation (5-16)	147
Equation (5-17)	147
Equation (5-18)	148
Equation (5-19)	148
Equation (5-20)	149

Chapter 1. INTRODUCTION

Grain harvest represents a substantial cost in terms of dollars, energy, fossil fuels, and environmental impacts. Expected yields, grain moisture content, and potential field losses, along with weather risks during the harvest window, influence the equipment set required to efficiently and economically move grain from the field to the first storage location. To minimize these costs, the optimal machinery set should be used. However, the interaction between several separate systems influences the overall system performance, making the selection of optimal power, number, and size of equipment a daunting challenge. Many algorithms and optimization schemes have been proposed, yet with a few exceptions, these models are rarely used in practice and could do with updating to reflect modern equipment and practices. This dissertation focuses on issues surrounding grain harvest, transportation, and drying at an on-farm storage facility.

Grain harvest can be classified into three interdependent systems: harvesting, transporting, and post-harvest drying/storage. A bottleneck in any one of these systems will directly affect the other two. Changes in field conditions during harvest can create or shift bottlenecks throughout the system. These systems are highly interrelated and require a whole-system approach. Figure 1-1 shows the typical flow of grain from the field to the first storage structure, and there could be a potential bottleneck at each operation. This dissertation focused on on-farm systems and did not investigate delivering grain directly to the elevator.

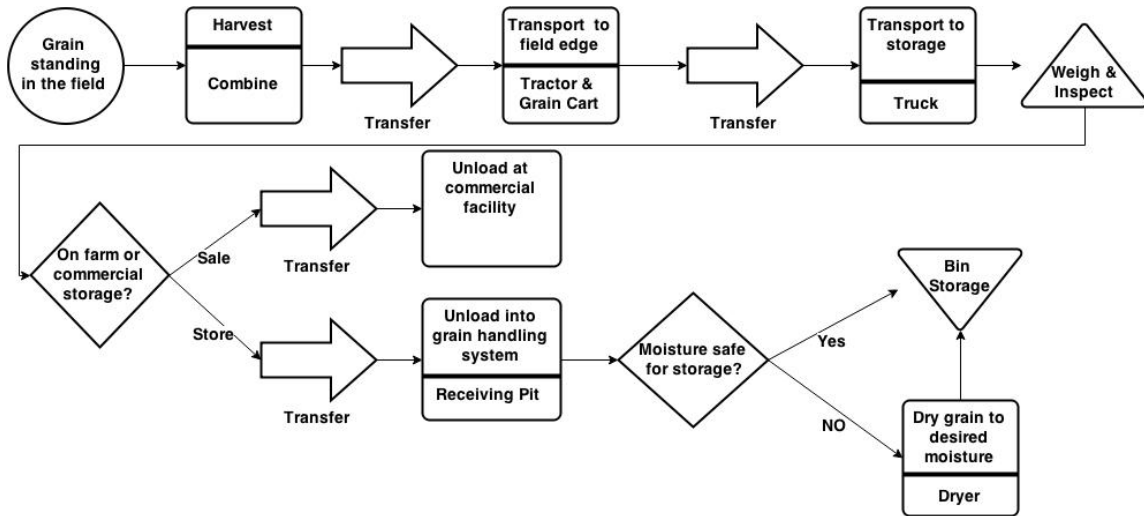


Figure 1-1: Typical flow of grain from the field to storage.

To examine the whole system, a large number of performance, logistical, temporal, and geospatial factors must be considered. The harvest capacity for field machinery is influenced by the machine complement (size, capacity, and number of combines and grain carts), grain moisture, field conditions (weather impacts), plant conditions (for example, lodging), field size, shape, and location. On the other end of the system are the grain storage and drying facilities. The moisture content of the grain and the capacity of the dryer change over the course of the season and can limit the rate at which grain can be placed into storage, especially during the initial harvest period when moisture is highest. The effective drying capacity is also influenced by the wet holding tank, which provides surge capacity, allowing the dryer to ‘catch up’ once harvest has stopped for the day or when the harvest is interrupted due to weather. Additionally, weighing, sampling, and the ability of the receiving pit to unload incoming grain impact the system. Transportation serves as the link between the field and the storage facility. It is limited by distance, capacity, and the number of vehicles. Extended wait times at any location in the system can lead to bottlenecks, and the on-board holding capacity of transportation vehicles can serve as additional surge capacity. This type of system can be examined through simulation or operations research.

Examining agricultural production from a whole system perspective to reduce waste and increase productivity has been of interest to the agricultural community for decades. Numerous techniques have been applied to this problem. These works have

generally addressed the problem through simulation or optimization techniques. Common simulation techniques are equation-based modeling (EBM) where governing equations are used to predict the response of key variables and agent-based modeling (ABM), where ‘agents’ emulate the behaviors of the individual components of the system (Parunak, Savit, & Riolo, 1998). By focusing on timing related to key events or interactions, these concepts can further be expanded to discrete event-based modeling (Loewer, Bridges, & Bucklin, 1994) and cycle analysis (Buckmaster & Hilton, 2005; Harrigan, 2003). Discrete event simulation (DES) modeling was chosen for this analysis, because it is well suited for examining resource utilization and system bottlenecks.

A large body of work was published in the literature related to grain harvest timing and logistics from the 1960’s to 1980’s, many of which are summarized in Loewer et al. (1994). However, there have been significant changes in field size, equipment size, stalk quality, yield, and other factors since that time, and minimal validation data were available. An additional weakness of these models has always been the ability to define variables and contend with dynamic conditions accurately.

For agriculture in general, models serve as decision support systems for many different types of farming operations. These models allow farmers, researchers, and extension personnel to interconnect multiple parameters and to ascertain what actions should be taken to improve and/or optimize system, labor, and/or cost performance. Models can also be used by producers to assist in the management of their operations. Commonly used within agriculture, static models possess fixed dates such as crop planting, fertilization, spraying, and scheduling management level activities. Nonetheless, actual conditions are subject to dynamic conditions and the cumulative effects of weather (i.e. temperature, humidity, and rainfall), price fluctuations, and resource availability. Inherent flexibility in the dates, time, and response to variables are essential to dynamic models (Baptist, 1992).

Several review articles have been published which attempt to summarize proposed models for agricultural production. Glen (1987) reviewed mathematical models used in farm planning and agricultural production. Models were broken down by focus area, and the solution approach and methodology employed by the models relevant to this

research were primarily simulations, linear programming, or dynamic programming with a stochastic weather element. A more recent review of machinery management studies, which classified their relationship to the American Society of Agricultural and Biosystems Engineers (ASABE) management phases (ASABE Standards, 2015d), was published by Bochtis, Sørensen, and Busato (2014). The studies relevant to this research were classified as capacity or task time planning.

1.1 Project Goals

The overall goal of this dissertation was to develop and validate a model to enable grain producers to make informed, data-driven decisions relevant to harvest and post-harvest logistics by integrating seasonal impacts of weather with transportation, harvest, and post-harvest equipment performance characteristics. A model to examine harvest logistics from the field to the first storage structure was developed and validated. The model allows changes in weather, field dry down, equipment capacity, infrastructure, or operational practices to be evaluated. Ultimately this model would allow producers to identify bottlenecks in their system and examine impacts and potential gains or losses from investments in equipment and/or additional labor. This dissertation was separated into four main objectives to address the issues surrounding grain harvest logistics.

1. Develop a DES model of grain transportation from the field to delivery at an on-farm storage facility and incorporate stochastic parameters to account for variability in equipment performance.
2. Evaluate yield and machine losses typically encountered during corn harvest in Kentucky.
3. Expand the DES model for grain transportation to include wet holding and drying capacity, accounting for changes in drying capacity due to drying temperature and grain moisture content.
4. Demonstrate the use of the model as a decision support tool to examine how system changes impact overall performance and costs and conduct a sensitivity analysis to evaluate system performance over a range of harvest rates and transportation times.

1.2 Organization of Dissertation

Chapter 1 provides a general introduction and rationale for this project, identifies the specific objectives explored, and outlines the organization of this dissertation. The main body of this dissertation was separated into separate chapters, each of which was self-contained, consisting of an introduction, literature review, methods, results and discussion, and conclusions section. Chapter 2 presents a discrete event simulation model of grain transportation from the field edge to an on-farm storage facility and explores how daily variability in equipment performance can impact the harvest system. Chapter 3 establishes a range of typical yield losses encountered by Kentucky producers and explores issues surrounding potential yield losses as grain dries in the field. Chapter 4 expands the grain transportation DES model to include on-farm wet holding and drying capacity. Chapter 5 demonstrates the application of the full model as a decision support tool. Whole harvest season simulations of a hypothetical operation were used to explore changes to the system and conduct a sensitivity analysis. Chapter 6 provides a general summary, conclusions, and expands on potential future work associated with this project. The appendix includes sample code, model details, and supplemental figures not included in the main body of the dissertation.

1.3 References

- ASABE Standards. (2015d). S495.1 Uniform terminology for agricultural machinery management. St. Joseph, MI: ASABE.
- Baptist, R. (1992). Derivation of steady-state herd productivity. *Agricultural Systems*, 39(3), 253-272. doi:[http://dx.doi.org/10.1016/0308-521X\(92\)90099-A](http://dx.doi.org/10.1016/0308-521X(92)90099-A)
- Bochtis, D. D., Sørensen, C. G., & Busato, P. (2014). Advances in agricultural machinery management: A review. *Biosystems Engineering*, 126, 69-81.
- Buckmaster, D. R., & Hilton, J. W. (2005). Computerized cycle analysis of harvest, transport, and unload systems. *Computers and Electronics in Agriculture*, 47(2), 137-147.
- Glen, J. J. (1987). Mathematical models in farm planning: A survey. *Operations Research*, 35(5), 641-666.
- Harrigan, T. (2003). Time-motion analysis of corn silage harvest systems. *Applied Engineering in Agriculture*, 19(4), 389-396.

Loewer, O. J., Bridges, T. C., & Bucklin, R. A. (1994). *On-farm drying and storage systems*. St. Joseph, MI: ASABE.

Parunak, H. V. D., Savit, R., & Riolo, R. L. (1998). *Agent-based modeling vs. Equation-based modeling: A case study and users' guide*. Paper presented at the Multi-agent systems and agent-based simulation.

Chapter 2. A DISCRETE EVENT SIMULATION MODEL FOR ANALYSIS OF FARM SCALE GRAIN TRANSPORTATION SYSTEMS

2.1 Summary

Grain transportation from the field to an on-farm storage facility is a critical component of the harvest system. A discrete event simulation model of grain transportation was developed to evaluate how truck and driver resource constraints impact material flow efficiency, resource utilization, and system throughput. Harvest rate and in-field transportation were represented as a stochastic entity generation process, and service times associated with various material handling steps were represented by a combination of deterministic times and statistical distributions. The model was applied to data collected for three distinct harvest scenarios (18 total days). Wheat and corn harvest from a large Kentucky operation was selected to evaluate the effect of different harvest rates (in wheat and corn), and corn harvest from a smaller Michigan operation was used to assess how the model handled situations where a single operator shuttled multiple trucks. The observed number of daily deliveries was within ± 2 standard deviations of the simulation for 15 of the 18 input conditions examined, and on a daily basis, the median error between the simulated and observed deliveries was -4.1%. This model can be used to simulate how changes in vehicle and labor constraints impact the overall system performance. An important extension of this concept is that, given an existing equipment set and labor force, a producer can estimate how often grain transportation is the system bottleneck and simulate the impact of additional vehicles or labor on grain transportation efficiency.

2.2 Introduction

2.2.1 Overview

As the capacity of grain harvesting machinery and yield continue to increase, there are corresponding increases in demand placed on material handling equipment, and increasingly semi-trailers are used for on-road grain transportation. In a recent Iowa State survey, semi-trailers made up 82% of grain trucks in 2015, up from 62% in 2006 (Edwards, Plastina, & Johanns, 2016). Investment in equipment for large harvesting

operations requires thoughtful planning because individual subsystem efficiency can impact the whole system (Sørensen & Bochtis, 2010). Additionally, difficulties finding reliable short-term labor to help with harvest activities, such as transporting grain from the field edge to storage, can result in producers using fewer drivers than trucks. A modeling tool that simulates grain transportation from the field edge to storage would be useful to producers by allowing them to evaluate how changes in the number of trucks and drivers used for on-road transportation affects overall productivity, transportation efficiency, and resource utilization. Selecting farm equipment requires a systems approach due to the need to evaluate interactions between field machinery, crop characteristics, and field conditions (Rotz, Muhtar, & Black, 1983; Sogaard & Sørensen, 2004); however, there is a need for a simplified approach that focuses on grain transportation without explicitly modeling the entire system. Specifically, in this study, field machinery and any sources of variability associated with harvest and field conditions are enveloped in a single parameter, representing the rate at which material enters the transportation system.

Assuming sufficient receiving and wet holding capacity at the destination facility, the effective harvest rate of the system will be set by in-field machinery (combine harvest rate ($t\ hr^{-1}$), in-field transportation rate ($t\ hr^{-1}$)), or by the on-road transport rate ($t\ hr^{-1}$). However, combine hoppers, grain tanks on in-field transporters, and trucks staged at the field edge act as surge capacity, providing a buffer between processes. This allows harvest to progress at a faster rate than the material can be transported away from the field. This also means that grain transportation operations can continue after harvest operations have stopped for the day, allowing for delivery of the remaining grain in the buffer. Because of these factors, an operation may have a single operator shuttling multiple trucks from the field to the destination facility, allowing them to operate with fewer drivers than trucks.

This study presents a discrete event simulation (DES) model of on-road grain transportation from the field to delivery at an on-farm storage facility. DES is a commonly used tool in manufacturing and operations research to examine resources utilization and identify bottlenecks and to assist in capacity planning (Allen, 2011). This approach uses a logical or mathematical model to represent state changes in a system at

discrete points in time, and the system is assumed constant between events, reducing modeling complexity (Tako & Robinson, 2012). In DES, material flows are represented by entities that enter the system at a determined rate and then flow through a network of queues and servers. In this study, entities represent full in-field transporters (tractor pulled grain carts) arriving at the field edge, and the rate at which they arrive represents the time required to harvest and transport the grain up to that point. Servers represent processing steps, and their duration represents the time required to complete the activity (time required to transport the grain to storage, time required to unload, etc.). The entity generation rate and service times can be deterministic or stochastic. Dynamic system behavior and variation in entity generation or processing times are represented with statistical distributions based on observations of the system (Spedding & Sun, 1999).

2.2.2 Literature Review

DES has been applied to a number of agricultural applications related to harvest logistics and grain handling. Simulation of Queues involving Unloading and Arrivals for Systems of Harvesting (SQUASH) was an early hybrid discrete-continuous simulation model used as a planning tool to evaluate grain harvesting efficiency and to size equipment components of many harvesting/delivery/handling/drying/storage systems (Benock, Loewer Jr, Bridges, & Loewer, 1981). This model calculated the operating efficiency of combines, hauling vehicles, wet grain receiving pit, wet holding bin, and grain dryer and was very useful for identifying potential problems with mismatched equipment before a purchase was made. Specifically, the model could be used to match the hauling capacity and transport time for in-field material transporter(s) and on-road transporter(s) with the harvest capacity of the combine(s) to optimize field efficiency and system performance. SQUASH allowed for the number of days to complete harvest to vary, but equipment performance was held constant over the course of the harvest season. Additionally, no stochastic processes were incorporated into the model. The number of harvest days could be varied, but not performance (for example, harvest rate and travel distance as grain moisture changes). This model was validated using time-motion analysis with manual stopwatches.

The SQUASH model could not identify the bottleneck in the system itself, so Loewer, Kocher, and Solaimanian (1990) expanded on the SQUASH model and used “expert rules” to identify bottlenecks in a grain harvest/handling/drying system. The model utilized a decision support tree to answer questions during harvest simulation that would identify the system bottleneck. Loewer, Benock, and Bridges (1980) simulated harvest and delivery systems over a range of efficiencies. The authors found the system may not be optimum if the material flow is the only evaluation criteria. They also found that a decrease in delivery vehicle performance was accompanied by an increase in combine efficiency. Flow-based optimization results in excess capacity in one or more system to increase utilization in another. Many of these works were consolidated in Loewer et al. (1994), which, in addition to the above, provided guidelines on selecting optimal equipment sets based on cycle time.

Several other efforts have applied DES to field machinery and grain harvesting operations. De Toro and Hansson (2004) applied a DES model to simulate daily farm operations to study timeliness costs for two methods of estimating field workability. The simulation spanned multiple farm operations, and the model parameters were taken from ASABE Standards (2000). Benson, Hansen, Reid, Warman, and Brand (2002) presented a DES model of in-field grain handling, which incorporated combine travel through the field but was unable to accurately estimate the time required to complete an operation due to limitations of the modeling environment selected. Busato, Berruto, and Saunders (2007) applied DES to wheat harvest in Australia where they simulated multiple harvest scenarios to evaluate the effect of yield, field characteristics, and temporary grain storage bin locations on combine efficiency.

A number of efforts, related to this research, have been made to model forage and silage harvest systems using DES or cycle analysis. Harrigan (2003) used observers with stopwatches to perform a time-motion analysis for corn silage harvest. This research was conducted at several Michigan dairy farms and identified average times for each step in the cycle and found, depending on configuration, harvesters were utilized 75%-85% of the cycle. Harmon, Luck, Shinnars, Anex, and Drewry (2017) improved the time-motion analysis by utilizing data collected from GPS and vehicles CAN bus. Buckmaster and Hilton (2005) proposed a system model for transport and unloading systems based on

cycle times and capacity. This tool was spreadsheet-based and allowed for the system capacity and machine utilization to be determined. Dudenhoeffer, Luck, Digman, and Drewry (2017) developed a model for silage harvesting that was found to produce errors comparable to Buckmaster and Hilton (2005) but allowed for the inclusion of transport vehicles with dissimilar capacity. Amiama, Pereira, Castro, and Bueno (2015) used a DES model to develop a decision support tool for corn silage. The model encompassed harvest, transport, and packing. It was intended to be used both for strategic planning and daily decision making. Results indicated the system was more sensitive to packing capacity than to the number of transporters used and noted that, while some models select the number of transport vehicles to keep the harvester fully utilized, this does not necessarily result in the lowest cost if the extra transporter is mostly inactive and has a low utilization rate.

Several studies have applied DES to model and evaluate commercial grain storage facilities. Berruto and Maier (2001) used DES to investigate how different queueing methods impacted the operation of a receiving pit at a country elevator. The model was validated using field observations and evaluated the queueing methods based on average customer wait times. Silva, Queiroz, Flores, and Melo (2012) noted the need to account for stochastic factors and model dynamic system behavior. The authors used DES combined with Monte Carlo to simulate grain arrival and departure for corn, wheat, and soybeans at a commercial facility over the course of a year.

2.2.3 Motivation

The majority of previous efforts at modeling grain harvest and transportation explicitly model every aspect of the system, and define the system using deterministic model inputs. There is a need to develop a simplified modeling approach to evaluate on-road transportation equipment that can account for variable transportation demand that results from fluctuations in the rate at which material leaves the field. The overall goal of this study was to develop a DES model of grain transportation from the field to delivery at an on-farm storage facility. The model differs from previous works in that it represents harvest rate and in-field machinery interactions as a stochastic entity generation processes, and models receiving capacity at the storage facility as a stochastic service

time. The distributions used to represent these inputs are system specific (equipment set, crop, yield, etc.) but can be developed from easily obtained data. Specific objectives were:

1. Develop a DES model for grain transportation from field to storage.
2. Account for complex system behavior by incorporating stochastic elements into the model.
3. Apply the developed model to case study operations to validate the model and assess the performance of the studied harvest systems.

2.3 Materials and Methods

2.3.1 Model Implementation

2.3.1.1 Description

The focus of this DES model was on-road grain transportation, and it spans from the arrival of full in-field transporters at the field edge to the delivery of that grain to an on-farm storage facility. Figure 2-1 shows a simplified flow diagram of the model, and subsequent sections expand on specific functionality. Entities, which represent a full grain cart arriving at the field edge, are created in load generation. The rate at which they enter the system is the time required to harvest the grain and transport it to the field edge and represents the demand for on-road transportation. This rate accounts for the in-field machinery parameters that have traditionally been explicitly modeled. The number of combines and grain carts, harvest rate of the combine(s) and the in-field machinery interactions were all reduced to the timing of arrivals at the field edge.

After creation, an entity proceeds into the system if the current simulation time is less than the duration of fieldwork and the number of entities waiting for a truck is less than the maximum. This accounts for entities arriving faster than they can be delivered to the storage facility (harvest rate is larger than the transportation rate). Transportation continues after load generation has stopped for the day, allowing entities waiting in the various queues to be delivered. The model could account for mismatched capacities between trucks and grain carts by allowing multiple full grain carts to be loaded onto a single truck. The first entity acquires the truck, and subsequent loads are transferred into the same truck until it reaches capacity. These entities are combined and move through

the remainder of the system as a batched entity. Once a truck is fully loaded, and a driver is acquired, the load is transported to the storage facility where it is weighed and inspected before being unloaded. The acquire truck/driver blocks in Figure 2-1 represent acquiring resources from the respective resource pools. Throughout this discussion, the grain receiving area is referred to generally as the pit, though it could be a pit, auger, or drive over hopper. After unloading, trucks, and drivers are delayed by the time required to return to the field before being made available again. In cases where harvest was stopped because of a transportation bottleneck (i.e., all trucks are in use and combine(s) and grain carts are full), the harvest is restarted once resources become free.

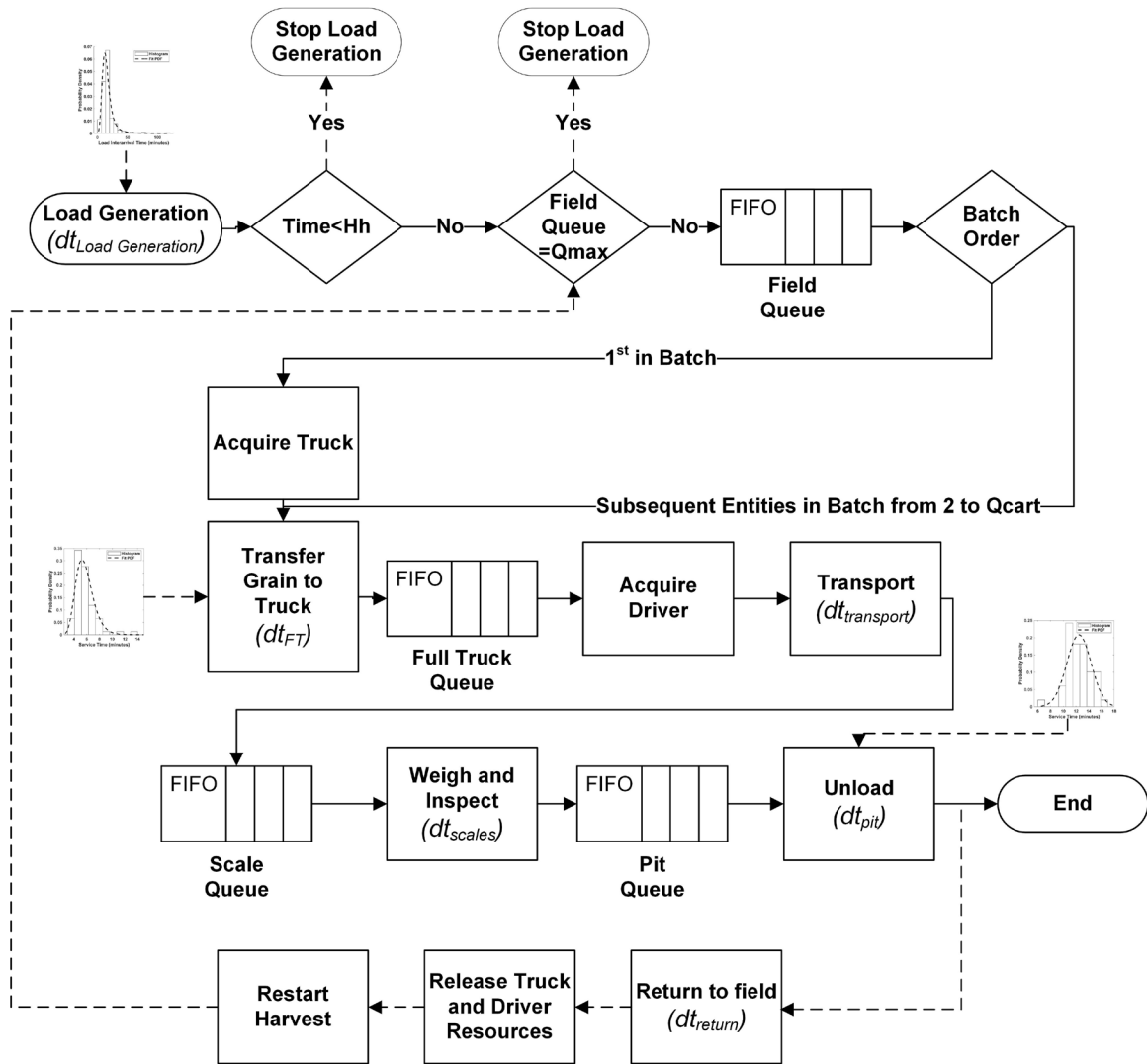


Figure 2-1: Simplified model structure. Solid lines represent the flow of material and dashed lines represent the flow of information. Graphs represent stochastic input parameters. See Table 2-1 for variable definitions.

2.3.1.2 Simulation

The DES model was created using MATLAB and Simulink (R2017b, The MathWorks Inc., Natick, MA), and required the use of the SimEvents toolbox. Table 2-1 lists the model inputs, along with a description and associated units. Model inputs were defined in the MATLAB workspace and passed to the Simulink model. The results of the simulation were passed back to the MATLAB workspace for further analysis. To examine the dynamic behavior of the system, 500 Monte Carlo simulations were run for each day for which data was available for the three operations (total of 18 daily input

conditions). Preliminary examination indicated 500 simulations were adequate to describe the variability and increasing the number of simulations by an order of magnitude had minimal effect on the results. In general terms of the model, the input parameters could be defined as constants or as random values depending on what characteristics of the system were of interest. For this study, the system characteristics, including the number of trucks, number of drivers, harvesting time, and transportation time were deterministic and unique to each day. The load generation rate, field transfer service time, and pit unloading service time were estimated from data collected during harvest and a distribution fit for each operation/crop (shown in the results section). The model simulates grain transportation for a single day, and it was assumed that adequate wet-holding capacity was available or would be accounted for by the duration of fieldwork for a given day. The effects of storing and drying wet grain were outside the bounds of this study.

Table 2-1: Model Variable Nomenclature*

Symbol	Description	Units
Model Inputs		
$dt_{Load\ Generation}^{**}$	Time between arrivals of full in-field transporters	Minutes cart ⁻¹
Q_{cart}	Number of field unloading events required to fill a truck	Carts truck ⁻¹
dt_{FT}^{**}	Field transfer time	Minutes
$dt_{transport}$	Time to transport from field to facility	Minutes
dt_{scales}	Weigh and inspect duration	Minutes
dt_{pit}^{**}	Unload duration	Minutes
dt_{return}	Time to return to the field from the facility	Minutes
$N_{drivers}$	Number of drivers	-
N_{trucks}	Number of trucks	-
Q_{Field_max}	Number of cart entities that can be harvested without a truck present	Entities
Hh	Harvest time	Minutes
Ht	Simulation time	Minutes
μ_L	Mass of grain per truckload, dry matter basis	Tonnes truck ⁻¹
Model Outputs		
Driver Utilization	Percentage of the day drivers were committed to transportation	%
Truck Utilization	Percentage of the day trucks were committed to transportation	%
Cumulative deliveries	Total number of arrivals at the storage facility	Trucks day ⁻¹
FTE	Flow time efficiency	Percent
WTF	Wait time for full grain carts at the field edge	Minutes
WTP	Wait time for trucks to unload at the receiving pit	Minutes

*Throughout this analysis all references to moisture content are on a wet basis, and all mass were on a dry matter basis.

**Parameters considered stochastic for this analysis.

Probability objects (MATLAB structures used to represent a statistical distribution) generated based on the collected data, and the *random* function were used to generate separate matrices of pseudorandom times for grain cart interarrival and each

process server. The distributions used are unique to each process and generally to each specific system examined. The matrices were predefined with enough random times for 500 simulation runs for each set of input conditions. Each individual simulation was allocated a unique array of random times from the matrices for each respective parameter. Every time a Simulink block that requires a random time was called, a new value from the corresponding time array was selected. Enough time values were included in each array to accommodate 100 Simulink block calls (i.e. 100-grain cart loads harvested per day). This was sufficient for all conditions in this study but could be adjusted as needed. The specific distributions used here are described in the results, and deterministic inputs were handled by populating the matrices with constant values.

The simulation was run for each day separately, and a different seed value was used in the random number generator to create unique matrices for each set of input conditions considered in the simulation. Deterministic model parameters were defined as constants in the workspace, and the daily simulations were independent, with the duration of fieldwork, number of trucks and drivers, and transportation time set as constants unique to each day. This resulted in input conditions that were unique to each day, and which allowed the simulation output to be repeatable. The simulations were run using a *parfor* loop with a parallel processing pool of four workers. Each day was evaluated separately, and a 1X500 *SimulationOutput* structure was saved from each day for further analysis.

2.3.1.3 Model Structure

Entity Generation

Figure 2-2 shows the Simulink model layout. This simulation is process-oriented, and arrivals to the system (entities) are created via a generator process (Rubinstein & Kroese, 2016). In this model, entities represent full in-field transporters arriving at the field edge with a specified rate, $dt_{Load\ Generation}$. Arrival generation is handled via the portion of the flow diagram in light blue. Since grain transportation can continue after harvest stops, a custom block was included to stop load generation after a specified time. This allows transportation to continue after harvest operations have ceased for the day. Additional gates and control functions in the light blue section were included to stop

entity generation when no trucks/drivers were available and when the field queue (representing harvested grain waiting in combine hoppers and grain carts) was full. These structures simulate situations where harvest was stopped due to lack of an on-road transporter. Once a transporter becomes available, it can be immediately loaded if there is an entity waiting in the field queue.

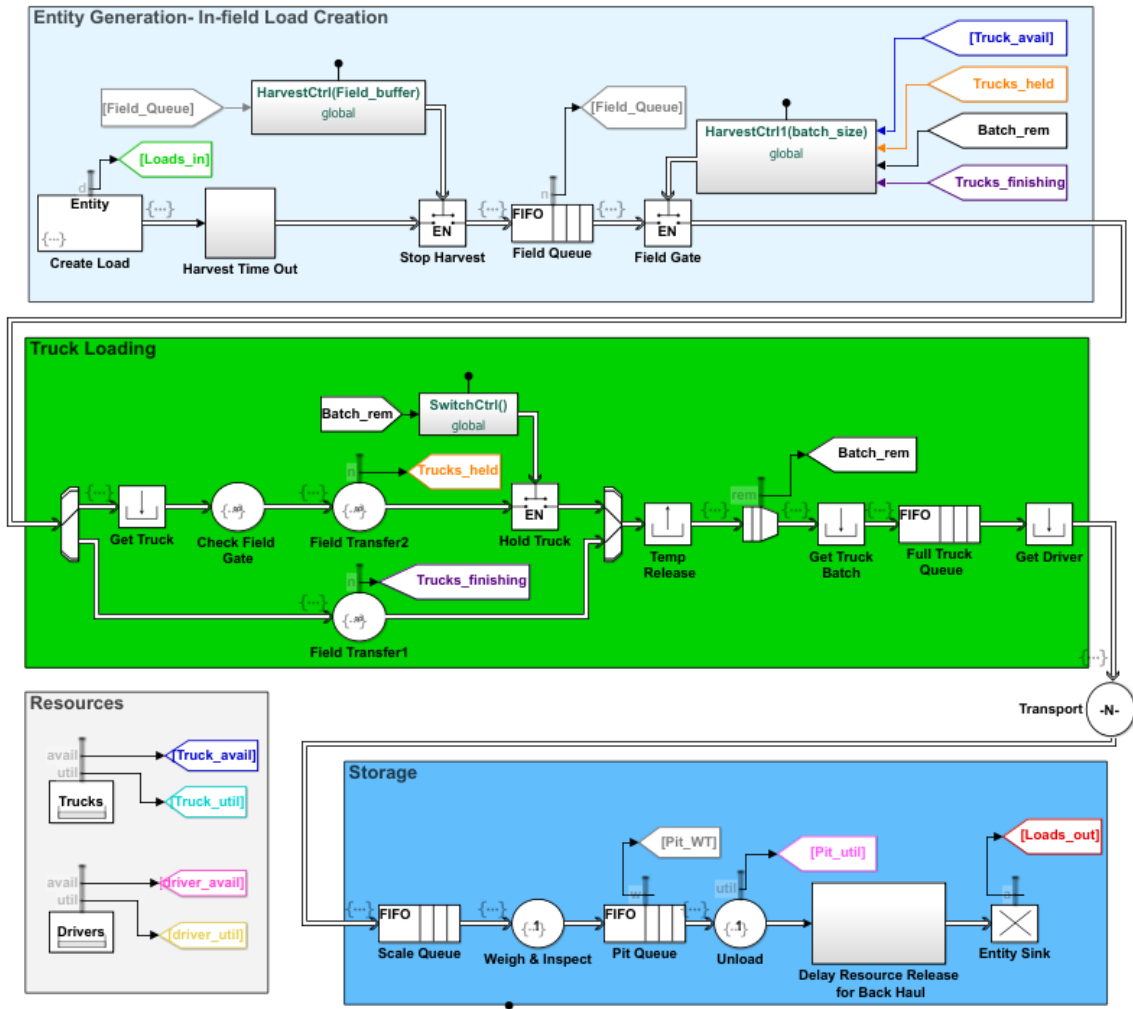


Figure 2-2: Simulink model flow diagram.

Field-Side Interactions and Transportation

Trucks and drivers are treated as resource pools in the model. The section of Figure 2-2 in green simulates the transfer of grain between in-field and on-road transportation. Accounting for unequal in-field and on-road transportation capacity was handled by the truck loading section of Figure 2-2 prior to the full truck queue. When

entities were created they were assigned an attribute based on which order they would be transferred to a truck, and the number of entities required to fill a truck, Q_{cart} , was required to be an integer value. The selection gate at the beginning of the truck loading section routes entities to either reserve a truck prior to being transferred, or to be transferred directly onto an already acquired truck. Once all the in-field arrivals required to fill a truck have been transferred, they are batched together and enter the full truck queue where they wait to acquire a driver before being transported to the storage facility. The service time to transfer the grain to the truck was stochastic, and the travel time was deterministic. Several items in the Truck Loading section of Figure 2-2 were a result of the programming environment. The check field gate server had a service time of zero and was required to ensure events were executed in the correct order when restarting harvest after a transportation delay. Temp Release and Get Truck Batch blocks were required to release a reserved truck and reassign it to the newly created batch when all entities required to fill a transporter are batched together (both of which happen at the same timestep).

Storage Facility and Empty Return to Field

Once an entity arrives at the storage facility, as shown in the blue section of Figure 2-2, it enters a first-in-first-out (FIFO) queue before being processed by a server which represents weighing/sampling the load. Next, the entities enter a queue in front of the last server, which represents unloading at the facility's receiving pit. The time to weigh and inspect the load was taken as deterministic, and the time unloading at the receiving pit was stochastic. After unloading, the entity was duplicated before being destroyed. The duplicated entity was then sent through a server with a service time that represented the time to make the return trip to the field before the truck and driver were released back into the resource pool. The model assumes that each transportation cycle begins and ends with the vehicle staged at the field edge. An additional server which evaluated the *HarvestCtrl* function after a service time equal to $dt_{Load\ Generation}$ delayed opening the stop harvest gate. This process only has an effect if harvest had previously been stopped, and the delay represents time required to harvest the next full load once harvest begins again. This was required to prevent a waiting entity in the generator from

being released immediately after the truck and driver resources were released. These steps were handled by the custom delay resource release block shown in Figure 2-2.

2.3.1.4 Analysis

The primary model output is the cumulative number of deliveries that were made per day for a given set of input conditions. This represents how much grain could be harvested on a given day and indicates the overall material handling capability of the system. The simulation output included the average total daily deliveries and corresponding 95% reference intervals (± 2 standard deviations) for each set of input conditions. The model validity was evaluated by comparing the actual number of truckloads delivered to the storage facility to the simulation result for each set of input parameters. The number of full truckloads delivered was the parameter of interest for this study, but it could easily be combined with the estimated load size to estimate the total mass of grain delivered.

Several other performance measures were used to evaluate the system. One way to evaluate how efficiently material moves through a system is to examine how long it takes the material to travel through the system from beginning to end (flow time, equation (2-1)). This can be compared to the minimum time required to complete all the required processing steps, which is productive time (equation (2-2)). Productive time for this study includes the time to transfer the material to the truck, transport it to the storage facility, weigh and inspect the material, and unload it at the receiving pit, but does not include delays. The time of events was estimated for each simulation run based on entity attributes, which are assigned timestamps as the entity moved through the system. The ratio between the productive time and flow time is the flow time efficiency (FTE), which was determined from equation (2-3). An FTE of 100% implies that no delays were observed in the system. An FTE of 50% reflects that half of the time it took an entity to flow through the was productive, performing the required tasks, and delays between processing steps consumed half of the time. Because FTE was based on the actual time required to complete each processing step, FTE only evaluated delays between productive steps and does not account for inefficiencies within processing steps (i.e., if the minimum time to transfer the grain was 2 minutes, but a given observation took 5 minutes, that would not be reflected in FTE).

$$Flow\ Time_i = (Tdi - Tci) \quad (2-1)$$

Where:

$Flow\ Time_i$ = Time required for the i^{th} entity to complete processing from arrival at field edge to delivery (minutes)

Tdi = Timestamp when the i^{th} entity was delivered to the storage facility (minutes)

Tci = Timestamp when the i^{th} entity was created (minutes)

$$Productive\ time_i = dt_{FT_i} + dt_{transport_i} + dt_{scales_i} + dt_{pit_i} \quad (2-2)$$

Where:

$Productive\ time_i$ = Total time to complete all necessary process steps for the i^{th} entity (minutes)

dt_{FT_i} = Time required to transfer the i^{th} entity from a grain cart to truck (minutes)

$dt_{transport_i}$ = Time required to transport the i^{th} entity from the field to storage (minutes)

dt_{scales_i} = Time required to weigh and inspect the i^{th} entity (minutes)

dt_{pit_i} = Time required to transfer the grain at the receiving pit (minutes)

i = entity number. Represents a single grain cart arriving to the field edge

$$Flow\ Time\ Efficiency_i = \frac{Productive\ time_i}{Flow\ time_i} * 100 \quad (2-3)$$

Where:

$Flow\ Time\ Efficiency_i$ = Ratio of the minimum time required to complete processing to the actual time for the i^{th} entity (%)

Similarly, wait times between processes served as indicators of how efficiently material moved through the system. The field and pit queue were the two primary points of interest for this study, and their associated wait times were estimated from equation (2-4) and equation (2-5), respectively. Wait time was estimated for each entity in

equation (2-4) and each full truckload delivered to the storage facility in equation (2-5). Time spent waiting in the field queue represented full in-field transporters that cannot be unloaded because no truck was available. Frequent or long wait times here indicate the potential for in-field operations to be slowed or stopped. Wait times associated with full trucks queuing before unloading at the receiving pit indicated trucks were arriving faster than they could be unloaded. For a given set of input conditions, the mean wait time and percentage of entities or loads with wait times greater than zero were estimated across all simulations.

$$WTF_i = (Tsl_i - Tci) \quad (2-4)$$

Where:

WTF_i = Time the i^{th} entity spent waiting in the field side queue before being transferred to a truck (minutes)

Tsl_i = Timestamp when the i^{th} entity began transfer to a truck (minutes)

$$WTP_j = (Tdj - Tfs_j) \quad (2-5)$$

Where:

WTP_j = Time the j^{th} truckload spent waiting in queue before unloading at the storage facility (minutes)

Tfs_j = Timestamp when the j^{th} truckload left the scales (minutes)

Tdj = Timestamp when the j^{th} truckload started unloading at the storage facility (minutes).

j = index for full trucks. Corresponds to full trucks moving through the system, consists of Q_{cart} entities.

The utilization of truck and driver resources was also a primary concern. The time a resource was dedicated to transporting a particular truckload was determined from equation (2-6) and equation (2-7) for trucks and drivers, respectively. Trucks were considered in use from the time the first entity begins to transfer to the time the vehicle returned to the field empty. The driver's time was estimated similarly, except a driver was not required until the truck was full and ready to begin transportation. The average

utilization of the resources over the course of the day was determined from the total utilized time, number of resources, and the time when the last truck returned to the field (equations (2-8) and (2-9) for trucks and drivers, respectively). The average truck utilization, driver utilization, and flow time efficiency were estimated over the 500 simulations for each set of given input conditions. The simulation automatically recorded resource utilization at discrete points over the course of the simulation. From this, the maximum resource utilization observed at any point over all simulations was determined. The discrete utilization estimates for all simulations were averaged using a five-minute window to show the trend of utilization over the course of the day.

$$\textit{Truck Utilized Time}_j = (Ttrj - Tslj) \quad (2-6)$$

Where:

$\textit{Truck Utilized Time}_j$ = Time a truck was committed to the j^{th} truckload
(minutes)

$Tslj$ = Timestamp when the first entity begins transfer to the j^{th} truckload
(minutes)

$Ttrj$ = Timestamp when the truck and driver return to the field after delivering the j^{th} truckload (minutes)

$$\textit{Driver Utilized Time}_j = (Ttrj - Tstj) \quad (2-7)$$

Where:

$\textit{Driver Utilized Time}_j$ = Time a truck was committed to the j^{th} truckload
(minutes)

$Tstj$ = Timestamp when the driver is acquired for transport of the j^{th} truckload
(minutes)

$$Truck\ Utilization = \frac{\sum_{j=1}^N Truck\ utilized\ time_j}{N_{trucks} * t_{max}} * 100 \quad (2-8)$$

Where:

Truck Utilization = Average truck utilization over a whole day for a given simulation (%)

t_{max} = Time when the final truck returns to the field (minutes)

N = Total number of deliveries

$$Driver\ Utilization = \frac{\sum_{j=1}^N Driver\ utilized\ time_j}{N_{drivers} * t_{max}} * 100 \quad (2-9)$$

Where:

Driver Utilization = Average driver utilization over a whole day for a given simulation run (%)

$N_{drivers}$ = Number of drivers

2.3.2 Case Studies

2.3.2.1 Operation 1—Data Collection

The data used to inform and validate the model were collected at two cooperating farms. The first cooperator (Operation 1) was a large grain farm in Western Kentucky, for which data was collected during the 2016 wheat (June) and corn (August/September) harvest. This provided the ability to look at the same system with different material handling demands due to the yield difference between the two crops. The producer operated multiple combines and utilized multiple grain carts for in-field transportation. During wheat harvest, the producer utilized up to four class 8 combines (grain tank capacity of approximately 14.5 m³) with 12.2 m platform headers and two 35.3 m³ (1,000 bu) capacity grain carts. For corn harvest, the producer utilized two class 8 combines with 12-row corn heads and the same two grain carts. On-road transportation utilized a combination of hopper and dump semi-trailers, and the grain carts were sized to match the capacity of the trucks (approximately 25 wet tonnes). The producer determined the number of unique trucks used on a given day, and it varied from 2 to 11 depending on

availability, crop, and field conditions. Grain was primarily delivered to an on-farm drying and storage facility equipped with scales and an estimated receiving capacity of 125 t hr^{-1} .

Scale records obtained from the producer were one of the primary sources of data for this analysis. The records included the date, field, destination, test weight, moisture content, truck number, mass of grain, and grain cart driver. The records also included timing information, recorded to the nearest minute, including when grain carts arrived at the field edge and when semi-trailers arrived and departed from the storage facility. Records were obtained for an entire season of winter wheat and white corn harvest, and only on days where 100% of the grain was delivered to the on-farm storage facility were tested using the model. For a given day, these records were used to determine: the number of unique trucks utilized; the number of truckloads delivered to the facility; and though not explicitly a model parameter, the total amount of grain harvested (adjusted to tonnes on a dry matter basis). The elapsed time between when full grain carts arrived at the field edge was utilized to determine the interarrival time for in-field transporters, $dt_{Load\ Generation}$. The total time harvesting each day, Hh , was estimated as the elapsed time between the first and last grain cart arrival plus the average time between arrivals (equation (2-10)). This additional time was included to account for the time harvesting before the first in-field transporter arrived at the field edge.

$$Hh = \Delta T + \frac{\Delta T}{TP} \quad (2-10)$$

Where:

ΔT = Elapsed time between the first and last grain cart arrival for the day
(minutes)

TP = Total number of truckloads delivered (trucks day^{-1})

The average transportation distance from each field to storage was estimated using the Network Analysis Toolbox in ArcMap 10.2.2 (ESRI, Redlands, CA). Field locations were imported as shapefiles, and the Kentucky road network shapefile was used to find the distance from each field to the storage facility. The average travel speed was

determined using a GPS data logger (Flashback GPS Tracker, LandAirSea, Woodstock, IL) that was installed on a truck that was operated for eight days during corn harvest. These were combined to estimate the average time required to transport grain from the field to storage, $dt_{transport}$, for each day. This data was also used to determine the average time spent weighing and sampling the grain upon arrival at the storage facility, dt_{scales} . For this operation, the time required to return to the field from the storage facility, dt_{return} , was assumed equal to $dt_{transport}$.

The service time for a truck to receive grain from a grain cart, tarp the load and depart the field (dt_{FT}) was determined through time-motion studies of the harvest operation over several days for both crops. Service times at the unloading pit, dt_{pit} , were determined in a similar fashion and were determined based on when the truck pulled into the pit to when it departed. These times were based on physical observation of the system and data was recorded to the nearest second.

2.3.2.2 Operation 2—Data Collection

A second location in Central Michigan (Operation 2) was used to evaluate how well the model could approximate an operation where multiple on-road transporters were shuttled from the field to storage by a single operator. For this location, three dump semi-trailers were shuttled by a single operator; a common configuration in smaller operations that can result in harvest rates higher than the grain transportation rate. This operation was equipped with a class 7 combine (grain tank capacity of approximate 10.6 m^3) running a 12-row corn head, and a single grain cart with a maximum capacity of 30.8 m^3 (875 bu) was used for in-field transportation. The full capacity of the grain cart was not utilized, and unloading events were timed so that each truck received two unloads from the grain cart. No scales were employed at this location, so no weight information was available. However, based on conversations with the producer, each truck had an approximate capacity of 28 tonnes on a wet basis (1,300 bu). For this operation, all model parameters were estimated from a time-motion study conducted for a single day during the 2016 corn harvest (November).

2.3.2.3 Data Analysis

The collected data were organized and preprocessed in a spreadsheet. The input parameters are shown in Table 2-1, except for: $dt_{Load\ Generation}$, dt_{ft} , and dt_{pit} , were considered deterministic and were taken as average values for each operation/day. The time associated with entity generation, field side grain transfer, and unloading at the destination facility were considered as stochastic. Observations for these parameters were imported to MATLAB for distribution fitting. The *allfitdist* function (downloaded from the MATLAB file exchange) was used to assist in determining the best distribution for modeling the data. Common distributions were fit to the data and ranked based on the Bayesian Information Criterion (BIC). The *fitdist* function was then used to create probability distribution objects for the top choices, which were further evaluated with manual observation of QQ plots. The selected distributions and associated parameters were saved as MATLAB formatted data files (*.mat*) containing the probability distribution objects that served as inputs to the model. Finally, the probability distribution for the selected distributions were overlaid with histograms of the observed data using the *histogram* function with normalization based on the probability density function.

2.4 Results and Discussion

2.4.1 Example Operation System Characteristics

2.4.1.1 Operation Summary

A summary of the operating characteristics for the example farms can be found in Table 2-2. The two crops examined in Operation 1 represent the same system with different material handling requirements, and Operation 2 represents a smaller operation. Operation 1 used two combines and two grain carts in corn, which resulted in an average harvest rate, HR, of 73.6 tonnes of corn per hour (adjusted to 0% moisture). The in-field transporters' capacity was matched to the semi-trucks used for on-road transportation ($Q_{cart} = 1$), and the average mass of grain, μ_L , was 21.0 tonnes of dry matter per truck. This combination resulted in an average time between full grain carts arriving at the field edge of 17.2 minutes. The operating characteristics were similar for Operation 1 in wheat, except up to four combines and two grain carts were used. The average HR was reduced to 44.7 t hr⁻¹ (at 0% moisture) and the time between grain cart arrivals increased to an

average of 26.7 minutes. This lower harvest rate and increased time between grain cart arrivals represents a lower material handling requirement and is consistent with the lower yield of wheat compared to corn in Kentucky. Operation 2 utilized a single combine and grain cart and no scale data was available at this operation, so it was evaluated based solely on the number of truckloads delivered. Additional axles and increased transportation weight limits allowed an increased mass of grain to be transported per truckload, and each truckload was approximately 28 tonnes (1,300 std. bu). The average time between cart arrivals was 20.5 minutes, with two partially full grain carts required to fill a single truck ($Q_{cart} = 2$). The characteristics of these three scenarios result in a transportation demand (λ) ranging from an average of 1.0 to 3.6 trucks per hour.

Table 2-2: Operation Characteristics*

Parameter	Operation 1 Corn	Operation 1 Wheat	Operation 2 Corn
Days	12	5**	1
HR (t hr ⁻¹)	86.5 (58.9-171.9)	51.7 (12.4-71.8)	-
H_h (minutes)	469 (268-590)	375 (149-521)	578
dt_{Load Generation} (minutes cart ⁻¹)	17.2 (3.0-120)	26.7 (1.0-95)	20.5 (4.7-30.9)
Tt (trucks day⁻¹)	28 (15-39)	13.8 (5.0-23)	10
TG (t day⁻¹)	673 (356-1000)	329 (72-574)	-
dt_{transport} (minutes)	11.6 (3.9-29.5)	5.0 (4.2-6.3)	11.8 (8.0-22.4)
N_{trucks}	8.6 (5-11)	3.2 (2-4)	3
N_{drivers}	8.6 (5-11)	3.2 (2-4)	1
λ (trucks hr⁻¹)	3.6 (2.5-4.5)	2.2 (0.9-2.9)	1.0
μ_L (t truckload ⁻¹)	21 (9.6-29.0)	21.5 (8.5-24.7)	-
Q_{cart} (Carts truck ⁻¹)	1		2
dt_{FT} (minutes)	5.76 (3.6-14.0)		2.3 (1.7-2.3)
dt_{scales} (minutes)	2		0
dt_{pit} (minutes)	12.5 (6.5-16.9)		26.1 (18.3-32.2)
dt_{return} (minutes)	dt_{transport}		9.5
Q_{Field_max} (loads)	3	4	1
Ht	960		960

*Average values, range shown in parenthesis.

**8 days were used for $dt_{Load Generation}$. The additional days were days when grain was delivered directly to a commercial elevator.

Table 2-2 also provides a summary of the transportation requirements for the operations. Operation 1 had access to a relatively large number of trucks and drivers, which for corn, ranged from 5 to 11 trucks and drivers used per day with an average of 8.6. In wheat, only 2 to 4 trucks were used per day, with an average of 3.2. The number of trucks and drivers used on a given day was determined by the producer based on availability, field and weather conditions, and locations. The transportation time from the field to the storage facility, $dt_{transport}$, had a daily average that ranged from 3.9 to 29.5 minutes for Operation 1 corn. The fields planted in wheat were generally closer to the storage facility, thus Operation 1 wheat had shorter transportation times averaging from

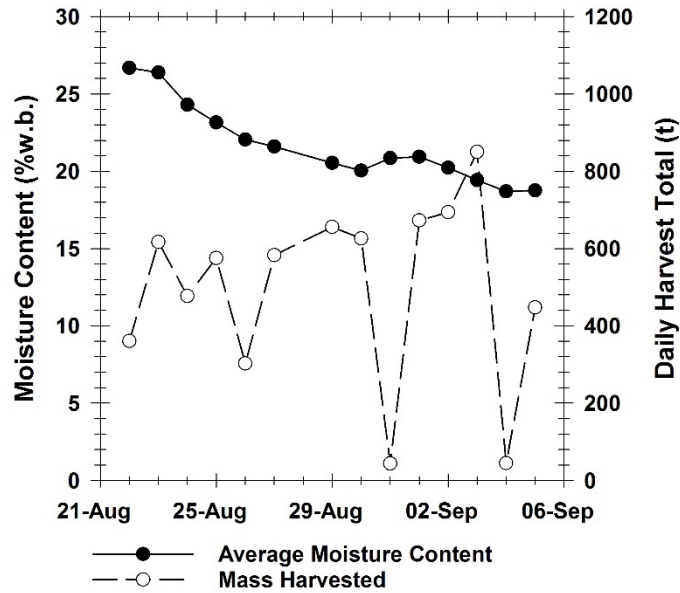
4.6 to 6.3 minutes. Operation 2 utilized three trucks that were shuttled to the storage facility by a single driver. The extra trucks were staged by the field edge where they served as temporary field side storage while waiting for a driver. No scales were used at Operation 2 ($dt_{scales} = 0$), and the average time unloading at the pit was more than double Operation 1 at 34.5 minutes, primarily due to the capacity of the wet grain receiving system.

2.4.1.2 Harvest Trends

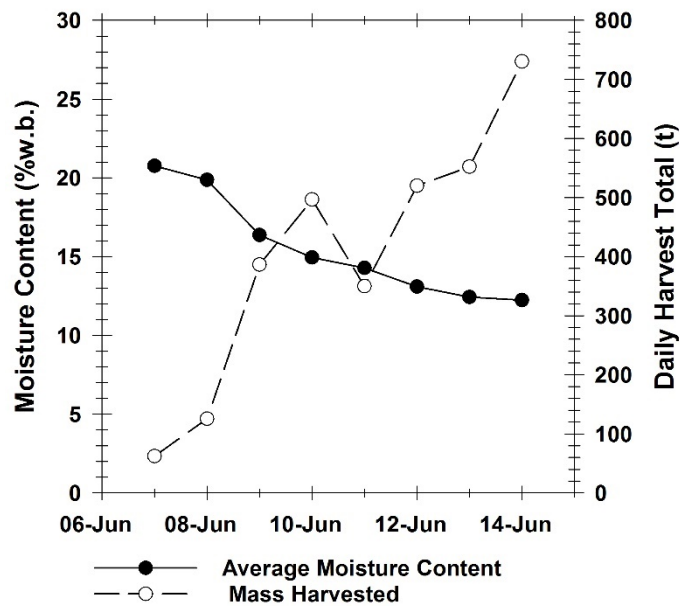
Data were only collected for a single day at Operation 2. Thus, discussion in this section is limited to Operation 1, where data was available for multiple days and crops. Figure 4-4 shows the trend in grain moisture content and the total mass of grain harvested over the course of the harvest season for Operation 1 (a) corn (b) wheat. Both plots show a general trend of decreasing moisture over the course of the season as the crop field dries, and the range of moistures encountered in corn was 26.7% w.b. to 18.8% w.b.. For wheat, the range encountered was 20.8% w.b. to 14.3% w.b., so both crops required some heated-air drying for the duration of the harvest season.

Figure 4-4 also shows the total mass of grain harvested on a given day, as determined from the scale records, adjusted to a dry matter basis. This shows the overall harvest system productivity and accounts for any variation in yield, field machinery performance, transportation distance, number of transporters, and the harvest duration for each day. For both crops, there is a general trend of increased daily productivity as the grain field dries. The trend was most pronounced in wheat where the productivity increased from 62.3 to 730 t day⁻¹. A large portion of the increased productivity can be explained by a corresponding increase in daily harvest duration. The harvest time was primarily determined by field conditions, or by the wet holding capacity at the storage facility. In corn, the trend was not as clear, and there was a larger amount of variability. Two days are shown in Figure 4-4 (a), which had drastically lower productivity. September 4th was a Sunday, which typically would not be a work day for this operation. The cause for the other low productivity day is unknown, but fieldwork only occurred for approximately 90 minutes. The last three days shown in Figure 4-4 (b), which had a much higher harvest rate because a large portion of the wheat was delivered directly to a commercial elevator, were included here for context. The two low productivity days in

corn and three high productivity days in wheat were excluded from Table 2-2 and subsequent sections.



(a)



(b)

Figure 2-3: Trends over the harvest window (Data shows average moisture content and the average mass of grain harvested (dry matter basis) over the span of data collection (a) Operation 1 corn (b) Operation 1 wheat).

One of the aims of this research was to evaluate if the complex interactions that affect the harvest rate (yield, moisture, field machinery performance, etc.) could be represented by the elapsed time between the arrival of full loads of grain at the field edge ($dt_{Load\ Generation}$). The distributions used to represent this value (shown in section 2.4.2) were estimated using data collected over a range of field conditions. One potential pitfall of using a single distribution to represent this relationship over the whole harvest season is the variation in field machinery performance as field conditions and moisture content change. Figure 2-4 shows the time between grain cart arrivals plotted against grain moisture content for (a) Operation 1 corn and (b) Operation 1 wheat. The moisture content shown here is the average moisture of the two subsequent grain cart arrivals used to calculate the interarrival time. There was no strong correlation between interarrival time and moisture for either crop ($r^2 < 0.02$ for both cases). A similar lack of correlation was observed between time of day and interarrival time. This indicates a single distribution is appropriate for use over the whole harvest season, and any moisture or non-stationary relationships were masked by other forms of variability.

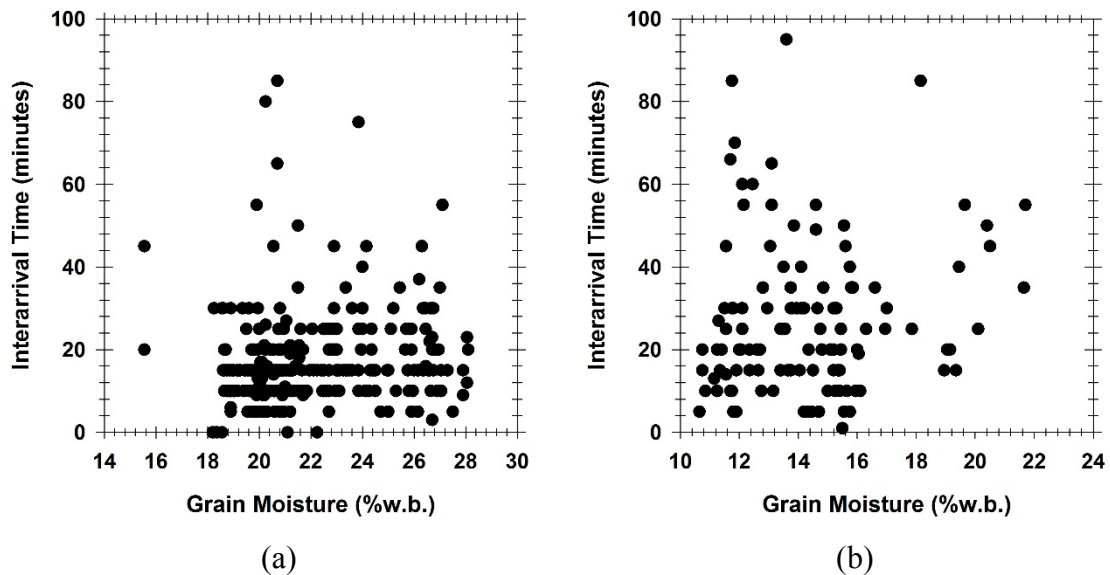


Figure 2-4: Grain moisture content plotted against the grain cart interarrival rate. Moisture content is the average of the two subsequent arrivals, and interarrival time is the time elapsed between their arrival at the field edge (a) Operation 1 corn (b) Operation 1 wheat

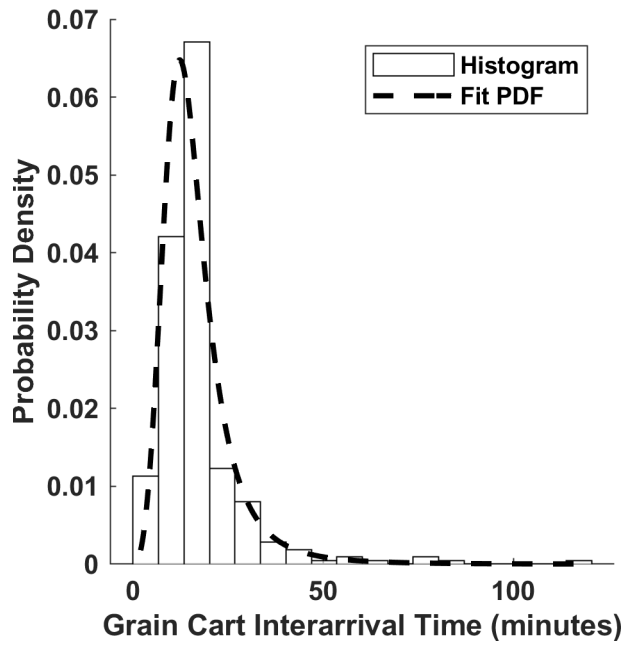
2.4.2 Distributions for Stochastic Elements

The full grain cart generation rate, service time to transfer grain to trucks, and the service time at the unloading pit were modeled as stochastic processes. Table 2-3 shows the selected distributions and associated parameters that were used to represent them. The values shown here represents the same data that was shown in Table 2-2, but here the data is presented in terms of the parameters of the associated distributions. Normalized histograms and the fitted probability functions chosen to represent the entity generation rate are shown in Figure 2-5. The low values on the histograms could represent instances when full grain carts arrive faster than the grain they contain could physically be harvested. There are numerous scenarios where this could be the case. For Operation 1, multiple full grain carts could be working in parallel and arrive at approximately the same time (Figure 2-5 (a) or (b)). Alternatively, Operation 2 used a single grain cart and required two grain cart unloads to fill a truck; entities are not required to be identical in size, so a smaller mass of grain could be dumped before moving to a new section of the field. The times on the long end of the distribution could represent delays due to breakdowns, changing fields, or adjusting equipment. These distributions are critical to the model because, given enough capacity in other areas of the system, they will govern how much grain enters the system and the total productivity.

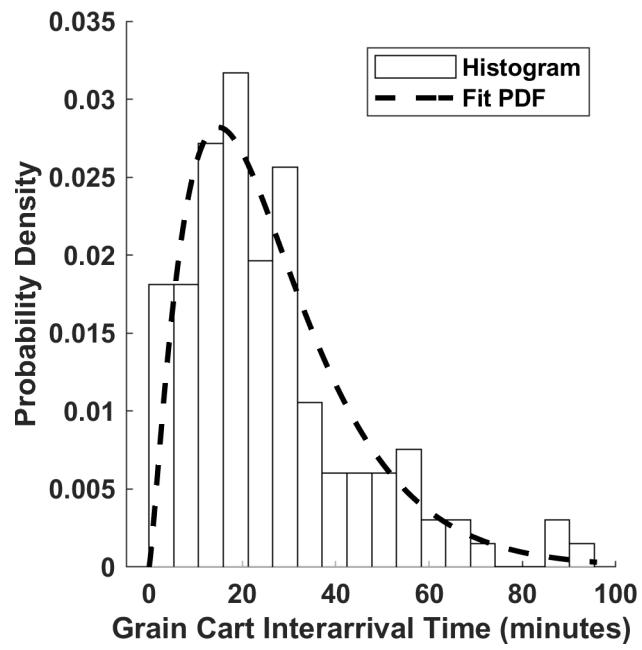
Table 2-3: Input Parameters and Associated Distribution for Model Validation

Symbol	Operation 1 Corn		Operation 1 Wheat		Operation 2 Corn	
	Parameters	Distribution	Parameters	Distribution	Parameters	Distribution
$dt_{Load\ Generation}$	$\mu=2.68$ $\sigma=0.29$ $n=317$	Log-Logistic	$\alpha=2.27$ $\beta=11.79$ $n=125$	Gamma	$\mu=3.12$ $\sigma=0.28$ $n=15$	Log-Logistic
dt_{FT}	$\mu=1.72$ $\sigma=0.24$ $n=69$			Lognormal	$\mu=2.37$ $\sigma=0.60$ $n=19$	Normal
dt_{pit}	$\mu=12.47$ $\sigma=1.92$ $n=45$			Normal	$\mu=26.1$ $\sigma=3.69$ $n=9$	Normal

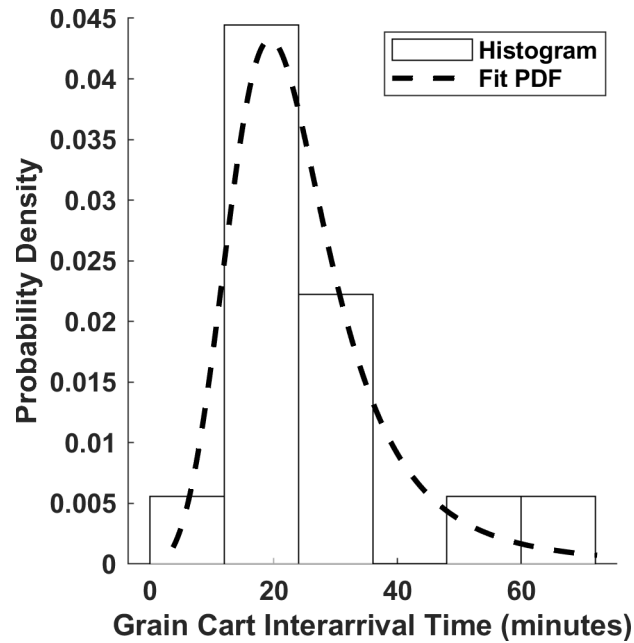
*n=number of observations used, α =shape parameter, β =scale parameter, μ =mean, σ =standard deviation or scale parameter. Note μ and σ are in terms of their distribution.



(a)



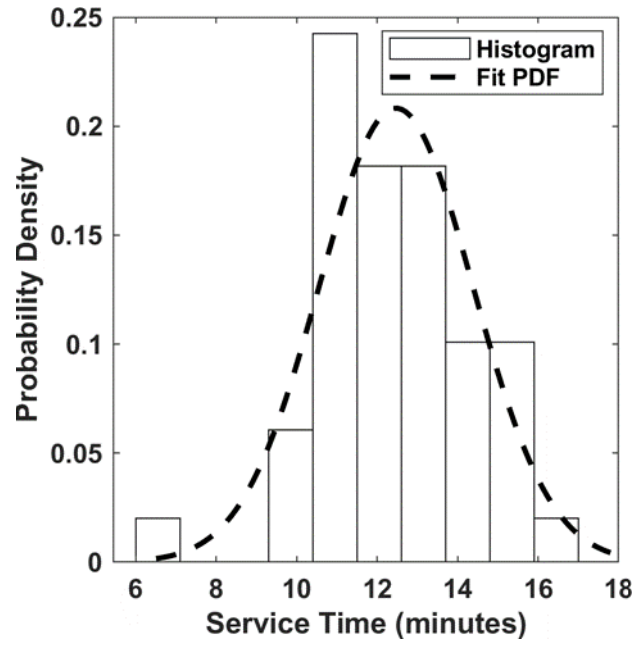
(b)



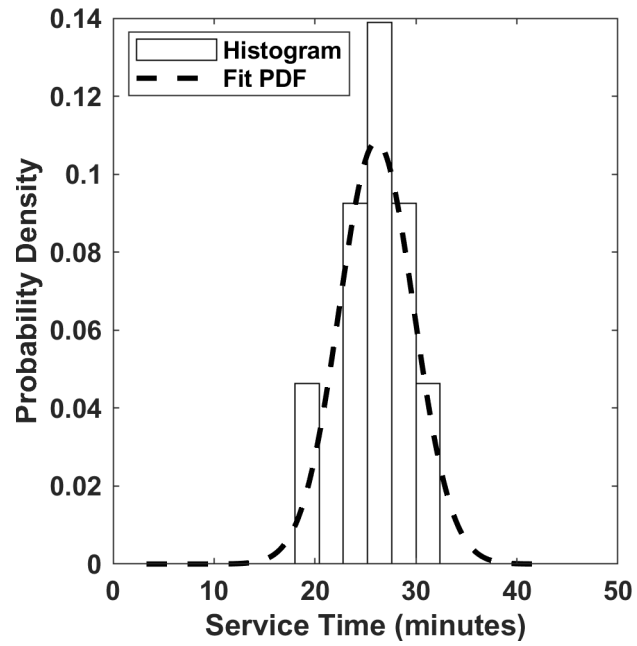
(c)

Figure 2-5: Grain cart interarrival time (a) Operation 1 corn (b) Operation 1 wheat (c) Operation 2 corn

Normalized histograms and the fitted probability functions chosen to represent the time spent unloading at the storage facility, dt_{pit} , and the time required to transfer the grain to a waiting truck, dt_{FT} , are shown in Figure 2-6 and Figure 2-7, respectively. A common distribution was used for both crops at Operation 1 (Figure 2-6 (a) and Figure 2-7 (a)). The intent was to increase the sample size and find a more representative distribution for these processes because limited observations were available. This was deemed acceptable because the same equipment was used in both cases, and no statistically significant differences were found between the means of the individual data sets. Crop and moisture content most likely caused differences in the physical material handling capacity of the equipment; however, in addition to the time required to physically transfer the material, dt_{FT} and dt_{pit} include ancillary time required to complete the operation (align the equipment, communication between operators, etc.). The distributions for dt_{FT} and dt_{pit} at Operation 2 are shown in Figure 2-6 (b) and Figure 2-7 (b), respectively. The time required to transfer the grain to the truck for Operation 2 was on average less than half of Operation 1, which is consistent with Operation 2 requiring two unloading events to fill a single truck.

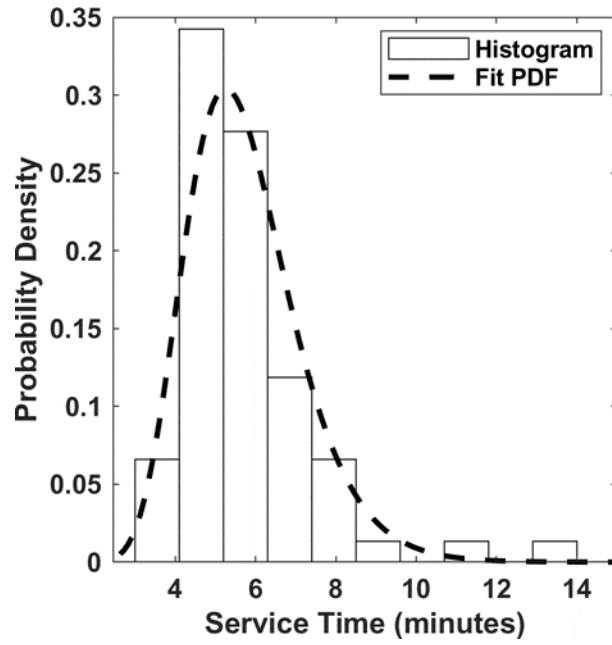


(a)

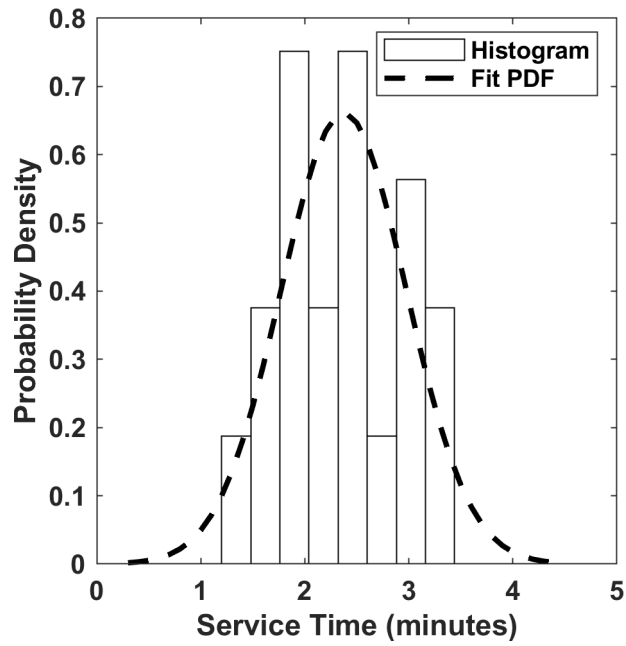


(b)

Figure 2-6: Pit service time (a) Operation 1 wheat and corn (b) Operation 2 corn



(a)



(b)

Figure 2-7: Loading service time (a) Operation 1 wheat and corn (b) Operation 2 corn

2.4.3 Model Application and Validation

2.4.3.1 Overall Performance

The simulation output was validated by comparing the number of deliveries estimated by the simulation to observed data. All available data was used to inform the model parameters for each operation/crop, and the model was applied to each individual set of input conditions. Figure 2-8 shows the observed number of deliveries plotted against the average simulation output, and Table 2-4 provides a tabular comparison. Overall, based on the daily input conditions, the simulation agreed well with the observed data, and the observed data was within the 95% reference interval for 15 of the 18 input conditions examined, and the median difference between the simulation and observed data was 0.8 deliveries, or -4.1%. Overall, the simulation underestimated the number of deliveries for 61% of the input conditions. The simulation underestimated the total number of grain deliveries by 0.5% for Operation 1 in corn and overestimated by 0.3% for Operation 1 in wheat, and 8% for Operation 2. It was also apparent that the simulation produced a relatively wide range of cumulative deliveries, with the half width of the 95% reference interval being on average 23%, 39%, and 24% of the average number of deliveries for Operation 1 corn, Operation 1 wheat, and Operation 2 corn, respectively. A closer examination of the three days that did not fall into the 95% reference interval gives insight as to why the simulation did not perform well for these observations. The simulation overpredicted the observed data on all three occasions. August 22 was the first day of harvest, and the arrival rate for the first third of the day was over double the season average. On 8/26, there was a single truckload harvested followed by a two-hour delay while switching farms. Similarly, on 06/07 there was a two-hour span where no truckloads arrived. Though the simulation was not able to capture these atypical scenarios, it does illustrate the amount of variability that can be encountered for a given day, and partially explains the relatively large variability in simulation output.

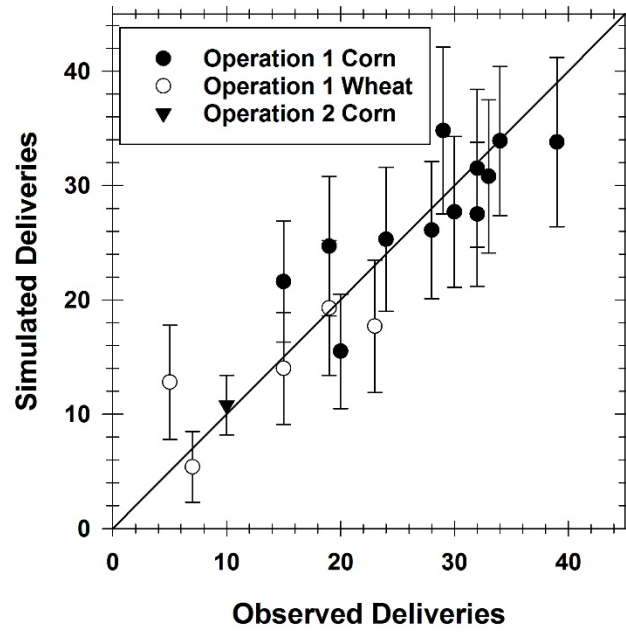


Figure 2-8: Observed versus simulated daily deliveries. Each series represents a different crop operation combination. Error bars represent the \pm two standard deviations for the simulated values ($n=500$).

Table 2-4: Simulation Results: Resource Utilization and Cumulative Deliveries

Scenario (operation- crop)	Day	Resources (Trucks/ Drivers)	Average Driver Utilization (%)	Max Driver Utilization (%)	Average Truck Utilization (%)	Max Truck Utilization (%)	Simulated Deliveries	Observed Deliveries
1 Corn	08/22	(5/5)	28.8	66.0	35.2	75.8	24.7±6.1	19
1 Corn	08/23	(11/11)	13.9	31.0	16.9	35.0	33.9±6.5	34
1 Corn	08/24	(10/10)	15.5	34.8	18.8	39.7	25.3±6.3	24
1 Corn	08/25	(6/6)	28.7	60.2	34.1	67.9	34.8±7.3	29
1 Corn	08/26	(7/7)	22.3	49.0	26.9	55.7	21.6±5.3	15
1 Corn	08/27	(10/10)	17.2	34.4	20.4	39.5	26.1±6.0	28
1 Corn	08/29	(9/9)	17.8	36.8	21.4	41.6	31.5±6.9	32
1 Corn	08/30	(9/9)	17.3	32.9	20.9	38.6	27.7±6.6	30
1 Corn	09/01	(8/8)	49.1	74.4	52.8	79.8	27.5 ±6.3	32
1 Corn	09/02	(10/10)	38.1	67.9	41.1	72.6	30.8±6.7	33
1 Corn	09/03	(11/11)	29.7	47.0	32.5	50.8	33.8 ±7.4	39
1 Corn	09/05	(7/7)	41.1	72.0	45.1	78.2	15.5 ± 5.0	20
1 Wheat	06/07	(2/2)	41.5	75.9	54.3	90.8	12.8±5.0	5
1 Wheat	06/08	(3/3)	26.9	69.8	33.3	85.1	5.4±3.1	7
1 Wheat	06/09	(3/3)	32.7	67.6	39.8	80.2	19.3±5.9	19
1 Wheat	06/10	(4/4)	23.2	56.3	28.4	70.0	17.7±5.8	23
1 Wheat	06/11	(4/4)	25.2	52.8	30.3	61.5	14.0±4.9	15
2 Corn	-	(3/1)	82.4	96.0	51.8	89.5	10.8± 2.6	10

Table 2-5 shows flow time efficiency and wait times, as estimated by the simulation. Operation 1 had extremely high flow time efficiency for both crops (average 92%), and on average, less than 0.2% of entities for corn and 4.4% of entities for wheat had wait times greater than zero at the field edge. This indicates that full in-field transporters rarely had to wait for a truck, and it was unlikely harvest operations were frequently stopped due to a lack of transportation resources. At the receiving pit, on average 50.6% of corn truckloads experienced wait times and the average wait was 7.1 minutes. For wheat, 23.6% truckloads had wait times at the pit greater than zero, and the average wait was 5.4 minutes. When compared to corn harvest, the reduction in wait time and the percentage of truckloads impacted is consistent with the reduced material handling requirements for wheat. Moreover, when combined with the apparent lack of delay on the field side, this indicates there was sufficient surge capacity in the transportation resources to prevent wait times at the receiving pit from impacting upstream processes.

Table 2-4 also shows resource utilization, and the columns for maximum driver and truck utilization represents the highest utilization that was recorded over all simulations. A large number of transportation vehicles employed at Operation 1 resulted in the low truck and driver utilization, especially in corn where the average truck utilization ranged from approximately 17% to 53%, with driver utilization being slightly lower because a driver was not considered necessary to load the truck. From a practical standpoint, the large number of trucks that were used by Operation 1 could serve as auxiliary wet holding capacity once regular wet bins were full. This would be accounted for by duration of harvest operations and would not impact the overall number of deliveries to the storage facility that were estimated. The only difference would be the time associated with waiting at the pit to unload the final entity before transport back to the field. The trucks would most likely queue at the storage facility with their last load, and they would be unloaded at a rate equal to the drying capacity before returning to the field the next morning. These aspects, and incorporating wet holding and drying capacity, will be addressed in future work.

Table 2-5: Simulated Results: Flow Time Efficiency and Wait Times

Scenario (operation- crop)	Day	Mean FTE* (%)	Mean WTF* (minutes)	Entities Impacted** (%)	Mean WTP* (minutes)	Truckloads Impacted*** (%)
1 Corn	08/22	89.8	3.9	0.2	7.0	50.5
1 Corn	08/23	89.1	-	0.0	7.4	51.8
1 Corn	08/24	89.5	-	0.0	7.4	50.6
1 Corn	08/25	90.0	7.5	0.3	7.4	50.6
1 Corn	08/26	90.2	-	0.0	6.9	50.6
1 Corn	08/27	89.9	-	0.0	7.3	51.4
1 Corn	08/29	89.6	-	0.0	7.2	51.1
1 Corn	08/30	90.1	-	0.0	7.1	49.9
1 Corn	09/01	94.3	5.0	0.8	6.8	50.2
1 Corn	09/02	93.7	-	0.0	7.2	50.9
1 Corn	09/03	93.2	-	0.0	7.0	50.5
1 Corn	09/05	93.3	7.5	0.5	7.0	49.0
1 Wheat	06/07	93.9	9.0	16.7	4.0	16.5
1 Wheat	06/08	95.5	4.8	1.5	5.6	24.5
1 Wheat	06/09	95.5	6.5	3.2	5.3	25.0
1 Wheat	06/10	95.2	9.1	0.2	6.1	26.2
1 Wheat	06/11	95.5	4.8	0.2	6.0	25.6
2 Corn	-	66.5	9.1	0.8	-	0

*WTF= wait time at field edge. WTP= wait time at the receiving pit. Mean wait time only considers entities that had a wait time>0. FTE=Flow time efficiency.

**Percentage of entities (full grain carts) created that experienced a delay at the field edge due to lack of an available truck

***Percentage of truckloads that experienced a delay before unloading at the storage facility

This simulation resulted in extremely high flow time efficiency for Operation 1 wheat, while also increasing the utilization of trucks and drivers. Fewer trucks were utilized during wheat harvest because of the lower harvest rate and shorter transportation distance. In this instance, the simulation shows the transportation equipment was better matched to the field conditions, with the average truck utilization ranging from 28% to 54%, with the maximum observed truck utilization topping out over 90%.

Operation 2 provided an example of a different system configuration where a single driver was responsible for handling multiple trucks, and the simulation estimated an average driver utilization of 82%. The average truck utilization was estimated at 52%,

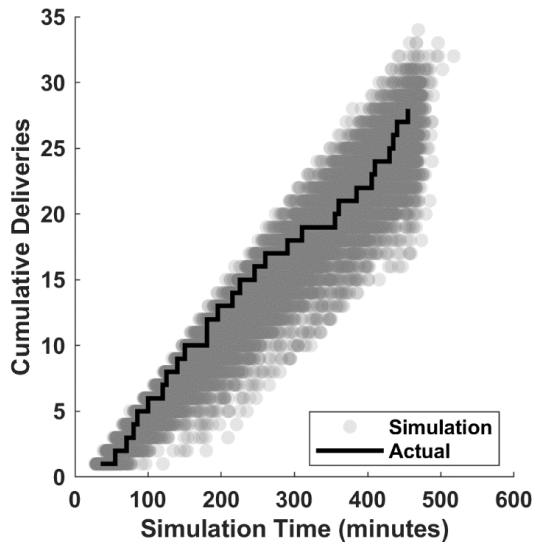
which includes the portion of the time the trucks served as temporary storage at the field edge. This operation had a lower flow time efficiency at 66.5%. This is indicative of the wait times for both fully loaded trucks and entities in partially loaded trucks. These wait times are not accounted for in WTF, which impacted less than 1% of entities, and which only accounts for full in-field transporters waiting for a truck. For this operation, there was never any wait time at the receiving pit because only a single driver was used, implying that only a single truck could be at the storage facility at any given time.

2.4.3.2 Example Performance

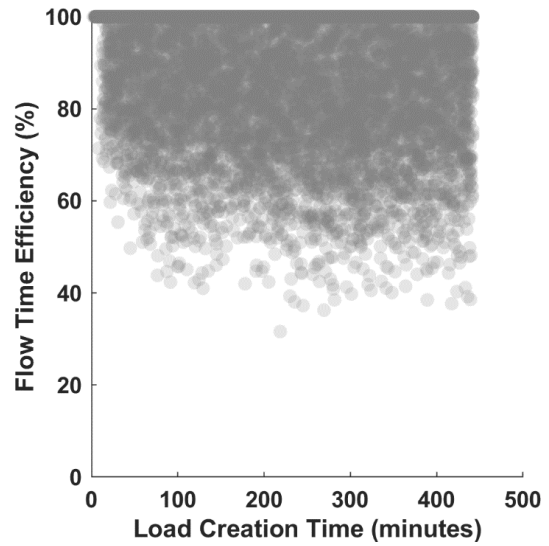
The following sections show example simulation output for three example harvest scenarios that were summarized in Table 2-4. The simulation output and performance metrics as determined by the simulation are shown for a single day for each harvest scenario. Figure 2-9, Figure 2-10, and Figure 2-11 show the output of 500 simulation runs for Operation 1 corn, Operation 1 wheat, and Operation 2 corn, respectively. These specific dates were chosen because they represent a variety of input conditions and simulation performance.

Figure 2-9 (a) shows the cumulative deliveries over the course of the day. The solid black line represents observed deliveries each semi-transparent gray circle represents a simulated delivery. Over the course of the day, the actual deliveries always fall within the range of simulation outputs, and the uneven spacing in the observed deliveries represents the variability in the system. For this example, the total time harvesting was 440 minutes. The total number of observed deliveries was 28, and the average simulation number of deliveries was 26.1, which represents an average of 6.8% underprediction of the total number of truckloads delivered. Figure 2-9 (b) shows the flow time efficiency for each full grain cart entity generated in the simulation. Points with 100% FTE represent entities that were delivered with no wait or delays between handling steps. The x-axis in this figure represents the time at which the entity enters the system, with zero corresponding to the start of the harvest on the day. Actual delivery time is not shown and could be outside of the time scale shown. Figure 2-9 (c) and (d) shows the respective average utilization of trucks and drivers over the course of the day. Semi-transparent gray circles in these figures represent resource utilization as determined by Simulink and represent an average utilization between system updates. The solid black

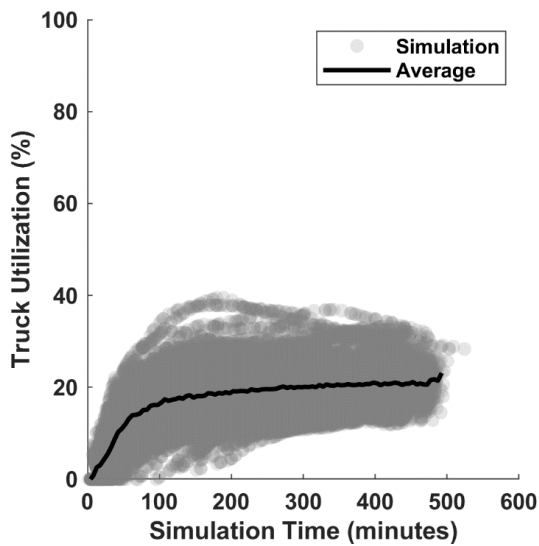
line shows utilization averaged across a five-minute window for all simulation runs. The utilization of trucks and drivers increases rapidly initially as material enters the system and then has a more gradual increase over the bulk of the day. The maximum utilization observed at any point occurs between 100 and 200 minutes. This most likely represents a simulation run where several entities were generated with small intergeneration times early in the simulation. This example utilized ten trucks and drivers, and average utilization never exceeded 40%. Truck utilization was always slightly higher than driver utilization because the simulation did not acquire a driver until the truck was full. For individual simulation runs, utilization decreases towards the end of the day as trucks and drivers complete their last run of the day, but the decrease was not dramatic because Simulink estimates utilization from the start of the simulation to each evaluation point.



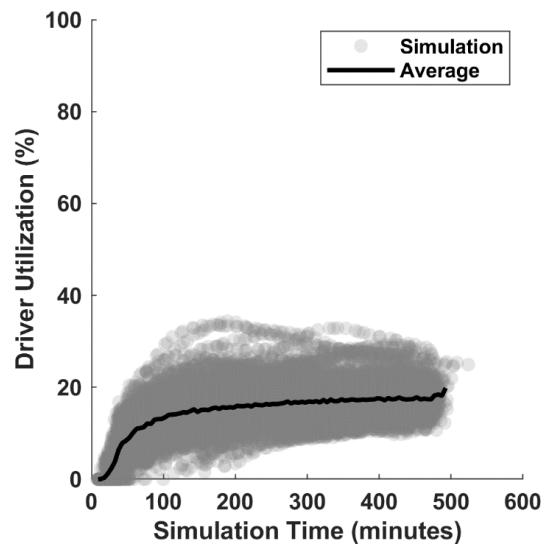
(a)



(b)



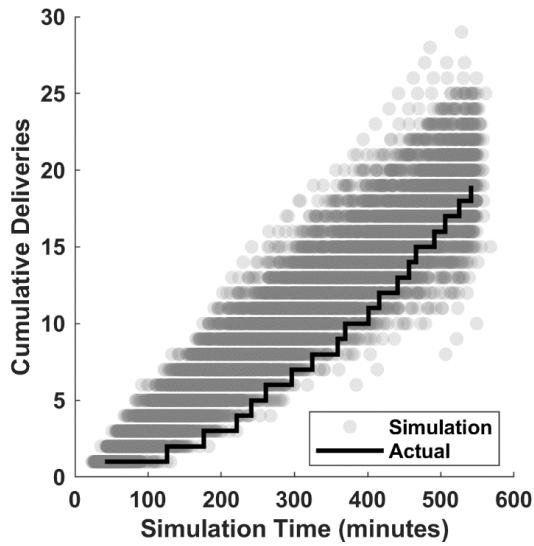
(c)



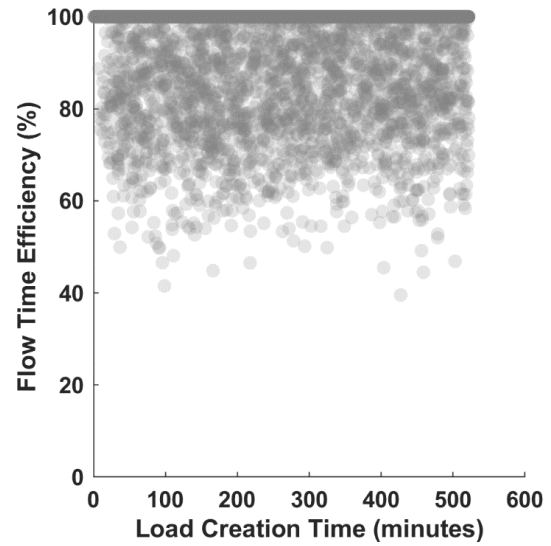
(d)

Figure 2-9: Example simulation output for all simulations ($n=500$) for a single day (08/27) for Operation 1 corn (Gray circles represent a single point, and darker areas represent a higher concentration of points). (a) Cumulative deliveries over the course of the day. Solid black line represents observed data. (b) Flow time efficiency, where 100% represents no delays between handling steps (average 89.9%). (c) Truck utilization. Black line represents average utilization across all simulation runs using a five-minute sampling window. (d) Driver utilization Black line represents average utilization across all simulation runs using a five-minute sampling window).

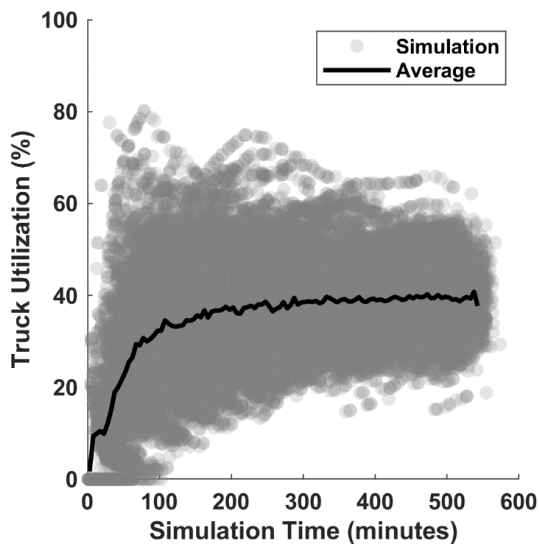
Figure 2-10 similarly shows results for Operation 1 in wheat. In this example, the observed deliveries tended to occur on the later end of the simulation output. This was primarily due to the long gap between the second and third arrival (Figure 2-10 (a)). However, simulation average total deliveries for the day was 19.3 truckloads, which was within 1.6% of the observed total. There were three trucks utilized in this example, and even with slightly higher utilization compared to Operation 1 corn, flow time efficiency still averaged 95% (Figure 2-10 (b)-(d)). This was primarily due to the proximity to the storage facility and lower material handling requirements for wheat.



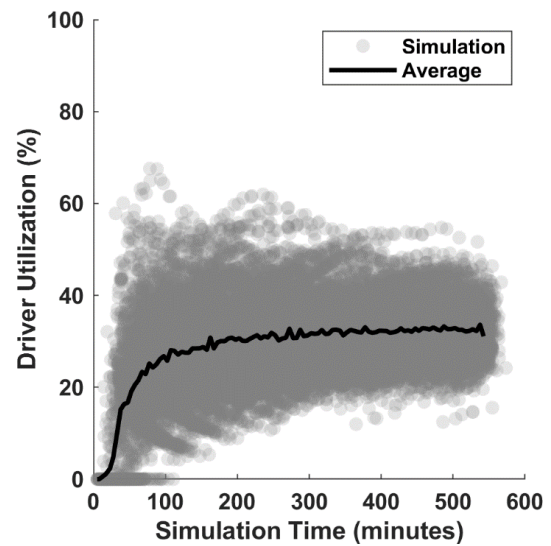
(a)



(b)



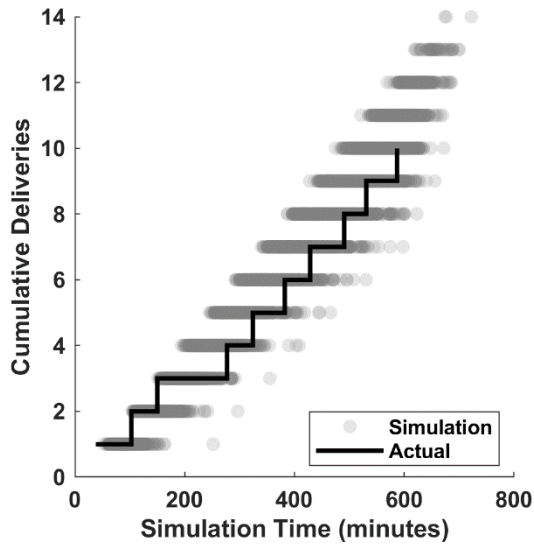
(c)



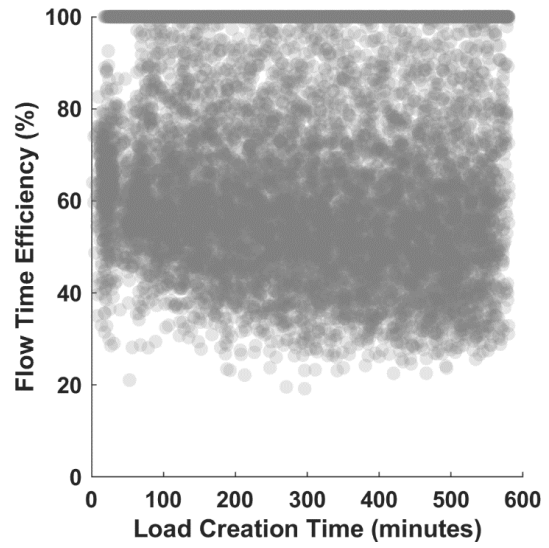
(d)

Figure 2-10: Example simulation output for all simulations ($n=500$) for a single day (06/09) for Operation 1 wheat (Gray circles represent a single point, and darker areas represent a higher concentration of points). (a) Cumulative deliveries over the course of the day. Black line represents observed data. (b) Flow time efficiency, where 100% represents no delays between handling steps (average 95.5%). (c) Truck utilization. Black line represents average utilization across all simulation runs using a five-minute sampling window. (d) Driver utilization. Black line represents average utilization across all simulation runs using a five-minute sampling window).

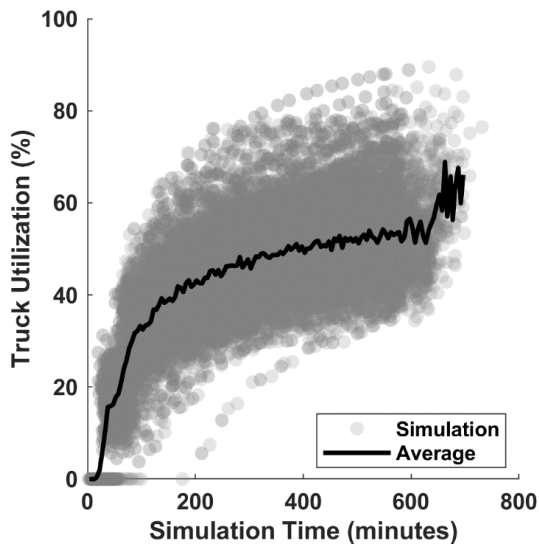
Figure 2-11 similarly shows the results for Operation 2. Over the course of the day, ten total truckloads were delivered, and the average after 500 simulations was 10.8 truckloads delivered. This operation was different from the previous examples in that two unloading events were required to fill a truck. The increased number of points in Figure 2-11 (b) that have Flow time efficiencies less than 100% visually represent the handling delays that resulted in this operation having an average flow time efficiency of 66.5%. Part of the lower FTE compared to Operation 1 is that multiple entities were required to fill a truck. The time required to harvest and load the second entity shows up as a delay in the transportation of the first. However, there is no major trend in FTE over the course of the day, indicating the system is adequately able to handle the transportation demand, at least over the given duration of harvest. Truck and driver utilization (Figure 2-11 (c)-(d)) are also quite different for this example because a single driver was responsible for three trucks. Truck utilization is higher in this example than in the other examples and includes not only productive time, but also accounts for a time when the trucks were fully or partially loaded waiting for a driver. The driver utilization quickly jumps to an average utilization of over 50% after sufficient time has passed for the first truck to be filled. Driver utilization continues to increase as time progresses, finally ending at an average utilization of over 80%.



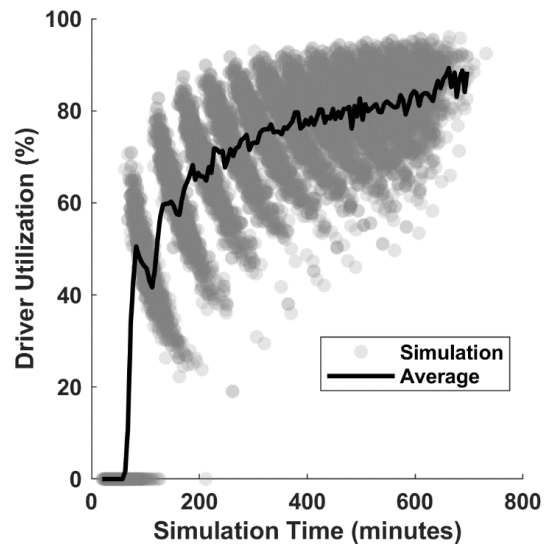
(a)



(b)



(c)



(d)

Figure 2-11: Example simulation output for all simulations ($n=500$) for a single day in Operation 2 (Gray circles represent a single point, and darker areas represent a higher concentration of points). (a) Cumulative deliveries over the course of the day. Black line represents observed data. (b) Flow time efficiency, where 100% represents no delays between handling steps (average 66.5%). (c) Truck utilization. Black line represents average utilization across all simulation runs using a five-minute sampling window. (d) Driver utilization. Black line represents average utilization across all simulation runs using a five-minute sampling window).

2.5 Conclusions

A DES model of grain transportation was developed to evaluate grain transportation capacity and aid in capacity planning. Field machinery characteristics were not explicitly modeled but were represented by a stochastic entity generation process, which represented the time required to harvest and transport a full load of grain to the field edge. The simulation accounted for dynamic system behavior by representing entity generation and service times as statistical distributions. The distributions presented here were determined from experimentally collected data and are specific to the operations and conditions encountered. The data needed to create these distributions is straight forward to collect, and any distributions could be used to evaluate other operations. Moreover, stochastic components could be incorporated into other model parameters, if they were of interest. For the scenarios examined, the model could satisfactorily represent the total number of deliveries to the storage facility. The model could represent operations with capacity matched between in-field and on-road transporters as well as operations with capacity for on-road transporters being integer multiples of in-field transporter capacity. Additionally, a single distribution was found to adequately represent harvest rate and in-field machinery interactions over the range of input conditions encountered.

The simulation output was used to evaluate the example system performance for the 18 given input conditions. FTE was very high for operation 1 in both crops, indicating there were few delays between handling steps and transportation capacity was sufficient. The relatively low utilization of trucks and drivers for Operation 1 indicate that the operation could be over-equipped. Operation 2 had lower FTE due to multiple entities being required to fill a truck. For this operation truck, and especially driver utilization, were relatively high, and there was no noticeable trend of decreased FTE over the course of the day, indicating the resources are adequately matched to the harvest rate. This model could be used to evaluate how changing resource quantities would impact utilization, throughput, and FTE, however assessing the overall implications of these changes would require discretion. Operation characteristics including if trucks are used as supplemental wet storage, resource availability, and how the transportation costs are structured (trucks owned vs. leased, contracted by load vs. hourly employee, etc.) all

affect the best decision. Further refinement could include the incorporation of drying and storage considerations as well as economic considerations.

2.6 References

- Allen, T. T. (2011). *Introduction to discrete event simulation and agent-based modeling: voting systems, health care, military, and manufacturing*. London, United Kingdom: Springer Science & Business Media.
- Amiama, C., Pereira, J. M., Castro, A., & Bueno, J. (2015). Modelling corn silage harvest logistics for a cost optimization approach. *Computers and Electronics in Agriculture*, 118, 56-65. doi:<http://dx.doi.org/10.1016/j.compag.2015.08.024>
- ASABE Standards (2000). D497.4 Agricultural Machinery Management Data. St. Joseph, MI: ASABE.
- Benock, G., Loewer Jr, O., Bridges, T., & Loewer, D. (1981). Grain flow restrictions in harvesting-delivery-drying systems. *Trans ASAE*, 24(5), 1151-1161.
- Benson, E. R., Hansen, A. C., Reid, J. F., Warman, B. L., & Brand, M. A. (2002). *Development of an in-field grain handling simulation in ARENA. ASABE Paper No. 023104*. ASAE, St. Joseph, MI.
- Berruto, R., & Maier, D. E. (2001). Analyzing the receiving operation of different grain types in a single-pit country elevator. *Trans. ASAE*, 44(3), 631-638.
- Buckmaster, D. R., & Hilton, J. W. (2005). Computerized cycle analysis of harvest, transport, and unload systems. *Computers and Electronics in Agriculture*, 47(2), 137-147.
- Busato, P., Berruto, R., & Saunders, C. (2007). Optimal field-bin locations and harvest patterns to improve the combine field capacity: study with a dynamic simulation model. *Agricultural Engineering International: CIGR Journal*, IX.
- De Toro, A., & Hansson, P. A. (2004). Analysis of field machinery performance based on daily soil workability status using discrete event simulation or on average workday probability. *Agricultural Systems*, 79(1), 109-129. doi:10.1016/s0308-521x(03)00073-8

- Dudenhoeffer, N. E., Luck, B. D., Digman, M. F., & Drewry, J. L. (2017). Simulation of the forage harvest cycle for asset allocation. *Applied Engineering in Agriculture*, 34(2), 327-334.
- Edwards, W., Plastina, A., & Johanns, A. (2016). Grain Harvesting Equipment and Labor in Iowa. *Ag Decision Maker*, 2017.
- Harmon, J. D., Luck, B. D., Shinnars, K. J., Anex, R. P., & Drewry, J. L. (2017). Time-motion analysis of forage harvest: A case study. *Trans ASABE*, 61(2), 483-491.
- Harrigan, T. (2003). Time-motion analysis of corn silage harvest systems. *Applied Engineering in Agriculture*, 19(4), 389-396.
- Loewer, O., Kocher, M., & Solaimanian, J. (1990). An expert system for determining bottlenecks in on-farm grain processing systems. *Applied Engineering in Agriculture*, 6(1), 69-72.
- Loewer, O. J., Benock, G., & Bridges, T. C. (1980). Effect of combine selection and harvesting rate on grain drying and delivery system performance. *Transactions of the ASAE*, 23(6), 1548-1553.
- Loewer, O. J., Bridges, T. C., & Bucklin, R. A. (1994). *On-farm drying and storage systems*. St. Joseph, MI: ASABE.
- Rotz, C. A., Muhtar, H. A., & Black, J. R. (1983). A multiple crop machinery selection algorithm. *Transactions of the Asae*, 26(6), 1644-1649.
- Rubinstein, R. Y., & Kroese, D. P. (2016). *Simulation and the Monte Carlo method* (3 ed. Vol. 10). Hoboken, NJ: John Wiley & Sons.
- Silva, L. C., Queiroz, D. M., Flores, R. A., & Melo, E. C. (2012). A simulation toolset for modeling grain storage facilities. *Journal of Stored Products Research*, 48, 30-36. doi:<https://doi.org/10.1016/j.jspr.2011.09.001>
- Søgaard, H. T., & Sørensen, C. G. (2004). A model for optimal selection of machinery sizes within the farm machinery system. *Biosystems Engineering*, 89(1), 13-28.
- Sørensen, C. G., & Bochtis, D. D. (2010). Conceptual model of fleet management in agriculture. *Biosystems Engineering*, 105(1), 41-50.
- Spedding, T. A., & Sun, G. Q. (1999). Application of discrete event simulation to the activity based costing of manufacturing systems. *International Journal of*

Production Economics, 58(3), 289-301. doi:[https://doi.org/10.1016/S0925-5273\(98\)00204-7](https://doi.org/10.1016/S0925-5273(98)00204-7)

Tako, A. A., & Robinson, S. (2012). The application of discrete event simulation and system dynamics in the logistics and supply chain context. *Decision Support Systems*, 52(4), 802-815. doi:<https://doi.org/10.1016/j.dss.2011.11.015>

Chapter 3. VARIABILITY IN CORN HARVEST LOSSES IN KENTUCKY

3.1 Summary

This study presents a single year evaluation of corn harvest losses in Kentucky. To evaluate typical harvest losses, losses were measured for four cooperating producers' combines operating under normal conditions and total losses were found to be between 0.8% to 2.4% of total yield (86 to 222 dry kg ha⁻¹). On average, the combine head accounted for 66% of the measured losses, and the total losses were highly variable, with coefficients of variation ranging from 21.7% to 77.2%. Yield and harvest losses were also monitored in a single field at four points over the course of the 2017 harvest season to assess loss changes with respect to time and moisture. Measurement points were selected to cover a wide range of grain moisture contents (33.9%, 26.4%, 19.8%, and 14.6% w.b.) representing high moisture corn, the upper limit for drying, normal drying, and corn field dried to nominally 15%. There was no significant difference in the potential yield at any moisture level, and the observed yield and losses displayed little variation for moisture levels from 33.9% to 19.8%, with total losses less than 1% (82 to 130 dry kg ha⁻¹). Large amounts of lodging occurred when the grain was allowed to field dry to 14.6%, which resulted in an 18.9% reduction in yield and measured harvest losses in excess of 9%. Allowing the grain to field dry generally improved test weight and reduced mechanical damage, however, there was a trend of increased mold and other damage in prolonged field drying.

3.2 Introduction

3.2.1 *Machine Losses*

Grain yield losses can be broken down into two primary components, machine and preharvest losses. Machine losses are associated with the combine physically gathering and processing the crop. The lost crop represents revenue that was left in the field and is a concern to producers because these losses can be minimized through proper combine adjustment. They occur at the head as the crop is gathered into the machine, during threshing, and when separating grain from the material other than grain (MOG). Losses at the head are often the largest component of the overall machine loss and occur

when whole ears fail to make it into the machine (gathering loss) and when kernels are dislodged from the ears by the deck plates or snapping rolls (butt shelling). Losses due to dropped ears are often associated with crop condition, travel speed, and uneven feeding, and can be exacerbated by lodging. Cylinder or rotor losses are associated with incomplete shelling and machine settings (rotor speed, concave clearance, etc.), and the machine settings should be adjusted to minimize both losses and damage that can result from threshing too aggressively. Separation and cleaning loss are composed of loose kernels that fail to separate from the MOG and are carried out the back of the combine with the MOG. Proper machine settings and operation help minimize all of these losses, and several extension sources provide producers with guidelines to adjust settings based on observed losses (Hanna, 2008; Huitink, 2001; McNeill & Montross, 2007; Sumner & Williams, 2009).

A large portion of the literature for machine losses comes from university-affiliated cooperative extension service sources, though there are a few peer-reviewed sources. Johnson, Lamp, Henry, and Hall (1963) presented a four-year study of changes in yield and quality as a function of harvest moisture. The authors found a range of snapping roll losses from 1.8% to 3.0% of total yield, cylinder losses less than 2%, and separation losses were less than 5%, with higher losses being associated with non-combine shellers. Ayres, Babcock, and Hull (1972) performed a survey of harvest losses from 84 combines in Iowa. They found an average loss of 232 kg ha⁻¹ (3.7 bu ac⁻¹), but a range of 31.4 to 1444 kg ha⁻¹ (0.5 to 23.0 bu ac⁻¹). Surprisingly, 48% of the combines had losses greater than 188 kg ha⁻¹ (3 bu ac⁻¹), while only 7% had losses less than 63 kg ha⁻¹ (1 bu ac⁻¹). Another study, by Hanna, Kohl, and Haden (2002), evaluated visible machine loss for conventional (76 cm) and narrow (38 cm) corn row spacing and found losses were similar for row spacings when the corn head was set to match. The authors found 90% of losses occurred at the head, with kernel loss at the head representing 1% of the total yield. Most recently, Paulsen et al. (2014) performed a more recent study specifically to determine a representative range of harvest losses for corn and soybeans in Brazil. They found that machine losses ranged from 1.2% to 5.5% of gross yield in soybeans, and 0.3% to 3.6% for corn.

3.2.2 Losses Associated with Harvest Timing

As grain dries in the field, energy costs associated with drying decrease, but there is an increased risk of lodging, reduction in yield, and quality degradation (Licht, Hurburgh, Kots, Blake, & Hanna, 2017). Preharvest losses are associated with a reduction in yield that results from allowing the grain to field dry. Visible preharvest losses are easily measured and observed based on ears that detach from the plant prior to harvesting. The potential for an additional drop in yield (referred to as invisible or phantom loss) is more difficult to quantify. A number of explanations for this loss have been proposed in the literature, including: changes in dry matter, predation, and incomplete shelling (broken kernel tips remaining on the cob) (Johnson et al., 1963; Nielsen, Brown, Wuethrich, & Halter, 1996; Sumner & Williams, 2009). These losses represent grain that never had the chance to make it into the combine and are a factor producers must consider when making management decisions regarding harvest timing.

Yield loss and dry matter changes as the crop field dries have been explored in several works with mixed results. Kernel dry matter losses have been estimated at approximately 1% per point of moisture when the crop was allowed to dry in the field (Nielsen et al., 1996). This was in contrast to Elmore and Roeth (1999), who evaluated corn yield as a function of harvest moisture using a combination of greenhouse experiments and field plots. The authors found no evidence of kernel dry matter losses following physiological maturity, after accounting for harvest losses. Thomison, Mullen, Lipps, Doerge, and Geyer (2011) also studied the effect of harvest date on yield loss in Ohio and found yield losses associated with delayed harvest did not exist until harvest was extended past November. Marley and Ayres (1972) studied the effect of planting and harvest date in Iowa and found no difference between date and total field losses. However, the harvest date did significantly impact yield. Johnson et al. (1963) found no significant differences in yield due to moisture for handpicked ears, but there was a significant correlation between moisture and machine yield.

Research efforts at modeling grain harvesting systems need to account for harvest timing, dry down, and yield losses with time. ASABE Standards (2015a) recommends a timeliness factor of 0.003% per day past the optimum day for shelled corn. This is a linear decrease based on the number of calendar days past the optimum crop value per

unit area. Many previous works, (Holtman, Pickett, Armstrong, & Connor, 1973; Loewer et al., 1994; Loewer, Bridges, White, & Overhults, 1980; Loewer, Bridges, White, & Razor, 1984; Morey, Zachariah, & Peart, 1971) utilized loss data cited from Johnson and Lamp (1966), which grew to 0.85% per day once grain field dried to 18%. However, this data does not reflect the capabilities of modern equipment and hybrids, which furthers the point that these values need to be updated (Loewer et al., 1984).

Other efforts have focused on losses for small grains. Klinner and Biggar (1972) measured field and header loss for wheat and barley for six dates over 5 weeks and found barley losses of 1% for every 5.5 days past ripeness. Wheat losses were not measurable until the final harvest date, but the grain was at high moisture for the entirety of the study. A two-part study of cereal harvest models (McGechan (1985a) and McGechan (1985b)) compared threshing losses and front-end loss studies as a function of days past ripeness. The goal of this study was to determine the optimum size and forward speed of the combine. They found variations in source data produced very different responses, but the influence of straw yield and combine capacity on the cost equations outweighed the variations in losses.

3.2.3 Motivation

The overall goal of this study was to evaluate yield and machine losses typically encountered during corn harvest in Kentucky. Paulsen et al. (2014) contend that because the combine operator adjusts the settings, a good operator who pays attention to losses can be worth the premium. By extension, it is also of interest to establish the range of losses that are typically encountered in a variety of geographies and operation types. Toward that end, preharvest and machine losses were evaluated for several producers to establish a range of losses typically encountered in Kentucky for current equipment and hybrids.

The second aspect of this study was to evaluate how losses and yield changed over the course of the harvest season. This relationship is of interest for researchers and producers who seek to balance the potential losses associated with field drying against fuel costs to dry wet grain. Generally, previous investigations in this area are dated or were conducted in field plots and may not be representative of current field scale

operations. A single field, at a university research farm, was harvested at multiple points as grain dried in the field to evaluate the impact of delayed harvest on yield, machine losses, and grain quality.

3.3 Materials and Methods

3.3.1 Measurement Locations:

Machine and preharvest losses were measured for four combines utilized by three producers during the 2017 corn harvest season. The producers were from across the state (Logan, Hardin, and Madison counties), and utilized a diverse set of combines (Table 3-1). This evaluation was used to determine the magnitude and variability of losses encountered in typical conditions. Three measurements were made per site, and were taken at random locations in the same field. An additional measurement site, at University of Kentucky's C. Oran Little Research Center in Versailles, KY., was measured multiple times over the course of the harvest season to evaluate how losses changed as the crop field dried. All combine settings and forward speed were determined by the operators, all of whom were experienced.

Table 3-1: Overview of Measurement Locations and Equipment*

County*	Date	Make-Model	Head Width (m)	# of Rows	Row Spacing (cm)	Speed (km h⁻¹)	Moisture Content (% w.b.)	Test Weight (kg m⁻³)
Woodford**	9/20 -12/01	CLAAS-730	4.57	6	76	5.6-6.4	33.9-14.6	681-752
Hardin	9/17	JD -*	9.14	12	76	4.6	23.4	657
Logan 1	9/27	CNH-8240	9.14	12	76	6.4	17.8	760
Logan 2	9/27	CNH-8240	9.14	12	76	6.4	17.9	764
Madison	10/4	Case IH-1666	3.66	4	91	5.2	13.3	739

* Logan County locations were white corn, all others were normal field corn

* *Combine utilized in the delayed harvest experiment

***Combine model number unknown

3.3.2 *Field Procedure*

Harvest losses were evaluated following a procedure similar to (Paulsen et al., 2014). Each loss component was measured as outlined in Figure 3-1. During each measurement, the combine was operating under normal conditions before abruptly stopping. After the combine was cleaned out, it was reversed 2-3 m to allow access to the head kernel loss area. Measurements were taken by staking out the requisite area across the full width of the head, which resulted in a variable length and width based on the size of the corn head on the combine being investigated. Teams of two to three people examined the sample area, which often required residue be removed from the area to ensure all the grain was collected (Figure 3-2). All loss components were evaluated on a dry matter (dm) basis, and the material collected from each sampling area was labeled and bagged separately before being transported to the lab for further analysis. Grain moisture content, test weight, damage, and BCFM (broken corn and foreign material) were estimated from grab samples of approximately 1 kg that were collected from the combine's clean grain sample door for each measurement. These samples were sealed in large plastic freezer bags and were placed in cold storage at approximately 4°C until processing.

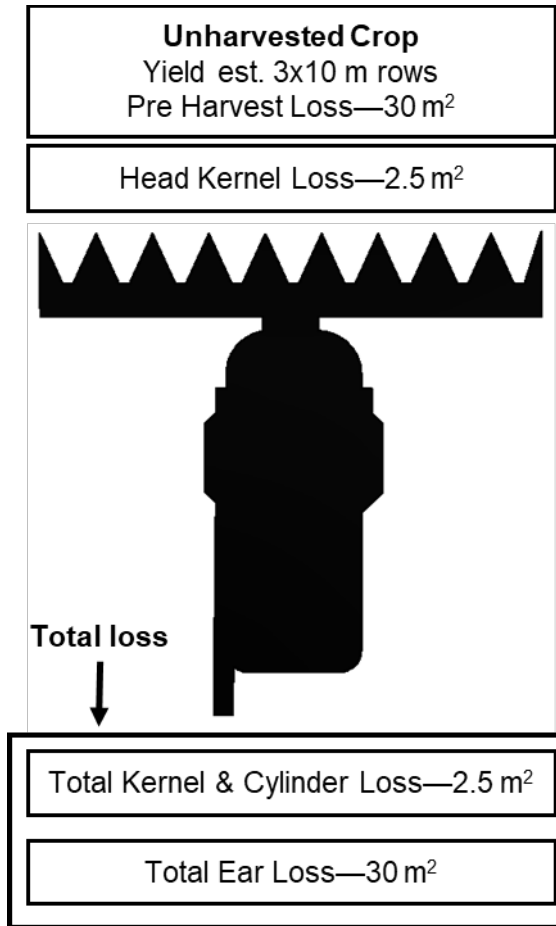


Figure 3-1: Overview of loss component measurement locations



Figure 3-2: Example staked out area to collect loose kernels. Photo was taken after the residue was removed and before kernels were collected

The unharvested crop in front of the combine was used to evaluate preharvest losses and to estimate the crop yield. Preharvest losses were evaluated by collecting downed ears in a 30 m² area of unharvested crop. The yield was estimated based on the plant population (ears ha⁻¹) and average yield per ear (kg dm ear⁻¹). The plant population was determined from the row spacing and number of ears in a 10-m row length. When counting ears, every 10th ear was collected for dry matter determination. The procedure was repeated for three rows, and the yield was estimated using the average per ear dry matter content for all three rows.

Head kernel loss represents kernels that were dislodged from the cob by the corn head and were evaluated by collecting loose kernels in a 2.5 m² area in front of the combine where the corn head had passed, but the combine had not fully traversed to avoid having cleaning losses from the combine. The total kernel loss was estimated by collecting loose kernels in a 2.5 m² area behind the combine, and this measurement consisted of a combination of kernel losses due to the head and machine losses. This area was selected sufficiently behind the combine, so it was not impacted by the residue that was discharged as the combine cleared out after stopping. Partially shelled ears found in this 2.5 m² area represent cylinder/rotor losses and were collected separately. Whole ears were collected in a 30 m² area behind the combine and represented a combination of preharvest loss and ear loss from the header. Ears attached to lodged stalks were not counted as preharvest loss. However, if the ears were still attached to the stalk after the header passed, it was considered being lost by the head.

The total loss was estimated using the two measurement locations behind the combine using equation (3-1). The other measurements, shown in Figure 3-1, were used to estimate how much various components contributed to the total loss. Losses that occurred at the head due to ears not being gathered into the combine were separated from preharvest losses using equation (3-2), and the total loss at the head was estimated by added head kernel loss measurement (equation (3-3)). Separation and cleaning losses were estimated by subtracting the head kernel loss from the total kernel loss (equation (3-4)). Finally, the total machine loss was estimated by subtracting preharvest losses from the total loss (equation (3-5)).

$$\text{Total loss} = \text{Total kernel loss} + \text{Total ear loss} + \text{Cylinder loss} \quad (3-1)$$

Where:

Total loss = Combination of preharvest and machine losses (kg ha⁻¹)

Total kernel loss = Total loss associated with loose kernels, as measured behind the combine, includes head, cleaning, and separation loss (kg ha⁻¹)

Cylinder loss = Loss due to partially shelled ears (kg ha⁻¹)

$$\text{Head ear loss} = \text{Total ear loss} - \text{Preharvest loss} \quad (3-2)$$

Where:

Head ear loss = Losses that occur at the combine head due to dropped ears (kg ha⁻¹)

Total ear loss = Total ear loss as measured behind the combine, includes head and preharvest loss (kg ha⁻¹)

Preharvest loss = Losses associated with dropped ears collected from an area of unharvest crop (kg ha⁻¹)

$$\text{Head loss} = \text{Head kernel loss} + \text{Head ear loss} \quad (3-3)$$

Where:

Head loss = Combination of missed ears and loose kernels due to the combine head (kg ha⁻¹)

Head kernel loss = Loose kernels collected in front of the combine (kg ha⁻¹)

$$\text{Separation loss} = \text{Total kernel loss} - \text{head kernel loss} \quad (3-4)$$

Where:

Separation loss = Loss associated with separating grain from the MOG (kg ha⁻¹)

$$\text{Machine loss} = \text{Total loss} - \text{Preharvest loss} \quad (3-5)$$

Where:

Machine loss = total mechanical loss due to gathering, shelling and cleaning the grain, excludes preharvest losses (kg ha⁻¹)

3.3.3 Tracking Yield Changes with Time

Recoverable yield and machine losses varied as grain dried in the field, losses were measured at four points over the course of the 2017 corn harvest season. The experiments were conducted in a single field at the University of Kentucky research farm in Versailles, KY. The field was planted in 76 cm rows with Becks 6225HR on 05/18/2017, and a CLAAS Lexion 730 combine with a 6-row Lexion corn head (CLAAS of America, Omaha, NE) was utilized to harvest the grain. The field was divided into four blocks with enough rows in each block for four replications per measurement date. On each measurement date a single pass was taken from each block, resulting in four measurements for each date/moisture level. The block sampling order and the section harvested from each block was chosen randomly (Figure 3-3). The study was conducted over 72 days, and moisture levels evaluated ranged from approximately 34% to 14.6%.

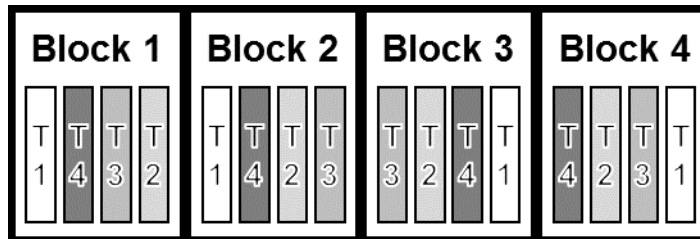


Figure 3-3: Plot sampling layout. Each block was sampled once per measurement date. The order each section of the blocks was harvested is separated by shade.

Loss measurements followed the same protocol as previously described, but in addition to the yield estimate made by hand picking ears, the actual recovered yield was measured for each pass through the field. After each pass was harvested, the grain was transferred to a truck and was weighed using truck scales with a 9 kg resolution. The length of each pass through the field was similar across the field and was determined using a gauge wheel (Rolatape 300, Rolatape Corporation, Watseka, IL). Each pass was approximately 230 m long and contained approximately 1,300 kg dm of shelled corn. Combine settings were adjusted by the operator in an adjacent field prior to harvesting the test field. The actual loss measurement locations were selected at random but were sufficiently far from the beginning of the row to allow the combine to reach steady-state operation.

3.3.4 Laboratory Procedure

All collected loss samples were dried at 103°C for 72 hours for dry matter determination (ASABE Standards, 2012). Whole ears that were collected in the field were hand shelled after partial drying, and then returned to the oven for complete drying. All weights were determined using an Ohaus Precision Advanced lab scale (Ohaus Corporation, Parsippany, NJ).

The grab samples of clean grain collected from the combine were used to estimate several quality parameters. Moisture content, test weight, and BCFM were determined for each measurement at both the Woodford County and cooperator sites (n=4 at Woodford County, otherwise n=3). The moisture content of the grain at the time of harvest was estimated by drying approximately 100 to 150 g samples, and the test weight of each sample was measured in triplicate using the Winchester test cup (USDA, 2013b). Test weight was measured at the incoming harvest moisture for all samples.

All clean grain samples were subjected to drying with unheated forced air in an environmental chamber with constant ambient conditions of 15.6 °C and 70% relative humidity. These ambient conditions were chosen to provide an equilibrium moisture content of approximately 15%. Drying was conducted using PVC aeration tubes, and the samples were subject to drying air at approximately 89.2 cmm m⁻³ (111 cfm bu⁻¹) for 72 hours, which previous tests determined was sufficient to reach equilibrium. Test weight was measured again after drying for the Woodford County samples, which allowed for better comparison of test weight between harvest dates.

BCFM was estimated for each sample using the hand sieving method as outlined in (USDA, 2013a). When required, a sample divider was utilized to separate approximately 1,000 g from the grab samples, and the percentage of BCFM was determined based on the weight of material passing through a 4.76 mm (12/64 inch) sieve. The sample divider was again used to separate an approximately 250 g sample to evaluate damage. The percentage (by mass) of damaged kernels was determined by visual inspection (USDA, 2013a). Though not an explicit grade factor, the samples were also evaluated for mechanical damage from the combine. This was done through visual inspection of the kernels on a light table (without green dye. See Chowdhury and Buchele (1976) for more information on the dye method) to better highlight any damage. For this

study, physical damage was defined as any observable damage to the seed coating, which included both chips and stress cracks. Although this is not an official standard, it was done in an attempt to capture differences in damage due to shelling at different moistures.

3.4 Results and Discussion

3.4.1 *Cooperator Locations*

Table 3-2 shows an overview of the loss measurements from all locations. Cooperator combines were measured over a range of moistures from 23.4% to 13.3%, and yield varied from 9.3 to 12.3 t ha⁻¹. All mass values in this paper are reported on a zero-moisture basis. The total losses were estimated from the total ear loss, total kernel loss, and cylinder loss measurements. Total losses ranged from 86 to 222 kg ha⁻¹, which was equivalent to 0.5% to 2.4% of the potential yield. This was consistent with Paulsen et al. (2014), who found a range of losses from 0.3% to 3.6% of total yield and Hanna et al. (2002), who found total losses over three years averaged 1.7% and 2.6% for 76-cm and 38-cm row spacing, respectively. There was a large amount of variability between measurements as manifested by the large coefficients of variation associated with the total loss estimate, which was up to 77.2%. Total kernel losses (combination of head kernel loss and separation/cleaning loss) was the largest contributing factor, and represented, on average, 62% of the total loss. Total ear and cylinder losses were highly variable, as shown by their large standard deviations, which often exceeded the mean. This resulted from the small magnitude of the losses and variability between measurement locations (e.g., the number of loose kernels found in front of the combine versus behind), and was consistent with what was observed by Hanna et al. (2002).

Table 3-2: Summary of Cooperator Combine Measurements ***

County	BCFM (%)	Yield** (t ha ⁻¹)	Total Ear (kg ha ⁻¹)	Total Kernel (kg ha ⁻¹)	Cylinder (kg ha ⁻¹)	Total Loss (kg ha ⁻¹)	CV* (%)
Hardin	0.57	10.6	10 ±17	76±8	0±0	86±19	21.7
Logan 1	0.19	12.1	65±113	72±42	22±27	160±123	77.2
Logan 2	0.15	12.3	60±82	131±20	7±15	198±85	43.0
Madison	0.52	9.3	33±38	110±3	79±133	222±138	62.3

*CV= coefficient of variation in total loss measurement

**Estimated from hand counting ears

***All yield and losses are expressed in terms of dry matter. Mean values shown, ± one standard deviation where applicable.

Figure 3-4 shows the components of the total loss for each cooperator combine that was evaluated. Negative loss components resulted from variability between measurement locations and the way components were estimated. For example, on a given replication if more kernels were found in the head kernel measurement area than in the total kernel measurement area, the separation and cleaning loss would appear negative. No preharvest losses were observed at any cooperating producer locations, which could be a result of the favorable conditions during harvest, or because measurements were taken during the peak of harvest and did not include late season harvest. On average, 66.9% of losses occurred at the head, which was slightly lower than Paulsen et al. (2014), and a good deal less than the 90% observed by (Hanna et al., 2002). The combine operating in Madison County was the oldest combine evaluated and was operating in the lowest moisture and yielding corn. This combine had the highest losses of any of the cooperator combines, which was a result of the distinctly higher cylinder and head kernel losses.

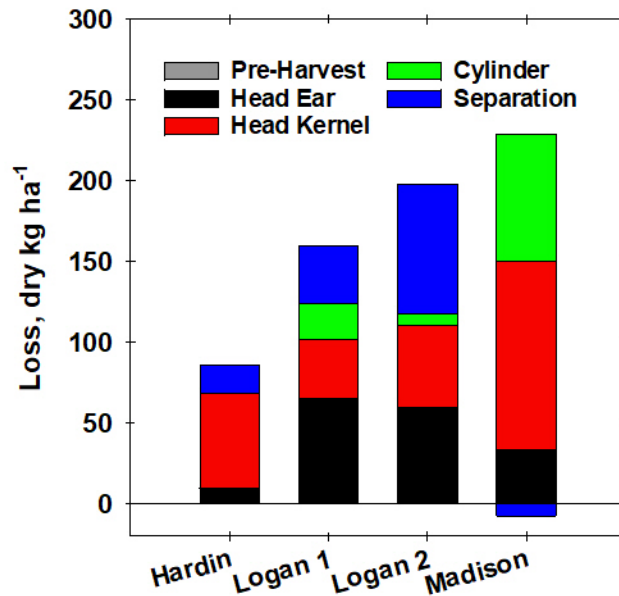


Figure 3-4: Approximate breakdown of loss components at cooperator other measurement locations. Average values are shown, and separation loss represents a combination of separation and cleaning loss.

3.4.2 Woodford County Location

Figure 3-5 shows the change in yield as the grain field dried at the Woodford County site. The observed yield represented the amount of grain that was recovered by the combine, and the potential yield represented the yield estimated by picking and drying ears. This would represent the upper bounds on yield if there were no mechanical harvest losses. There were no significant differences between the two yield estimates or between yields at different moisture levels for the first three observations. The initial moisture content of the grain harvested on September 20th was 33.9% (all moisture contents are expressed on a wet basis) and was above the typical upper limit for corn harvest. The moisture content observed on the subsequent two observations averaged 24.6% and 19.8%, respectively. This moisture range is representative of the typical harvest conditions. There was no significant change in potential yield as the field drying occurred, and there was no significant difference between the observed and potential

yield for the first three observations. Across the first three measurement dates, the average for both the observed and potential yield was 13.3 t ha⁻¹.

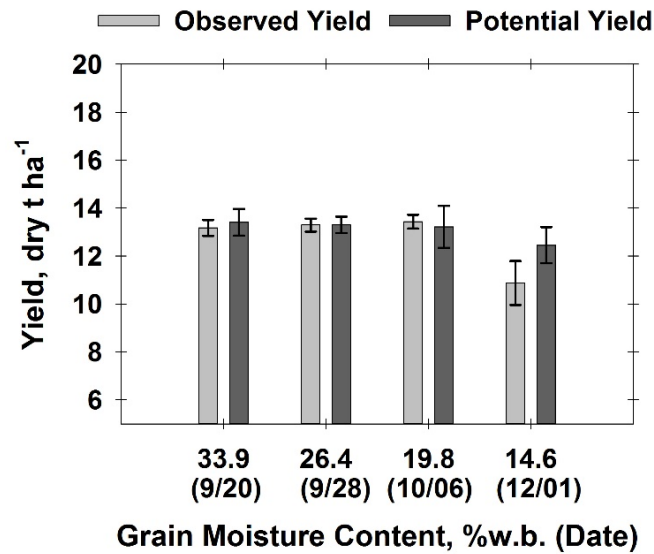


Figure 3-5: Change in yield as grain was allowed to dry in the field. Observed yield represents the actual grain harvested by the combine. Potential yield was estimated by hand picking ears. Error bars represent \pm one standard deviation and was based on four replications.

Fifty-six days passed between the 19.8% and 14.6% moisture level observations. This was a result of a prolonged stretch of rain and unfavorable field conditions, and when the field was once again suitable for harvesting, a large majority of the stalks were lodged to some degree (Figure 3-6). This also resulted in increased variability and a decrease yield. Table 3-3 shows the breakdown of the losses at the 14.6% moisture level. Observed yield showed a statistically significant drop to 10.9 t ha⁻¹, from 13.3 t ha⁻¹, which represented an 18.9% yield decrease when compared to the maximum potential yield observed on 9/20. Over the same period, the potential yield decreased by 7.1% (not significant), which accounted for 37.6% of the total loss. Visible or measured losses increased from less than 1% of the potential yield for the first three measurement dates to over 9.1% of the potential yield on the final measurement (Table 3-4). This was equivalent to 8.5% of the maximum potential yield (measured on 9/20) and accounted for 44.9% of the total loss measured on 12/01. Another 3.3% of the total yield was lost to unknown sources and could be attributed to variations in the field or to the increased

variability in losses that were observed on 12/01. This is consistent with Thomison et al. (2011) who found yield loss associated with field drying was only apparent if harvest extended past November in Ohio.



Figure 3-6: Lodged and wind damaged corn observed during 12/01 loss measurement.

Table 3-3: Yield Loss Breakdown for the Measurements Taken at the 14.6% Moisture Level (12/01)

Component	Loss Component (kg ha⁻¹)	Percent of Maximum Yield*(%)	Fraction of Total Loss (%)
Potential yield loss	954	7.1	37.6
Measured losses	1138	8.5	44.9
Unknown	442	3.3	17.5
Observed yield loss	2534	18.9	100.0

*Maximum yield was taken as the highest potential yield, which was observed on 09/20

Table 3-4: Summary Measurements at Woodford County Location ***

Date	Speed (km h⁻¹)	BCFM (%)	Yield** (t ha⁻¹)	Total Ear (kg ha⁻¹)	Total Kernel (kg ha⁻¹)	Cylinder (kg ha⁻¹)	Total Loss (kg ha⁻¹)	CV* (%)	Percent of Yield (%)
9/20	6.4	0.96	13.4	93±61	24±8	3±5	119±62	52	0.9
9/28	5.6	0.26	13.3	107±139	24±6	0±0	130±139	107	1.0
10/6	6.1	0.14	13.2	35±48	47±8	0±0	82±49	59	0.6
12/1	-	0.62	12.5	930±416	208±93	0±0	1138±426	37	9.1

*CV= coefficient of variation in total loss measurement

**Estimated from hand counting ears

*** Woodford county was the location used to track losses as the grain field dried. All yield and losses are expressed in terms of dry matter. Mean values shown, ± one standard deviation where applicable

Total losses averaged between 82 and 130 kg ha⁻¹ between the 33.9% and 19.8% moisture level (Table 3-4). This resulted in total losses between 0.6% and 1.0% of the total yield, which was better than average when compared to the cooperator combines. For these measurements, ear loss comprised the majority of the losses and was the most variable component. For these observations, the coefficient of variation in total loss ranged from 37% to 107%. The observation on 9/28 had a coefficient of variation of 107%, which was largely influenced by the total ear loss and varied from 0 to 292 kg ha⁻¹. Figure 3-7 shows a further breakdown of the loss components that were measured as the grain dried in the field. Minimal cylinder losses were found on any date, and preharvest losses did not appear to have a trend with delayed harvest. The maximum preharvest loss occurred on 9/28, where it represented 93% of the total loss. The large fraction of losses associated with head ear loss observed on 12/01 was a result of ears that were missed because the crop was lodged. This was consistent with Paulsen et al. (2014), who concluded lodged corn increased loss more than any other factor.

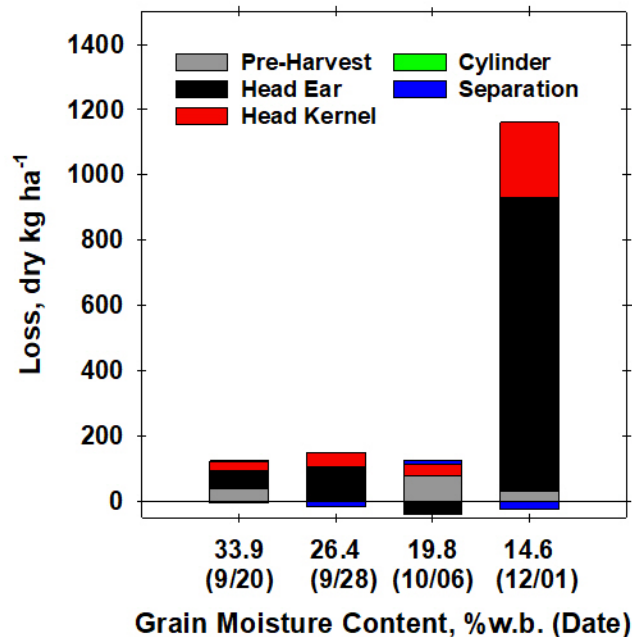


Figure 3-7: Approximate breakdown of loss components as the grain field dried at the Woodford County location. Average values are shown, and separation loss represents a combination of separation and cleaning loss.

3.4.3 *Quality Changes*

Figure 3-8 shows the changes in both mechanical and mold/other damage as the grain dried in the field. Mechanical damage was initially very high and generally decreased with decreasing moisture. There was no significant difference in mechanical damage between the 26.4% and 19.8% moisture levels, but the 14.6% moisture level was significantly different from the 33.9% and 26.4% moisture level. The damage reported here does not impact the official grade or price received, but does impact storability, and indicates an increased susceptibility to breakage and quality degradation with further handling and drying (Ng, Wilcke, Morey, Meronuck, & Lang, 1998). Conversely, as the grain was allowed to dry in the field, there was a trend of increasing mold and other damage. This represented damage that would impact the grade and marketability of the grain. The increase in damaged kernels was only significantly different for the final observation on 12/01, which displayed the highest percentage of damaged kernels and greatest variability. The damage levels observed over the range of dates would only impact the grade for the final observation, which on average exceeded the 5.0% limit for U.S. No. 2 corn (USDA, 2013a). However, the higher moisture samples would require drying which could result in increased final levels of damage, at the point of storage.

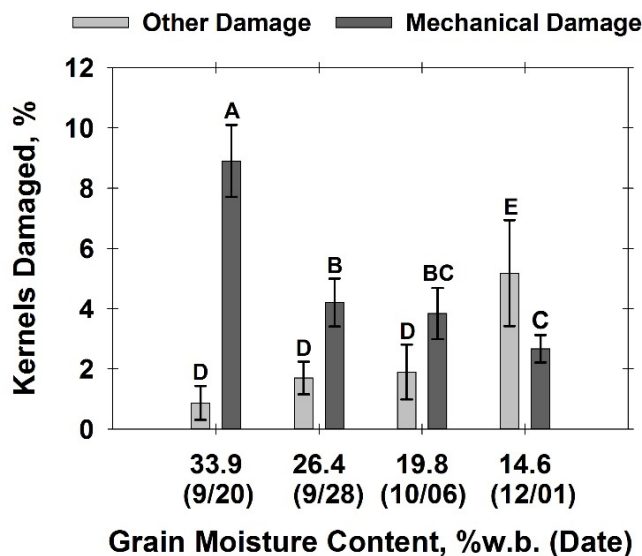


Figure 3-8: Percentage of kernels damaged, on a mass basis, as grain was allowed to dry in the field. Mechanical damage represents broken kernels or kernels with visible cracks. Other damages represents damage as included in the grain inspection guidelines (USDA, 2013a). Error bars represent \pm one standard deviation, and different letters indicate significant differences (A-C for mechanical damage and D-E for other damage).

Figure 3-9 shows the test weight of samples that were taken from the same field at multiple points as the grain field dried. Test weight at field moisture represents the test weight of the sample measured at the incoming moisture. This series displays the expected trend of increasing test weight as the moisture content is reduced (due to field drying). Dry test weight represents the test weight measured after the samples were dried in the environmental chamber. At this point, the samples were all nominally at a moisture of 15%, but the data still shows a trend of increasing test weight as the samples field dried. This indicates that some process other than moisture change contributes to the test weight change, and was consistent with Johnson et al. (1963). The samples collected on the final observation were not dried in the environmental chamber because the grain was already below market moisture at the time of harvest. Test weight was significantly different for all dates both before and after drying. This change in test weight has a direct impact on which grade requirements the grain meets. Before natural air drying, the grain grade, based on test weight alone, progresses from U.S. No. 3 on 9/20 to U.S. No. 2 on 9/28 to U.S. No. 1 on 10/06 and 12/01. After natural air drying, the highest moisture

sample meets the requirement for U.S. No. 2 corn, and the remaining dates qualify for U.S. No. 1 (USDA, 2013a) in terms of test weight.

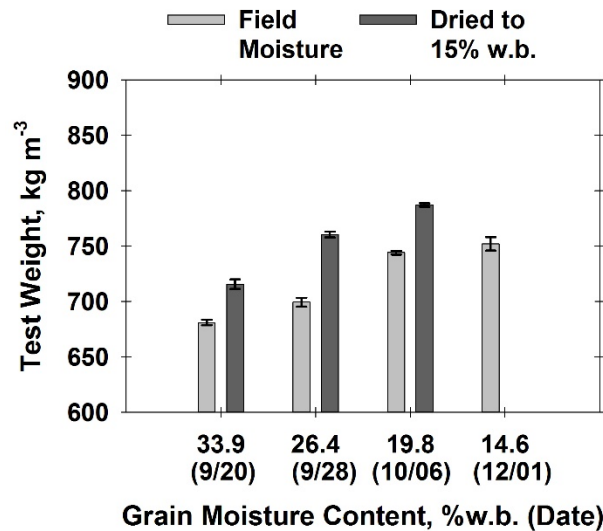


Figure 3-9: Test weight of samples harvested at various field moistures. Initial TW represents the test weight of samples at the incoming field moisture. Final TW represents the test weight of the samples after drying to ~15%. Error bars represent \pm one standard deviation.

3.5 Conclusions

This study evaluated preharvest and machine yield losses for multiple producers and in a variety of settings to establish a typical range of machine losses in Kentucky corn harvest. Total losses ranged from 19 to 138 kg ha⁻¹, which was equivalent to 0.8% to 2.4% of total yield. Losses were highly variable for a given combine, with coefficients of variation in total loss ranging from 21.7% to 77.2% of the total loss. Even though minimal preharvest losses were observed, the total ear loss was the largest source of variability, and losses at the combine head amounted to between 55.7% and 80.0% of the total loss. This indicates that combine operators should pay close attention to factors that influence losses that occur at the head (speed, deck plate spacing, etc.).

This study also attempted to quantify potential changes in losses, quality, and yield as grain was allowed to field dry. Harvest date (and moisture content) had no significant impact on the potential yield in the field, and the recovered yield was only significantly impacted by the long delay as the crop field dried from 19.8% to 14.6%.

This delay resulted in a large increase in the number of missed ears as well as increased mold damage. Test weight and mechanical damage generally improved with decreased moisture, but the test weight after drying was always sufficient to at least meet U.S. No 2 corn standards.

Lodging and weather impacts will have a strong effect on the results presented here, but these results indicate the loss relationships used in previous harvest logistics models are not representative of current practices. Conditions were favorable for much of the harvest season, and for this specific year, losses associated with field drying would not have been a factor until lodging occurred. This suggests an alternative approach, based on the chance of a weather event causing crop lodging, could be useful as a way to evaluate harvest timing. Ultimately, this study should be repeated for additional years to examine more variability in weather and to obtain finer resolution results.

3.6 References

- Allen, T. T. (2011). *Introduction to discrete event simulation and agent-based modeling: Voting systems, health care, military, and manufacturing*. London, United Kingdom: Springer Science & Business Media.
- Amiama, C., Pereira, J. M., Castro, A., & Bueno, J. (2015). Modelling corn silage harvest logistics for a cost optimization approach. *Computers and Electronics in Agriculture*, 118, 56-65. doi:<http://dx.doi.org/10.1016/j.compag.2015.08.024>
- ASABE Standards (2000). D497.4 Agricultural machinery management data. St. Joseph, MI: ASABE.
- ASABE Standards. (2012). S352.2 Moisture measurement- unground grain and seeds. St. Joseph, MI: ASABE.
- ASABE Standards. (2015a). D497. 6 Agricultural machinery management data. St. Joseph, MI: ASABE.
- Ayres, G. E., Babcock, C., & Hull, D. O. (1972). *Corn combine field performance in iowa*. Paper presented at the Grain Damage Symposium, The Ohio State University, Columbus, Ohio.
- Benock, G., Loewer Jr, O., Bridges, T., & Loewer, D. (1981). Grain flow restrictions in harvesting-delivery-drying systems. *Trans ASAE*, 24(5), 1151-1161.

- Benson, E. R., Hansen, A. C., Reid, J. F., Warman, B. L., & Brand, M. A. (2002). *Development of an in-field grain handling simulation in arena. Asabe paper no. 023104*. ASAE, St. Joseph, MI.
- Berruto, R., & Maier, D. E. (2001). Analyzing the receiving operation of different grain types in a single-pit country elevator. *Trans. ASAE, 44*(3), 631-638.
- Buckmaster, D. R., & Hilton, J. W. (2005). Computerized cycle analysis of harvest, transport, and unload systems. *Computers and Electronics in Agriculture, 47*(2), 137-147.
- Busato, P., Berruto, R., & Saunders, C. (2007). Optimal field-bin locations and harvest patterns to improve the combine field capacity: Study with a dynamic simulation model. *Agricultural Engineering International: CIGR Journal, IX*.
- Chowdhury, M. H., & Buchele, W. F. (1976). Colorimetric determination of grain damage. *Transactions of the ASAE., 19*(5), 807-0808.
doi:<https://doi.org/10.13031/2013.36122>
- De Toro, A., & Hansson, P. A. (2004). Analysis of field machinery performance based on daily soil workability status using discrete event simulation or on average workday probability. *Agricultural Systems, 79*(1), 109-129. doi:10.1016/s0308-521x(03)00073-8
- Dudenhoeffer, N. E., Luck, B. D., Digman, M. F., & Drewry, J. L. (2017). Simulation of the forage harvest cycle for asset allocation. *Applied Engineering in Agriculture, 34*(2), 327-334.
- Edwards, W., Plastina, A., & Johanns, A. (2016). Grain harvesting equipment and labor in iowa. *Ag Decision Maker*. Retrieved from <https://www.extension.iastate.edu/agdm/crops/pdf/a3-16.pdf>
- Elmore, R. W., & Roeth, F. W. (1999). Corn kernel weight and grain yield stability during post-maturity drydown. *Journal of production agriculture, 12*(2), 300-305.
- Hanna, H. M. (2008). Pm 574 profitable corn harvesting. Retrieved from <https://store.extension.iastate.edu/product/Profitable-Corn-Harvesting>
- Hanna, H. M., Kohl, K., & Haden, D. A. (2002). Machine losses from conventional versus narrow row corn harvest. *Applied Engineering in Agriculture, 18*(4), 405-410.

- Harmon, J. D., Luck, B. D., Shinnars, K. J., Anex, R. P., & Drewry, J. L. (2017). Time-motion analysis of forage harvest: A case study. *Trans ASABE*, 61(2), 483-491.
- Harrigan, T. (2003). Time-motion analysis of corn silage harvest systems. *Applied Engineering in Agriculture*, 19(4), 389-396.
- Holtman, J. B., Pickett, L. K., Armstrong, D., & Connor, L. J. (1973). A systematic approach to simulating corn production systems. *Transactions of the ASAE*, 16(1), 19-0023.
- Huitink, G. (2001). Mp 437 corn production handbook, 65-72. Retrieved from <https://www.uaex.edu/publications/pdf/mp437/chap8.pdf>
- Johnson, W., & Lamp, B. (1966). *Principles, equipment and systems for corn harvesting*. Wooster, OH: Agricultural Consulting Associates, Inc.
- Johnson, W. H., Lamp, B., Henry, J., & Hall, G. (1963). Corn harvesting performance at various dates. *Transactions of the ASAE*, 6(3), 268-0272.
- Klinner, W. E., & Biggar, G. W. (1972). Some effects of harvest date and design features of the cutting table on the front losses of combine-harvesters. *Journal of Agricultural Engineering Research*, 17(1), 71-78.
doi:[http://dx.doi.org/10.1016/S0021-8634\(72\)80016-7](http://dx.doi.org/10.1016/S0021-8634(72)80016-7)
- Licht, M., Hurburgh, C., Kots, M., Blake, P., & Hanna, M. (2017). *Is there loss of corn dry matter in the field after maturity?* Paper presented at the 29th Annual Integrated Crop Management Conference.
- Loewer, O., Kocher, M., & Solaimanian, J. (1990). An expert system for determining bottlenecks in on-farm grain processing systems. *Applied Engineering in Agriculture*, 6(1), 69-72.
- Loewer, O. J., Benock, G., & Bridges, T. C. (1980). Effect of combine selection and harvesting rate on grain drying and delivery system performance. *Transactions of the ASAE*, 23(6), 1548-1553.
- Loewer, O. J., Bridges, T. C., & Bucklin, R. A. (1994). *On-farm drying and storage systems*. St. Joseph, MI: ASABE.
- Loewer, O. J., Bridges, T. C., White, G. M., & Overhults, D. G. (1980). The influence of harvesting strategies and economic constraints on the feasibility of farm grain drying and storage facilities. 23(2). doi:10.13031/2013.34605

- Loewer, O. J., Bridges, T. C., White, G. M., & Razor, R. B. (1984). Optimum moisture content to begin harvesting corn as influenced by energy cost. *Transactions of the ASAE.*, 27(2), 362-365.
- Marley, S. J., & Ayres, G. E. (1972). Influence of planting and harvesting dates on corn yield. *Transactions of the ASAE.*, 15(2), 228-231.
doi:<https://doi.org/10.13031/2013.37873>
- McGechan, M. B. (1985a). A parametric study of cereal harvesting models i. Critical assessment of measured data on parameter variability. *Journal of Agricultural Engineering Research*, 31(2), 149-158. doi:[http://dx.doi.org/10.1016/0021-8634\(85\)90067-8](http://dx.doi.org/10.1016/0021-8634(85)90067-8)
- McGechan, M. B. (1985b). A parametric study of cereal harvesting models ii. Analysis of sensitivity to parameter variability. *Journal of Agricultural Engineering Research*, 31(2), 159-170.
- McNeill, S., & Montross, M. (2007). Corn harvesting, handling, drying, and storage. Retrieved from <http://www2.ca.uky.edu/agcomm/pubs/id/id139/harvesting.pdf>
- Morey, R. V., Zachariah, G. L., & Peart, R. M. (1971). Optimum policies for corn harvesting. *Transactions of the ASAE.*, 14(5), 787-792.
- Ng, H., Wilcke, W., Morey, R., Meronuck, R., & Lang, J. (1998). Mechanical damage and corn storability. *Transactions of the ASAE.*, 41(4), 1095-1100.
- Nielsen, R. L., Brown, G., Wuethrich, k., & Halter, A. (1996). *Kernel dry weight loss during post-maturity drydown intervals in corn*. Purdue University. West Lafayette, IN. Retrieved from <http://www.agry.purdue.edu/ext/corn/research/rpt94-01.htm>
- Paulsen, M. R., de Sena, D. G., Jr., de Assis de Carvalho Pinto, F., Zandonadi, R. S., Ruffato, S., Gomide Costa, A., . . . Danao, M. G. C. (2014). Measurement of combine losses for corn and soybeans in brazil. *Applied Engineering in Agriculture*, 60(6), 841-855.
- Rotz, C. A., Muhtar, H. A., & Black, J. R. (1983). A multiple crop machinery selection algorithm. *Transactions of the Asae*, 26(6), 1644-1649.
- Rubinstein, R. Y., & Kroese, D. P. (2016). *Simulation and the monte carlo method* (3 ed. Vol. 10). Hoboken, NJ: John Wiley & Sons.

- Silva, L. C., Queiroz, D. M., Flores, R. A., & Melo, E. C. (2012). A simulation toolset for modeling grain storage facilities. *Journal of Stored Products Research*, 48, 30-36. doi:<https://doi.org/10.1016/j.jspr.2011.09.001>
- Søgaard, H. T., & Sørensen, C. G. (2004). A model for optimal selection of machinery sizes within the farm machinery system. *Biosystems Engineering*, 89(1), 13-28.
- Sørensen, C. G., & Bochtis, D. D. (2010). Conceptual model of fleet management in agriculture. *Biosystems Engineering*, 105(1), 41-50.
- Spedding, T. A., & Sun, G. Q. (1999). Application of discrete event simulation to the activity based costing of manufacturing systems. *International Journal of Production Economics*, 58(3), 289-301. doi:[https://doi.org/10.1016/S0925-5273\(98\)00204-7](https://doi.org/10.1016/S0925-5273(98)00204-7)
- Sumner, P. E., & Williams, E. J. (2009). Bulletin 973: Measuring field losses from grain combines. Retrieved from <http://hdl.handle.net/10724/12068>
- Tako, A. A., & Robinson, S. (2012). The application of discrete event simulation and system dynamics in the logistics and supply chain context. *Decision Support Systems*, 52(4), 802-815. doi:<https://doi.org/10.1016/j.dss.2011.11.015>
- Thomison, P. R., Mullen, R. W., Lipps, P. E., Doerge, T., & Geyer, A. B. (2011). Corn response to harvest date as affected by plant population and hybrid. *Agronomy Journal*, 103(6), 1765-1772.
- USDA. (2013a). Grain inspection handbook *Book ii, chapter 4 corn*. Washington, DC: Grain Inspection, Packers and Stockyards Administration.
- USDA. (2013b). Grain inspection handbook *Book ii, chapter 1 general information*. Washington, DC: Grain Inspection, Packers and Stockyards Administration.

Chapter 4. DISCRETE EVENT SIMULATION OF GRAIN TRANSPORTATION AND DRYING

4.1 Summary

Examining grain harvest logistics from a whole system perspective is important to identify system bottlenecks and increase productivity. This study presents a whole season discrete event simulation model of corn harvest from the field through the first storage structure. It was an expansion of the previously proposed transportation model and included wet holding capacity and grain drying at an on-farm facility. A simple method was proposed to estimate dryer capacity relative to its rating at standard conditions, and field dry down was modeled based on weather data and grain equilibrium moisture content relationships. The model was applied to an operation to assess the suitability of both the drying capacity adjustment and the overall harvest model. There was large variability in the observed data, which made assessing the accuracy of the drying model difficult. Dryer capacity was generally underpredicted and in some instances had large errors. The method did however, agree well with the previous literature data from which it was derived. The proposed relationship for field dry down accurately represented the change in incoming grain moisture, with a root mean squared error of 0.73 points. The overall harvest model showed good agreement with the observed data based on the cumulative mass of grain delivered over the season.

4.2 Introduction

4.2.1 Overview

Determining a harvest strategy is an important decision for producers, and it requires an evaluation of the whole harvest system. On-farm drying and storage provides producers with flexibility in harvest timing by avoiding constraints associated with elevator business hours and long waits to unload during peak times. Producers may also see benefits from reduced drying costs and better marketability. On-farm storage is a critical component of the US grain infrastructure, with 54.5% of the total storage capacity located on farm (USDA-NASS, 2017). In some regions, this value increases to over 80% (Figure 4-1), and in wetter regions or areas with shorter harvest windows, the ability to

effectively dry wet grain to levels safe for storage, without sacrificing efficiency in other areas of the harvest system, is key to utilizing this storage capacity.

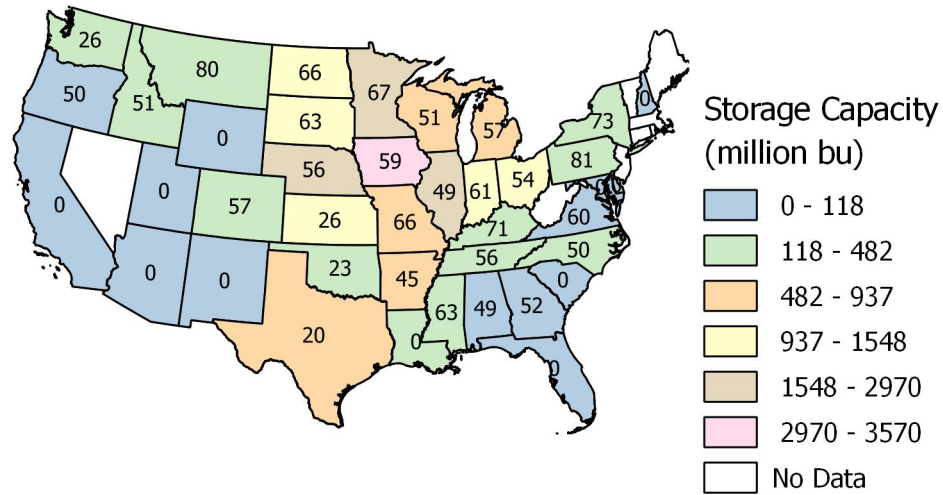


Figure 4-1: Combined on-farm and off-farm storage for 2017. Labels indicate the percentage of capacity on the farm, and 0% indicates no on-farm storage data were available. The national average was 54.5% on-farm. (USDA-NASS, 2017).

When harvesting and drying wet grain, the grain dryer, and temporary wet holding bins can often become the system bottleneck and limit the daily productivity of an operation. The dryer capacity depends on its configuration, drying temperature, and weather conditions. Additionally, incoming grain moisture (and associated quantity of water that must be removed) plays a large role in drying energy use and capacity. As the harvest season progresses, the incoming grain moisture generally decreases and drying capacity increases. Producers must balance costs associated with drying high moisture grain and potential weather delays, losses, and logistical issues that come along with allowing grain to dry in the field. Many operations grow a mix of wheat, corn, full-season soybeans, and double-crop soybeans. Harvest, transportation, and drying systems need to accommodate a range of planting systems. To further complicate the issue, low corn prices have led some producers to explore higher value commodities, such as food grade corn, that require additional planning and management to avoid quality discounts.

4.2.2 *Wet Holding*

Typically, on-farm drying systems require temporary wet-holding storage bins prior to the dryer. These bins serve as a buffer between processes and allow harvest and grain delivery to progress faster than the grain can be dried. Wet holding capacity of at least 25%-50% of the peak daily intake is suggested by Maier and Bakker-Arkema (2002), and Loewer et al. (1994) suggested sizing wet holding based on the deficit between the daily harvest and drying capacity. Wet holding bins provide temporary storage for grain delivered in excess of the drying capacity and allows the drying window to be extended so the dryer can ‘catch up’ once the drying demand is reduced. This occurs overnight after harvest stops, once the grain moisture drops, or on days with unfavorable harvesting weather. When managing wet grain, care must be taken to stay within the recommended storage times, and grain is typically held for less than 24 hours prior to drying to reduce heating (MWPS-13, 1987).

4.2.3 *Drying*

The dryer often has the lowest capacity in a harvest system, at least for a portion of the harvest season if wet grain is harvested. Several factors including the expected daily harvest, moisture content, wet holding, and weather conditions must be considered to match drying and harvest capacity. When determining the capacity of grain handling and drying equipment, another important consideration is future growth, where double the drying capacity could be required in ten years (MWPS-13, 1987). Many options exist for grain drying, but dryers can be broken down into low temperature/low capacity systems versus high temperature/high capacity systems. Generally, as the drying rate increases due to high temperatures, so does energy consumption. Several resources cover drying methods in detail (Edwards, 2014; Hellevang, 2013; Maier & Bakker-Arkema, 2002; Maier & Watkins, 1998; MWPS-13, 1987; Nichols, n.d.). Natural air drying is the most energy efficient, but runs the risk of spoilage, depending on moisture content and temperature. Low-temperature drying is a step up from natural air drying in that a burner is added in line with the fan so air is heated approximately 5.6°C (10°F) above ambient. This study was primarily concerned with high capacity, high-temperature dryers. These systems have the highest capacity and are classified as cross-flow, counter-flow, or

mixed-flow depending on the direction of airflow relative to grain flow. These are generally referred to as column dryers or tower dryers. High-temperature on-floor or on-roof bin-batch dryers are also available that use air temperatures ranging from 49°C to 82°C (120°F to 180°F.). High-temperature, crossflow dryers are generally considered in the US once the required drying capacity is greater than 38 tonnes day⁻¹ (1,500 bu day⁻¹) (Loewer et al., 1994).

Dryer performance has been explored extensively in the literature, and several mathematical and simulation models have been developed. This study primarily focuses on cross-flow dryers, which are typically modeled using deep bed drying models (Liu & Bakker-Arkema, 1997; Thompson, Peart, Foster, Loewer, & Bridges, 1994). These deep bed models utilize air psychrometric properties and a series of thin layer drying models (ASABE Standards, 2014) to represent the drying process. Morey, Cloud, and Lueschen (1976) utilized a simulation model to evaluate the energy use in a crossflow dryer for various drying strategies including changing drying temperature and air flow rates, delayed harvest, and combination drying (high temperature drying to 18-20%, followed by natural air drying). The general recommendations from the study were to: dry at the highest temperature that allows quality to be maintained, plant as early as possible, and to use combination drying where possible. Pierce and Thompson (1981) evaluated the performance of a normal crossflow dryer and several modifications to the heating and cooling sections as a function of airflow rate and drying air temperature. The results were consistent with previous research, which showed higher drying air temperature and lower airflow rates were generally more energy efficient and increasing the airflow rate resulted in increased capacity but sacrificed energy efficiency.

Drying grain in a high-temperature dryer can have adverse effects on quality, and the number of stress cracked kernels, which can increase breakage and BCFM (broken corn and foreign material) (Brooker, Bakker-Arkema, & Hall, 1992). These stress cracks result from large moisture or temperature gradients in the kernel and when grain is dried at high temperatures to low moistures. Higher drying temperature increases drying efficiency and capacity, but an acceptable level of damage in regular No. 2 field corn might be detrimental for waxy, food grade, white corn, or other instances where high quality is demanded. Kernel temperature, not drying temperature is what leads to

breakage, and should be kept below 60°C for yellow corn and 43°C for food grade or white corn (Montross & Maier, 2000). Reducing the drying temperature has the effect of reducing drying efficiency and drying capacity and reducing the drying air temperature to 60°C has been recommended to maintain quality in white corn. Ambient conditions and varietal difference influence drying, and simulation models are reportedly within 10%-20% of experimental data (Brooker et al., 1992). Additionally, dryer performance is generally shown as a function of moisture, drying air flow rate, and drying air temperature (Morey et al., 1976; Pierce & Thompson, 1981). However, an end user has minimal control over the airflow rate, and from their perspective, it would be more beneficial to know how the dryer performance changes with temperature and moisture relative to a known rating. Dryer manufacturers specify dryer capacities, in terms of wet grain per hour, drying from 25 to 15% (10 point removal) and 20 to 15% (5 point removal) (ASABE Standards, 2015c). These ratings are given based on drying and cooling the grain, and where applicable, when full heat is used (grain discharged hot at an elevated moisture and cooled in a bin). These ratings are established using a combination of computer simulation and field testing and are based on the conditions defined in the standard (ASABE Standards, 2015c). The drying temperature used to produce the ratings is generally the highest temperature the dryer will operate at continuously (usually ~104°C for a cross flow dryer), and actual capacity observed in the field is often 70% of the manufacturer's rating (MWPS-13, 1987). Most dryers could, in theory, operate continuously, but Maier and Bakker-Arkema (2002) suggested a more realistic value is 20 hours per day, which further reduces that total daily drying capacity.

4.2.4 Harvest System Models

An important consideration for harvest models that simulate operations over a span of dates is the probability that fieldwork can occur on a given day. This probability is largely influenced by the type and timing of the operation, geographical region, weather, soil type, and the slope of the field. ASABE Standards (2015a) provides the probability of working days, separated by the time of year, for several geographic locations. These probability models use historical weather data and a moisture balance to determine the status of the field. Field operations are classified as traffic or tillage, and

the field is deemed suitable for work if the moisture is below a specified threshold. Similar methods have been applied in a number of farm simulation models (Babeir, Colvin, & Marley, 1986; Hwang, Epplin, Lee, & Huhnke, 2009; Rotz & Harrigan, 2005; Sorensen, 2003).

A group of related publications that explored harvesting systems were summarized in Loewer et al. (1994), and the associated models were distributed in Thompson et al. (1994). Many of these works were also previously described in the discrete event simulation of grain transportation that was the starting point for this study. Benock, Loewer, Bridges, and Loewer (1981) developed a simulation model that could be used to examine material flow and delays in the harvesting, handling, and drying system. The model assumed a constant harvest rate and allowed multiple drying practices to be evaluated. Bridges, Loewer, Walker, and Overhults (1979) presented a similar program that ranked costs associated with predetermined equipment sets and drying methods. O. J. Loewer et al. (1980) utilized the previous models to evaluate how changes in system components from an 'optimum' capacity influenced the overall system capacity and found the dryer capacity was generally the most influential factor on field equipment and transportation efficiency. O.J. Loewer et al. (1980) presented a sensitivity analysis of harvest and management strategies on the economics of on-farm drying and storage. The study indicated approximately 26% to 28% was the ideal moisture content to begin harvesting.

Morey et al. (1971) developed a dynamic model for corn harvesting which operated based on the decision variable of how many hours to harvest per day for a given week. A sensitivity analysis showed extending the working day during peak harvest time was often the best policy even accounting for overtime labor rates. The number of acres remaining to be harvested and moisture content were considered state variables. Field trafficability was evaluated using historical weather data and a soil moisture budget, and recoverable yield and field dry down were modeled using data from Johnson and Lamp (1966). The dryer capacity for a given moisture content was estimated as a function of the 5-point dryer rating with a linear correction for different moisture spans (based on the drying model from Thompson, Peart, and Foster (1968)).

Loewer et al. (1984) developed a model to determine the optimum moisture content to start harvest when evaluated based on costs associated with drying. Days suitable for fieldwork were determined from a probability of rainfall greater than 0.25 mm, and it was assumed no work occurred on Sundays. The grain moisture in the field was evaluated using the relationship proposed by Morey et al. (1971) and the field losses based on Johnson and Lamp (1966). Dryer capacity was based on Thompson et al. (1968) and evaluated continuous flow drying, batch-in-bin-drying, and layer drying. The goal of the study was to balance field losses, grain prices, and energy costs, and empirical relationships were proposed to identify the optimum moisture to start harvest based on the number of days required to harvest the grain, grain prices, and energy costs. Relationships were developed to determine the optimum moisture content to begin harvest based on harvesting capacity, drying method, and the price ratio of drying energy to grain value.

A number of modeling efforts in regions outside the United States focused on cereal grain production. Abawi (1993) developed a broad model of wheat harvesting and drying in Australia to evaluate the costs associated with field versus artificial drying. The model was based on an hourly simulation and was evaluated using 30 years of historical data. Conditions for field tractability were set based on the magnitude of rain events, and field and harvest losses were modeled as a function of the number of days past maturity and moisture content. Grain drying was modeled as a function of temperature and moisture removal using the relationship presented by Radajewski, Jolly, and Abawi (1987), and was an empirical fit derived from simulation data. The simulation indicated harvesting and removing 2-5 pts of moisture with artificial drying resulted in the highest returns, with harvest capacity significantly influencing the optimum moisture content. This model neglected transportation and found returns were more sensitive to drying capacity than to harvest capacity.

Another early linear programming model of cereal grain harvesting and drying was published by Audsley and Boyce (1974). This model accounted for harvest, wet storage, and drying costs along with field losses. The model neglected transportation costs, and moisture content was assumed to be independent of weather. The amount of time available for field work was estimated using a simple rainfall accumulation and 10

years of historical data. This analysis showed the importance of planting to achieve varying maturity dates and concluded reduced field losses could offset the costs incurred by drying early wet grain.

Sorensen (2003) used historical weather data to predict crop moisture and available harvest hours and simulated combine performance for various crops in Denmark. Combine capacity was determined through time-motion studies, and the overall capacity included adjustments related to field shape and a stochastic parameter related to field conditions. The authors found that under capacity was 50% more costly than over-capacity, and a 30% reduction in crop price reduced the optimal capacity by 15%.

De Toro and Hansson (2004) used a discrete event simulation and 20 years of historical records of operation completion dates to estimate timeliness and the total cost for planting and harvesting operations. The model was applied to a hypothetical farm in Sweden, and two methods were used to estimate the workability of the fields. Daily workability was estimated using a soil model and a simple probability of working days (ASABE Standards, 2015a). They found the simpler method was difficult to implement for harvest operations due to varying field maturation times, and the compounding effects of delays resulted in an underestimation of timeliness cost using the ASABE method. De Toro (2005) was an expansion of De Toro and Hansson (2004), which analyzed the effects of weather on timeliness costs on cereal farms in Sweden. The authors found multiple least cost machinery sets for a given farm. This was further expanded to include crop moisture content as a function of weather in De Toro, Gunnarsson, Lundin, and Jonsson (2012). The study utilized 30 years of historical weather data from Sweden and modeled field drying based on evapotranspiration and grain equilibrium moisture content relationships. The model also accounted for precipitation and grain rewetting. Here the authors found timeliness and drying costs were the largest contributors to annual variation.

4.2.5 Motivation

This study expands on a previously developed discrete event simulation (DES) model for grain transportation by including system constraints related to wet holding and

drying capacity. The intended application of this study is to provide decision support to producers by allowing them to explore how changes in their production system could impact the overall harvest operation. The proposed model can be used to explore the relationship between grain drying capacity and harvest/transportation capacity, and the implications of reduced drying temperature, that need to be considered when maintaining high levels of grain quality are important (specialty crops, food grade, etc.). Specific objectives of this study were:

1. Develop a simple relationship to adjust grain dryer capacity as a function of drying temperature and moisture removal.
2. Account for seasonal dryer performance by modeling field dry down based on weather data.
3. Adapt the previously developed model of grain transportation to include wet holding storage and grain drying and expand the model to simulate a whole harvest season.
4. Validate the model using data collected from a cooperating producer.

4.3 Materials and Methods

This study presents a DES simulation model of grain harvest from the field through delivery, drying, and storage at an on-farm storage facility. The model was developed using MATLAB and the SimEvents toolbox in Simulink (R2017b, The MathWorks Inc., Natick, MA). It consists of two major components – the daily harvest model and its application over the whole harvest season. The daily harvest model was used to evaluate wait times, system throughput, and resource utilization on a daily basis and the whole system portion utilized multiple daily simulations, aggregated the daily outputs, and updated input conditions between days. Models for field drying of grain and dryer performance as a function of drying temperature and moisture were used to account for changes in drying capacity over the course of the harvest season. Input and output variables along with their description and associated units are given in Table 4-1.

Table 4-1: Model Variable Nomenclature

Symbol	Description	Units
Daily Simulation Inputs		
$dt_{Load\ Generation}$	Time between arrivals of full in-field transporters	Minutes load ⁻¹
dt_{FT}	Field transfer time	Minutes
$dt_{transport}$	Time to transport from field to facility	Minutes
dt_{scales}	Weigh and inspect duration	Minutes
dt_{pit}	Unload duration	Minutes
dt_{return}	Time to return to the field from storage facility	Minutes
Hh	Duration of field work	Minutes
Ht	Total length of daily simulation, 1440 minutes (24 hours)	Minutes
$N_{drivers}$	Number of drivers	-
N_{trucks}	Number of trucks	-
Q_{cart}	Number of field unloading events required to fill a truck	Carts truck ⁻¹
Q_{Field_max}	Number of loads that can be harvested without a truck present	Loads
μ_L	Mass of grain per truck load, dry basis	Tonnes load ⁻¹
Q_{wh}	Capacity of the wet holding bins	Loads
Q_{Carry}	Fill level of wet holding bins at start of daily simulation	Loads
dt_{dry}	Time to dry a full truck load of grain	Minutes
Whole Season Parameters		
W_T	Total mass of grain to be harvested, zero moisture basis	Tonnes
β	Field dry down rate coefficient	Day ⁻¹
MC_{in}	Incoming grain moisture content	% w.b.
MC_{out}	Final moisture content after drying, nominally 15%	% w.b.
MC_0	Initial know moisture content for dry down equation	%w.b.
MC_E	Equilibrium moisture content estimated from weather data	%w.b.
T_{dry}	Actual drying air temperature	°F
T_{rated}	Air temperature used to determine dryer capacity	°F
SDC	Stated drying capacity at T_{rated} and 5 pts removal	bu hr ⁻¹
RDC	Relative drying capacity at a given temperature and moisture, dry basis	Tonnes hr ⁻¹
Model Outputs		
$Loads_{in}$	Total number of arrivals at storage facility	Trucks day ⁻¹
W_{in}	Total mass of grain delivered to the storage facility, dry basis	Tonnes day ⁻¹
W_{out}	Total mass of grain dried on a given day, dry basis	Tonnes day ⁻¹
WT Field Side	Average time full loads coming from the field wait for a truck	hours
WT Pit	Average wait time for trucks to unload at the receiving pit	hours
FTE	Flow time efficiency, from field to wet holding	Percent
$Q_{wh\ Final}$	Wet holding bin fill level at the end of the daily simulation	Loads
HTL	Harvest time lost. Portion of the day harvest was stopped due to a bottleneck somewhere in the system	Hours
Driver Utilization	Percentage of the day drivers were committed to transportation	%
Truck Utilization	Percentage of the day trucks were committed to transportation	%
Dryer Utilization	Percentage of the day the dryer was in use	%

4.3.1 Dryer Capacity

One of the goals of this model was to simulate the impact of harvest moisture and drying temperature on overall system capacity, and specifically to this study, high-temperature continuous flow dryers were considered. Dryer manufacturers' product literature typically provides estimated drying capacity (in wet bushels per hour) at 5 and 10 points of moisture removal, and where applicable provide this data under various modes of operation (ex. dry and cool vs. full heat). The stated drying capacity (SDC) was taken as the dryer specification at five points of moisture removal at a given drying temperature (typically 104 °C), operating in dry/cool mode.

A number of factors influence dryer performance including: incoming grain moisture, drying temperature, amount of cooling in the dryer, final moisture content, ambient conditions, and variety, among others. To account for seasonal variation in performance, and to evaluate potential changes in system performance due to drying at lower temperatures for specialty grains, the drying capacity was adjusted by scaling the 5-pt rated dryer capacity. This was done by estimating a relative drying capacity (RDC) ratio similar to Morey et al. (1971), except for this study, the capacity was adjusted for both moisture content and drying temperature. The ratio of the dryer performance at a given moisture removal relative to the capacity at 5-pts removal was estimated from equation (4-1), and was a function of the amount of water removed and the incoming and outgoing grain moisture content. The temperature effects were approximated as a linear function of the difference between the rated and reduced drying temperature and was estimated using equation (4-2).

$$R(MC_{in}, MC_{out}) = a * e^{-b * Pts} + c * \frac{MC_{in} * MC_{out}}{Pts} \quad (4-1)$$

Where:

$R(MC_{in}, MC_{out})$ = Moisture correction function. Ratio of dryer capacity with a variable initial moisture content, variable final moisture content, and decreased drying air temperature compared to the stated drying capacity provided from the manufacturer drying at 104 C from 20 to 15% w.b.

MC_{in} = Actual moisture content of incoming grain (% w.b.)

MC_{out} = Final grain moisture content. Typically, 15% or 15.5% (%w.b.)

Pts = Moisture removal, $(MC_{in} - MC_{out})$, in percentage points of moisture removed

a, b, c = Regression coefficients.

$$R(\Delta T) = d + f * \Delta T \quad (4-2)$$

Where:

$R(\Delta T)$ = Temperature correction function. Ratio of dryer capacity at a given temperature to the stated drying capacity

ΔT = Difference between rated and actual drying temperature, $T_{actual} - T_{rated}$, (°C)

d, f = Regression coefficients.

The relative capacity functions were developed based on multiple simulations using the cross-flow drying simulation model developed by Thompson et al. (1994). Simulations were run using an airflow rate of 64.3 cmm m⁻³ (80 cfm bu⁻¹), that was estimated from manufacturers published specifications, and ambient conditions of 10°C and 60% relative humidity. The relative drying ratio was determined based on estimated drying time from the simulations. The relative change in capacity due to grain moisture was estimated from simulations over all combinations of MC_{in} (%w. b.) = [30,27,25,22,20], MC_{out} (%w. b.) = [17,16,15,14,13], T_{actual} (°C) = [104,93,82,71,60]. Additionally, simulations were run for: MC_{in} = [18], MC_{out} = [14,13], at the same drying temperatures. The relative capacity due to decreased drying

temperature was calculated relative to 104 °C, and was estimated based on simulation results for all combinations of MC_{in} (%w. b.) = [27,25,22,20,18], MC_{out} = [15], and T_{actual} (°C) = [104,98, 93,82,71,60,49,43]. The best fit regression coefficients for equationd (4-1) and (4-2) were determined using the Curve Fitting toolbox in MATLAB.

Typical dryer ratings are given in U.S. customary units of wet bushels per hour, so before scaling the dryer performance, SDC was adjusted to dry t hr⁻¹ using equation (4-3). RDC was then determined for a given set of conditions using equation (4-4). The dryer service time for a given day and entity was determined using equation (4-5). Because RDC was based on a stated capacity for a given dryer, the effects of airflow rate and heat recovery were neglected.

$$SDC_{dry} = SDC / 39.368 * (1 - \frac{20}{100}) \quad (4-3)$$

Where:

SDC_{dry} = Drying capacity in terms of dry matter throughput (dry t hr⁻¹)

SDC = Stated drying capacity of wet grain from manufacturer data at 5 pts moisture removal (20% to 15%) and a known temperature (typically 104°C) (wet bu hr⁻¹)

39.368 = conversion factor from bushels of corn to tonnes

$$RDC(MC_{in}, MC_{out}, \Delta T) = SDC_{dry} * R(MC_{in}, MC_{out}) * R(\Delta T) \quad (4-4)$$

Where:

$RDC(MC_{in}, MC_{out}, \Delta T)$ = Relative drying capacity as a function of moisture content in and out of the dryer and drying air temperature (dry t hr⁻¹)

$$dt_{dry_j} = \frac{\mu_{L_j}}{RDC(Pts, T)} / 60 \quad (4-5)$$

Where:

dt_{dry_j} = Dryer service time for the jth load (minutes)

60 = Conversion from hours to minutes

4.3.2 Modeling Incoming Grain Moisture

The change in moisture content of grain coming out of the field directly impacts how much moisture needs to be removed from the grain and in turn the dryer capacity. The change in grain moisture over the course of the season was estimated using equation (4-6) (Morey et al., 1971). Previous works that utilized this equation treated it like the exponential drying model and assumed a linear increase in equilibrium moisture content as the harvest season progresses (Loewer et al., 1994; Loewer et al., 1984; Morey et al., 1971). In this study weather records of temperature and relative humidity were used to estimate the average daily equilibrium moisture content. A function, written in MATLAB was used to estimate the daily change in moisture and moisture content over a range of dates using Euler's method and equation (4-6). The function required a known initial moisture content (MC_0) and hourly weather data, over the range of dates that are of interest. The hourly observations of temperature and relative humidity were consolidated into daily averages, which were used to estimate the equilibrium moisture content, MC_{Et} , of the grain in the field using the Modified Henderson Equation from ASABE Standards (2007). If there was precipitation on a given day, it was assumed no drying occurred. Throughout this manuscript all moisture contents are expressed in percent wet basis.

$$\frac{dMC}{dt} = -\beta(MC_t - MC_{Et}) \quad (4-6)$$

Where:

$\frac{dMC}{dt}$ = Change in moisture content with time (pts day⁻¹)

MC_t = Moisture content on a specific day t (% w.b.)

β = Field drying rate coefficient (day⁻¹)

MC_{Et} = Equilibrium moisture content on a specific day t, determined from weather data and the Modified Henderson Equation from ASABE Standards (2007) (% w.b.)

4.3.3 Daily Model Implementation

The daily harvest simulation was a DES model and was an expansion of the previously proposed model of grain transportation. Figure 4-2 shows the general flow of full loads of grain through the system. The simulation was driven by an entity generation process which represented full grain carts arriving at the field edge. The arrival of loads of grain at the field edge, acquisition of truck and driver resources, transportation of grain to the storage facility, and weighing and inspecting the grain was handled as previously described. These portions of the model are represented by broken lines in Figure 4-2. After arriving at the receiving pit, the grain was either placed directly into storage or transferred to the wet holding bins in front of the grain dryer. Once an entity exited the receiving pit, it was duplicated with one copy representing the grain as it flows through wet holding and drying, and the other retains the truck and driver resources and accounts for empty haul back to the field, as described in the previous manuscript. After duplication, the entities were routed either directly into storage or through wet holding and drying. This decision is based on a threshold moisture content of 15 % w.b. and when the moisture is below this level the system behaves identically to the previous model with grain going directly into storage.

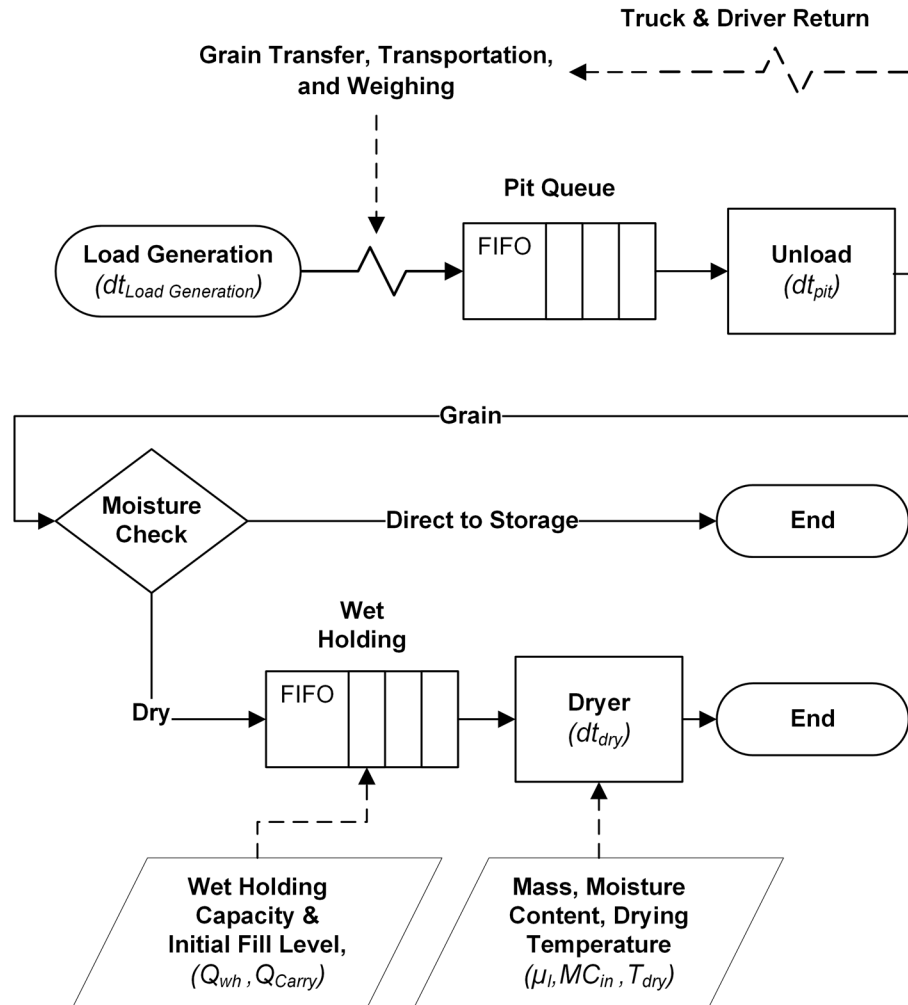


Figure 4-2: Simplified diagram of the DES model. Solid lines represent the flow of material, and dashed lines represent information flow. The break lines represent portions of the model unchanged from the previous transportation model.

To fit within the DES modeling framework, the continuous drying process was represented with an analogous discrete process. A queue and entity server represented wet holding capacity and drying. Wet holding, capacity, Q_{wh} , was a whole number multiple of entities that could be held in front of the dryer. This represents the combination of the wet holding bin capacity and dryer holding capacity. The maximum queue length in the model was the total holding capacity minus one to account for the entity in the dryer server. This could result in a small portion of the wet holding capacity that is never utilized, but that portion of the storage capacity would have little impact on a real system because the entire truck has to be unloaded before it can leave the pit. The

service time associated with unloading at the receiving pit, dt_{pit} represented the minimum time required to unload a truck. However, once the wet holding capacity was reached, the truck was held at the receiving pit until the grain could be transferred to wet holding. When this occurred, the total time spent at the receiving pit was the elapsed time from when the entity entered the unload server to the time it could pass to the wet holding bin. This represents the time to transfer the whole contents of the truck and would only come into account when the wet holding bin is full and the pit unloading rate was higher than the drying rate. In this situation, the unloading rate at the receiving pit was essentially controlled by the drying rate. The serviced time was associated with drying the grain, dt_{dry} , was determined by dividing the mass of grain per truck load, μ_L by the drying rate, which varied by day as described in subsequent discussion. Because the simulation was run in 24-hour intervals, the amount of grain waiting to be dried at the end of each day was carried over as an initial condition for the next daily simulation.

4.3.3.1 Analysis

Much of the resource utilization and material flow was analyzed as described in the previous transportation model. Wait times between processes, truck and driver utilization, and flow time efficiency FTE were identical. However, the productive time for a given entity was modified to account for instances when unloading at the pit takes longer than the pit service time (equation (4-7)). The time the dryer was utilized was estimated from equation (4-8), and the dryer utilization over the 24-hour daily simulation period was estimated from equation (4-9).

$$Productive\ time_i = dt_{FT_i} + dt_{transport_i} + dt_{scales_i} + (T_{fpi} - T_{spi}) \quad (4-7)$$

Where:

$Productive\ time_i$ = Total time to complete all necessary process steps for the i^{th} entity (minutes)

dt_{FT_i} = Time required for the i^{th} entity to be transferred to a truck (minutes)

$dt_{transport_i}$ = Time required for the i^{th} entity to be transported to storage (minutes)

dt_{scales_i} = Time required for the i^{th} entity to be weighted (minutes)

T_{spi} = Timestamp when the i^{th} entity started unloading at the storage facility (minutes)

T_{fpi} = Timestamp when the i^{th} entity finished unloading at the storage facility (minutes)

i = entity number. Represents a single load arriving to the field edge

$$Dryer\ Utilized\ Time_j = (T_{fdj} - T_{sdj}) \quad (4-8)$$

Where:

$Dryer\ Utilized\ Time_j$ = Time the dryer was committed to the j th load (minutes)

T_{sdj} = Timestamp when the j th load starts drying (minutes)

T_{fdj} = Timestamp when the j th load exits the dryer (minutes)

j = Load number. Represents a full truck load of grain

$$Dryer\ Utilization = \frac{\sum_{j=1}^N Dryer\ Utilized\ Time_j}{1440} * 100 \quad (4-9)$$

Where:

$Dry\ Utilization$ = Dryer utilization over a 24-hour period (%)

1440 = Length of dryer simulation assuming dryer could run continuously (minutes)

N = Total number of deliveries in a day

In addition to the average resource utilization, instantaneous resource utilization was estimated at discrete points in the system when the resource state changed. Equation (4-10) was applied to the truck, driver, and dryer resources to evaluate the instantaneous utilization as the simulation progressed. The instantaneous utilization was determined from the Simulink output, and estimates occurred when the resource states changed. A new parameter was proposed to quantify the amount of field time lost due to a bottleneck in the system. A full field side queue represented a situation where harvest had to be stopped because all grain carts and combines were full and there was no place for the entities to move downstream. The time between when this occurred and when an entity left the queue (allowing harvest to restart) represented lost productive time, and harvest time lost (HTL) was defined as the total amount of time this occurred (equation (4-11)). If the next load did not leave the queue until after the harvest window had ended for the day, the difference was taken between when the queue became full and when the window for fieldwork expired.

$$Instant\ Utilization = \left(1 - \left(\frac{Resources_{available}}{Resources_{total}}\right)\right) * 100 \quad (4-10)$$

Where:

Instant Utilization = Resource utilization after a resource state change (%)

Resources_{available} = Quantity of resources not currently in use

Resources_{total} = Total quantity of resources

$$HTL = \sum_{idx=1}^{Idx} (\min(T_{idx+1}, Hh) - T_{idx}) \quad (4-11)$$

Where:

HTL = Harvest Time Lost. Total time harvest was stopped due to a bottleneck (minutes)

T_{idx} = Timestamp when the field queue becomes full, $\{Q_{Field} = Q_{Field_max}, T_{idx} < Hh\}$ (minutes)

T_{idx+1} = Next timestamp. Corresponds to the next entity leaving the queue (minutes)

idx = Timestamp index corresponding to state change that caused the queue to become full

Idx = Final timestamp when the queue was full

4.3.4 Whole Season Simulation

Figure 4-3 shows the flow diagram representing how the daily harvest model was applied to the whole harvest season. The model required the total mass of grain to be harvested, M_T , the moisture content at the beginning of harvest, weather data spanning the harvest window, and the other inputs to the daily simulation outlined in Table 4-1. After initialization, the model runs in a loop over the daily harvest model until the total mass of grain is harvested. A summary including: resource utilization, loads into the system, loads out of the system, wait time between processes, and the final level of the wet holding bins was generated for each day. The starting level of the wet holding bins, grain moisture content, and drying capacity were updated each day. All trucks had to be unloaded on the same day. If there was insufficient time to complete all unloading events, the daily simulation was run again using a reduced time that would allow all material to be delivered.

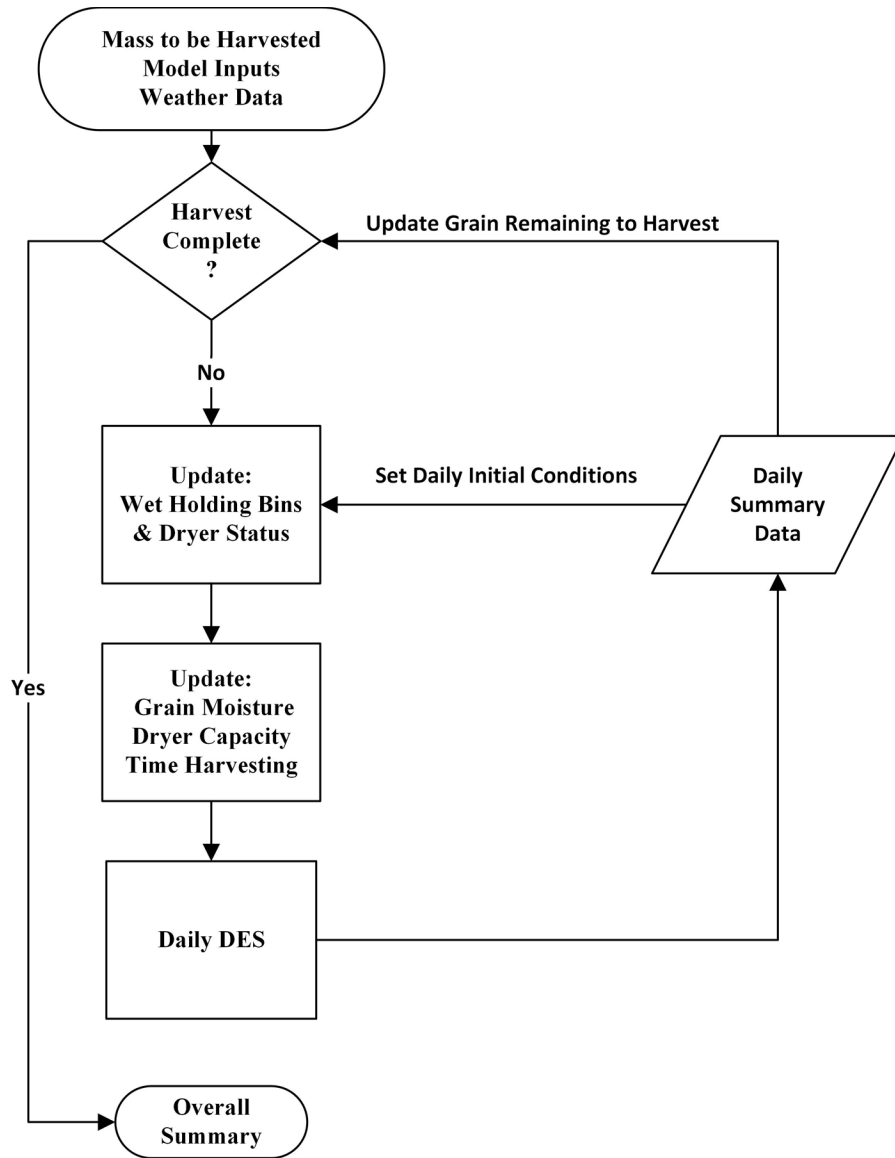


Figure 4-3: Whole season flow diagram.

Time harvesting, Hh , was the variable used to control if new grain was harvested on a given day. A standard eight-hour work day was used for the time harvesting occurred, and it was assumed no fieldwork occurred on Sunday. A simple rainfall threshold similar to (Audsley & Boyce, 1974) and (Loewer et al., 1984) was used to account for weather delays (equation (4-12)). It was assumed that 20% of the precipitation carried forward between days and if the accumulated rainfall threshold was greater than 6.35 mm no fieldwork occurred. Applying this method to ten years of records for the weather data for Bowling Green, Kentucky over a range of dates from

September 1 to October 31 resulted in an 83% average probability of fieldwork. This was within the range of values provided in ASABE Standards (2015a), and estimating field days from equation (4-12) can be applied to specific sites, if weather data is available. The dryer was allowed to run continuously and dry any grain present in the wet holding bins on days when no harvest occurred. The final iteration of the model was run twice, once to determine if it was the last simulation day, and a second time with a harvest time equal to the amount of time required to harvest the last grain. This prevented the model from overshooting the total mass to be harvested. After harvest was complete, the daily results were compiled into an overall summary.

$$\begin{aligned} Z_t &= P_t \quad t = 1 \\ Z_t &= 0.2 * P_{t-1} + P_t \quad t > 1 \end{aligned} \quad (4-12)$$

Where:

Z_t = Accumulated rainfall threshold, (mm of precipitation)

P_t = Precipitation on a given day (mm of precipitation)

t = Day relative to the start of the simulation

4.3.5 Model Application

The data used to evaluate the proposed field drying model, dryer capacity adjustment, and DES harvest simulation model were collected on a large grain farm in Western Kentucky during the 2016 corn harvest season. The harvest and transportation characteristics of this operation were described in detail in the previous grain transportation study. In addition to the previously described data, the mass of grain delivered in each truck, μ_L , was used to quantify how much grain needed to be dried. The dryer used at the example operation was a Sukup tower dryer (model U4018, Sukup Manufacturing Co., Sheffield, IA) with a 5-pt capacity (from 20 to 15% w.b.) of 102 t hr⁻¹ (4,000 bu hr⁻¹), a 91 m³ heating section capacity. It should be noted that the capacity ratings are based on wet grain, 20% w.b. in this example. A maximum unloading rate of approximately 140 t hr⁻¹ (5,500 bu hr⁻¹) (Sukup, 2016). The operation was harvesting white corn, and the dryer was operated at 60 °C as a result.

The method used to adjust drying capacity was evaluated using two approaches. First, RDC estimated from equation (4-4) was compared to RDC as determined from Thompson et al. (1994). This primarily served to evaluate how well the empirical relationships developed approximated the output of the more complex model. Secondly, both the Thompson et al. (1994) model and the proposed RDC adjustment were compared to producer maintained drying records. The records utilized included incoming grain moisture, outlet grain moisture, and unload roller set point. The dryer was operated in manual mode, and the roller set point was given as a percentage of the maximum capacity. The daily operating parameters were estimated using a time-weighted average of moisture grab samples and unload roller set points. The drying capacity estimated from Thompson et al. (1994) was based on the required retention time and the holding capacity of the heating section of the dryer.

Field drying of grain was modeled using equation (4-6) and weather data that was obtained from the Midwestern Regional Climate Center (2018), for the nearest weather station which was located in Bowling Green, KY. A value for β was estimated using the weather data in combination with actual moisture content measurements taken from inbound trucks. The moisture content was determined using a commercial moisture analyzer (model GAC 2100, DICKEY-john Corporation, Auburn, IL), and a total of 339 moisture samples over 14 days were used in the analysis. The best fit value for β was determined from an exhaustive search of values in the range of $0 < \beta < 0.1$ in 0.0001 increments. The final value of β was taken as the value which resulted in the lowest sum of squared errors.

4.4 Results and Discussion

4.4.1 Relative Dryer Capacity

Relative drying capacity (RDC) was determined by running the crossflow drying simulation from Thompson et al. (1994) over a range of drying air temperatures, initial and final moisture contents (135 combinations total). The best fit line for the moisture adjustment function (equation (4-1)) resulted in coefficients of $a=1.610$, $b=0.2022$, and $c=0.006901$, and the resulting fit matched the simulated data with an $r^2=0.99$. The linear temperature adjustment (equation (4-2)) had an r^2 of 0.98 using regression coefficients of

$d=1.0$ and $f=0.0136$. Figure 4-4 shows a comparison of the overall RDC adjustment determined from equation (4-4) and the estimated relatively drying capacity predicted using the individual model runs from Thompson et al. (1994). The RDC values developed in this study cover a broad range of drying conditions and included the effects of drying air temperature, initial moisture content, and final moisture content. Values for RDC are relative to the manufacturer's stated drying capacity at 5-pt moisture removal with a drying air temperature of 104°C. The values for RDC in Figure 4-4 were determined using equation (4-4) with SDC_{dry} set equal to one, and each point represented a different moisture removal and temperature combination. The solid line was included for reference and represents perfect agreement between the two methods. The results shown in Figure 4-4 indicates the method used to adjust drying capacity in this study provides good agreement with those obtained from individual model runs from Thompson et al. (1994), and was appropriate for use. An overview of the relative drying capacity for various temperature reductions and moisture removal levels is shown in Figure 4-5.

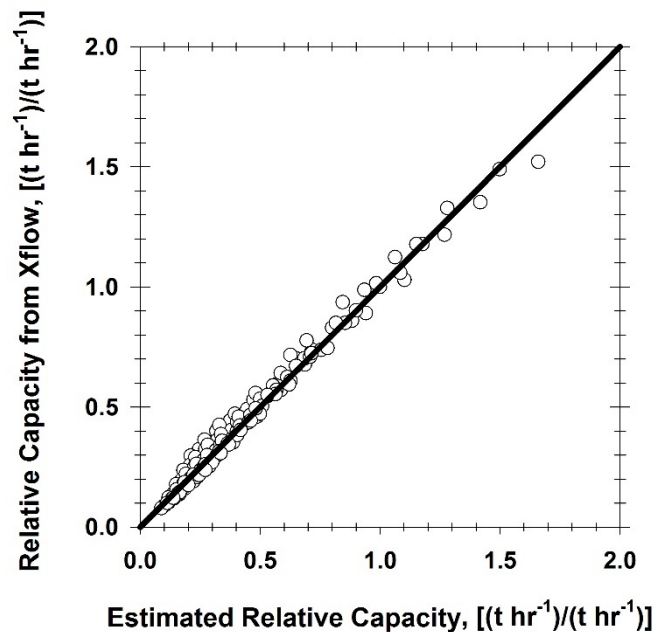


Figure 4-4: Plot of relative drying capacity estimated from Thompson et al. (1994) plotted against the estimated ratio from equation (4-4). 1 to 1 line shown for reference.

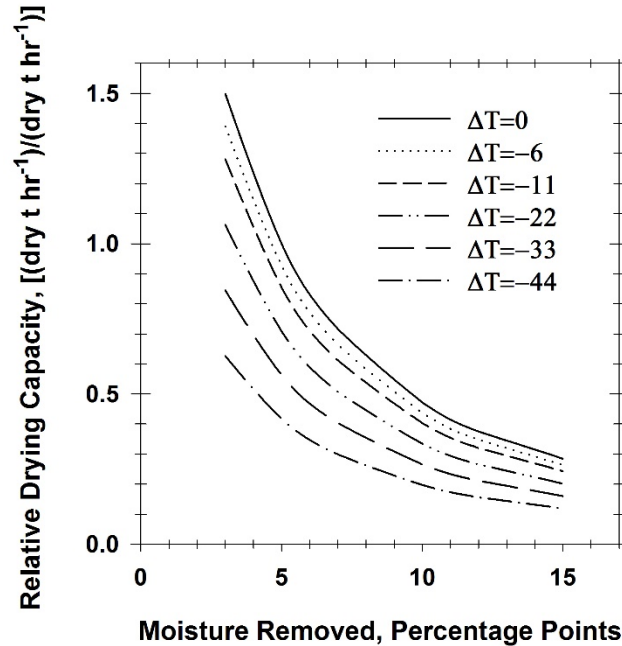


Figure 4-5: Relative drying capacity estimated for various moisture removal levels and temperature reductions. All ratios are relative to 5 points of moisture removal at 104°C.

Table 4-2 shows the average and range in the hourly drying capacity estimated for the example operation. RDC estimated using equation (4-4), and RDC estimated from the crossflow drying model (Thompson et al., 1994) in conjunction with the observed ambient conditions are also shown in Table 4-3. Both methods generally underpredicted the estimated drying capacity. Previous work (Brooker et al., 1992) has shown that drying simulation models often have an error range of $\pm 20\%$ and in this instance 4 out of 11 of the daily drying estimates were outside of that range for both methods. Additionally, both methods evaluated dramatically under predicted the drying capacity for the first two days of drying. This time coincided with the highest moisture incoming grain, yet the estimated drying capacity was the highest on the first two days. The cause of this variation was unknown, but it indicated that there were other factors that were not accounted for occurring on those days. The dryer was operated at 60°C, which was on the low end of typical operation for continuous flow dryers. In this region, ambient conditions play a larger role in dryer performance and could contribute to the variation in dryer performance. The mean daily temperature over the course of the harvest window was 25.5 °C, which is 15.5 °C higher than standard conditions used to simulate dryer

performance. Applying the observed ambient conditions to Thompson et al. (1994) resulted in up to a 15% change in RDC.

Table 4-2 Comparison of Estimated Drying Capacity to Producer Drying Log¹

Day	Estimated Capacity ² (t hr ⁻¹)	Eq. (4-4)		Xflow	
		RDC (t hr ⁻¹)	Error (%)	RDC (t hr ⁻¹)	Error (%)
23-Aug	32.9 [30.7-37.7]	18.0	-45.3	17.2	-47.8
24-Aug	27.9 [27.9-27.9]	15.8	-43.4	14.3	-49.0
25-Aug	20.4 [18.2-23.8]	19.0	-6.5	17.1	-15.9
26-Aug	17.8 [15.4-18.2]	23.5	30.5	21.4	20.4
27-Aug	24.3 [16.8-34.9]	21.8	-10.4	19.7	-19.1
29-Aug	21.4 [16.8-22.4]	20.8	-2.8	18.6	-13.1
30-Aug	23.4 [21.0-27.9]	25.0	6.9	23.3	-0.4
31-Aug	22.4 [21.0-25.2]	22.0	-1.9	19.7	-12.2
1-Sep	27.3 [25.2-30.7]	20.4	-25.3	18.9	-30.9
2-Sep	27.0 [23.8-32.1]	28.5	5.5	25.2	-6.7
3-Sep	29.9 [25.2-32.1]	32.6	8.8	34.1	13.9

1 All capacities are on a dry basis, and the following assumptions were used: drying temperature was 60°C, 139.7 t hr⁻¹ maximum unload capacity, 5-pt rated capacity was 81.3 t hr⁻¹, capacity of heating section was 93 m³. Xflow refers to the granary model (Thompson et al., 1994) run using average daily conditions at the test site. RDC=Relative drying capacity.

2. Estimated drying capacity observed at cooperating farm. Average value is given, range is shown in brackets.

Table 4-3 Summary of Weather Data from the Midwestern Regional Climate Center (2018) for Bowling Green, KY.*

Day	Ambient Temperature (°C)	RH (%)	MC _{in} (%w.b.)	MC _{out} (% w.b.)	Precipitation (mm)	MC _E (% w.b.)
22-Aug	21.8	71.0	26.7	15.5	0	14.7
23-Aug	23.1	72.6	26.4	16.9	0	14.8
24-Aug	27.1	73.8	24.3	14.7	0	14.7
25-Aug	28.6	72.4	23.2	14.9	0	14.3
26-Aug	28.5	73.8	22.1	15.1	0	14.6
27-Aug	27.2	77.0	21.6	14.4	0	15.3
28-Aug	27.0	74.8	-	-	10.2	14.9
29-Aug	26.6	75.3	20.5	13.4	0	15.0
30-Aug	27.5	73.4	20.0	13.9	0	14.6
31-Aug	27.2	75.0	20.9	13.9	0	14.9
1-Sep	24.1	74.9	20.9	13.6	0	15.2
2-Sep	22.0	62.2	20.2	14.6	0	13.1
3-Sep	21.8	69.0	19.4	14.6	0	14.3
4-Sep	24.2	70.5	18.7	-	0	14.3
5-Sep	25.8	68.8	18.8	-	0	13.9
6-Sep	26.1	69.2	-	-	0	13.9

*MC_{in}= average harvest moisture content, MC_{out}= average moisture content out of dryer, and MC_E= equilibrium moisture content using the Modified Henderson Equation from ASABE Standards (2007), RH=average relative humidity.

The method for estimating observed dryer capacity also introduced uncertainty into the analysis. The unloading metering roll settings were used to estimate drying capacity based on the manufacture specified maximum unload rate of 5500 bu hr⁻¹. This was a large assumption because actual unloading rates vary based on variety and flow gate settings, and an error in the maximum capacity results in a proportional error in the estimated capacity. A change of one point in the unload roller setting equates to an approximate 5% change in unload capacity, over the range of unloader settings observed. The estimated drying capacity exhibited large variations as the set point was manually adjusted (Table 4-2-values in brackets are the daily minimum and maximum setting), and varied by an average of 26% on a given day. This illustrates the difficulty in evaluating dryer performance and shows the need for more comprehensive evaluation data. However, similar methods for adjusting drying capacity using the concept of RDC based on simulation outputs have been employed in other studies (Abawi, 1993; Morey et al., 1971), and equation (4-4) generally agreed well with Thompson et al. (1994), although it

underpredicted the capacity by 6.4% (when standard test conditions were used). This changed to an over prediction of 8.2% when Thompson et al. (1994) was run using observed ambient conditions.

4.4.2 Weather Impacts and Grain Moisture Content

Table 4-3 included a daily summary of the weather conditions used to estimate if field work occurred and field drying. The date range when harvest occurred was generally considered early for the area, was considered drier than normal, and precipitation only occurred on a single day over the harvest window, which happened to coincide with Sunday. Due to this, weather delays had no impact over the range of dates examined. Figure 4-6 shows the average daily incoming grain moisture over the course of the harvest window. The observed incoming moisture varied from 26.7% to 18.7% and generally decreased as the season progressed. The slight uptick in moisture later in the harvest window could be due to changes in varieties or planting date. The equilibrium moisture content, based on average daily conditions, varied from 13.1% to 15.3% over the range of dates of interest to this study. The best fitting value for β in equation (4-6) determined from the exhaustive search was 0.081 day^{-1} , and this resulted in a root mean squared error (RMSE) of 0.73 points. The model adequately represented the trend in field drying.

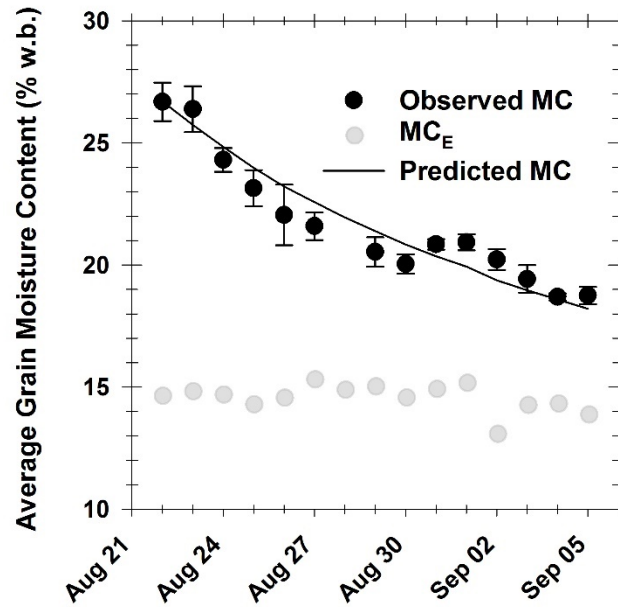


Figure 4-6 Change in harvest moisture content over season. Observed MC is the average daily moisture of incoming grain, MC_E is the grain equilibrium moisture content calculated based on daily weather data and Predicted MC is the predicted moisture content using $\beta=0.081 \text{ day}^{-1}$ using equation (4-6). Error bars represent \pm one standard deviation.

4.4.3 Example Operation System Characteristics

The proposed model was applied to a case study operation to assess its suitability. Table 4-4 provides an overview of the model parameters that were used in the simulation, and the weather data used in the simulation are shown in Table 4-3. Many parameters associated with this operation and their variability were described in detail in the previous study. For this study, load generation rate, $dt_{Load\ Generation}$, and all service times were treated as deterministic values. They were based on all observations over the harvest season. The load generation rate of 17.2 minutes, and average mass of 21 dry tonnes per load corresponded to an average harvest rate of $73.3 \text{ dry tonnes hr}^{-1}$ ($3394 \text{ std. bu hr}^{-1}$). The average time field work occurred over all days was approximately eight hours, so a constant value 480 minutes was used for Hh , on days when harvest occurred. The operation utilized two hopper bottom wet holding bins (5.5 m diameter x 5.7 m tall and 6.1 m diameter x 11.5 m tall), that when combined with the wet holding on the dryer

provided enough wet holding capacity, Q_{wh} , for approximately 18 loads or 378 dry tonnes.

Table 4-4: Parameters Used for the Example Simulation *

Symbol	Value	Units
Daily Simulation Inputs		
$dt_{Load\ Generation}$	17.2	Minutes load ⁻¹
dt_{FT}	5.76	Minutes
$dt_{transport}$	11.6	Minutes
dt_{scales}	2	Minutes
dt_{pit}	12.5	Minutes
dt_{return}	11.6	Minutes
Hh	Max: 480	Minutes
Ht	1440	Minutes
$N_{drivers}$	8	-
N_{trucks}	8	-
Q_{truck}	1	Field unloads truck ⁻¹
Q_{Field_max}	3	Loads
μ_L	21	Tonnes load ⁻¹
Q_{wh}	18	Loads
Q_{Carry}	VBD	Loads
dt_{dry}	VBD	Minutes
Whole Season Parameters		
W_T	6959	Tonnes
β	.0940	Day ⁻¹
MC_{in}	VBD	% w.b.
MC_{out}	15	% w.b.
MC_0	26.7	%w.b.
MC_E	VBD	%w.b.
T_{dry}	140	°F
T_{rated}	220	°F
SDC	4000	bu hr ⁻¹
RDC	VBD	Tonnes hr ⁻¹

*VBD= Variable by day. These are parameters that change over the course of the simulation

4.4.3.1 Example Single Day Simulation

Figure 4-7, Figure 4-8, and Figure 4-9 provide an overview of the harvest simulation for a single day. Aug-27 was selected because it was near the middle of the simulated harvest season and exhibited a number of the behaviors the model was intended to capture. The top portion of Figure 4-7 shows the timing of entities entering (loads generated from harvest) and exiting the system (out of the dryer) over the course of the day, and the bottom portion shows the number of entities waiting at various processes. In this example, loads exiting the system appear at two equal intervals. The mass of grain in each load was constant over the course of the simulation, and the drying rate was determined based on the day the material was harvested. Drying begins as soon as the simulation starts because there was a surplus of 15 truckloads in the wet holding bins from the previous day. The first load dried quickly because it was partially finished drying when the previous day simulation ended. After that point, loads exit the system at constant intervals until all of the previous day's grain was dried. Then new grain exits at a slightly faster pace due to its lower moisture content. The constant load generation rate (harvest rate) resulted in consistent timing between loads entering the system early in the simulation. On the bottom of Figure 4-7, loads from the field arrive faster than they can be dried, causing the wet holding bins to reach capacity approximately two hours into the simulation (simulation begins at the start of harvest). After that point, trucks were slowed down unloading at the pit, causing the number of trucks waiting at the pit to increase. This is shown as up to seven entities, full trucks in this case, being in process. Around 5 hours into the simulation full loads of grain coming out of the field are waiting for a truck to unload onto. At this point in the simulation, grain drying was the system bottleneck and the wet bins, trucks, and in-field holding capacity was full. This resulted in delays for new material entering the system, as shown by the longer period between loads entering the system for the last two loads. After eight hours, the fieldwork window is over and the remainder of the simulation is already harvested grain being moved from the field through drying and storage. The number of entities waiting field side decreases first, followed by full trucks waiting at the pit to unload, and finally, the level of the wet holding bins begins to drop before the simulation ends at 24 hours.

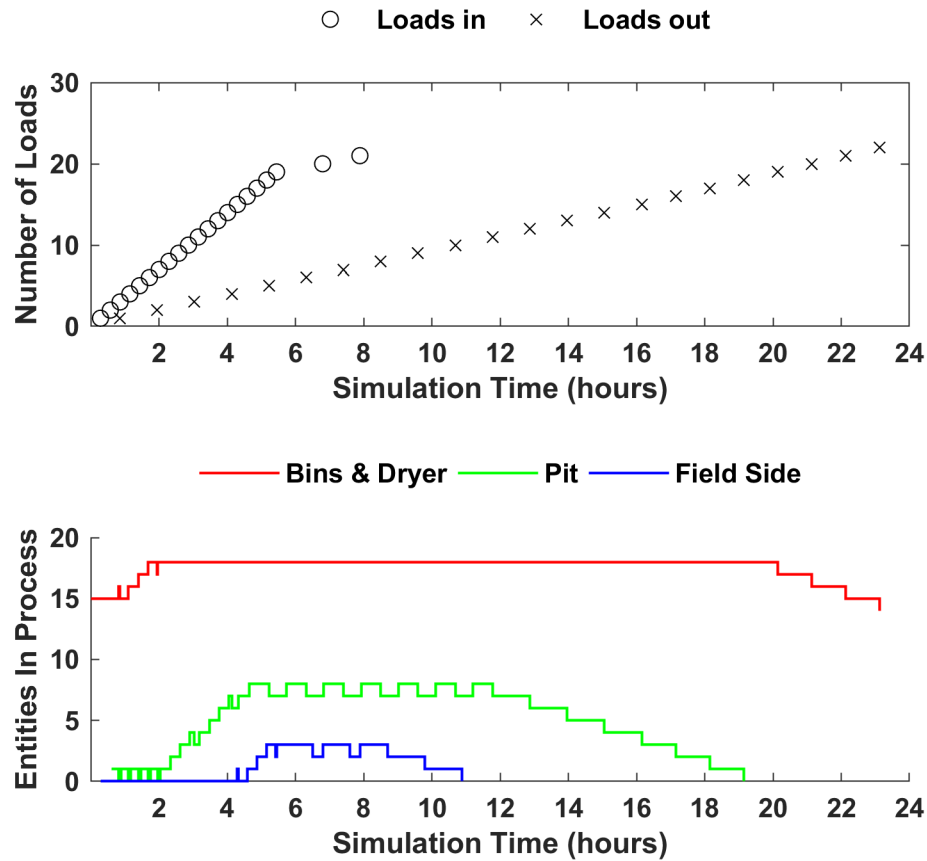
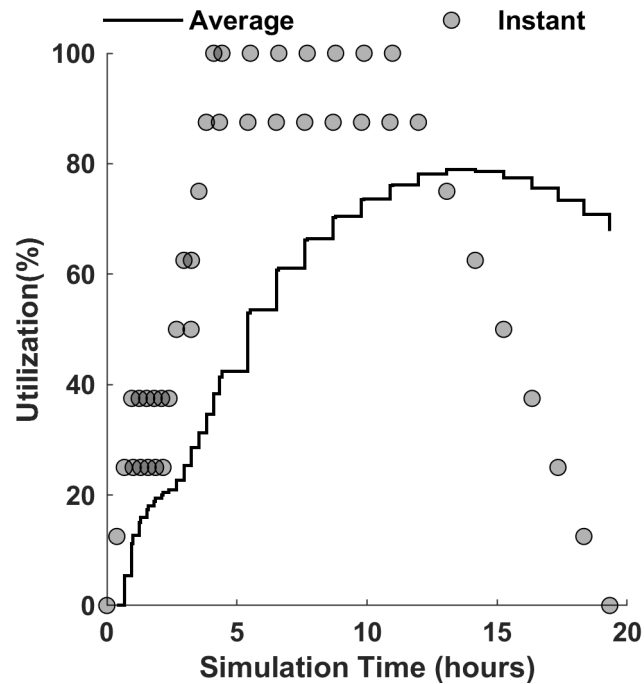


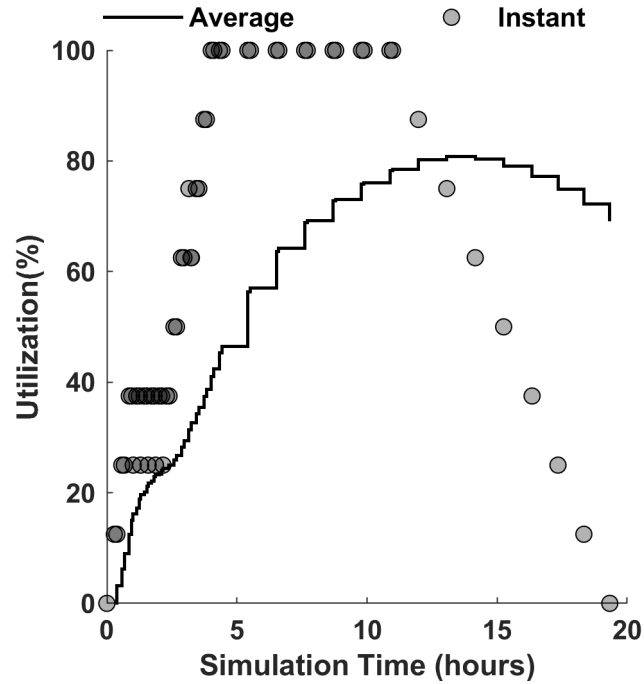
Figure 4-7 Overview of material flow through the harvest system on Aug-27. The top portion of the figure shows loads into and out of the system, and the bottom portion shows the number of entities in process.

Figure 4-8 shows the utilization of driver, truck, and dryer resources over the course of the simulation on Aug-27. The solid black line represents a moving average of utilization of the resources to that point in the simulation. The gray circles represent instantaneous resource utilization estimated when the system state changes. Driver and truck utilization, Figure 4-8 (a), and Figure 4-8 (b), respectively, display very similar trends over the course of the day. Figure 4-8 (a) shows fluctuations in instantaneous driver utilization since, by definition, a truck did not require a driver to be loaded at the field edge. The instantaneous utilization stays between 20-40% for the first portion of the harvest simulation, until the wet holding bins are full, causing the truck and driver utilization to increase as the trucks wait to unload at the storage facility. In the overnight

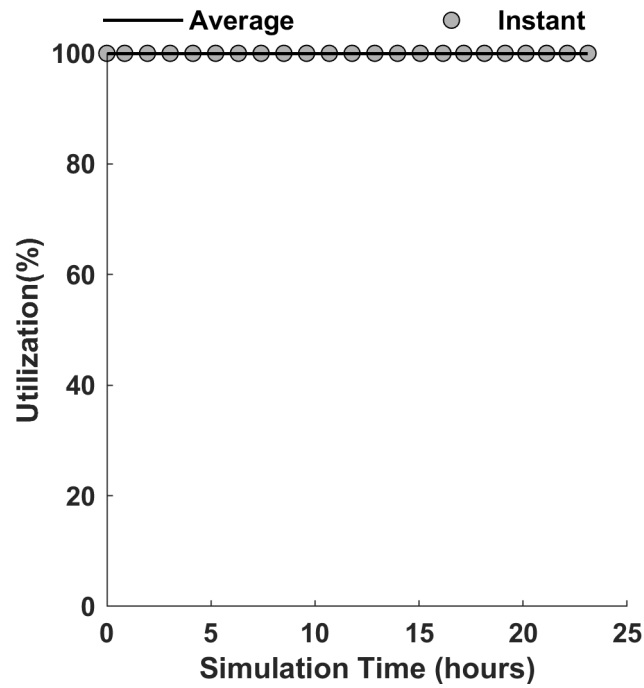
hours, additional loads from the field were transported and all trucks were empty by approximately 19 hours into the simulation. This additional wait time after fieldwork stopped for the day was the behavior that was not explicitly captured by the previous transportation model that assumed unlimited receiving capacity and utilized a variable fieldwork duration. The slight differences between the truck and driver utilization was a result of the model not requiring a driver until after the grain had been transferred to the truck. There was grain in the wet holding bins at the start of the simulation, and the dryer was never able to catch up, resulting in a utilization of 100% over the whole simulation (Figure 4-8 (c)). In this model, the dryer ran continuously, and no time was allotted for breakdowns or maintenance.



(a)



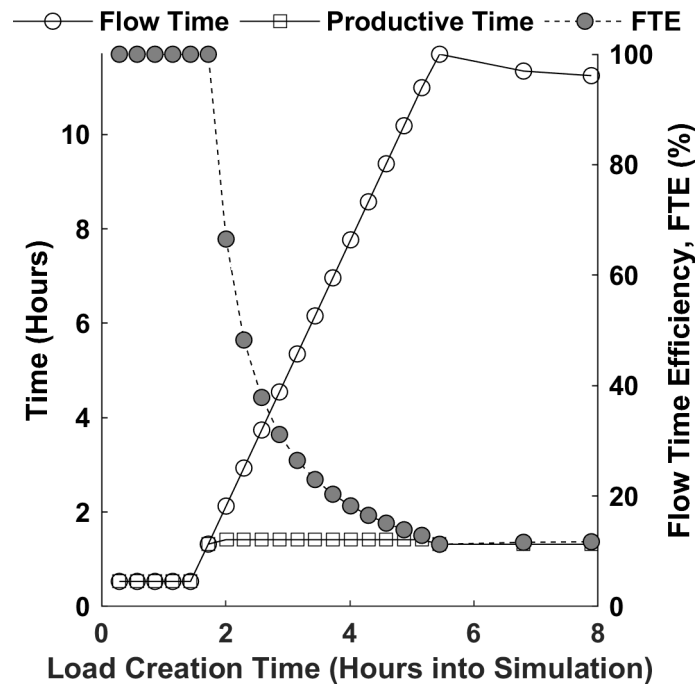
(b)



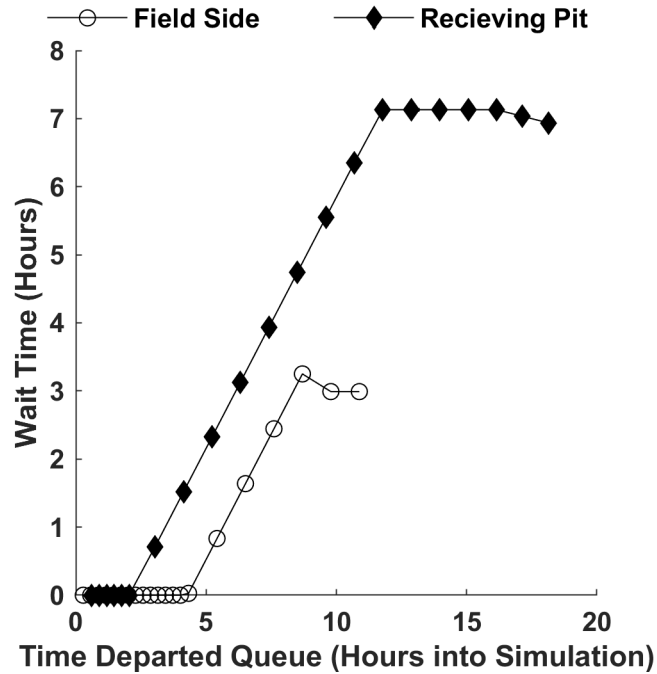
(c)

Figure 4-8 Resource utilization over the course of an example day (Aug-27). The solid line represents the average utilization to that point in the simulation, and gray circles represent the instantaneous utilization. (a) Driver (b) Truck (c) Dryer.

Figure 4-9 provides an overview of material flow through the simulation for Aug-27. Figure 4-9 (a) shows the productive time, flow time, and FTE over the course of the simulation. These concepts were defined in the previous study, but briefly, flow time represented the time span from when a load entered the system to when it was emptied into the receiving pit. Productive time was defined as the time required to complete all handling steps. Flow time efficiency (FTE) was the ratio between the two and was an indicator of the magnitude of the delays in the system. The horizontal axis in Figure 4-9 (a) references the time when the entity entered the system. Initially, there were no delays in the system, so productive time and flow time were equal resulting in FTE equal to 100%. In the context of this analysis, productive time was a measure of how long the entity was in process, and once the wet holding bins were full, productive time increased slightly because the unloading rate at the pit was governed by grain leaving the dryer. In this case, an increase in the productive time is not desirable, but reflects an increase in the time required to handle a load of grain. FTE rapidly decreased after approximately two hours due to the longer flow times that resulted from extended wait time at the receiving pit and field edge (Figure 4-9 (b)).



(a)



(b)

Figure 4-9 Overview of wait time and material flow efficiency for an example day of the simulation (Aug-27). (a) Flow time from the field to unloading at the storage facility, Total productive time, and FTE. These values do not include time spent in wet holding or dryer. (b) Wait time for full loads at the receiving pit, and full grain carts waiting field side.

4.4.3.2 Whole Season Simulation

Table 4-5 shows an overall summary of the simulated resource utilization and wait times described in the previous section, expanded over the whole harvest season. $Q_{wh} Final$ indicates the final fill level of the wet bins at the end of the daily simulation. It peaks on the second day of the simulation, with the wet bins completely full at the end of the day (with 18 entities in the bins). As the incoming grain moisture dropped, the drying capacity increased, and the dryer was able to catch up to harvest after Aug-29. After that point, dryer capacity was sufficient to dry all incoming grain during the same day. The wait time at the field edge was the average time full loads from the field were required to wait for a truck to receive the grain, and the wait time at the receiving pit represented the average time full trucks waited in the queue ahead of the receiving pit. These wait times are reflected in FTE, which varied from a minimum of 32% on to 100% later in the simulation. The minimum value of FTE indicated that the average load required

approximately three times longer than the minimum time to be delivered and was a result of the extended wait times to unload once the wet holding bins were full. Harvest time lost (HTL) represented the amount of time harvest was completely shut down due to a downstream bottleneck. The maximum value of HTL was 3.4 hours and represented a loss of 43% of the available harvesting time.

Table 4-5 Whole Season Overview of Simulated Resource Utilization and Material Flow

Day	WT Field (hours)	WT Pit (hours)	FTE (%)	Truck Util. (%)	Driver Util. (%)	Dryer Util. (%)	HTL (hours)	Q_{wh} Final
22-Aug	0	0.9	87	38.3	36.4	91.3	0	15
23-Aug	0.7	5.4	47	71.8	64.7	96.6	1.9	18
24-Aug	1.2	6.5	32	81.3	70.4	97.9	3.4	18
25-Aug	1.1	5.8	33	82.2	70.8	98.1	3.1	17
26-Aug	0.8	4.6	39	78.4	68.3	96.4	2.8	15
27-Aug	0.7	3.7	46	78.3	67.8	96.3	2.2	14
28-Aug	0	0	0	0.0	0.0	57.6	0	0
29-Aug	0	0	100	28.0	24.4	93.2	0	1
30-Aug	0	0	100	29.0	25.1	91.6	0	0
31-Aug	0	0	100	29.0	25.1	81.3	0	0
1-Sep	0	0	100	29.0	25.1	75.4	0	0
2-Sep	0	0	100	29.0	25.1	68.0	0	0
3-Sep	0	0	100	29.0	25.1	62.7	0	0
4-Sep	0	0	0	0.0	0.0	0.0	0	0
5-Sep	0	0	100	29.0	25.1	53.4	0	0
6-Sep	0	0	100	27.7	24.0	31.6	0	0

WT Field=Wait time at field edge. WT Pit= wait time at receiving pit. HTL= harvest time lost due to a downstream bottleneck. Q_{wh} Final=number of truckloads in the wet holding bins/dryer at the end of the day.

Table 4-6 shows a summary of the actual observed harvest from the farm and the daily simulation expanded over the whole season. There were day-to-day variations between the simulated and observed mass of grain entering the system. The simulation used average values for the whole season, which could explain a portion of the daily variation. The actual operation was able to vary the number of trucks used on a given day and would have allowed more grain to be harvested on days when the lack of wet holding or drying capacity limited harvest. Excluding the first day, the simulation underpredicts the amount of grain harvested early in the season. Large values of HTL on these days and the full wet bin at the end of the daily simulation indicated drying was the bottleneck in

the simulation. This combined with the RDC adjustment that underpredicted the drying rate on these days indicate the dryer operating conditions may have not been fully accounted for. This could have included a drying air temperature higher than recorded, changes in the amount of cooling performed in the dryer, and/or significant differences in hybrid drying rates in the early part of the season. The largest variation between the observed system and the simulation occurred on Aug-31 when only three loads were harvested in the observed system, the cause of the limited harvest on that day was unknown. The first-day harvest also exhibited large variation between the simulated and observed system. The simulation overpredicted the amount of grain harvested, which resulted in a large amount of grain in the wet holding bin at the end of the daily simulation. This combined with a fixed number of transportation vehicles used in the model resulted in an underprediction on the second day. After the sixth day of the simulation, the dryer was able to accommodate the total mass of incoming grain, and for subsequent days the mass of grain into and out of the system was governed by the time harvesting and the load generation rate. The actual operation varied how long fieldwork occurred, and later in the season the producer was able to run longer. The simulation predicted the harvest would require a single day longer than was observed, however in the observed data, grain was harvested on the second to last day, which was a Sunday and violated the assumptions used in the simulation. Additionally, the simulation required all grain be unloaded into storage on the same day it was harvested. In reality, a single load or two would have sufficient time to complete unloading the following day and return to the field before they were needed. Despite the daily variation, Figure 4-10 shows good agreement between the observed and simulated cumulative mass harvested, which indicated the model was adequate to serve as a decision support tool.

Table 4-6 Summary of Grain Entering and Leaving the System

Day	Observed Deliveries	Observed W_{in} (dry t)	Simulated Deliveries	Simulated W_{in} (dry t)	Simulated W_{out} (dry t)
22-Aug	19	361	28	588	273
23-Aug	34	617	17	357	294
24-Aug	24	477	16	336	336
25-Aug	29	575	17	357	378
26-Aug	15	303	18	378	420
27-Aug	28	583	21	441	462
28-Aug	0	0	0	0	294
29-Aug	32	656	28	588	567
30-Aug	30	626	28	588	609
31-Aug	3	44	28	588	588
1-Sep	32	673	28	588	588
2-Sep	33	694	28	588	588
3-Sep	39	850	28	588	588
4-Sep	2	45	0	0	0
5-Sep	20	447	28	588	588
6-Sep	0	0	19	399	399

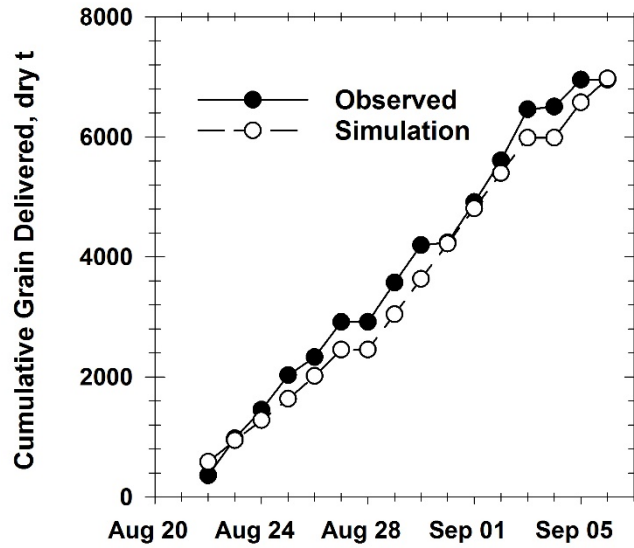


Figure 4-10 Observed and simulated cumulative mass of grain delivered, dry t. Simulation data was based on average input conditions.

4.5 Conclusions

This study presented a whole season simulation model of corn harvest logistics. To account for temperature and incoming moisture content effects on drying capacity, a simplified method to adjust drying capacity relative to the manufacturer's rated capacity was proposed. When applied to the dryer used in this study, and when compared based on relative drying capacity, the proposed method agreed well with simulation results from Thompson et al. (1994). However, the model underpredicted the observed data and in some instances had large errors. There were large amounts of variability in the observed data, and ambient conditions have a large impact on dryer performance at the low drying temperatures observed in this study. The variability in estimated drying capacity made it difficult to accurately assess the proposed method and showed the need to obtain better data for validation. Field dry down was accurately represented over the range of moistures from 26.7% to 18.7%, with an RMSE of 0.73 points. The simulation estimated harvest would require an additional partial day over the observed data, and overall the harvest model showed good agreement with the observed data, based on the cumulative mass of grain delivered over the season. The wait times and HTL early in the harvest simulation were consistent with the expected behavior, and this information could be combined with economic information to evaluate potential system changes.

4.6 References

- Abawi, G. Y. (1993). A simulation model of wheat harvesting and drying in northern Australia. *Journal of Agricultural Engineering Research*, 54(2), 141-158.
doi:<http://dx.doi.org/10.1006/jaer.1993.1009>
- ASABE Standards. (2007). D245. 6—Moisture relationship of plant-based agricultural products (pp. 604-638). St. Joseph, MI: ASABE.
- ASABE Standards. (2014). S448.2: Thin-layer drying of agricultural crops. St. Joseph, MI: ASABE.
- ASABE Standards. (2015a). D497. 6 Agricultural machinery management data. St. Joseph, MI: ASABE.
- ASABE Standards. (2015b). Ep 496.3 Agricultural machinery management. St. Joseph, MI: ASABE.

- ASABE Standards. (2015c). S248.3 Construction and rating of equipment for drying farm crops. St. Joseph, MI: ASABE.
- ASABE Standards. (2015d). S495.1 Uniform terminology for agricultural machinery management. St. Joseph, MI: ASABE.
- Audsley, E., & Boyce, D. (1974). A method of minimizing the costs of combine-harvesting and high temperature grain drying. *Journal of Agricultural Engineering Research*, 19(2), 173-188.
- Babeir, A. S., Colvin, T. S., & Marley, S. J. (1986). Predicting field tractability with a simulation model. *Transactions of the ASAE.*, 29(6). doi:10.13031/2013.30347
- Benock, G., Loewer, O., Bridges, T., & Loewer, D. (1981). Grain flow restrictions in harvesting-delivery-drying systems. *Transactions of the ASAE.*
- Bridges, T. C., Loewer, O. J., Walker, J. N., & Overhults, D. G. (1979). A computer model for evaluating corn harvesting, handling, drying and storage systems. *Transactions of the Asae*, 22(3), 618.
- Brooker, D. B., Bakker-Arkema, F. W., & Hall, C. W. (1992). *Drying and storage of grains and oilseeds*: Springer Science & Business Media.
- Carpenter, M. L., & Brooker, D. B. (1972). Minimum cost machinery systems for harvesting, drying and storing shelled corn. *Transactions of the ASAE.*, 15(3), 515-519. doi:<https://doi.org/10.13031/2013.37942>
- Davis, S., Diegel, S., & Boundy, R. (2007). Transportation energy data book: Edition 26. Oak ridge national laboratory. *ORNL*, 6978.
- De Toro, A. (2005). Influences on timeliness costs and their variability on arable farms. *Biosystems Engineering*, 92(1), 1-13.
- De Toro, A., Gunnarsson, C., Lundin, G., & Jonsson, N. (2012). Cereal harvesting – strategies and costs under variable weather conditions. *Biosystems Engineering*, 111(4), 429-439. doi:<http://dx.doi.org/10.1016/j.biosystemseng.2012.01.010>
- De Toro, A., & Hansson, P. A. (2004). Analysis of field machinery performance based on daily soil workability status using discrete event simulation or on average workday probability. *Agricultural Systems*, 79(1), 109-129. doi:10.1016/s0308-521x(03)00073-8

- Edwards, W. (2014). Estimating the cost for drying corn. *Ag Decision Maker*. Retrieved from <https://www.extension.iastate.edu/agdm/crops/pdf/a2-31.pdf>
- Edwards, W., & Johanns, A. (2012). Wages and benefits for farm employees. *Ag Decision Maker*. Retrieved from <https://www.extension.iastate.edu/agdm/wholefarm/html/c1-60.html>
- Edwards, W., Plastina, A., & Johanns, A. (2016). Grain harvesting equipment and labor in iowa. *Ag Decision Maker*. Retrieved from <https://www.extension.iastate.edu/agdm/crops/pdf/a3-16.pdf>
- Farm Fans Inc. (1999). *Operator's manual c-2130b, c-2140b, c-2160b, c-2175b, and c-21100b grain dryers*. Indianapolis, IN: FFI Corporation.
- Halich, G. (2018). Custom machinery rates applicable to kentucky (2018). *University of Kentucky Cooperative Extension Service*. Retrieved from <https://www.uky.edu/Ag/AgEcon/pubs/customratesKY.pdf>
- Hellevang, K. J. (2013). *Ae701 grain drying*. North Dakota State University.
- Hwang, S., Epplin, F. M., Lee, B.-h., & Huhnke, R. (2009). A probabilistic estimate of the frequency of mowing and baling days available in oklahoma USA for the harvest of switchgrass for use in biorefineries. *Biomass and Bioenergy*, 33(8), 1037-1045. doi:<http://dx.doi.org/10.1016/j.biombioe.2009.03.003>
- Isaac, N. E., Quick, G. R., Birrell, S. J., Edwards, W. M., & Coers, B. A. (2006). Combine harvester econometric model with forward speed optimization. *Applied Engineering in Agriculture*, 22(1), 25-31.
- Jackson, J. J. (2015). *Optimal uses of biomass resources in distributed applications*. (PhD), University of Kentucky, Lexington, KY.
- Johnson, W., & Lamp, B. (1966). *Principles, equipment and systems for corn harvesting*. Wooster, OH: Agricultural Consulting Associates, Inc.
- Kiker, C., & Lieblich, M. (1986). Financial analysis of on-farm grain drying. *Journal of Agricultural and Applied Economics*, 18(2), 73-84.
- Licht, M., Hurburgh, C., Kots, M., Blake, P., & Hanna, M. (2017). *Is there loss of corn dry matter in the field after maturity?* Paper presented at the 29th Annual Integrated Crop Management Conference.

- Liu, Q., & Bakker-Arkema, F. W. (1997). Stochastic modelling of grain drying: Part 2. Model development. *Journal of Agricultural Engineering Research*, 66(4), 275-280. doi:<https://doi.org/10.1006/jaer.1996.0145>
- Loewer, O. J., Benock, G., & Bridges, T. C. (1980). Effect of combine selection and harvesting rate on grain drying and delivery system performance. *Transactions of the ASAE.*, 23(6), 1548-1553.
- Loewer, O. J., Bridges, T. C., & Bucklin, R. A. (1994). *On-farm drying and storage systems*. St. Joseph, MI: ASABE.
- Loewer, O. J., Bridges, T. C., White, G. M., & Overhults, D. G. (1980). The influence of harvesting strategies and economic constraints on the feasibility of farm grain drying and storage facilities. 23(2). doi:10.13031/2013.34605
- Loewer, O. J., Bridges, T. C., White, G. M., & Razor, R. B. (1984). Optimum moisture content to begin harvesting corn as influenced by energy cost. *Transactions of the ASAE.*, 27(2), 362-365.
- Maier, D. E., & Bakker-Arkema, F. W. (2002). *Grain drying systems*. Paper presented at the Proceedings of the 2002 Facility Design Conference of the Grain Elevator & Processing Society, St. Charles, Illinois, USA, July.
- Maier, D. E., & Watkins, A. E. (1998). *Drying of white food corn for quality*. Purdue University.
- Martin, B. A. (2018). *Two essays on whole farm modeling and crop marketing in western kentucky*. (MSc), University of Kentucky, Lexington, KY.
- Midwestern Regional Climate Center. (2018). Cli-mate application tools environment sub_daily data(database). Retrieved 6/15/2018
<https://mrcc.illinois.edu/CLIMATE/>
- Montross, M. D., & Maier, D. E. (2000). Simulated performance of conventional high-temperature drying, dryeration, and combination drying of shelled corn with automatic conditioning. *Transactions of the ASAE.*, 43(3), 691.
- Morey, R. V., Cloud, H. A., & Lueschen, W. E. (1976). Practices for the efficient utilization of energy for drying corn. *Transactions of the ASAE.*, 19(1), 151-0155.
- Morey, R. V., Zachariah, G. L., & Peart, R. M. (1971). Optimum policies for corn harvesting. *Transactions of the ASAE.*, 14(5), 787-792.

- MWPS-13. (1987). Grain drying handling and storage handbook: Midwest Plan Service, Ames, IA.
- Nichols, T. E. (n.d.). *Economics of on-farm corn drying*. NCH-21. North Carolina State University.
- Paulsen, M. R., de Sena, D. G., Jr., de Assis de Carvalho Pinto, F., Zandonadi, R. S., Ruffato, S., Gomide Costa, A., . . . Danao, M. G. C. (2014). Measurement of combine losses for corn and soybeans in Brazil. *Applied Engineering in Agriculture*, 60(6), 841-855.
- Pierce, R., & Thompson, T. (1981). Energy use and performance related to crossflow dryer design. *Transactions of the ASAE.*, 24(1), 216-0220.
- Plastina, A. (2018). *Ag decision maker-estimated costs of crop production in Iowa*. Iowa State University.
- Radajewski, W., Jolly, P., & Abawi, G. Y. (1987). Optimization of solar grain drying in a continuous flow dryer. *Journal of Agricultural Engineering Research*, 38(2), 127-144.
- Rotz, C. A., & Harrigan, T. M. (2005). Predicting suitable days for field machinery operations in a whole farm simulation. *Applied Engineering in Agriculture*, 21(4). doi:10.13031/2013.18563
- Sorensen, C. (2003). Workability and machinery sizing for combine harvesting. *Agricultural Engineering International*, V.
- Sukup. (2016). *Tower dryer owner's operation manual*. Sheffield, IA: Sukup Manufacturing Co.
- Thomison, P. R., Mullen, R. W., Lipps, P. E., Doerge, T., & Geyer, A. B. (2011). Corn response to harvest date as affected by plant population and hybrid. *Agronomy Journal*, 103(6), 1765-1772.
- Thompson, T. L., Peart, M., & Foster, G. H. (1968). Mathematical simulation of corn drying — a new model. *Transactions of the ASAE.*, 11(4), 582.
doi:<https://doi.org/10.13031/2013.39473>
- Thompson, T. L., Peart, R. M., Foster, G. H., Loewer, O., & Bridges, T. (1994). Granary. University of Florida.

- Tippayawong, K. Y., Piriyaageera-anan, P., & Chaichak, T. (2013). Reduction in energy consumption and operating cost in a dried corn warehouse using logistics techniques. *Maejo International Journal of Science and Technology*, 7(2), 258.
- Trego, T., & Murray, D. (2010). *An analysis of the operational costs of trucking*. Paper presented at the Transportation Research Board 2010 Annual Meetings, Washington, DC.
- U.S. Energy Information Administration. (2018). Data for petroleum & other liquids. Retrieved from <https://www.eia.gov/petroleum/data.php>
- USDA-NASS. (2017). Quick stats. *Washington, DC*.

Chapter 5. SENSITIVITY ANALYSIS OF GRAIN TRANSPORTATION AND DRYING SYSTEMS

5.1 Summary

Simulation models for grain harvest systems provide a useful tool to evaluate economic and productivity implications of changes in equipment, operation harvest strategies when specialty grains with differing drying rates are incorporated, and seasonal variability. This study demonstrated the application of a discrete event simulation model for corn harvest, transportation, and drying at an on-farm storage facility. A hypothetical operation was evaluated for a range of seasonal effects. When compared to the baseline configuration, a dry year, where the corn field dried faster, and a slow drying crop slower field dry down rate had the largest impact on the system's operating and drying costs (12.7% decrease and 10.8% increase, respectively). The impact of reducing the drying temperature to maintain quality in drying white corn was also examined. For this specific configuration, there was no impact on the total operating and drying cost, and harvest took six days longer. The reduced drying capacity at lower temperatures resulted in more field drying which counteracted the reduced drying efficiency and increased field time. The use of the model to evaluate impacts of additional equipment on both cost and system performance were demonstrated, and a sensitivity analysis demonstrated how the benefits of increased drying and hauling capacity varied based on how often these systems created a bottleneck in the operation. Based on this hypothetical operation, some combinations of longer transportation distance, and higher harvest rates, increasing hauling and drying capacity could shorten the harvest window by a week or more at an increase in costs of less than \$12 ha⁻¹.

5.2 Introduction

5.2.1 Overview

Grain harvest systems function at their highest level when decisions are made using the best information available. Grain harvest is capital, labor, and energy intensive, and producers must develop their operational plan and select equipment to efficiently and economically move grain from the field through drying and into storage. This is a

complex task that should consider both year to year variability in weather and crop conditions, as well as seasonal variation in equipment performance. Improving the overall harvest capacity of the system can shorten the time required to complete the harvest and mitigate potential yield and quality losses associated with prolonged harvest. It also frees up time and resources to complete other field tasks. The benefits of increasing capacity in one portion of the system is directly dependent on the capacity of the other system components, and for additional grain drying equipment, improved drying capacity can lead to increased energy costs because more grain can be harvested at higher moistures. Harvest simulation models can be used as decision support tools to allow producers to evaluate the potential implications of changes to their system.

Since the 1970's a number of harvest simulation models have been developed to examine aspects of harvest systems. Carpenter and Brooker (1972) examined several farmer-owned and custom harvest system configurations to find the least cost equipment to harvest and dry corn. The model was based on 20 years of weather data and included costs associated with equipment, drying, and losses. The relationship between system components was relatively simple, with daily harvest rates estimated from a normal distribution, and empirical relationships were used to approximate field drying, yield losses, and dryer capacity. Constant hauling costs were based on the annual volume of grain handled, and suitability for fieldwork was estimated based on precipitation and temperature. Harvest rates examined varied from 3.2 to 8.9 t hr⁻¹, which is several times lower than typical harvest rates in modern equipment. This study indicated continuous flow drying should be considered once annual volume was above 1,093 tonnes (43,000 bu). Kiker and Lieblich (1986) used a Monte Carlo simulation to evaluate the profitability of artificial drying equipment in Florida. This model incorporated variability in grain price received and indicated a high probability of a positive return for drying once the annual volume increased above 508 tonnes (20,000 bu).

Morey et al. (1971) presented a dynamic programming simulation to determine the optimum number of hours to harvest each week as a function of the recoverable yield and dryer capacity. Recoverable yield was a function of moisture based on data from Johnson and Lamp (1966), and also assumed a linear decrease in yield as a function of time past November 1st. The results indicated overtime pay could be justified during the critical

harvest periods, which occurred early in the season, and again late in the season as losses began to grow.

Loewer et al. (1984) estimated the ideal moisture content to start harvest by balancing the increased energy used to dry grain at higher moistures against the value of potential losses. This study also utilized the loss data from Johnson and Lamp (1966), and the field drying equations from Morey et al. (1971). The optimum moisture content was shown as a function of the ratio between price of fuel energy to value of grain. For continuous flow dryers, the optimum starting moisture decreased as the price of fuel increased relative to the value of the grain, and generally the more time required to complete the harvest, the higher the optimum starting moisture. The potential benefits of increasing drying capacity were not considered as part of this study. O.J. Loewer et al. (1980) examined the economics of on-farm drying and storage. This study showed harvest should begin around 28% moisture, and indicated drying high moisture grain was more beneficial than field drying for most situations examined.

Many of the previous works discussed here utilized a potential yield loss to justify the additional expense of drying high moisture grain. Generally they relied on loss data from Johnson and Lamp (1966), however, this potential yield and loss data does not reflect improvements in modern hybrids and equipment. The loss evaluation associated with this research showed there was no change in yield or losses until prolonged field drying created lodging in the crop. This was consistent with Thomison et al. (2011) who found increased losses only occurred if harvest was delayed into November where greater lodging occurred, and Licht et al. (2017) who found no dry matter loss as corn was allowed to field dry. It is likely that a major cause of harvest losses is a result of lodging (Paulsen et al., 2014), which can result from weather events or from stalk quality degradation as the crop field dries. Considering these more recent evaluations, a more appropriate evaluation metric for changes to the harvest system would be how much the potential change could reduce the harvest window. The shorter window would have the benefits of freeing resources for other fall operations (planting wheat, harvesting soybeans, etc.), and would reduce the opportunities for a storm to cause lodging and losses.

Other previous works have examined impacts of various components on the overall system. O. J. Loewer et al. (1980) evaluated resource utilization for a range of harvest rates and receiving / wet holding/ drying capacities. Combine and hauling efficiencies were determined relative to their theoretical maximum performance over the simulation, and dryer capacity generally had the largest impact on overall capacity. Isaac, Quick, Birrell, Edwards, and Coers (2006) developed an economic model of combine harvest with a focus on selecting the optimum harvest speed for wheat harvest. The ratio of grain to material other than grain (MOG), yield, daily time available for operations, price, and timeliness influenced the optimum speed and net income. This model was based around a single crop with a constant yield and grain/MOG ratio and knowledge of the combine's functional performance. A constant drying cost was applied to grain harvested above safe storage moisture, and field losses were estimated from a John Deere service publication combined with a shrink adjustment. The authors found a combine speed of 7.9 kph produced the highest net return for the hypothetical operation considered in the model. Tippayawong, Piriyaageera-anan, and Chaichak (2013) presented a case study that demonstrated how logistic techniques could be applied to a grain storage facility in Thailand. The system in their study was much different than what would typically be encountered in the US, but it did demonstrate how activity-based costing (ABC) could be applied in an agricultural setting to reduce energy use.

5.2.2 Drying Efficiency

Artificially drying grain to levels safe for storage is a key component in on-farm storage systems. Energy used in drying is highly variable and is influenced by variety, the initial moisture content, final moisture content, drying airflow rate, and drying air temperature. Pierce and Thompson (1981) and Morey et al. (1976) showed heat energy requirements as a function of drying air temperature and airflow rate for crossflow dryers. Increasing the airflow rate increases the drying capacity but decreases the drying efficiency. Reducing the drying temperature decreases both the drying capacity and energy efficiency but can be necessary to maintain quality, especially in specialty grains. Typical drying efficiencies for continuous flow dryers is in the range of 4 to 10 MJ per kg of water removed from the grain. This range could extend even further at high airflow

rates and low drying temperatures. Additionally, many dryers improve efficiency by recovering a portion of the heat from the grain in the cooling section. The amount of air reclaimed can be adjusted to increase drying airflow based on the incoming moisture to balance energy savings and capacity (Farm Fans Inc, 1999). These aspects were beyond the current investigation.

Current estimated expenditures for corn production (with a yield of 8.5 tonnes per hectare) following soybeans in Iowa have been estimated to total approximately \$1380 ha⁻¹. Rates to custom harvest and haul corn have been estimated at \$104 ha⁻¹, and grain elevators charge approximately \$1.57 per t-pt (\$0.04 per bu-pt) to dry wet grain (Halich, 2018). Another extension source estimated roughly \$120 ha⁻¹ was required to harvest and haul the grain to the first storage facility; while drying and handling would require an additional \$89 ha⁻¹ (Plastina, 2018). These costs are highly variable and depend in large part on the organization of the operation along with labor and energy prices.

5.2.3 Motivation

This study was the culmination of the previous modeling efforts aimed at developing a system model for grain harvest logistics. The overall objective of this analysis was twofold. First the potential of the model as a decision support tool was demonstrated by applying it to examine performance and cost changes associated with changes made to a hypothetical farm. Secondly, a sensitivity analysis was conducted to explore how changes in material handling and drying demand due to increased harvest rate and transportation time impacted the overall system. Whole season utilization of the available harvest capacity, time required to complete the operation, and operating costs associated with harvesting, transporting and drying the grain were determined for each system configuration. The specific objectives of this analysis were:

1. Examine seasonal variations in system performance due to changing weather conditions and field dry down rates.
2. Evaluate the impact of reduced drying temperature required to maintain quality in food grade white corn.
3. Demonstrate how the model could be applied to evaluate changes in the harvest system.

4. Conduct a sensitivity analysis by evaluating system performance and operating costs over a range of harvest rates and transportation times.

5.3 Materials and Methods

5.3.1 Model Application

This study utilizes the previously developed whole season discrete event simulation (DES) model of grain harvest to conduct a sensitivity analysis and explore performance and economic impacts of changing system parameters. Two approaches were used when applying the model. The first portion of the analysis utilized a baseline system configuration with a series of whole season simulations, in which parameters were changed to demonstrate their impact on the overall system. Secondly, the baseline operation and several other configurations were evaluated over a range of transportation distances and harvest rates to evaluate changes associated with increased material handling and transportation demand. All model development, processing and analysis was conducted using MATLAB and the SimEvents toolbox in Simulink (R2017b, The MathWorks Inc., Natick, MA).

The model was driven by an entity generation process, which allows material to enter the system at predetermined time intervals. Previous efforts in this project incorporated these values explicitly as inputs to the model. For this discussion, model field equipment characteristics and performance were utilized to determine the rate at which material enters the system. Field equipment characteristics (speed, width, etc.) were used along with (ASABE Standards, 2015b) to estimate the effective area capacity (C_a) and material harvest capacity (C_m). This was combined with the grain cart capacity, number of unloading events required to fill a truck and the average mass loaded on a truck to estimate the entity interarrival time or load generation rate (equation (5-1)). The harvest rate, C_m , was assumed constant, and it was assumed the grain cart was sufficient to not impede the combine. All other model parameters were defined as previously described. Throughout this analysis dry mass refers to 0% moisture material.

$$dt_{Load\ generation} = \frac{\mu_L}{Cm * Q_{truck}} * 60 \quad (5-1)$$

Where:

$dt_{Load\ generation}$ = Time between arrivals of full grain carts (minutes)

μ_L = Mass of grain per truck (dry t truck⁻¹)

Cm = material harvest capacity from ASABE Standards (2015b), dry t hr⁻¹

Q_{truck} = number of unloading events to fill a truck

60 = number of minutes in one hour

5.3.2 System Configurations

The system configuration with the operational parameters outlined in Table 5-1 served as a baseline configuration for evaluating changes to the system. The simulated operation was assumed to operate a single combine and grain cart to harvest 810 ha (2000 ac) of field corn. A class 7 combine with a 12-row head that had a constant field speed of 5.6 kph (3.5 mph) was selected based on data from ASABE Standards (2015a) and Edwards et al. (2016). The average yield was assumed to be 8.11 dry tonnes per ha (152 std. bu ac⁻¹), which was the ten year average for the Midwestern agricultural region of Kentucky (USDA-NASS, 2017). Three semi-trucks and two drivers hauled grain from the field to the storage facility, which had a single worker present at all times when harvest and drying occurred. The average transportation time was assumed to be 20 minutes, and a truck could unload in a minimum of 15 minutes. The minimum unload time was an optimistic estimate for an operation this size, and O. J. Loewer et al. (1980) indicated pit and receiving conveyor size can influence combine and delivery equipment efficiency. However, grain receiving equipment was not specifically examined in this analysis, and it was beneficial to avoid it becoming the system bottleneck. A 320 m³ (9088 bu) hopper bottom wet holding bin was selected, along with a cross-flow dryer with 14.7 dry t hr⁻¹ (730 bph at 20% moisture) rating at 5-pts moisture removal. A drying temperature of 104 °C (220 °F) was selected, and it was assumed harvest started at 9:00 am each morning. A period of 10 hours each day were allotted for fieldwork and grain transportation and drying could occur continuously.

Table 5-1: System Characteristics for Baseline System

Parameter	Value	Description	Unit
<i>Hh</i>	600 (10)	Duration of fieldwork	Minutes (hr)
<i>Ht</i>	1440 (24)	Total length of daily simulation	Minutes (hr)
<i>Area</i>	810 (2000)	Total area to harvest	ha (ac)
<i>Yield</i>	8.11 (152)	Average yield	dry t ha ⁻¹ (std bu ac ⁻¹)
<i>N_{combines}</i>	1	Number of combines	-
<i>S_{combine}</i>	5.6 (3.5)	Average Combine speed	kph (mph)
<i>RowSpace</i>	0.762 (30)	Row spacing	m (in)
<i>N_{row}</i>	12	Number of rows on corn head	-
<i>V_{combine}</i>	12.3 (350)	Combine onboard storage	m ³ (bu)
<i>E_f</i>	0.7	Field Efficiency	-
<i>Cm</i>	29.25 (1354)	Combine material harvest capacity	dry t ha ⁻¹ (std bu ac ⁻¹)
<i>Ca</i>	3.6 (8.9)	Combine area harvest capacity	ha hr ⁻¹ (ac hr ⁻¹)
<i>dt_{Load generation}</i>	42	Time between arrivals of full grain carts	Minutes cart ⁻¹
<i>N_{cart}</i>	1	Number of grain carts	-
<i>V_{cart}</i>	35.3 (1000)	Maximum cart capacity	m ³ (bu)
<i>dt_{FT}</i>	6	Field transfer time	Minutes
<i>Q_{Cart}</i>	1	Number of field unloading events to fill a truck	Carts truck ⁻¹
<i>N_{drivers}</i>	2	Number of drivers	--
<i>N_{trucks}</i>	3	Number of trucks	--
<i>dt_{transport}</i>	20	Time from field to facility	Minutes
<i>μ_L</i>	20.5 (950)	Mass of grain per truck load	dry t load ⁻¹ (std. bu load ⁻¹)
<i>dt_{scales}</i>	4	Weigh and inspect duration	Minutes
<i>dt_{pit}</i>	15	Unload duration	Minutes
<i>V_{bins}</i>	320 (9088)	Storage capacity of wet bins	m ³ (bu)
<i>T_{dry}</i>	104 (220)	Actual drying air temperature	°C (°F)
<i>T_{rated}</i>	104 (220)	Air temperature used to determine dryer capacity	°C (°F)
<i>SDC</i>	14.8 (730)	Stated drying capacity at <i>T_{rated}</i> and 5 pts removal	dry t hr ⁻¹ (20% bu hr ⁻¹)
<i>SEF</i>	4651 (2000)	Stated drying efficiency 25%-15%	kJ kgH ₂ O ⁻¹ (BTU lbH ₂ O ⁻¹)
<i>V_{dryer}</i>	82	Wet holding before dryer	m ³ (bu)
<i>β</i>	0.0812	Field dry down rate coefficient	day ⁻¹
<i>Year</i>	2016	Year weather data was used from	year
<i>MC₀</i>	28	Initial moisture content on Sept 1	(%w.b.)
<i>MC_{out}</i>	15	Moisture content out of the dryer	(%w.b.)
<i>N_{Storage}</i>	1	Workers at storage facility	persons

An overview of the alternative system configurations evaluated are shown in Table 5-2. All changes were relative to the baseline configuration described in Table 5-1, and all system characteristics except those explicitly stated remained unchanged. Parameters examined are separated into several subsections. Seasonal effects were examined by changing the input weather data and field dry down rate, the effect of reduced drying temperature associated with changing to a specialty crop, such as white corn, was evaluated. Finally, the impact of increasing the capacity of specific components in the system was examined.

Table 5-2: System Variations Explored

Name	Description	Summary of Changes
Baseline	Basic operations outlined in Table 5-1	-
Seasonal		
Slow drying	Base operation, with a slower field dry down rate	$\beta = 0.06$ (Morey et al., 1971)
Fast drying	Base operation, with a faster field dry down rate	$\beta = 0.10$
Dry year	Base operation, simulated using weather data from a dry year	2009 Weather data 49 working days est. Sept 1-Oct 31
Wet year	Base operation, simulated using weather data from a wet year	2010 Weather data 34 working days est. Sept 1-Oct 31
Wet year, double drying capacity	Base operation, simulated using weather data from a wet year	2010 Weather data 34 working days est. Sept 1-Oct 31
Crop / drying temperature		
White Corn	Base operation, assuming producer was growing white corn.	Yield Reduced by 13% (Martin, 2018) Dryer Operated at 60 °C
White Corn Delayed	Base operation, assuming producer was growing white corn and delayed harvest until field moisture was 25%.	Yield Reduced by 13% (Martin, 2018) Dryer Operated at 60 °C No harvest until MC _{in} <25 %w.b.
Equipment		
Additional driver	Base operation with an additional driver.	$N_{drivers} = 3$
Double dryer capacity	Base operation with doubled dryer capacity.	Included annual cost of ownership for new equipment SDC=29.7 dry t hr ⁻¹ (1460 BPH at 20%)
Equipment for changes for a minimally equipped operation		
Minimally Equipped	Base operation, minus one truck and with half the drying and wet holding capacity	$N_{trucks} = 2, V_{bins} = 160 \text{ m}^3$ SDC=7.4 dry t hr ⁻¹
Additional truck	Minimally equipped operation with an additional truck.	Included annual cost of ownership for new equipment $N_{trucks} = 3$
Double dryer capacity and additional truck	Minimally equipped operation with an additional truck and larger dryer.	Included annual cost of ownership for new equipment $N_{trucks} = 3,$ SDC=14.8 dry t hr ⁻¹ (730 BPH at 20%)

Field dry down of grain and suitability for fieldwork was modeled using hourly weather data for Bowling Green, KY obtained from the Midwestern Regional Climate Center (2018). Ten years of hourly data (2008-2017) were evaluated for field dry down and days suitable for fieldwork. Field dry down was estimated using a field dry down rate parameter and grain equilibrium moisture content relationships as previously described. It was assumed the starting moisture content was 28% w.b. on Sept. 1 and the baseline dry down rate parameter was carried forward from the previous whole farm application ($\beta = 0.0812$). All configurations utilized the same initial moisture content, and the effects of delayed harvest was not a major focus of this analysis. The baseline weather data used was for 2016, and effects of a slower or faster drying variety were examined by changing the dry down rate parameter. A slower drying crop was simulated using $\beta = 0.06$, which was the value assumed by Morey et al. (1971). A faster drying crop was simulated by increasing β by a similar amount ($\beta = 0.1$). Conditions suitable for fieldwork were determined as previously described, using a daily accumulated precipitation threshold < 6.35 mm. Field drying and days suitable for field work were determined for each of the ten years of weather data, and seasonal effects were examined by applying the simulation to one of the wettest years (2009) and one of the driest (2010).

Switching from field corn to a specialty or food grade variety can provide producers a premium at market, but these crops require careful processing to maintain quality. Specifically, drying temperature should be reduced to minimize stress cracks in the kernels and using a drying air temperature of 60°C has been recommended (Montross & Maier, 2000). This has the effect of reducing the dryer capacity and efficiency. These effects were examined using the white corn and white corn delayed configurations outlined in Table 5-2. It was assumed white corn had an average yield that was 87% of regular yellow corn (Martin, 2018). It should be noted that the area capacity of the field equipment was not changed in this evaluation, and the baseline initial moisture content and dry down coefficients were used. Reducing the drying temperature greatly reduced the drying capacity at the highest moisture levels, so a second scenario was examined where the grain was allowed to field dry to 25% before harvest began. This was the only configuration where effects of delayed harvest were considered.

Finally, system components were changed to demonstrate how the developed model could be used as a decision support tool to simulate impacts of new equipment on the overall system. Changes resulting from increasing drying capacity, adding additional trucks, and increasing the number of truck drivers were evaluated. Two changes were evaluated for the baseline configuration. Adding a driver to the baseline has the potential to increase the transportation capacity of the system and doubling the size of the dryer could increase overall system capacity early in the season. The baseline configuration was relatively well equipped, so an alternate system that was minimally equipped, which could show larger changes in performance as system parameters were adjusted, was also examined. The minimally equipped configuration was identical, except only two trucks were employed, and the wet holding and drying capacity were reduced by half. The effects of adding a truck and adding a truck plus doubling the dryer size were examined in this case. These changes were outlined under the equipment section of Table 5-2, and the annual ownership cost for the new equipment was included in the harvest costs.

The final portion of this analysis focused on examining system performance over a range of transportation distances and harvest rates. The whole season was simulated over all combinations of transportation times from 15 to 60 minutes, in 5-minute intervals, and harvest rates in nine equal intervals over the range 2.5 ha hr⁻¹ to 4.7 ha hr⁻¹. This represented the baseline harvest rate $\pm 30\%$. The sensitivity analysis was run for the baseline configuration, the baseline configuration with doubled drying capacity, the baseline configuration with doubled drying capacity plus an additional driver, and for the minimally equipped operation. For each case, the seasonal average cost per unit area, field capacity utilization, and length of harvest were determined.

5.3.3 Harvest Costs

The values used to estimate the total operating costs for each system configuration are summarized in Table 5-3. Cost associated with equipment operation are classified as operating costs, which depend directly on how much the equipment is used and ownership costs, which are independent of equipment use (ASABE Standards, 2015d). This analysis was presented in terms of operating costs associated with harvesting, transporting, and drying grain. Ownership costs associated with the baseline operation

were not included because they would remain essentially unchanged regardless of how the system was operated. However, when considering additional equipment added to the system, the annual ownership cost of the additional equipment was considered. Additionally, timeliness and the value of potential yield losses were neglected from this analysis.

Table 5-3: Labor and Equipment Cost Estimates*

Parameter	Value	Notes
<i>Propane</i>	\$0.53 l ⁻¹ (\$2 gal ⁻¹)	Midwest regional average (U.S. Energy Information Administration, 2018)
<i>Electric</i>	\$0.1 kWh	
<i>Diesel</i>	\$0.93 l ⁻¹ (\$3.5 gal ⁻¹)	5 year average (U.S. Energy Information Administration, 2018)
<i>LR_{combine}</i>	\$20.1 hr ⁻¹	Labor rate (LR) for crop production supervisor (Edwards & Johanns, 2012)**
<i>LR_{cart}</i>	16.7 hr ⁻¹	Average hourly rate (Edwards & Johanns, 2012)**
<i>LR_{Truck}</i>	16.7 hr ⁻¹	Average hourly rate (Edwards & Johanns, 2012)**
<i>LR_{dryer}</i>	18.4 hr ⁻¹	Average salary rate (Edwards & Johanns, 2012)**
Combine fuel use	\$55.2 hr ⁻¹	Calculated from ASABE Standards (2015b), Assuming 268 kW
Combine lube	\$5.5 hr ⁻¹	10% of fuel use
Combine R&M	\$29.92 hr ⁻¹	Repair and Maintenance (R&M) (Edwards et al., 2016)
<i>ER_{Combine}</i>	\$90.6 hr⁻¹	Total combine operating cost per hour
Cart tractor fuel use	\$42.2 hr ⁻¹	Calculated from ASABE Standards (2015b), Assuming 205 kW
Tractor and cart lube	\$4.2 hr ⁻¹	10% of fuel use
Tractor R&M	\$5.0 hr ⁻¹	1% of purchase price (\$250k tractor/ @ 500 hr yr ⁻¹)
<i>ER_{Cart}</i>	\$51.4 hr⁻¹	Total grain cart tractor operating cost per hour
Truck travel speed	72.4 kph (45 mph)	(Jackson, 2015)
Truck fuel economy	2.55 km ¹ (6 mpg)	(Davis, Diegel, & Boundy, 2007)
Truck R&M	\$ 24.3 hr ⁻¹	based on \$0.54 mi ⁻¹ (Edwards et al., 2016)
Truck fuel use	\$26.25 hr ⁻¹	Based on speed and transport time
Insurance & other	\$3.0 hr ⁻¹	(Trego & Murray, 2010)
<i>ER_{trucks}</i>	\$53.55 hr⁻¹	Total operating cost per hour transport time
Additional truck AoC	\$2,500 yr⁻¹	Annual ownership cost from (ASABE Standards, 2015b) based on \$20k purchase price, \$0 salvage, i=5%, 10 yr service life
Large dryer upgrade AoC	\$8,200 yr⁻¹	Annual ownership cost from ASABE Standards (2015b) based on \$80k purchase price, 10% salvage, i=5%, 20 yr service life
Small dryer upgrade AoC	\$4,100 yr⁻¹	Annual ownership cost from ASABE Standards (2015b) based on \$40k purchase price, 10% salvage, i=5%, 20 yr service life

* Parameters in bold were used in the analysis. Others were intermediate.

** Adjusted to 2018 dollars.

The labor rates for the various positions in the operation were estimated from the average hourly total compensation from the survey conducted by (Edwards & Johanns, 2012). The values were adjusted to 2018 dollars, and it was assumed the combine operator would be the highest paid person and was assigned the average rate for row crop production personnel with supervisor duties. Grain cart operators and truck drivers were given the average hourly rate, and the manager at the storage facility was assumed to receive the average salaried rate. These values assumed all workers were employees of the farm, and a different organizational structure could greatly impact the labor rates.

The variable operating cost for field equipment were fuel use, oil for lubrication, and repair and maintenance (R&M). Fuel use was estimated using the formulas from (ASABE Standards, 2015b) and was based on an assumed horsepower for each piece of equipment (Throughout this section refer to notes in Table 5-3 for details regarding the cost estimation). Propane and diesel fuel prices were estimated using data from U.S. Energy Information Administration (2018). Lubrication costs were assumed to be 10% of fuel costs and combine R&M were based on the values reported in Edwards et al. (2016). R&M for the tractor pulling a grain cart was more difficult to estimate in this context, so 1% of the initial purchase price was assumed. Costs associated with trucking were estimated using an assumed average speed of 72.4 kph (Jackson, 2015) and an average fuel economy of 2.55 km l⁻¹. Fuel consumption was estimated for travel time only, and no idle fuel consumption was accounted for in this analysis. Truck R&M was estimated from Edwards et al. (2016), which was high compared to sources from traditional trucking (Trego & Murray, 2010). However, this value was deemed more appropriate for this application because grain trucks tend to be older and driven fewer miles per year. Taxes, insurance and other costs associated with trucking were estimated at \$3 hr⁻¹ based on Trego and Murray (2010).

The initial purchase price was used to estimate the annual ownership costs when additional equipment was added to the system. For this analysis that included additional trucks and two different size dryers (one each as an upgrade to the baseline and minimally equipped configurations). The initial purchase prices were estimated from a brief survey of online classified advertisements, and the annual ownership cost (AoC)

was determined using the standard formulas in (ASABE Standards, 2015b) and the values given in Table 5-3.

5.3.4 *Drying Energy Use and Cost*

Drying efficiency as a function of incoming moisture content and drying temperature was estimated from multiple simulation runs of the cross flow drying model developed by Thompson et al. (1994). The simulation was run using an airflow rate of $64.3 \text{ m}^3 \text{ min}^{-1} \text{ m}^{-3}$ (80 cfm bu^{-1}) and ambient conditions of 10°C and 60% relative humidity. Estimated energy use per unit mass of water removed was estimated for a range of drying temperatures from 104°C to 49°C and a range of initial moisture contents from 30% to 18%. A constant final moisture content of 15% was assumed, and all references to moisture content in this study were on a wet basis. To incorporate changes in drying efficiency into the simulation, a second order polynomial was fit to the simulation output using the Curve Fitting toolbox in MATLAB. The best fit equation that was used to estimate drying efficiency is shown in equation (5-2). To apply the drying efficiency relationship to a specific case, a known or assumed drying efficiency from 25% to 15% was used to offset the estimated drying capacity using equation (5-3), where the offset of $6797 \text{ kJ kgH}_2\text{O}^{-1}$ was the 25% to 15% drying efficiency from Thompson et al. (1994). Visual assessment indicated equation (5-2) was in line with (Morey et al., 1976), however this drying efficiency estimation did not account for potential heat reclamation or other energy saving options.

$$\begin{aligned} \text{drying}_{eff}(MC_{in}, T_{dry}) \\ = 18053 + 239 * MC_{in} - 236 * T_{dry} + 7.92 * MC_{in}^2 \\ - 7.80 * T_{dry} * MC_{in} + 2.10 * T_{dry}^2 \end{aligned} \quad (5-2)$$

Where:

$\text{drying}_{eff}(MC_{in}, T_{dry})$ = Drying efficiency for a given drying temperature and incoming moisture. Energy used per unit mass of water removed ($\text{kJ kgH}_2\text{O}^{-1}$)

MC_{in} = Incoming grain moisture content, (%w.b.)

T_{dry} = Drying temperature ($^\circ\text{C}$)

$$adj_drying_{eff}(MC_{in}, T_{dry}) = drying_{eff}(MC_{in}, T_{dry}) + (SEF - 6797) \quad (5-3)$$

Where:

$adj_drying_{eff}(MC_{in}, T_{dry})$ = Adjusted drying efficiency, offset to accounting for known drying efficiency

SEF = Known or assumed drying efficiency from 25% to 15% (kJ kgH₂O⁻¹)

Total drying energy used and costs were estimated on a daily basis. The overall season fuel use and costs were calculated utilizing the sum of the daily costs. To estimate fuel use on a given day, the amount of water removed needed to be known. Equation (5-4) provides the total amount of water removed based on the moisture content and dry mass of grain harvested on a given day. Once the mass of water removed is known, equation (5-5) was used to estimate the fuel energy needed to evaporate the water. It was assumed the dryer ran on propane for this study, and equation (5-6) was used to estimate the daily propane use. Equation (5-7) was used to estimate the daily fuel cost, and equation (5-8) was used to estimate electricity costs associated with drying based on 5% of fossil fuel use (Edwards, 2014). The total drying cost for each day was determined from equation (5-9).

$$H2O_{out} = M_{in} * 1000 * \left(\frac{100}{100 - MC_{in}} - \frac{100}{100 - MC_{out}} \right) \quad (5-4)$$

Where:

$H2O_{out}$ = Mass of water removed by the dryer (kgH₂O)

M_{in} = Total mass of grain harvested on a given day (tonnes dry basis)

MC_{out} = Dryer exiting moisture, assumed 15% (%.w.b.)

$$Drying_{energy} = adj_drying_{eff}(MC_{in}, T_{dry}) / 1000 * H2O_{out} \quad (5-5)$$

Where:

$Drying_{energy}$ = Fuel energy used in drying (MJ)

$$Drying_{fuel} = Drying_{energy}/LHV * .93 \quad (5-6)$$

Where:

$Drying_{fuel}$ =Fuel used in drying (l)

LHV = Heating value of propane, assumed 25.3 MJ l⁻¹

0.93=Combustion efficiency

$$Drying_{FC} = Drying_{fuel} * Propane \quad (5-7)$$

Where:

$Drying_{FC}$ = Daily cost for propane \$ day⁻¹

$Propane$ = Propane unit cost, assumed \$0.53 l⁻¹ (\$ l⁻¹)

$$Drying_{EC} = Drying_{energy}/3.6 * 0.05 * Electric \quad (5-8)$$

Where:

$Drying_{EC}$ = Electricity costs associated with operating the dryer (\$)

$Electric$ =Electric price, assumed to be 0.10\$ kWh⁻¹

3.6=conversion factor from MJ to kWh

$$DE = Drying_{FC} + Drying_{EC} \quad (5-9)$$

Where:

DE = Daily total drying energy cost (\$ day⁻¹)

5.3.5 Labor and Equipment Cost Estimation

Cultural practices and the availability of labor can play a large role in the labor and equipment costs associated with a specific operation. The following section describes the method and assumptions used for this analysis. The combine field time on each day was estimated utilizing equation (5-10). This equation only charged time to the combine from the beginning of the simulation until the last load was delivered to the field edge. This did not penalize the combines for remaining time in the work day that was not sufficient to harvest additional loads. For example, if the last load arrives 15 minutes

before the end of fieldwork and it takes 20 minutes to harvest the next load, no additional grain would be harvested and that 15 minutes would not count against the combine. This assumption also mimics a producer stopping harvest early if there is a downstream bottleneck. For example, early in the harvest season if fieldwork is stopped and would not resume until after the fieldwork window had passed, the model only charges combine time until the last load was created. This may result in partial days being harvested early in the season. Combine labor was assumed to be 110% of the combine operating time (equation (5-11)). The total labor and equipment operating cost for the combine was estimated from equation (5-12).

$$FT_{combine} = T_{fwe} * N_{combines} \quad (5-10)$$

Where:

$FT_{combine}$ = Combine field time (hr day⁻¹)

T_{fwe} = Timestamp when the last entity was created (hours)

$N_{combines}$ = Number of combines operating in the field

$$Labor_{combines} = T_{fwe} * N_{combines} * 1.1 \quad (5-11)$$

Where:

$Labor_{combines}$ = Total manhours for combining on a given day (hours)

$$Cost_{combine} = Labor_{combines} * LR_{combine} + FT_{combine} * ER_{combine} \quad (5-12)$$

Where:

$Cost_{combine}$ = Total operating cost for combines (\$ day⁻¹)

$LR_{combine}$ = Combine labor rate (\$ hr⁻¹)

$ER_{combine}$ = Combine hourly operation costs (\$ hr⁻¹)

Equation (5-13) was used to estimate the number of hours charged to tractors operating grain carts, and the operator's time was assumed equal to the grain cart tractor field time. The full duration of fieldwork was charged to the number of grain carts

operating in the field until after the last load was created. After that point it was assumed that a single operator could manage transferring any remaining grain, and their time was charged until the field queue was empty. The total operating cost for grain cart tractors was determined from equation (5-14).

$$FT_{carts} = T_{fwe} * N_{carts} + (T_{FQe} - T_{fwe}) * 1 \quad (5-13)$$

Where:

FT_{carts} = Field time for tractors pulling grain carts (hr day⁻¹)

T_{FQe} = Timestamp when the field queue was empty (hours)

N_{carts} = Number of grain carts operating in the field

$$Cost_{carts} = FT_{carts} * (LR_{cart} + ER_{cart}) \quad (5-14)$$

Where:

$Cost_{cart}$ = Total operating cost for grain cart tractors (\$ day⁻¹)

LR_{cart} = Labor rate for grain cart operator (\$ hr⁻¹)

ER_{cart} = Grain cart tractor hourly operating costs (\$ hr⁻¹)

The time spent transporting grain was determined from Equation (5-15). No idle time was included when determining the field time for transportation equipment, and fuel use while trucks were idling was neglected. Labor hours for truck drivers were estimated from equation (5-16). It was assumed all drivers were working from the start of the day until their last load for the day arrived on farm. Once a driver's last load for the day was placed in the queue in front of the receiving pit, it was assumed the driver could quit for the day and the worker monitoring the storage facility would be responsible for unloading the trucks overnight. If fewer loads were delivered to the storage facility than drivers were present in the system configuration, it was assumed that fewer drivers were used on that day. The total operating cost to haul grain from the field to the storage facility was determined from equation (5-17). The last cost component that needed to be estimated was the labor to manage the storage facility and dryer. It was assumed an employee was dedicated to the dryer the entire time it was in operation. Equation (5-18) was used to

estimate the dryer labor requirement and accounted both continuous and partial day operation. The costs associated with labor at the dryer was estimated from equation (5-19).

$$FT_{Trucks} = \sum_{j=1}^J dt_{transport_j} \quad (5-15)$$

Where:

FT_{Trucks} = Transportation equipment field time (hours day⁻¹)

j = number of the load delivered on a given day

J = Total number of loads delivered

$$Labor_{drivers} = \begin{cases} \sum_{j=J-N_{drivers}}^J Tfs_j, & \text{if } J > N_{drivers} \\ \sum_{j=1}^J Tfs_j, & \text{otherwise} \end{cases} \quad (5-16)$$

Where:

$Labor_{drivers}$ = Total manhours for hauling on a given day (hours day⁻¹)

Tfs_j = Timestamp when the j^{th} load finished at the scales and enters the pit queue (hours)

$N_{drivers}$ = Number of workers hauling grain on a given day

$$Cost_{trucks} = Labor_{drivers} * LR_{Truck} + FT_{Trucks} * ER_{Truck} \quad (5-17)$$

Where:

$Cost_{trucks}$ = Total operating costs for hauling grain (\$ day⁻¹)

LR_{Truck} = Labor rate for truck drivers (\$ hr⁻¹)

ER_{Truck} = Hauling hourly operation costs (\$ hr⁻¹)

$$Labor_{dryer} = \begin{cases} Tfd_j * N_{Storage}, & \text{if } Q_{wh_end} = 0 \\ Ht, & \text{otherwise} \end{cases} \quad (5-18)$$

Where:

$Labor_{Dryer}$ = Total manhours for hauling on a given day (hr day⁻¹)

Tfd_j = Timestamp when the final load finished drying (hours)

$N_{Storage}$ = Number of workers at the storage facility

Ht = Total simulation time (hours)

Q_{wh_end} = Wet holding level at the end of the day

$$Cost_{dryer\ labor} = Labor_{dryer} * LR_{dryer} \quad (5-19)$$

Where:

$Cost_{dryer\ labor}$ = Labor cost associated with operating the dryer (\$ day⁻¹)

LR_{dryer} = Labor rate paid to the person supervising the dryer (\$ hr⁻¹)

5.3.6 Evaluation

This analysis was focused on system performance over the whole season, and seasonal totals were determined by summing the results from the individual days. In addition to the overall total harvest operating cost, the data was separated by total drying energy costs and equipment operating costs. The equipment operating costs were comprised of the equipment operating cost (fuel, repairs, lube, maintenance), labor cost, and where applicable the annualized ownership cost of additional equipment. All costs were normalized on a per unit area basis. In addition to cost, several other metrics were used to evaluate the various system configurations. The number of calendar days required to complete the harvest was determined for each configuration and served as an indicator of how changing the system impacted the time required to complete the harvest. Field capacity utilization (FCU) was a performance measure used to evaluate how much material was harvested compared to the maximum. FCU was the ratio of the mass of material harvested on a given day to the maximum if there were no delays in harvest (equation (5-20)). This value varied by day and generally increased to some steady state value as the season progressed. The number of days into the simulation when FCU

reached its sustained maximum value was also reported for each configuration. This was an indicator of how long into the season incoming moisture and drying capacity were restricting harvest.

$$FCU = \frac{Min}{Cm * Hh} * 100 \quad (5-20)$$

Where:

FCU = Field capacity utilization (%)

Cm = Material capacity of the field machinery (t hr⁻¹)

Min = Total mass of grain harvested on a given day (t)

5.4 Results and Discussion

5.4.1 Simulation Overview

Figure 5-1 provides an overview of the field capacity utilization over the course of the harvest season for both the baseline configuration as well as the minimally-equipped configuration. This figure illustrates how harvest capacity changes over the course of the season. On the first day of the simulation, the baseline configuration had sufficient hauling and wet holding capacity to use full harvest capacity. On subsequent days the utilization changed based on the initial level in the wet holding bins and drying capacity. As the season progresses and the incoming moisture content decreases, the system eventually comes to a steady-state level of field capacity utilization, which was 10 calendar days for the baseline configuration. In contrast, the minimally equipped configuration had reduced transportation, wet holding, and drying capacity. This configuration took 22 days before it was able to utilize the full field capacity available and took 19% longer to complete harvest. Over the whole season, the average field capacity utilization was 90% and 75% for the baseline and minimally equipped configuration, respectively. The model allowed grain to be harvested until wet holding was full, regardless of how long the wet material would be held before drying. Allowable storage time was not included in this model but incorporating it would have the effect of reducing the wet holding capacity early in the simulation.

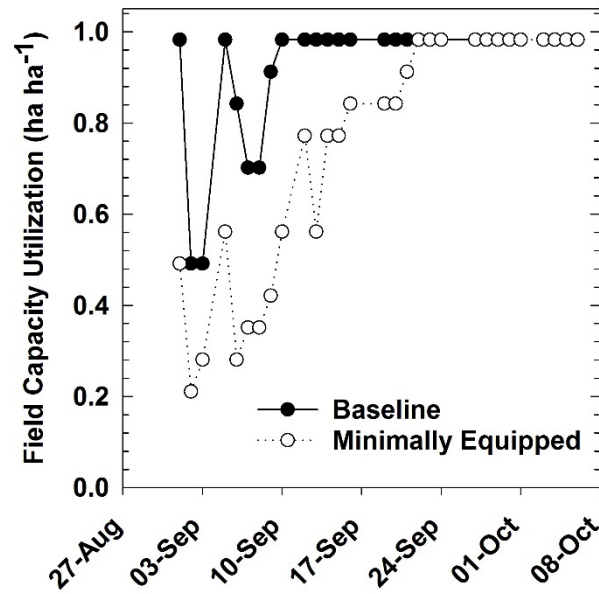


Figure 5-1: Change in field capacity utilization over the course of the simulated harvest season.

The amount of time field equipment operated each day was calculated taking into account occasions when harvest stopped early due to a downstream bottleneck that prevented additional grain from being harvested before the end of the fieldwork period. Figure 5-2 shows the actual duration of fieldwork for each day over the course of the season. This represented the time from the start of the daily simulation to the time the final load entered the system. Sundays and days not suitable for fieldwork were omitted from the figure for clarity. The figure displays a similar trend to Figure 5-1, where the duration of fieldwork was limited for some days early in the season, before reaching a maximum value as the season progressed. The shorter duration of fieldwork combined with temporary delays due to downstream bottlenecks manifested in the reduced field capacity utilization shown in Figure 5-1. The shorter fieldwork duration on the last point in each series represents the final partial day required to finish the harvest.

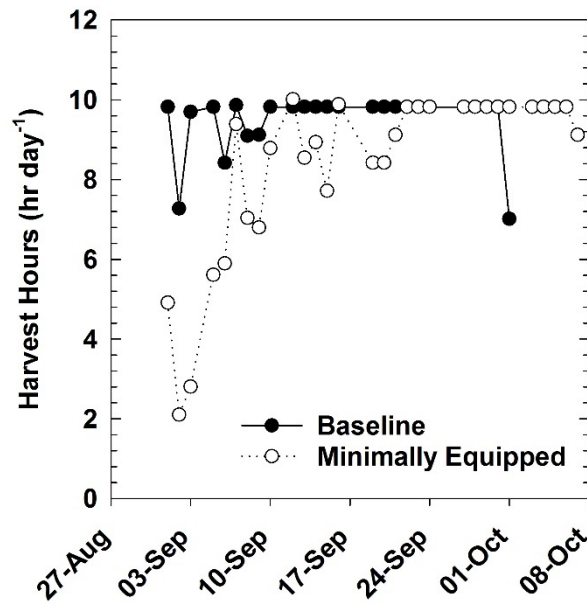


Figure 5-2: Change in field time over the course of the harvest season.

Figure 5-3 shows the total energy costs (propane + electric) associated with drying the grain for the baseline and minimally equipped configuration. The totals are shown for the day the material was harvested, and do not necessarily represent the day the material was dried. For example, if there was a surplus of five loads harvested over what could be dried on a given day, the energy cost for those loads were counted on the day they were harvested, even though they would not be dried until the following day. Drying costs generally decreased as the grain field dried, and local variations were due to changes in the total mass harvested on a given day. Increased drying capacity had the effect of increasing drying energy used. The baseline configuration in Figure 5-3 had higher energy costs because more grain was harvested at higher moisture contents early in the season. The decision to dry or place the grain directly in storage was based on a moisture content threshold of 15% for all configurations. This level could be increased slightly if natural air drying was used to condition grain in bins. However, that was beyond the scope of this investigation, and utilizing the same moisture content threshold allowed a uniform comparison between days.

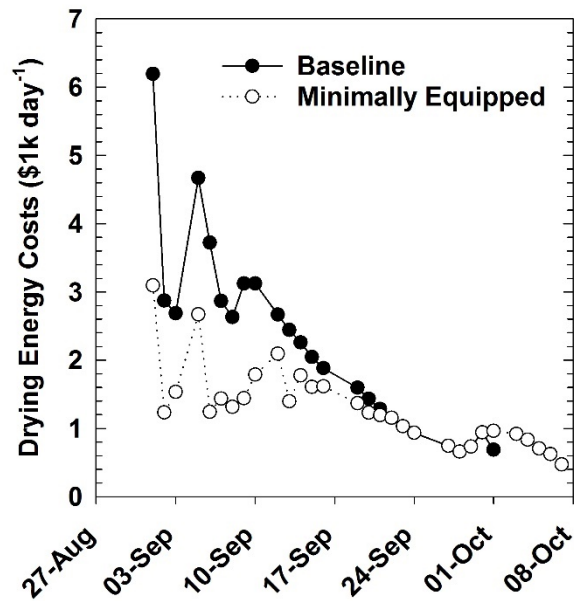


Figure 5-3: Change in drying energy usage over the course of the harvest season.

5.4.2 Seasonal Impacts

Table 5-4 shows a summary of the results from the seasonal variations explored. Calendar days was the number of days required to complete the operation and included both working days and days when no fieldwork occurred. The minimum, maximum, and average FCU indicated the variability in and overall utilization of the available harvest capacity, over the whole season. Many of the configurations in Table 5-4 had the same minimum and maximum values of FCU, which does not fully describe the variability between configurations. The number of days into the simulation before field capacity utilization reached its maximum sustained utilization indicated how long the system operated at a reduced capacity. Sustained implies that the occasional day with high utilization early season was ignored (Figure 5-1). This generally represented the point when the system was no longer sensitive to the incoming grain moisture content. The bottleneck once the maximum level of FCU was obtained could still be any component of the system. E&L represented the total per unit area equipment operating and labor costs. This included the operating costs for combines, grain cart tractors, and trucks plus labor costs to operate the field equipment, drive trucks, and manage the storage facility. Where

applicable, this value included the additional annual ownership cost of additional resources. DE represented per unit area costs associated with electricity and propane used in grain drying. Average values shown were in terms of the whole season. The baseline configuration is shown in bold, and subsequent tables follow a similar layout.

Table 5-4: Seasonal Impacts on System Performance

	Calendar days (days)	Average MC (% w.b.)	Average FCU (ha ha⁻¹)	Min FCU (ha hr⁻¹)	Max FCU (ha hr⁻¹)	Time to Max FCU (days)	E&L (\$ ha⁻¹)	DE (\$ ha⁻¹)	Total (\$ ha⁻¹)
Baseline	31	19.2	80	49	98	10	89	67	157
Slow drying	33	20.3	86	42	98	13	91	83	174
Fast drying	31	18.5	90	49	98	8	88	56	144
Dry year	31	18.2	90	49	98	6	86	51	137
Wet year	43	19.1	94	49	98	5	85	66	151
Wet year, 2x dryer capacity	42	19.3	98	98	98	1	91	69	159

*Average MC= weight average moisture content of all grain harvested over the season. FCU=Field capacity utilization.

Time to Max FCU= number of days until the system reaches its sustained maximum FCU.

E&L=Equipment operating and labor costs. Includes annual ownership cost for additional equipment, where applicable.

DE=Drying energy costs

All configurations evaluated in Table 5-4 eventually reached a field capacity utilization of 98%. The baseline operation took a total of 31 days to complete harvest at an average cost of \$157 ha⁻¹. Drying energy use was estimated at \$67 ha⁻¹, which was 6% higher than the drying cost estimated from Halich (2018) (\$67 ha⁻¹ using 4.2 pts removed at \$0.04 per bu-pt). Equipment and labor charges were lower than the custom combine, grain cart, and hauling rate of \$104 ha⁻¹ from Halich (2018). However, the values in Table 5-4 did not include fixed costs for the field equipment but did include labor at the storage facility. The Iowa State University production cost estimate bulletin estimated the cost of harvesting, transporting, and drying corn at approximately \$212 ha⁻¹ (Plastina, 2018). If the fixed costs used by Plastina (2018) were included here, the baseline configuration estimated a 4.7% higher total cost. These values are highly dependent on the assumed price of diesel fuel, propane, and the assumed labor rate and structure. This discussion is not intended as a comment on the referenced values but serves to illustrate the model and baseline configuration produce values that are reasonable and realistic.

When the dry down coefficient was reduced to $\beta = 0.06$, the number of days required to complete the operation increased by two days. The average field capacity utilization decreased 3.5 percentage points, primarily due to the increased number of days before the system reached steady state utilization. The slow field drying rate had the highest average moisture at 20.3% and was the most expensive of all the seasonal variations explored. Operating costs increased slightly, but increased drying costs accounted for the majority of the \$17 ha⁻¹ increase in harvest costs. The major difference between the baseline configuration and the dry year was the lower equilibrium moisture contents predicted in the dry year, which effectively resulted in a faster drying crop, especially later in the season. The dry year and the faster dry down rate ($\beta = 0.10$) produced similar behavior. In both cases, maximum capacity utilization was reached earlier in the season, but the overall harvest took the same length of time as the baseline configuration. Faster field drying resulted in a decrease in both operating and drying costs, with an 8.2% and 12.5% decrease in total costs for the faster dry down rate and dry year respectively.

When applied to a wet year the total length of harvest increased to 43 days. This increase was primarily due to six consecutive days during the middle of the harvest that

were not suitable for fieldwork. Additionally, days not suitable for fieldwork early in the season allowed the dryer to ‘catch up’ with harvest and resulted in an average field capacity utilization over the course of the season of 94%. The higher field capacity utilization resulted in a reduction in operating costs, and the average moisture content and drying energy costs were similar to the baseline configuration. The effects of doubling the drying capacity during the wet year had no impact on the length of harvest but did increase field capacity utilization to 98% for the entire season, indicating drying capacity was not the overall system bottleneck in this case. The additional annual ownership cost of the larger dryer account for the majority of the increase in cost (5%) relative to the base configuration during the wet year.

5.4.3 Drying Temperature

The impact of growing white corn on the system performance is shown in Table 5-5. The main differences considered in this configuration was a 13% reduction in yield and reducing the drying temperature to 60°C. Field equipment operation, initial moisture content, and dry down rate remained consistent with the baseline configuration. The total length of the harvest was increased to 37 days, and the average field capacity utilization was reduced to 75%. It took 19 days for the system to reach the sustained maximum field capacity utilization, which was 84%. The delays in the system that prolonged harvest were due primarily to the reduced drying capacity that resulted from the temperature decrease. The per unit area equipment and labor costs were increased due to the extended harvest period, but the lower capacity meant that more grain was harvested at lower moistures, reducing the drying energy costs. These tradeoffs between energy savings and increased harvesting costs surprisingly resulted in no change in total per ha⁻¹ costs. However, these costs resulted from harvesting 13% less material. This indicates, for this specific example, that the premium for growing white corn would only need to surpass the value of the lost yield. However, in practice, differences in drying rates and maturity dates between the varieties would impact the analysis. The reduced yield could also impact field machinery capacity, but these effects were beyond the scope of the current investigation.

Table 5-5: Impacts of Switching Reduced Drying Temperature*

	Calendar days (days)	Average FCU (ha ha⁻¹)	Min FCU (ha hr⁻¹)	Max FCU (ha hr⁻¹)	Time to Max FCU (days)	E&L (\$ ha⁻¹)	DE (\$ ha⁻¹)	Total (\$ ha⁻¹)
Baseline	31	90	49	98	10	89	67	157
White corn	37	75	21	84	19	93	64	157
White corn, delayed start	38	80	28	84	19	91	50	142

*FCU=Field capacity utilization. Time to Max FCU= number of days until the system reaches its sustained maximum FCU.

E&L=Equipment operating and labor costs. Includes annual ownership cost for additional equipment, where applicable.

DE=Drying energy costs

The reduced drying capacity resulted in grain spending excessive time in wet holding early in the season (data not are shown). This excess grain would require special management to prevent spoilage and could be controlled by limiting the daily harvest at higher moistures or by delaying harvest altogether to allow more field drying. Delaying the start of harvest until the incoming grain moisture was 25% was evaluated in Table 5-5. This had the effect of increasing the average field capacity utilization and reducing the total harvest costs by 9.6%, primarily through reduced drying costs. However, this came at the cost of increasing the length of harvest by one day over the base case white corn configuration.

5.4.4 Operating Characteristics

This section illustrates how the model could be applied as a decision tool to evaluate changes in equipment capacity. The impact of changing the system configuration was summarized in Table 5-6. This table includes changes to the baseline configuration as well as to the alternate minimally equipped configuration. The addition of a driver to the baseline configuration resulted in the number of trucks and drivers being matched. This change to the system did not have any impact on the overall system performance, at least with the relatively short transportation time used in the baseline configuration. The additional driver did, however, result in a slight increase in labor costs. Doubling the size of the dryer (large dryer upgrade) reduced the length of harvest by two days and increased the average field capacity utilization to 98%. The reduction in equipment and labor costs largely offset the \$10.1 ha⁻¹ annual ownership cost for the dryer. The total costs increased by 6.4%, most of which was a result of drying more grain at higher moistures.

Table 5-6: Impacts of Additional Equipment*

	Calendar days (days)	Average FCU (ha ha⁻¹)	Min FCU (ha hr⁻¹)	Max FCU (ha hr⁻¹)	Time to Max FCU (days)	E&L (\$ ha⁻¹)	DE (\$ ha⁻¹)	Total (\$ ha⁻¹)
Baseline	31	90	49	98	10	89	67	157
Additional driver	31	90	49	98	10	93	67	160
Double dryer size	29	98	98	98	1	91	76	167
Minimally Equipped	37	75	21	98	22	100	48	148
Additional truck	37	75	21	98	20	100	49	149
Double dryer size & additional truck	33	86	42	98	10	97	63	160

*FCU=Field capacity utilization. Time to Max FCU= number of days until the system reaches its sustained maximum FCU.

E&L=Equipment operating and labor costs. Includes annual ownership cost for additional equipment, where applicable.

DE=Drying energy costs

The minimally equipped operation utilized two trucks, two drivers, and had half of the wet holding and drying capacity compared to the baseline configuration. The base case for this configuration took 37 days to complete, with an average field capacity utilization of 75%. It took 22 days before the sustained maximum capacity was reached, and the harvesting cost per hectare was estimated at \$148. Aside from reaching maximum capacity two days earlier, adding an additional truck to this configuration had little impact on the overall system performance. Savings in operating costs offset almost half of the annual cost for the additional truck, and this configuration resulted in a \$1.6 ha⁻¹ increase in cost overall. If the dryer size was doubled and an additional truck was added to the system, the total length of harvest would be reduced by four days, and the average field capacity utilization increased to 86%. The upgraded dryer, in this case, was the small dryer upgrade shown in Table 5-3, and the additional costs for the upgrades was \$8.2 ha⁻¹. For this configuration, the decrease in equipment and labor costs, more than made up for the annual ownership costs of the additional truck and dryer upgrade. However, the larger capacity resulted in more grain dried at higher moistures, which increased drying energy costs. Overall the increased capacity comes at the cost of \$12 per ha. This configuration was identical to the baseline operation, except for having half the wet holding capacity. This lack of wet holding prolonged the season by two days.

5.4.5 Sensitivity Analysis

The final portion of this study examined how the system performance changed with respect to transportation distance and harvest rate. Figure 5-7 shows a contour plot of the seasonal average field capacity utilization over a range of transportation distances from 15-60 minutes and a harvest rate of 2.5 to 4.7 ha hr⁻¹. The baseline configuration was operating at the point noted as **A** on the figure and was the baseline shown in Table 5-4 through Table 5-6. If the transportation time was doubled to 40 minutes (**B**), the field capacity utilization would remain unchanged. This indicates that between those two points over the course of the season there was a surplus in transportation capacity. Point **C** represents the same system with a 40-minute transportation time and a 4.5 ha hr⁻¹ harvest rate. Moving to this area of operation decreased the field capacity utilization to approximately 70%, over the whole season. After accounting for field capacity

utilization, points **A**, **B**, and **C** all have essentially the same effective area capacities. This indicated, for the 40-minute transportation distance, increasing the harvest rate of the field equipment (by increasing combine speed) would not improve the effective harvest rate for the whole system. Figure 5-5 shows the combine status for an example day for both the baseline configuration (**B**) and the increased harvest rate (**C**). The horizontal axis represents the simulation time, and the shaded area represents portions of time when the harvest was stopped due to a downstream bottleneck. The configuration with the higher harvest rate hits a bottleneck sooner in the day, and they occur more often. Field capacity utilization can be interpreted as the portion of time harvest occurs over the fieldwork window. For example, at a field capacity utilization of 70%, harvesting would occur on average 7 out of the 10 hours available for fieldwork. These are seasonal totals, and day to day the operation would vary, especially early in the season when the moisture content was high.

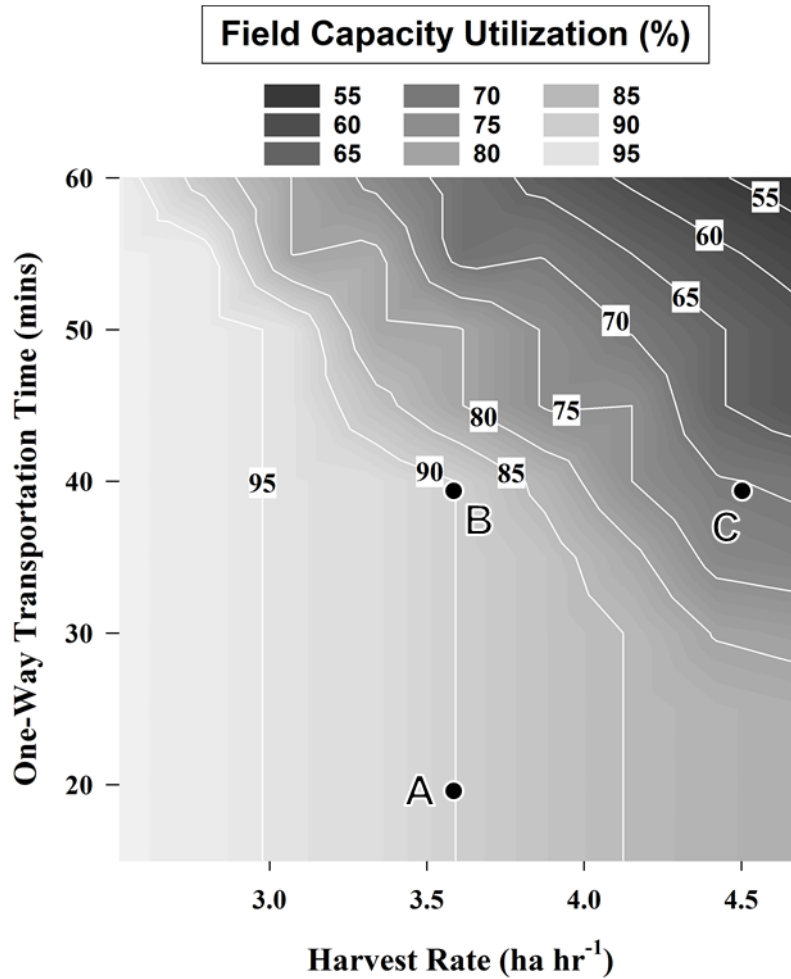


Figure 5-4: Whole season field equipment area capacity utilization as a function of transportation distance and harvest rate. Shown for the baseline configuration. **A** represents the operating point of the baseline configuration. **B** represents doubling the transportation time, and **C** represents a point with an increased harvest rate and transportation time.

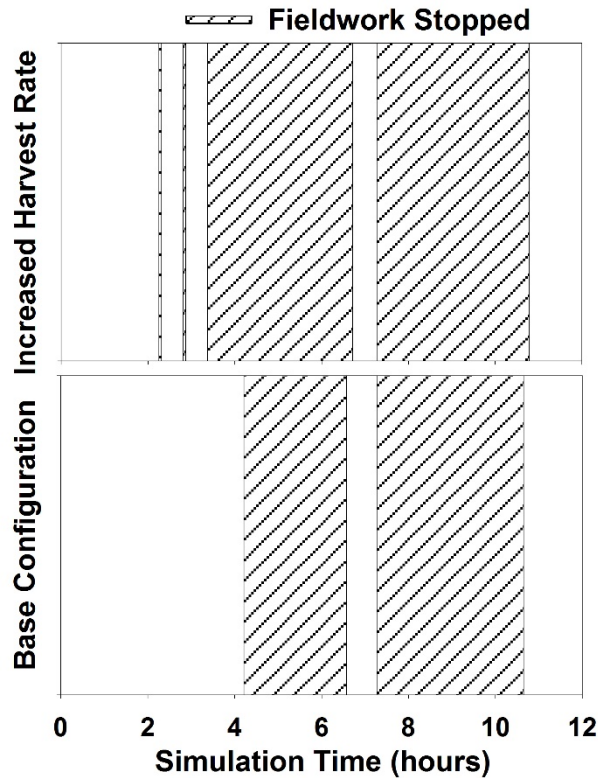


Figure 5-5: Comparison of fieldwork delays due to a downstream bottleneck for the base configuration and an increased harvest rate of 4.5 ha hr^{-1} . The transportation time was 40 minutes, and the timescale was relative to 9:00 am (Day 2 of simulation).

Figure 5-6 shows field capacity utilization for the minimally equipped operation. This configuration shows more sensitivity to the transportation distance and harvest rate than the baseline configuration (Figure 5-4). The difference in field capacity utilization was due to the limitations of the transportation, wet holding, and drying equipment. In contrast to the baseline configuration, moving from **A** to **B** decreased the overall field capacity utilization by approximately 5 percentage points. (75% to 70%), which indicated that doubling the transportation time resulted in an increased occurrence of bottlenecks downstream from the field equipment. Moving from point **B** to **C** also produced a larger decrease in field capacity utilization, with only 55% of the available field capacity being utilized at the higher harvest rate.

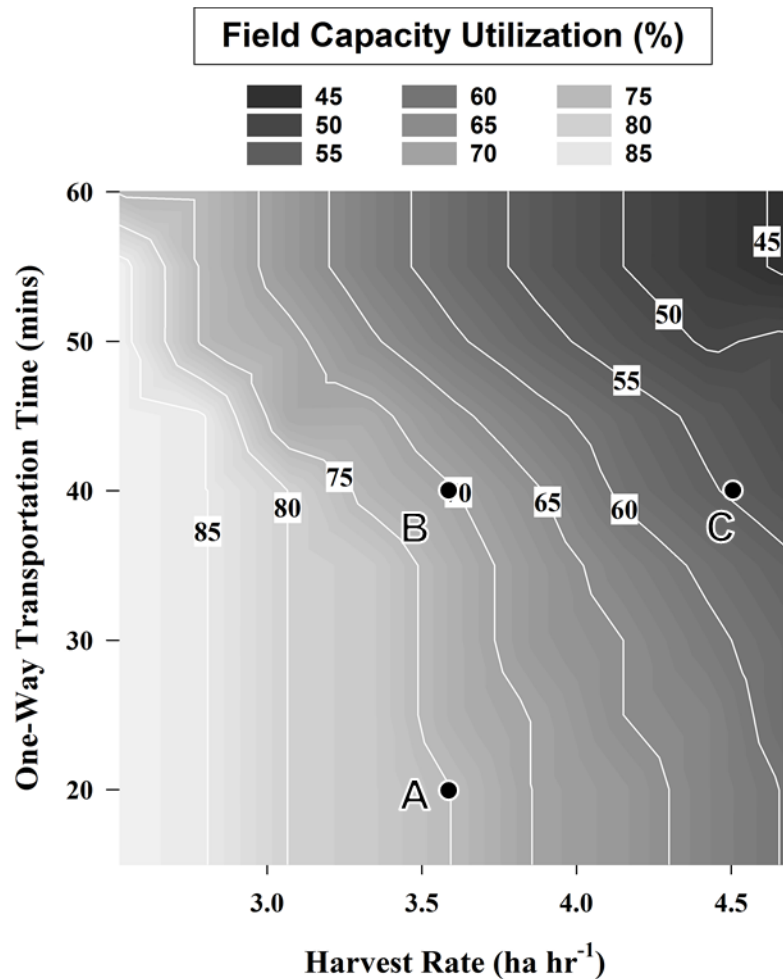


Figure 5-6: Whole season field equipment area capacity utilization as a function of transportation distance and harvest rate. Shown for the minimally-equipped configuration. **A** represents the operating point of the baseline configuration. **B** represents doubling the transportation time, and **C** represents a point with an increased harvest rate and transportation time.

The effect of doubling the drying capacity for the baseline configuration can be seen in Figure 5-7. The region of operation where the average field capacity utilization was greater than 90% expanded to cover a wider range of transportation times and harvest rates. Points **A** and **B** both had a field capacity utilization of approximately 97%, indicating at these points there were rarely downstream bottlenecks. At point **C** increasing the drying capacity increased field capacity utilization from 70% to 74%. Figure 5-8 shows the impact of utilizing an additional driver along with doubled drying capacity. At short transport times, field capacity utilization was greater than 90% for the entire range of harvest rates. Field capacity utilization was also improved for areas with

longer transportation distances and higher harvest rates. Point C on Figure 5-8 has a field capacity utilization of 90%. This improvement over Figure 5-7 indicates that transportation was the system bottleneck, at least for a portion of the season, and this prevented the full drying capacity from being utilized.

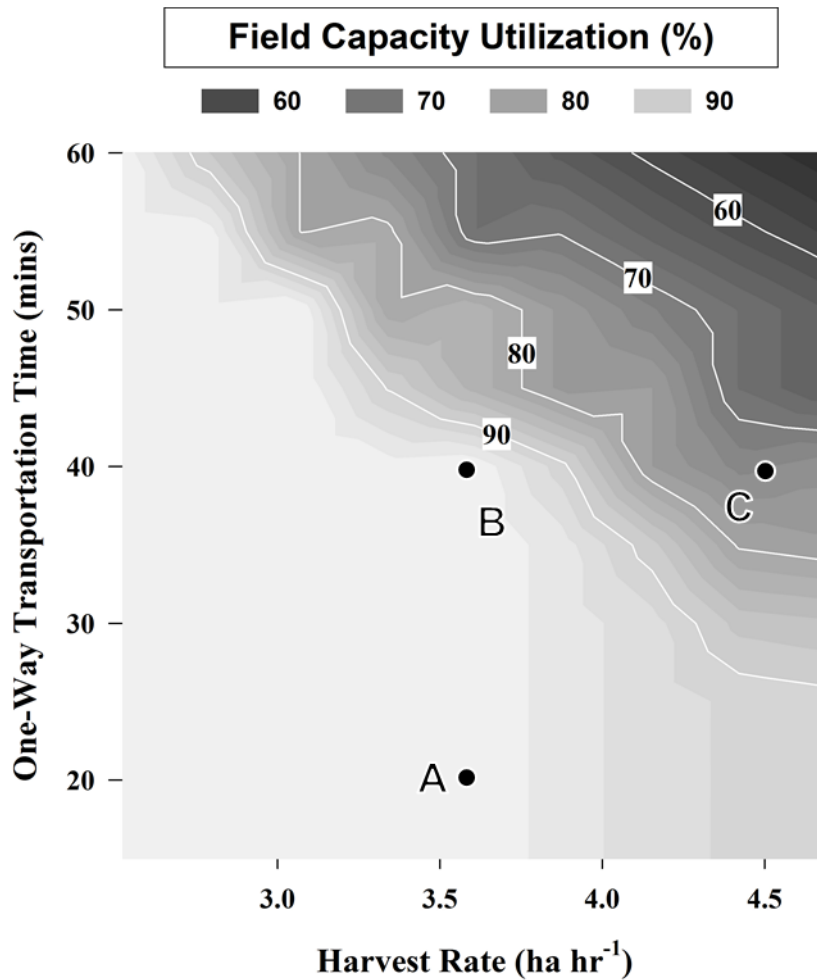


Figure 5-7: Whole season field equipment area capacity utilization as a function of transportation time and harvest rate. Shown for the baseline configuration with doubled drying capacity. **A** represents the operating point of the baseline configuration. **B** represents doubling the transportation time, and **C** represents a point with an increased harvest rate and transportation time.

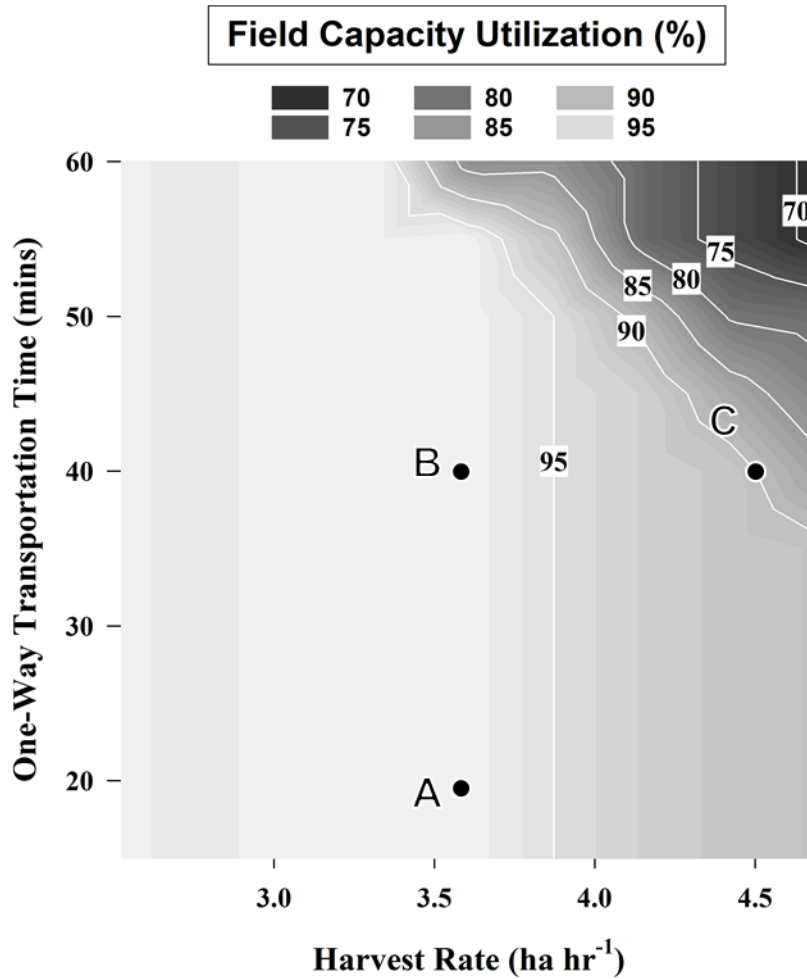


Figure 5-8: Whole season field equipment area capacity utilization as a function of transportation time and harvest rate. Shown for the baseline configuration with doubled drying capacity and an additional driver. **A** represents the operating point of the baseline configuration. **B** represents doubling the transportation time, and **C** represents a point with an increased harvest rate and transportation time.

Figure 5-9 shows the total harvest operating cost per unit area. These values represent the seasonal total drying energy, labor, and equipment operating costs divided by the total area harvested. The baseline configuration, operating at point **A**, had an estimated cost of \$157 ha⁻¹. When the transportation distance was doubled the cost increased to \$172 ha⁻¹, with the increased transportation demand accounting for the majority of the increase. Moving from **B** to point **C** had minimal impact on the overall cost. This was because the increased field capacity largely could not be taken advantage of due to downstream bottlenecks (Figure 5-4 & Figure 5-5). Increasing the harvest rate could come as a result of improved field efficiency or increased ground speed. If the

travel speed was increased beyond the optimum point for given field conditions, harvest losses can increase, however, these impacts would be highly variable and were not included in this analysis.

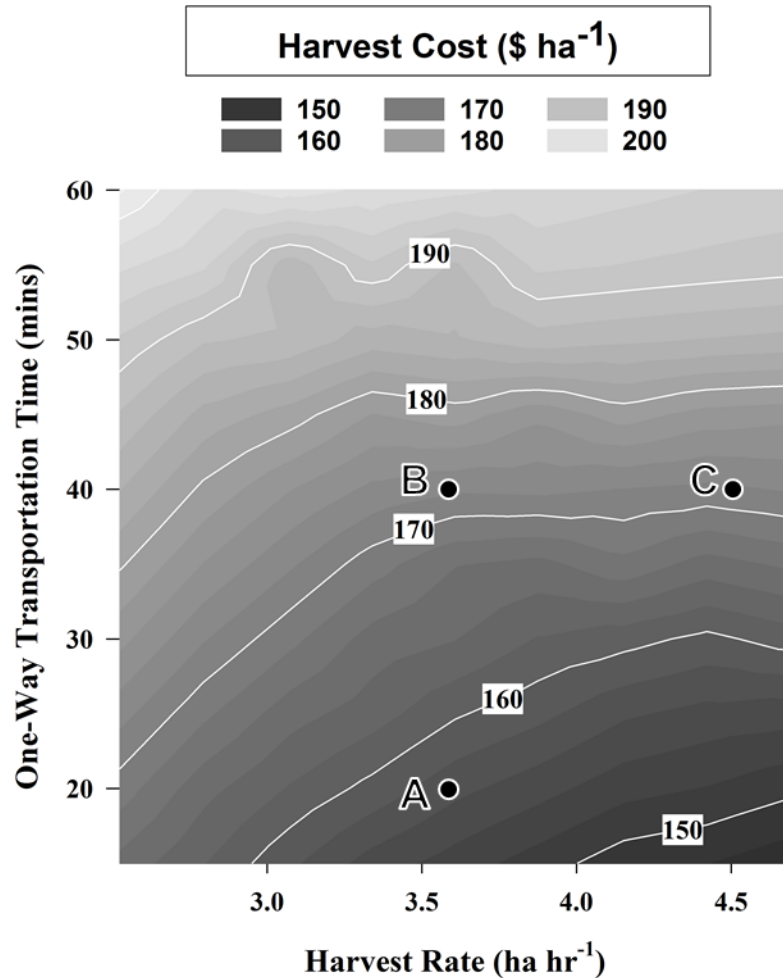


Figure 5-9: Per area costs of harvesting, transporting, and drying grain as a function of transportation time and harvest rate. Shown for the baseline configuration. **A** represents the operating point of the baseline configuration. **B** represents doubling the transportation time, and **C** represents a point with an increased harvest rate and transportation time.

Figure 5-10 shows the per hectare costs of harvesting for the baseline configuration with doubled drying capacity. Increasing the drying capacity resulted in an additional annual ownership cost of \$10.1 ha⁻¹. Here point **A** corresponded to the baseline configuration with doubled drying capacity shown in Table 5-6. For point **A** and **C**, the labor and equipment operating cost reductions that resulted from higher resource

utilization were counteracted by increased drying energy costs that resulted from harvesting more grain at high moisture contents. Overall, this resulted in a cost increase approximately equal to the annual ownership cost of the dryer. Point **B** showed an increase slightly higher at approximately \$12 ha⁻¹.

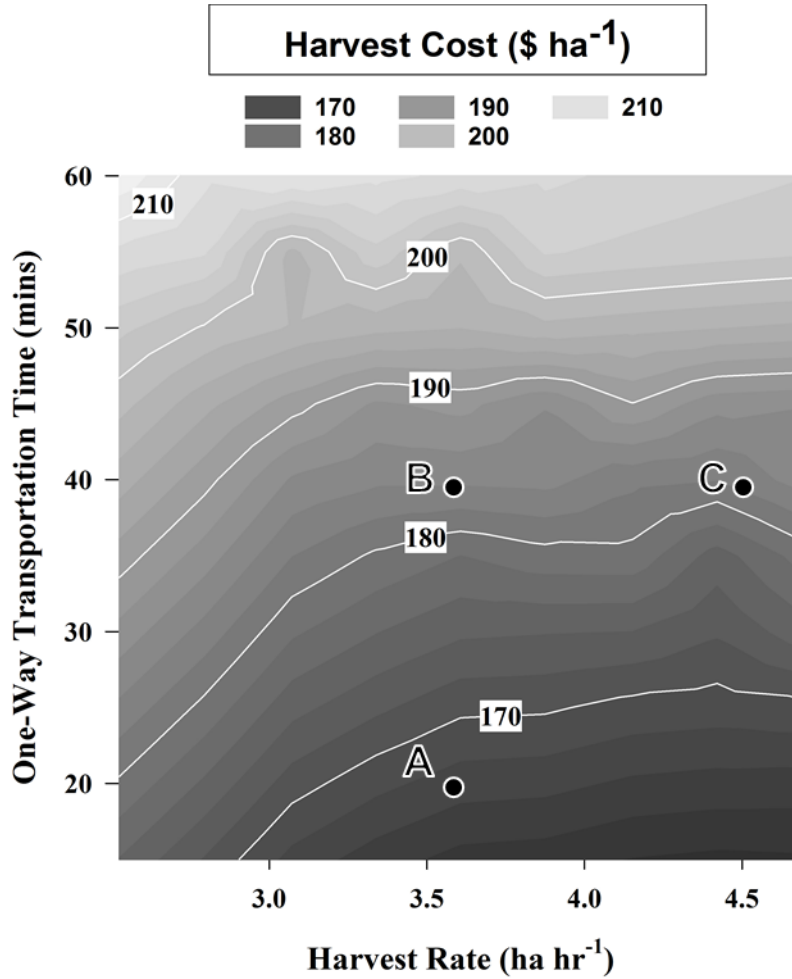


Figure 5-10: Per area costs of harvesting, transporting, and drying grain as a function of transportation time and harvest rate. Shown for the baseline configuration with doubled drying capacity. Value includes the annual cost of ownership for the large dryer upgrade. **A** represents the operating point of the baseline configuration. **B** represents doubling the transportation time, and **C** represents a point with an increased harvest rate and transportation time.

Figure 5-11 shows how the harvest costs changed when an additional driver was added to the configuration with double the drying capacity. In this instance, the additional costs included were the same \$10.1 ha⁻¹ ownership cost for the dryer plus the wages for

the extra employee. This addition increased the per hectare costs by approximately \$4 ha⁻¹ at point **A** and by approximately \$2 ha⁻¹ at points **B** and **C**, when compared to the configuration with doubled drying capacity. Compared to the baseline configuration, the total cost increase was \$14.5 ha⁻¹ and \$13 ha⁻¹ for **A** and **B**, respectively. The additional resources always increased the per hectare harvest costs; there were however many instances where the increase was less than the annual ownership costs of the new dryer. This indicates the improvement in efficiency helped offset the additional cost. These offsets were generally higher at longer transportation times and higher harvest rates. For example, if the system were operating at 4.42 ha hr⁻¹ with a transportation time of 55 minutes, the cost increase was only \$1.7 ha⁻¹. This effectively offset over 80% of the additional ownership costs for the larger dryer.

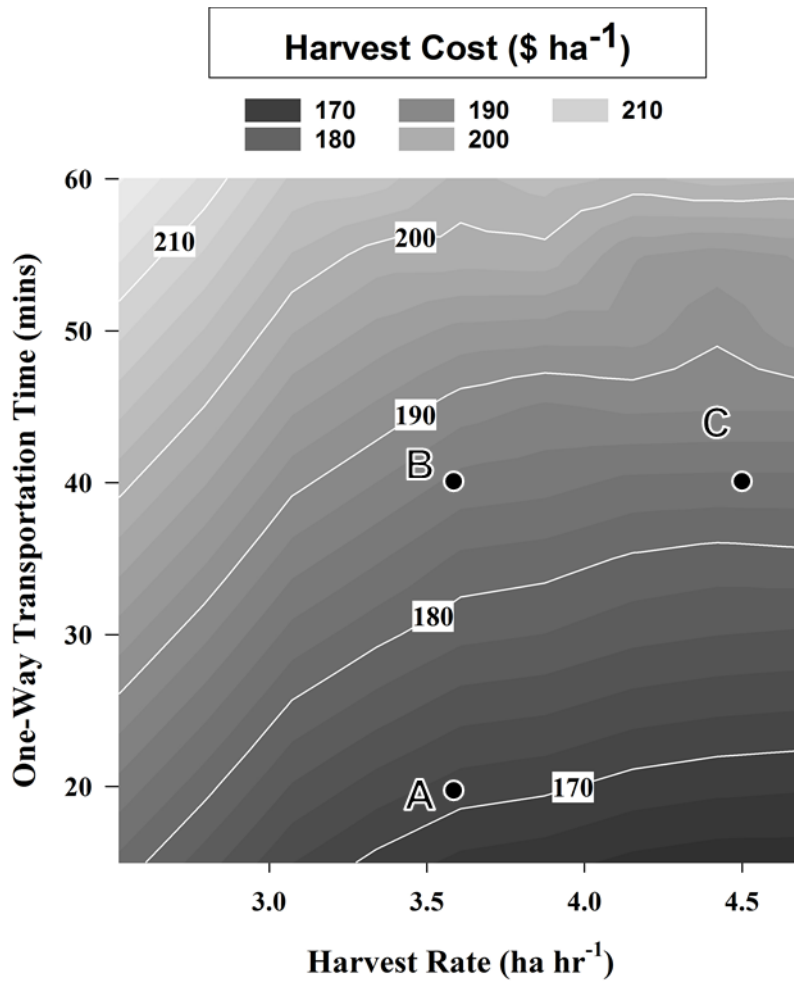


Figure 5-11: Per area costs of harvesting, transporting, and drying grain as a function of transportation time and harvest rate. Shown for baseline configuration with doubled drying capacity and an additional driver. **A** represents the operating point of the baseline configuration. **B** represents doubling the transportation time, and **C** represents a point with an increased harvest rate and transportation time.

Ultimately, the increased costs associated with additional equipment needs to be justified. This study was not concerned with the ideal moisture to start harvest but rather focused on how additional equipment would impact the overall cost and time to complete the operation. The change in the length of harvest when comparing the baseline configuration to the improved system with doubled drying capacity and an additional driver is shown in Figure 5-12. The larger dryer and additional truck had a varied impact on the system and ranged anywhere from no change to reducing the time required to complete harvest by 10 calendar days. Generally, the increased capacity produced a greater benefit in areas of operation with higher harvest rates and increased transportation times.

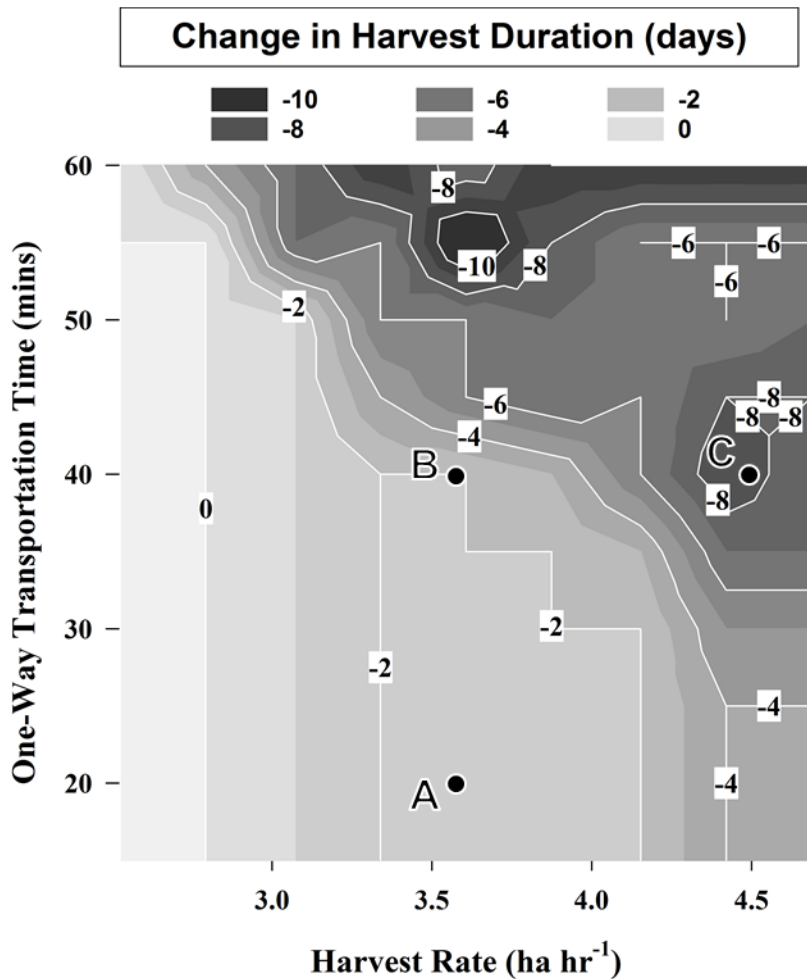


Figure 5-12: Change in harvest length with doubled drying capacity and three drivers **A** represents the operating point of the baseline configuration. **B** represents doubling the transportation time, and **C** represents a point with an increased harvest rate and transportation time.

Traditionally, the tradeoff between yield loss due to delayed harvest and fuel used in drying has been used to evaluate harvest costs and timing. This balance was highly dependent on the price of grain, and in many cases, small levels of loss prevention would justify the additional equipment. This small level of loss is difficult to quantify accurately due to the highly variable nature of losses and yield in general, and in this analysis a loss prevention of 1.5% would more than cover the increased harvest costs for all harvest rate and transport times considered in Figure 5-13 (assuming a corn price of \$3.50 bu). Decreasing the number of days required to complete harvest can free resources for other activities and provide a buffer on years with unfavorable weather conditions. One

solution to evaluate changes in the system would be to evaluate the additional costs for new equipment against the potential to shorten the harvest window. Figure 5-13 shows the change in harvest costs over the baseline operation for the additional driver and larger dryer. This could be used with the reduced harvest length in Figure 5-12 to evaluate the cost for a shortened harvest window. For example, at point C, a producer could weigh the additional $\$12 \text{ ha}^{-1}$ in harvest costs against being able to finish harvest 8 calendar days sooner. Areas on the left-hand side of the figures generally did not have transportation and drying bottlenecks but incurred an additional $\$16 \text{ ha}^{-1}$ cost for no reduction in time required to complete the operation. In contrast, some areas with higher harvest rates and longer transportation distances reduced the duration of harvest for as little as $\$2 \text{ ha}^{-1}$.

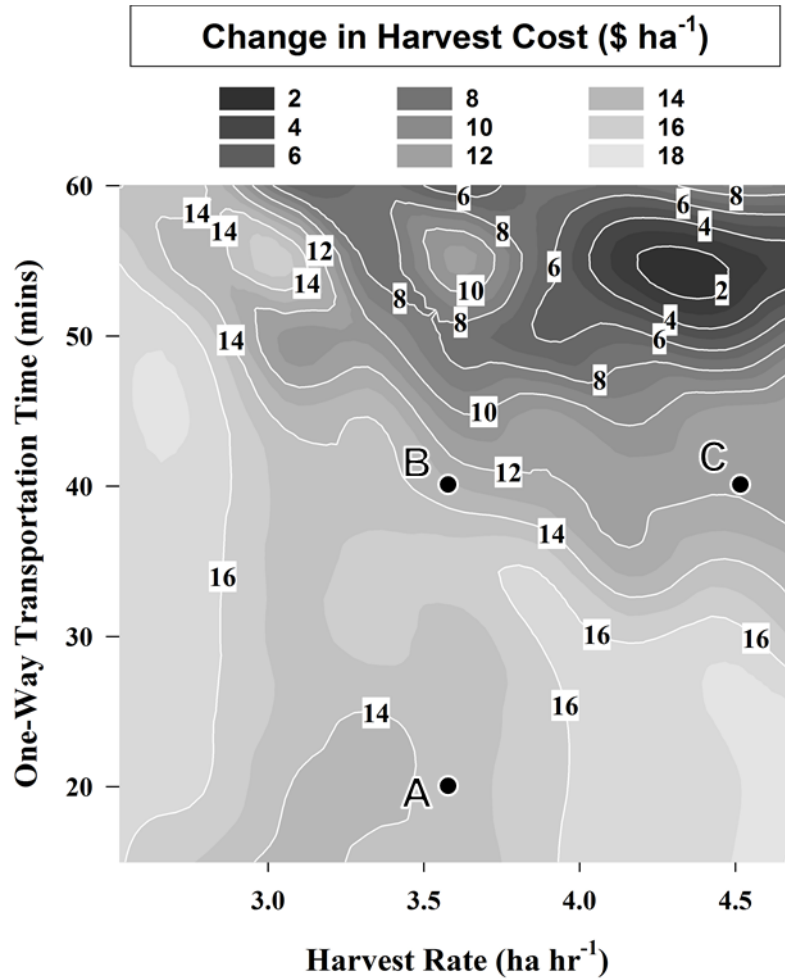


Figure 5-13: Change in harvest costs with doubled drying capacity and three drivers **A** represents the operating point of the baseline configuration. **B** represents doubling the transportation time, and **C** represents a point with an increased harvest rate and transportation time.

5.4.6 Assumptions and Limitations

There were several limitations associated with this study. All equipment included in the model was assumed to be the same size (ex. all trucks had the same capacity), and constant values were used for harvest rate and transportation time. The model could be improved by incorporating varying harvest rates and transportation distances to account for more local variation (similar to the grain transportation analysis). The boundary of the discrete event simulation could also be moved to incorporate interactions of field machinery.

Several other drying considerations were not included in this analysis. Allowable storage time was not considered but could have the effect of limiting harvest early in the simulation. Additionally, a constant final moisture was assumed, and all grain was dried to 15% until the incoming moisture was below that level. A producer could employ combination drying or operate the dryer in full heat mode early in the season to increase the dryer throughput. Additionally, once the incoming moisture approaches safe limits for storage, the dryer could be bypassed completely in favor of natural air drying.

The cost structure used to demonstrate the model could also have an impact on the results. For example, truck drivers are commonly independent of the farm operation and are paid on a per load, mile, or bushel basis. In this case, transportation costs would be insensitive to wait times and delays in grain transportation. An operation of the size examined here may not have the resources to dedicate personnel to the storage facility fulltime, and the labor rates used in this analysis were somewhat generous. The costs associated with purchasing a larger dryer could vary widely based on purchasing new or used equipment and any material handling infrastructure upgrades that could be required. These changes would not impact the system performance but would change the cost implications.

5.5 Conclusions

This study demonstrated the application of a model for corn harvest, transportation, and drying at an on-farm storage facility. A hypothetical operation was defined to show how the model could be used as a decision support tool. The impact of drying capacity varied based on the configuration examined, ranging anywhere from 1 to 22 days before the sustained maximum field capacity utilization was reached. The baseline operation was evaluated for a range of seasonal effects, and it was found that a dry year (12.7% decrease over baseline) and a slow field drying rate (10.8% increase over baseline) had the largest impact on the system's operating and drying costs. The model was also used to evaluate the impacts of the reduced drying temperature associated with drying white corn. For this specific configuration, harvest took six days longer, but after accounting for the reduced yield, there was no impact on the total operating and drying cost. The reduced drying capacity forced more field drying which counteracted the increased operating cost and decreased drying efficiency. The use of the model to

evaluate impacts of additional equipment on both cost and system performance were demonstrated, and a sensitivity analysis demonstrated how the benefits of increased drying and hauling capacity varied based on how often these systems created a bottleneck in the operation. For some combinations of higher field capacity and longer transportation distance, the time required to complete the operation could be shortened by a week or more for an additional cost of \$12 ha⁻¹ or less.

5.6 References

- ASABE Standards. (2015a). D497. 6 Agricultural Machinery Management Data. St. Joseph, MI: ASABE.
- ASABE Standards. (2015b). EP 496.3 Agricultural Machinery Management. St. Joseph MI: ASABE.
- ASABE Standards. (2015c). S495.1 Uniform Terminology for Agricultural Machinery Management. St. Joseph, MI: ASABE.
- Carpenter, M. L., & Brooker, D. B. (1972). Minimum Cost Machinery Systems for Harvesting, Drying and Storing Shelled Corn. *Transactions of the ASAE.*, 15(3), 515-0519. doi:<https://doi.org/10.13031/2013.37942>
- Davis, S., Diegel, S., & Boundy, R. (2007). Transportation Energy Data Book: Edition 26. Oak Ridge National Laboratory. *ORNL*, 6978.
- Edwards, W. (2014). Estimating the Cost for Drying Corn. *Ag Decision Maker*. Retrieved from <https://www.extension.iastate.edu/agdm/crops/pdf/a2-31.pdf>
- Edwards, W., & Johanns, A. (2012). Wages and Benefits for Farm Employees. *Ag Decision Maker*. Retrieved from <https://www.extension.iastate.edu/agdm/wholefarm/html/c1-60.html>
- Edwards, W., Plastina, A., & Johanns, A. (2016). Grain Harvesting Equipment and Labor in Iowa. *Ag Decision Maker*. Retrieved from <https://www.extension.iastate.edu/agdm/crops/pdf/a3-16.pdf>
- Farm Fans Inc. (1999). *Operator's Manual C-2130B, C-2140B, C-2160B, C-2175B, and C-21100B Grain Dryers*. Indianapolis, IN: FFI Corporation.
- Halich, G. (2018). Custom Machinery Rates Applicable to Kentucky (2018). *University of Kentucky Cooperative Extension Service*. Retrieved from <https://www.uky.edu/Ag/AgEcon/pubs/customratesKY.pdf>

- Isaac, N. E., Quick, G. R., Birrell, S. J., Edwards, W. M., & Coers, B. A. (2006). Combine harvester econometric model with forward speed optimization. *Applied Engineering in Agriculture*, 22(1), 25-31.
- Jackson, J. J. (2015). *Optimal uses of biomass resources in distributed applications*. (PhD), University of Kentucky, Lexington, KY.
- Johnson, W., & Lamp, B. (1966). *Principles, equipment and systems for corn harvesting*. Wooster, OH: Agricultural Consulting Associates, Inc.
- Kiker, C., & Lieblich, M. (1986). Financial analysis of on-farm grain drying. *Journal of Agricultural and Applied Economics*, 18(2), 73-84.
- Licht, M., Hurburgh, C., Kots, M., Blake, P., & Hanna, M. (2017). *Is there loss of corn dry matter in the field after maturity?* Paper presented at the 29th Annual Integrated Crop Management Conference.
- Loewer, O. J., Benock, G., & Bridges, T. C. (1980). Effect of combine selection and harvesting rate on grain drying and delivery system performance. *Transactions of the ASAE.*, 23(6), 1548-1553.
- Loewer, O. J., Bridges, T. C., White, G. M., & Overhults, D. G. (1980). The Influence of Harvesting Strategies and Economic Constraints on the Feasibility of Farm Grain Drying and Storage Facilities. 23(2). doi:10.13031/2013.34605
- Loewer, O. J., Bridges, T. C., White, G. M., & Razor, R. B. (1984). Optimum moisture content to begin harvesting corn as influenced by energy cost. *Transactions of the ASAE.*, 27(2), 362-365.
- Martin, B. A. (2018). *Two Essays on Whole Farm Modeling and Crop Marketing in Western Kentucky*. (MSc), University of Kentucky, Lexington, KY.
- Midwestern Regional Climate Center. (2018). cli-MATE Application Tools Environment Sub_daily Data(DATABASE). Retrieved 6/15/2018
<https://mrcc.illinois.edu/CLIMATE/>
- Montross, M. D., & Maier, D. E. (2000). Simulated performance of conventional high-temperature drying, dryeration, and combination drying of shelled corn with automatic conditioning. *Transactions of the ASAE.*, 43(3), 691.
- Morey, R. V., Cloud, H. A., & Lueschen, W. E. (1976). Practices for the efficient utilization of energy for drying corn. *Transactions of the ASAE.*, 19(1), 151-0155.

- Morey, R. V., Zachariah, G. L., & Peart, R. M. (1971). Optimum policies for corn harvesting. *Transactions of the ASAE.*, 14(5), 787-792.
- Paulsen, M. R., de Sena, D. G., Jr., de Assis de Carvalho Pinto, F., Zandonadi, R. S., Ruffato, S., Gomide Costa, A., . . . Danao, M. G. C. (2014). Measurement of Combine Losses for Corn and Soybeans in Brazil. *Applied Engineering in Agriculture*, 60(6), 841-855.
- Pierce, R., & Thompson, T. (1981). Energy use and performance related to crossflow dryer design. *Transactions of the ASAE.*, 24(1), 216-0220.
- Plastina, A. (2018). *Ag Decision Maker-Estimated Costs of Crop Productin in Iowa*. Iowa State University.
- Thomison, P. R., Mullen, R. W., Lipps, P. E., Doerge, T., & Geyer, A. B. (2011). Corn response to harvest date as affected by plant population and hybrid. *Agronomy Journal*, 103(6), 1765-1772.
- Thompson, T. L., Peart, R. M., Foster, G. H., Loewer, O., & Bridges, T. (1994). Granary. University of Florida.
- Tippayawong, K. Y., Piriyaageera-anan, P., & Chaichak, T. (2013). Reduction in energy consumption and operating cost in a dried corn warehouse using logistics techniques. *Maejo International Journal of Science and Technology*, 7(2), 258.
- Trego, T., & Murray, D. (2010). *An analysis of the operational costs of trucking*. Paper presented at the Transportation Research Board 2010 Annual Meetings, Washington, DC.
- U.S. Energy Information Administration. (2018). Data for Petroleum & Other Liquids. Retrieved from <https://www.eia.gov/petroleum/data.php>
- USDA-NASS. (2017). Quick Stats. *Washington, DC*.

Chapter 6. SUMMARY, CONCLUSIONS, AND FUTURE WORK

6.1 Summary and Conclusions

This dissertation explored issues surrounding grain harvest and transportation logistics with the overall objective of developing a simulation model that could be utilized to explore how changes in the system configuration (equipment, weather, labor, drying temperature, dry down rate, etc.) impacts the overall system performance and operating costs. Model development was broken into several stages. Initially a discrete event simulation (DES) model of grain transportation from the field edge to storage was proposed to evaluate how truck and driver resource constraints impact material flow efficiency, resource utilization, and system throughput. This work differed from previous efforts in that harvest rate and in-field transportation were not explicitly modeled, but were represented as a stochastic entity generation process. Service times associated with various material handling steps were represented by a combination of deterministic times and statistical distributions. The model was applied to data collected for three distinct harvest scenarios (18 total days). Key results from this objective were:

- For the scenarios examined, the model could satisfactorily represent the total number of deliveries to the storage facility.
- A single distribution for each operation or crop was found to adequately represent harvest rate and in-field machinery interactions over the range of input conditions encountered.
- The observed number of deliveries was within ± 2 standard deviations of the simulation for 15 of the 18 input conditions examined.
- The median error between the model and observed deliveries was -4.1%.
- The model could represent operations with capacity matched between in-field and on-road transporters as well as operations with capacity for on-road transporters being integer multiples of in-field transporter capacity.
- Flow time efficiency was very high for both crops in one operation evaluated, indicating there were few delays between handling steps, so transportation capacity was sufficient.

- The other operation examined had lower flow time efficiency because multiple grain cart loads (entities) were required to fill a truck. In contrast to the larger operation, truck, and especially driver utilization, were relatively high.

A field study was conducted to examine corn harvest losses in Kentucky. This included establishing a range of losses commonly encountered by cooperating producers around the state, and an evaluation of yield and loss changes over a range of dates/moisture contents (09/20/2017 to 12/01/2017 / 33.9% to 14.6%) from a single field at a University of Kentucky research farm. Key conclusions from this evaluation were:

- Total losses for producer combines were found to be between 0.8% to 2.4% of total yield (86 to 222 kg ha⁻¹), and on average 66% of the measured losses occurred at the head.
- Total losses were highly variable, with coefficients of variation ranging from 21.7% to 77.2%.
- For the single field evaluation, there was no significant difference in the potential yield at any moisture level, and the observed yield and losses displayed little variation for moisture levels from 33.9% to 19.8%, with total losses less than 1% (82 to 130 kg dry matter ha⁻¹).
- Large amounts of lodging occurred during the long delay while the grain field dried to the final moisture level, resulting in a 18.9% reduction in yield and harvest losses in excess of 9%.
- Test weight and mechanical damage generally improved with decreased moisture and post-drying test weight was always sufficient to at least meet the U.S. No. 2 test weight requirement.
- Results should be replicated for additional years or locations but indicate the loss relationships used in previous harvest logistics models are not representative of current practices.

The DES grain transportation model was expanded to include temporary wet storage capacity and grain drying to evaluate how these components impact the overall system. A method to adjust the capacity of the dryer based on drying temperature,

incoming, and exiting moisture was proposed. The model was validated by applying it to the whole season of corn harvest used in the grain transportation model. In this instance, average values for grain cart arrivals (entities) and transportation distance were used, but the duration of field work each day was determined from the model, and the status of the system on the previous day was carried forward, so days were no longer independent. The moisture content and field dry down of incoming grain was modeled based on weather data and the equilibrium moisture content of the grain. The model was evaluated by comparing the estimated drying capacity to an estimate derived from producer records, and by comparing the observed cumulative mass of grain delivered to storage to the model prediction. Key results from this objective were:

- Based on relative drying capacity, the proposed method agreed well with the established model from Thompson et al. (1994), with an average over prediction of 8.2%.
- The variability in estimated drying capacity made it difficult to accurately assess the proposed method against field data and showed the need to obtain better data for validation.
- Both Thompson et al. (1994) and the method used in this analysis underpredicted the observed data and in some instances had large errors.
- The best fit for field dry down rate, based on the collected data was $\beta=0.0812$, which had an RMSE of 0.73 points over the range of moistures from 26.7% to 18.7%.
- The simulation estimated harvest would require an additional partial day over the observed data, and overall the harvest model showed good agreement with the observed data, based on the cumulative mass of grain delivered over the season.

The final portion of this dissertation demonstrated the application of the full model to a hypothetical operation. This served to demonstrate how the model could be used as a decision support tool, and a sensitivity analysis was conducted over a range of transportation times and harvest rates to demonstrate how the benefits of potential changes in one portion of the system were affected by the operating parameters of the whole system. The number of days required to complete the operation, equipment

operating cost, labor costs, and drying costs were estimated for each configuration examined. Ownership costs were only taken into account when additional equipment was added to the system, and no preharvest losses or yield changes were included in this evaluation. Key conclusions from this analysis were:

- Utilization of the available field capacity and duration of fieldwork generally increased as the grain field dried.
- The system bottleneck could change over the course of the season, and the number of days into the simulation before field capacity utilization reached its sustained maximum varied from 1 to 22 days, depending on which configuration was examined.
- A dry year and a slow field drying rate had the largest impact on the system's operating and drying costs, resulting in a respective 12.7% decrease and 10.8% increase in costs.
- For this specific configuration, reducing the drying temperature to dry white corn prolonged harvest, but had no impact on the total operating and drying cost, after accounting for a yield reduction (operating and drying cost only, not accounting for changes in gross revenue).
- The reduced drying capacity forced more field drying which counteracted the increased operating cost and decreased drying efficiency.
- For some combinations of longer transportation times and higher harvest rates, doubling the dryer size and finding an additional truck driver could shorten the harvest window by a week or more at a cost of less than \$12 ha⁻¹.

To summarize, this dissertation focused on the development, testing, and application of a grain harvest system model that spanned from the field through drying and storage. It can be used to simulate how changes in equipment capacity, labor, weather, and crop characteristics (ex: food grain corn, or dry down rate) impact the overall system performance and operating costs. An important extension of this concept is that, given an existing equipment set and labor force, a producer can estimate how much increasing capacity in one area would increase the system capacity over the whole

season, and the cost of the additional equipment can be evaluated against the potential to shorten the harvest.

6.2 Future Work

From a model development prospective, there are several directions the model could be expanded to provide enhanced usefulness. The approach used here was a discrete event simulation from the arrival of full grain carts at the field edge through delivery and drying at an on-farm storage facility. Field equipment characteristics were represented by modeling the time required to fill a grain cart and transport the grain to the field edge. This time was estimated from observations of actual operations, or from a harvest rate and assuming sufficient in-field transportation capacity. The boundary of the discrete portion of the model could be expanded to include interactions of in-field equipment and spatial variability in performance. This would allow the model to be better equipped to evaluate changes in field equipment. Moreover, the variability in entity generation, service times, and transportation distance explored in the hauling model could be applied to the whole season model. This would allow more spatial and temporal effects of operational decisions to be examined. For example, strategies for determining the order in which fields are harvested could be explored (furthest first, earliest planted first, etc.). This work could also benefit from additional validation data for the drying capacity adjustment, and development of a user interface would allow the model to be used by producers.

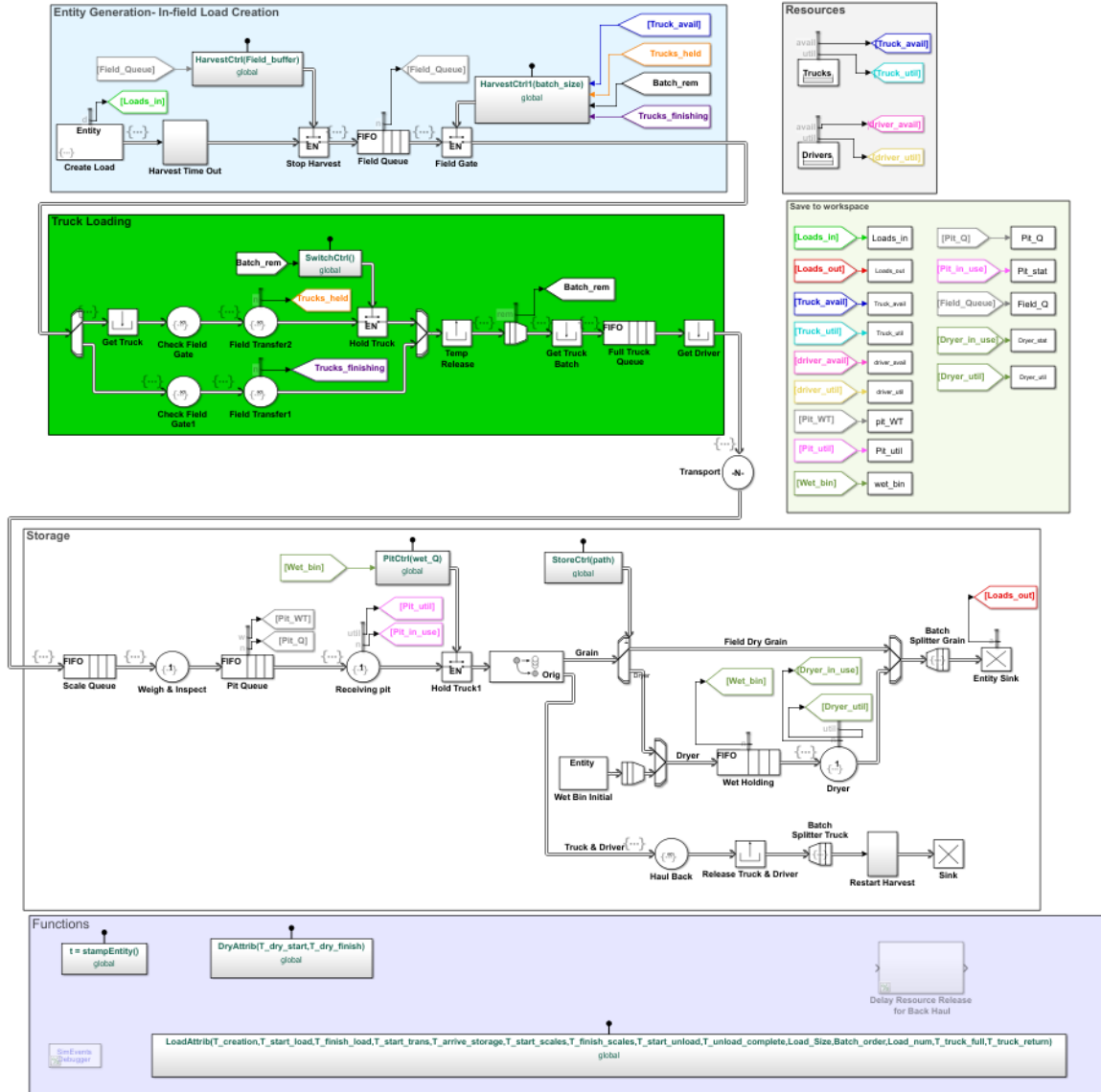
The sensitivity analysis indicated the rate at which grain dried in the field was one of the most influential factors on total drying energy costs. The dry down rate is relatively unexplored and is dependent on weather, planting date, and variety. More detailed information in this area could allow the model to be applied to evaluate the operational decisions described above and better estimate drying costs. Additionally, evaluation of yield changes and losses measured over the course of the harvest season in this study indicate the traditional loss and recoverable yield functions used to balance the costs of early harvest and artificial drying may not be the most appropriate method for modern equipment and hybrids. Losses are highly variable, and the results presented here should be replicated for additional years and/or locations. There still are clear timeliness benefits to starting harvest early. However, an alternate method to evaluate these benefits, perhaps

based on the likelihood of a weather event causing significant damage or lodging to the crop could be explored.

APPENDICES

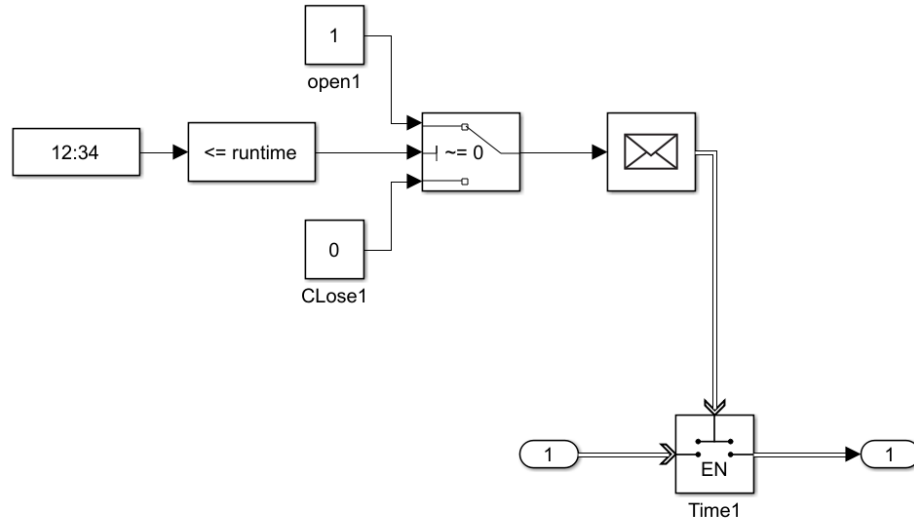
Appendix A. Simulink Model Details

Whole Model Diagram

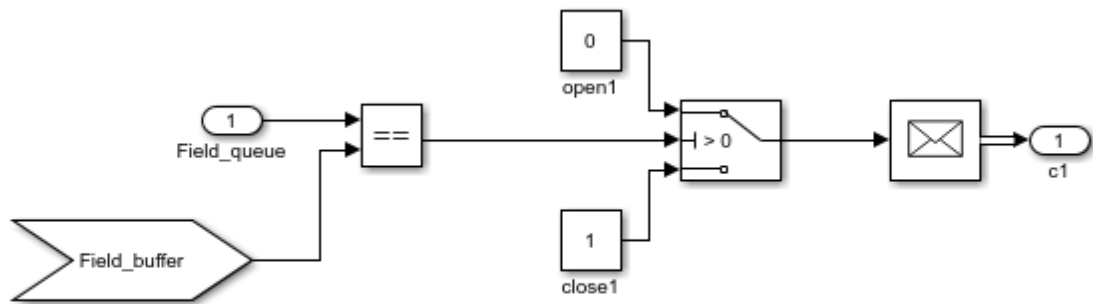


Harvest Time Out Subsystem

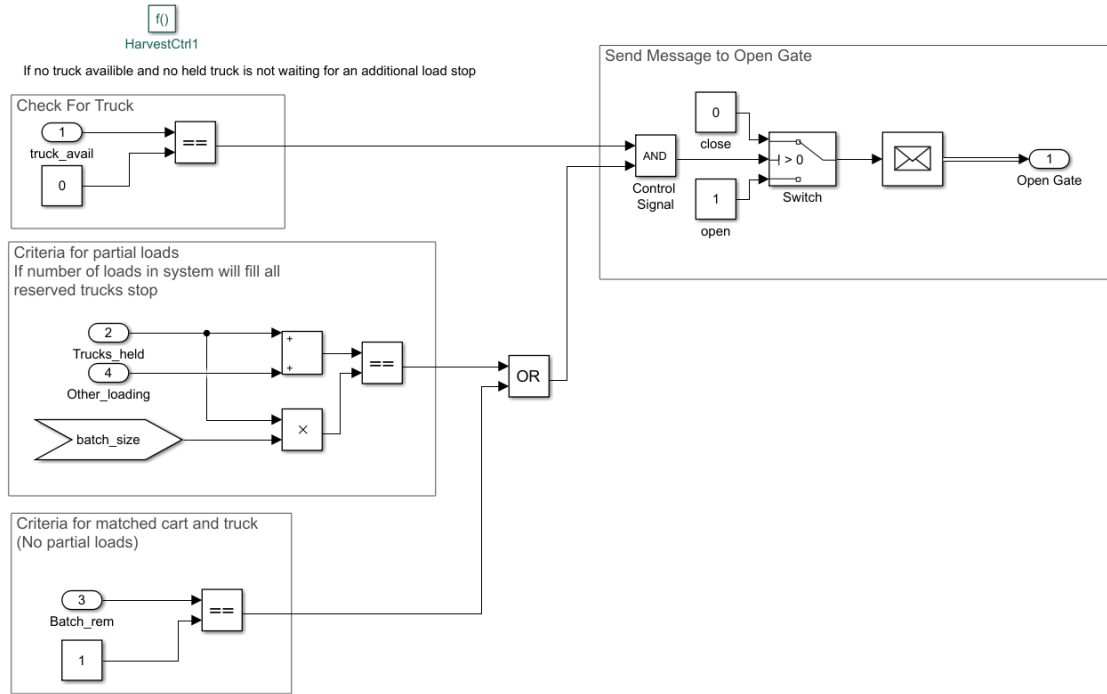
Gate closes after specified time to stop generation of new loads.
Allows transportation simulation to continue after harvest has stopped



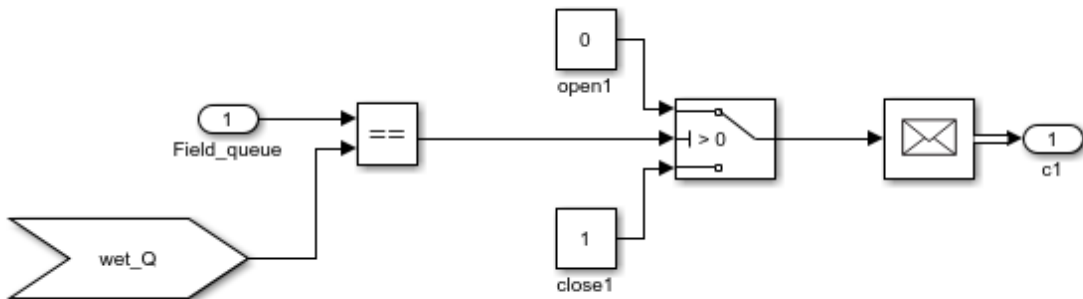
Harvest Gate Control Logic



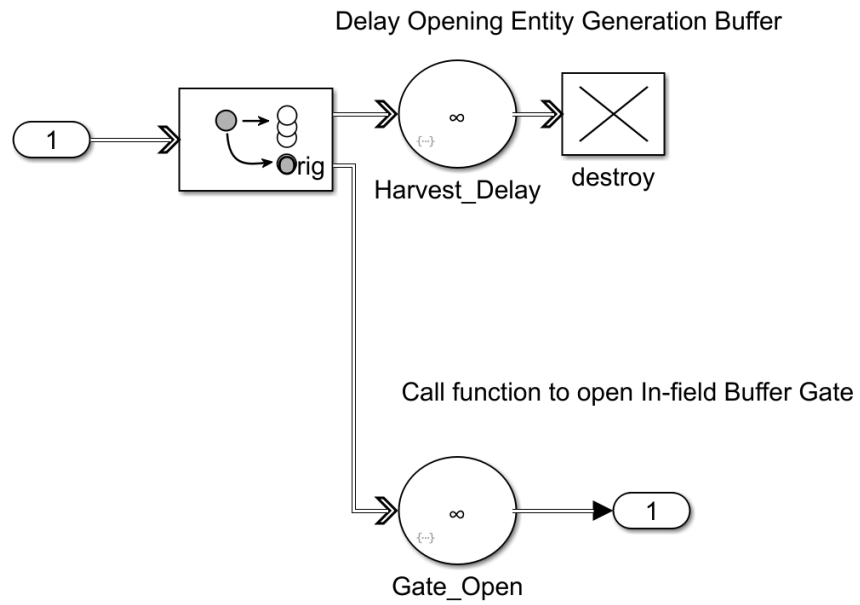
HarvestCtrl1 Logic for Gate to Control Loading Partial Trucks



Pit Control Gate Logic



Restart Harvest Subsystem



Entity Generation Block Code

```
Block Parameters: Create Load
Entity Generator
Generate entities using intergeneration times from dialog or upon arrival of events. Optionally, specify entity types as anonymous, structured, or bus.
Entity generation Entity type Event actions Statistics
Generation method: Time-based
Time source: MATLAB action
Intergeneration time action:
1 %create index var to read value from workspace
2 persistent ii;
3 if isempty(ii)
4     ii=1;
5 else
6     ii=ii+1;
7 end
8
9 dt = load_gen_rate(ii);
```

Block Parameters: Create Load

Entity Generator
Generate entities using intergeneration times from dialog or upon arrival of events. Optionally, specify entity types as anonymous, structured, or bus.

Entity generation | Entity type | Event actions | Statistics

Event actions

Generate action:

Called after entity is generated.
To access attribute use: entity.T_creation

```

1 HarvestCtrl(field_buffer);% check if harvest can continue
2
3
4 %Variable to create load number
5 persistent j;
6 if isempty(j)
7     j=1;
8 else
9     j=j+1;
10 end
11
12 entity.Load_num=j;%Load number
13
14 %Determine which route load takes. IF cart and truck size are ma
15 %If batching is used, first load on a trailer is held to reserve
16 %until only one more load is required, at which point the held l
17 %This releases the truck but it is required by the new batched
18
19 if batch_size==1
20     entity.Batch_order=1; %If batching is not needed go through
21 else
22     if mod(j,batch_size)==1 %First load in a batch, go through t
23     entity.Batch_order=1;%Reserve truck
24 else
25     entity.Batch_order=2;%continue filling truck.
26     end
27 end

```

Entity structure

- entity
 - T_creation
 - T_start_load
 - T_finish_load
 - T_start_trans
 - T_arrive_storage
 - T_start_scales
 - T_finish_scales
 - T_start_unload
 - T_unload_complete
 - Load_Size
 - Batch_order
 - Load_num
 - T_truck_full
 - T_start_dry
 - T_finish_dry
 - T_truck_return
- entitySys
 - id
 - priority

Block Parameters: Create Load

Entity Generator
Generate entities using intergeneration times from dialog or upon arrival of events. Optionally, specify entity types as anonymous, structured, or bus.

Entity generation | Entity type | Event actions | Statistics

Event actions

Exit action:

Called just before entity exits this block.
To access attribute use: entity.T_creation

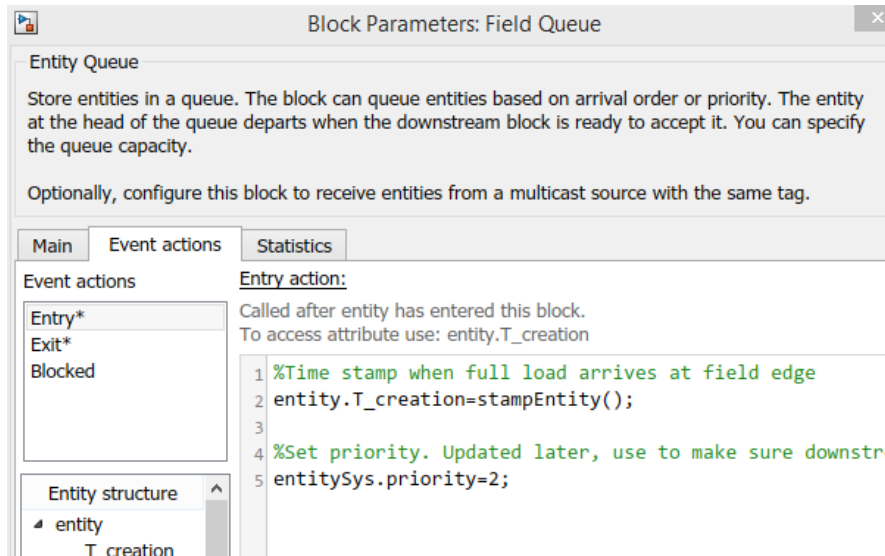
```

1 HarvestCtrl1(batch_size);% Check if truck is available

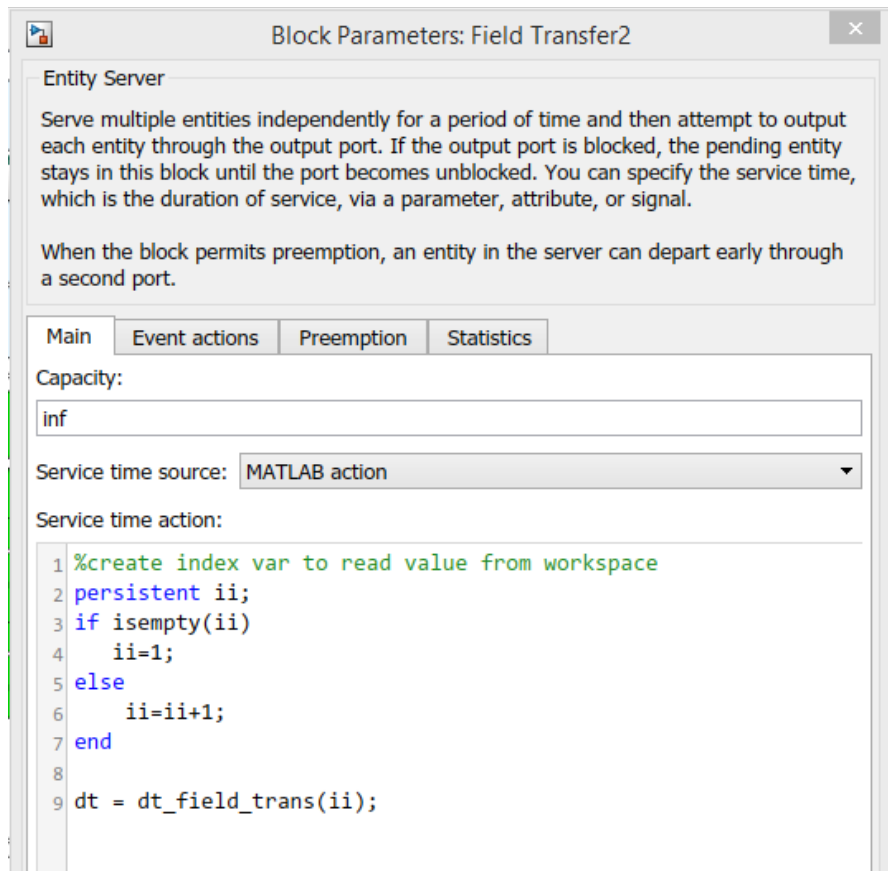
```

Entity structure

Example Timestamp Between Processes & Priority Setting



Example Service Time Selection



Entity Generation Block to Fill Wet Holding at the Start of the Daily Simulation

Block Parameters: Wet Bin Initial

Entity Generator

Generate entities using intergeneration times from dialog or upon arrival of events. Optionally, specify entity types as anonymous, structured, or bus.

Entity generation Entity type Event actions Statistics

Generation method: Time-based

Time source: MATLAB action

Intergeneration time action:

```
1 %Initialized ammount of grain in wet bin @ start of day
2 persistent count igt;
3
4 if isempty(count)
5     igt=[wet_bin_initial inf] ;
6     count=1;
7
8 end
9
10 dt=count;
11 dt=igt(count);
12 count=count+1;
```

Appendix B. Sample code for DES Transportation Model

Script to Create PDF Objects

```
%*****
% TITLE: Fit_dist
% AUTHOR: Aaron P. Turner
% DATES: Jan 2018
% DESCRIPTION: Main script to fit distribution objects to logistic data
%collected from MI and Western Kentucky. Uncomment selected
%crop/location to run
%Creates distributions, can be compared using allfitdist, Selected
%distributions can be manually saved as .mat files.
%Also exports paper quality figures
clear; clc; close all;
%*****

clear; clc; close all;
%*****Import data and set file save location*****
load inputdata.mat %Import source data contains raw data
figpath='C:\XXXXX\'

%*****
%Operation1

%Corn
%[D1] = allfitdist(Load_generation_rate_corn,'PDF');

%Time between corn loads
PD_load_gen_corn=fitdist(Load_generation_rate_corn,'loglogistic')

%%{
figure('Name','Corn Interarrival','Units','inches','Position',[0 0 3.5
3.5],'InvertHardcopy','off','Color',[1 1 1]);
hold on
%histogram(Load_generation_rate_corn,18,'Normalization','pdf')
histogram(Load_generation_rate_corn,18,'FaceColor','w','EdgeColor','k',
'Normalization','pdf')
x_values = min(Load_generation_rate_corn)-
1:0.1:max(Load_generation_rate_corn)+1;
y = pdf(PD_load_gen_corn,x_values);

hold on
plot(x_values,y,'--k','LineWidth',2)
xlabel('Load Interarrival Time (minutes)'); ylabel('Probability
Density');
xlabel('Grain Cart Interarrival Time (minutes)'); ylabel('Probability
Density');
a=gca;
a.Title=[]; a.FontWeight='bold'; a.FontSize=10; a.FontName='arial';
legend('Histogram', 'Fit PDF')
export_fig([figpath 'Corn Interarrival miles hist BW1'],'-png', '-
r300')

hold on
```



```

figure('Name','Corn Interarrival QQ','Units','inches','Position',[0 0
3.5 3.5],'InvertHardcopy','off','Color',[1 1 1]);
qqplot(Load_generation_rate_corn,PD_load_gen_corn)
a=gca;
a.Title=[]; a.FontWeight='bold'; a.FontSize=10; a.FontName='arial';
%export_fig([figpath 'Corn Interarrival miles QQ'],'-png', '-r300')
%}

%D2] = allfitdist(corn_bu,'PDF');
%Corn Load Size

PD_load_size_corn=fitdist(corn_bu,'logistic')%English
%%{
%metric for figures
corn_ton=corn_bu*56/2204*(1-15/100);%convert to t@ 0% mc

PD_load_size_corn=fitdist(corn_ton,'logistic')

hold on
figure('Name','Corn Load size','Units','inches','Position',[0 0 3.5
3.5],'InvertHardcopy','off','Color',[1 1 1]);
histogram(corn_ton,20,'FaceColor','w','EdgeColor','k','Normalization','
pdf')
x_values = min(corn_ton)-1:0.1:max(corn_ton)+1;
y = pdf(PD_load_size_corn,x_values);
hold on
plot(x_values,y,'--k','LineWidth',2)
xlabel('Load size (t)'); ylabel('Probability Density');
a=gca;
a.Title=[]; a.FontWeight='bold'; a.FontSize=10; a.FontName='arial';
%export_fig([figpath 'Corn Load Size Miles hist'],'-png', '-r300')

hold on
figure('Name','Corn Load size QQ','Units','inches','Position',[0 0 3.5
3.5],'InvertHardcopy','off','Color',[1 1 1]);
qqplot(corn_bu,PD_load_size_corn)
a=gca;
a.Title=[]; a.FontWeight='bold'; a.FontSize=10; a.FontName='arial';
%export_fig([figpath 'Corn Load Size Miles QQ'],'-png', '-r300')
%}

%Wheat

%Load generation
%D1] = allfitdist(Load_generation_rate_wheat,'PDF');%compare dist
%PD_load_gen_wheat=fitdist(Load_generation_rate_wheat,'loglogistic')
PD_load_gen_wheat=fitdist(Load_generation_rate_wheat,'gamma') r
%%{
figure('Name','Wheat Interarrival','Units','inches','Position',[0 0 3.5
3.5],'InvertHardcopy','off','Color',[1 1 1]);
hold on
%histogram(Load_generation_rate_wheat,18,'Normalization','pdf')
histogram(Load_generation_rate_wheat,18,'FaceColor','w','EdgeColor','k'
,'Normalization','pdf')

```

```

x_values = min(Load_generation_rate_wheat)-
1:0.1:max(Load_generation_rate_wheat)+1;
y = pdf(PD_load_gen_wheat,x_values);

hold on
plot(x_values,y,'--k','LineWidth',2)
xlabel('Load Interarrival Time (minutes)'); ylabel('Probability
Density');
xlabel('Grain Cart Interarrival Time (minutes)'); ylabel('Probability
Density');
legend('Histogram', 'Fit PDF')
a=gca;
a.Title=[]; a.FontWeight='bold'; a.FontSize=10; a.FontName='arial';
export_fig([figpath 'Wheat Interarrival miles hist BW1'],'-png', '-
r300')
hold on
figure('Name','Wheat Interarrival QQ','Units','inches','Position',[0 0
3.5 3.5],'InvertHardcopy','off','Color',[1 1 1]);
qqplot(Load_generation_rate_wheat,PD_load_gen_wheat)
a=gca;
a.Title=[]; a.FontWeight='bold'; a.FontSize=10; a.FontName='arial';
export_fig([figpath 'Wheat Interarrival miles QQ'],'-png', '-r300')
%}

%Load Size
%D2] = allfitdist(wheat_bu,'PDF');%Compare dist
PD_load_size_wheat=fitdist(wheat_bu,'logistic')%English
%%{
%Metric for figure
wheat_ton=wheat_bu*60/2204*(1-.135);%metric ton at 0. mc
PD_load_size_wheat=fitdist(wheat_ton,'logistic')

hold on
figure('Name','Wheat Load size','Units','inches','Position',[0 0 3.5
3.5],'InvertHardcopy','off','Color',[1 1 1]);
histogram(wheat_ton,20,'Normalization','pdf')
x_values = min(wheat_ton)-1:0.1:max(wheat_ton)+1;
y = pdf(PD_load_size_wheat,x_values);
hold on
plot(x_values,y,'LineWidth',2)
xlabel('Load size (t)'); ylabel('Probability Density');
a=gca;
a.Title=[]; a.FontWeight='bold'; a.FontSize=10; a.FontName='arial';
export_fig([figpath 'Wheat load size miles hist'],'-png', '-r300')
hold on
figure('Name','Wheat Load size QQ','Units','inches','Position',[0 0 3.5
3.5],'InvertHardcopy','off','Color',[1 1 1]);
qqplot(wheat_bu,PD_load_size_wheat)
a=gca;
a.Title=[]; a.FontWeight='bold'; a.FontSize=10; a.FontName='arial';
export_fig([figpath 'Wheat load size miles QQ'],'-png', '-r300')

%}

%Combined properties
%Pit service time

```

```

PD_pit=fitdist(service_time_pit,'normal')
%%{
hold on
figure('Name','Pit Service','Units','inches','Position',[0 0 3.5
3.5],'InvertHardcopy','off','Color',[1 1 1]);
%histogram(service_time_pit,10,'Normalization','pdf')
histogram(service_time_pit,10,'FaceColor','w','EdgeColor','k','Normaliz
ation','pdf')
x_values = min(service_time_pit):0.1:max(service_time_pit)+1;
y = pdf(PD_pit,x_values);
hold on
plot(x_values,y,'--k','LineWidth',2)
xlabel('Service Time (minutes)'); ylabel('Probability Density');
legend('Histogram', 'Fit PDF','Location','Best')
a=gca;
a.Title=[]; a.FontWeight='bold'; a.FontSize=10; a.FontName='arial';
export_fig([figpath 'Pit service miles hist BW'],'-png', '-r300')

hold on
figure('Name','Pit Service QQ','Units','inches','Position',[0 0 3.5
3.5],'InvertHardcopy','off','Color',[1 1 1]);
qqplot(service_time_pit,PD_pit)
a=gca;
a.Title=[]; a.FontWeight='bold'; a.FontSize=10; a.FontName='arial';
export_fig([figpath 'Pit service miles QQ'],'-png', '-r300')

%}

%Field transfer time
%[D] =
allfitdist([service_time_corn_load;service_time_wheat_load],'PDF');
service_time_load=[service_time_corn_load;service_time_wheat_load];
PD_loading=fitdist(service_time_load,'lognormal')

%%{
hold on
figure('Name','Loading Service','Units','inches','Position',[0 0 3.5
3.5],'InvertHardcopy','off','Color',[1 1 1]);
%histogram(service_time_load,10,'Normalization','pdf')
histogram(service_time_load,10,'FaceColor','w','EdgeColor','k','Normali
zation','pdf')
x_values = min(service_time_load)-1:0.1:max(service_time_load)+1;
y = pdf(PD_loading,x_values);
hold on
plot(x_values,y,'--k','LineWidth',2)
xlabel('Service Time (minutes)'); ylabel('Probability Density');
legend('Histogram', 'Fit PDF','Location','Best')
a=gca;
a.Title=[]; a.FontWeight='bold'; a.FontSize=10; a.FontName='arial';
export_fig([figpath 'Loading service miles hist BW'],'-png', '-r300')
hold on
figure('Name','Loading Service QQ','Units','inches','Position',[0 0 3.5
3.5],'InvertHardcopy','off','Color',[1 1 1]);
qqplot(service_time_load,PD_loading)
a=gca;

```

```

a.Title=[]; a.FontWeight='bold'; a.FontSize=10; a.FontName='arial';
export_fig([figpath 'Loading service miles QQ'],'-png', '-r300')
%}

%*****
*****
%Andy

%Load generation rate
%D1] = allfitdist(Load_generation_rate_andy,'PDF');
PD_load_gen_andy=fitdist(Load_generation_rate_andy,'loglogistic')

%%{
figure('Name','Corn Interarrival Andy','Units','inches','Position',[0 0
3.5 3.5],'InvertHardcopy','off','Color',[1 1 1]);
hold on
%histogram(Load_generation_rate_andy,6,'Normalization','pdf')
histogram(Load_generation_rate_andy,6,'FaceColor','w','EdgeColor','k','
Normalization','pdf')
x_values = min(Load_generation_rate_andy)-
1:0.1:max(Load_generation_rate_andy)+1;
y = pdf(PD_load_gen_andy,x_values);

hold on
plot(x_values,y,'--k','LineWidth',2)
xlabel('Load Interarrival Time (minutes)'); ylabel('Probability
Density');
xlabel('Grain Cart Interarrival Time (minutes)'); ylabel('Probability
Density');
legend('Histogram', 'Fit PDF','Location','Best')
a=gca;
a.Title=[]; a.FontWeight='bold'; a.FontSize=10; a.FontName='arial';
export_fig([figpath 'Load Interarrival andy hist BW1'],'-png', '-r300')

hold on
figure('Name','Corn Interarrival Andy
QQ','Units','inches','Position',[0 0 3.5
3.5],'InvertHardcopy','off','Color',[1 1 1]);
qqplot(Load_generation_rate_andy,PD_load_gen_andy)
a=gca;
a.Title=[]; a.FontWeight='bold'; a.FontSize=10; a.FontName='arial';
export_fig([figpath 'Load Interarrival andy QQ'],'-png', '-r300')
%}

%Pit service time
service_time_andy_pit(service_time_andy_pit>100)=[];%Delete the really
high service time ( It was due to breakdown/ lunch)
[D1] = allfitdist(service_time_andy_pit,'PDF');
PD_andy_pit=fitdist(service_time_andy_pit,'normal')
%%{
hold on
figure('Name','Pit Service Andy','Units','inches','Position',[0 0 3.5
3.5],'InvertHardcopy','off','Color',[1 1 1]);
%histogram(service_time_andy_pit,6,'Normalization','pdf')
histogram(service_time_andy_pit,6,'FaceColor','w','EdgeColor','k','Norm
alization','pdf')

```

```

x_values = min(service_time_andy_pit)-
15:0.1:max(service_time_andy_pit)+10;
y = pdf(PD_andy_pit,x_values);
hold on
plot(x_values,y,'--k','LineWidth',2)
xlabel('Service Time (minutes)'); ylabel('Probability Density');
legend('Histogram', 'Fit PDF','Location','Best')
a=gca;
a.Title=[]; a.FontWeight='bold'; a.FontSize=10; a.FontName='arial';
export_fig([figpath 'Pit service andy hist BW'],'-png', '-r300')

hold on
figure('Name','Pit Service Andy QQ','Units','inches','Position',[0 0
3.5 3.5],'InvertHardcopy','off','Color',[1 1 1]);
qqplot(service_time_andy_pit,PD_andy_pit)

a=gca;
a.Title=[]; a.FontWeight='bold'; a.FontSize=10; a.FontName='arial';
export_fig([figpath 'Pit Service andy QQ'],'-png', '-r300')

%}

%Field transfer
service_time_load=service_time_andy_load;
%[D] = allfitdist(service_time_load,'PDF');
PD_andy_loading=fitdist(service_time_load,'normal')

%%{
hold on
figure('Name','Loading Service','Units','inches','Position',[0 0 3.5
3.5],'InvertHardcopy','off','Color',[1 1 1]);
%histogram(service_time_load,8,'Normalization','pdf')
histogram(service_time_load,8,'FaceColor','w','EdgeColor','k','Normaliz
ation','pdf')
x_values = min(service_time_load)-1:0.1:max(service_time_load)+1;
y = pdf(PD_andy_loading,x_values);
hold on
plot(x_values,y,'--k','LineWidth',2)
xlabel('Service Time (minutes)'); ylabel('Probability Density');
legend('Histogram', 'Fit PDF','Location','Best')
a=gca;
a.Title=[]; a.FontWeight='bold'; a.FontSize=10; a.FontName='arial';
export_fig([figpath 'Loading service andy hist BW'],'-png', '-r300')
hold on
figure('Name','Loading Service QQ','Units','inches','Position',[0 0 3.5
3.5],'InvertHardcopy','off','Color',[1 1 1]);
qqplot(service_time_load,PD_andy_loading)
a=gca;
a.Title=[]; a.FontWeight='bold'; a.FontSize=10; a.FontName='arial';
export_fig([figpath 'Loading service andy QQ'],'-png', '-r300')
%}

```

Script to Run the Simulation Model

```
%*****
% TITLE: Run DES model
% AUTHOR: Aaron P. Turner
% DATES: Feb 2018
% DESCRIPTION: Main script to run Simulink DES simulation model      of
%grain transportation.
%Reads in .mat file with PDF objects for service times and entity
%generation.
%Simulation time and resource constraints defined in the script
%PDF's are from recorded data and fit using Fit_dist script
%Script to call Simevents DES model for grain hauling
%Outputs model results as a 1X500 simulation output
clear; clc; close all;
%*****
%Define variables
tic
load PD_objects.mat %Read in PDF objects
load seed_val.mat %Array of random seed values used to seed random
number generation for each day
mdl='Hauling_model_sto_batch.slx';
%mdl='test_model.slx';
load_system(mdl);
numsims=500;%number of times to run the simulation
parpool;

sim_out(numsims)= Simulink.SimulationOutput;% Initialize output

%*****
%Inputs are set for each day considered in the simulation. Uncomment a
day to evaluate

%Example change to run different days
%8/29
%%{
seed=master_seed(7);
runtime=531.1;%Time harvesting
num_truck=9;% number of trucks in resource pool
num_driver=9;% number of drivers in resource pool
field_buffer=3;%Field side storage buffer
batch_size=1;
dt_transport=5.0;%time traveling from field to storage
dt_inspect=2;% time to weigh and inspect
dt_return=dt_transport;% time to return to the field, equal to
dt_transport+ offset to position
%}

%Rename PDF objects here
PD_load_gen=PD_load_gen_corn;
PD_field_trans=PD_loading;
PD_pit=PD_pit;
PD_size=PD_load_size_corn;
```

```

%Define matrix of random numbers for simulation. rows=simulation #.
columns
%number of random vars. arbitrary at 100 so there is more than enough.

rng(seed);%Set seed val so can be replicated

%Generate random vars
load_gen_rate=random(PD_load_gen,numsims,100);
dt_field_trans=random(PD_field_trans,numsims,100);
dt_unload=random(PD_pit,numsims,100);

%*****

%Define outputs
operating_cost1=zeros(numsims,1);
WIP_finall=zeros(numsims,1);
Loads_theory1=zeros(numsims,1);
sys_eff1=zeros(numsims,1);
system_throughput1=zeros(numsims,1);
loads_missed1=zeros(numsims,1);
man_hrs1=zeros(numsims,1);

%*****

%use parallel processing
%%{
% 3) Need to switch all workers to a separate tempdir in case
% any code is generated for instance for StateFlow, or any other
% file artifacts are created by the model.
spmd
    % Setup tempdir and cd into it
    currDir = pwd;
    addpath(currDir);
    tmpDir = tempname;
    mkdir(tmpDir);
    cd(tmpDir);
    % Load the model on the worker
    load_system mdl;
end

parfor j=1:numsims% Run the simulation multiple times

    sim_out(j)=fun_run_mdl(...

num_truck,num_driver,load_gen_rate(j,:),dt_field_trans(j,:),dt_transpor
t,dt_unload(j,:),dt_return,field_buffer,dt_inspect,mdl,runtime,batch_si
ze);

end

% 5) Switch all of the workers back to their original folder.
spmd

```

```

        cd(currDir);
        rmdir(tmpDir,'s');
        rmpath(currDir);
        close_system mdl, 0);
end

close_system mdl, 0);
delete(gcp('nocreate'));
%}
toc

function
[res]=fun_run_mdl(num_truck,num_driver,Cost,load_gen_rate,dt_field_tran
s,dt_transport,dt_unload,dt_return,field_buffer,dt_inspect,mdl,runtime,
batch_size)
%Main function calls model and Stores results

%set model workspace to function and call model
options =
simset('SrcWorkspace','current','ReturnWorkspaceOutputs','on');

res=sim(mdl,[],options);
end

```

Script to Analyze Simulation Output

```

%*****
% TITLE: DES Analysis
% AUTHOR: Aaron P. Turner
% DATES: March 2018
% DESCRIPTION: Script reads in 1X500 Simulink output files for DES
%transportation model and performance analysis on the system
%Also generates High quality figures
%*****

clc; close all; clear;
%load andy_simout.mat

figpath='C:\XXX\';

%Example inputs. Each day was unique
%%{
folder='XXX\';
load wheat_delivered_actual.mat; %actual arrivals from spread sheet
only days w/ on-farm deliveries.

%0611
%Load Simulink output
load wheat0611.mat
day1='0611';

```



```

actual=wheat_actual(wheat_actual(:,1)==11,3:4); %select day and only
time and load #
t_harvest_stop=380;
batch_size=1;
num_truck=4;
num_driver=4;
%}

%Define vars
loads_delivered=[];
Flow_time=[];%Load creation to unload finish
batch_order=[];%order in batch
Truck_time=[];
productive_time=[];
loads_in=[];
loads_WIP=[];
Field_delay=[];
pit_delay=[];
truck_util=[];
driver_util=[];

%Loop to go through each simulation and aggregate results
for i=1:length(sim_out)

%*****Loads delivered, Productive time and Flow time*****
    %loads delivered
    res=[sim_out(i).Loads_out.Time sim_out(i).Loads_out.Data];
    loads_delivered=[loads_delivered; res];
    Cum_total(i)=sim_out(i).Loads_out.Data(end);

    %Flow time. Time from when load is generated till it is unloaded.
    res=[sim_out(i).T_creation.Data (sim_out(i).T_unload_complete.Data-
sim_out(i).T_creation.Data)];
    Flow_time=[Flow_time; res];

    %Productive time transfer, transport, weigh, unload
    res=[sim_out(i).T_creation.Data...
(sim_out(i).T_finish_load.Data-sim_out(i).T_start_load.Data)...
(sim_out(i).T_arrive_storage.Data-
sim_out(i).T_start_trans.Data)...
(sim_out(i).T_finish_scales.Data-
sim_out(i).T_start_scales.Data)...
(sim_out(i).T_unload_complete.Data)-
sim_out(i).T_start_unload.Data];
    productive_time=[productive_time; res];

    %*****Wait Time*****
    %Time entities wait for trucks
    res=[sim_out(i).T_creation.Data (sim_out(i).T_start_load.Data-
sim_out(i).T_creation.Data)];
    Field_delay=[Field_delay; res];

    %time trucks wait @ unload

```

```

    res=[sim_out(i).T_creation.Data (sim_out(i).T_start_unload.Data-
sim_out(i).T_finish_scales.Data)];
    pit_delay=[pit_delay; res];

% *****Resource utilization*****

    %Final time. when all resources return to field. all
    %sim_out(i).XXX.Time are the same time. And it is the time stamp
%whenthe haul back is complete and the resource is released.
    t_max=sim_out(i).T_creation.Time(end);
    t_OT(i)=t_max-t_harvest_stop; %Amount of time hauling continues
after harvest stops
    %Truck utilization, account for truck being "utilized" from first
unload
    %Batch order
    batch_temp=sim_out(i).Batch_order.Data;
    batch_order=[batch_order; batch_temp];

    %Truck total time including empty haul back
    res=[sim_out(i).T_creation.Data (sim_out(i).T_start_load.Time-
sim_out(i).T_creation.Data)];
    Truck_total_time=res(batch_temp==1,2);

    %Truck utilization, averaged for the day
    Daily_truck_util(i)=(sum(Truck_total_time)/num_truck)/t_max*100;

    %Driver Utilization
    res=[sim_out(i).T_creation.Data (sim_out(i).T_start_trans.Time-
sim_out(i).T_start_trans.Data)];
    %Driver_time=[Driver_time; res];
    Driver_total_time=res(batch_temp==1,2);

    %Driver utilization, averaged for the day
    Daily_driver_util(i)=(sum(Driver_total_time)/num_driver)/t_max*100;

%***** Parameters calculated in simulink*****
%Truck utilization
res=[sim_out(i).Truck_util.Time sim_out(i).Truck_util.Data];
truck_util=[truck_util; res];
%truck_util_max(i)=max(sim_out(i).Truck_util.Data);

%Driver utilization
res=[sim_out(i).driver_util.Time sim_out(i).driver_util.Data];
driver_util=[driver_util; res];
%driver_util_max(i)=max(sim_out(i).driver_util.Data);

%
end

%Average Deliveries
average_deliveries=mean(Cum_total);

```

```

std_dev=sqrt((1/(length(Cum_total)-1))*sum((Cum_total-
average_deliveries).^2));%std. dev eq 4.2 sim and monte carlo book

%Average Flow time.
average_flow_time=mean(Flow_time(:,2));

% Productive time
total_productive_time=[productive_time(:,1)
productive_time(:,2)+productive_time(:,3)+productive_time(:,4)+producti
ve_time(:,5)];

%Flow time efficiency
flow_time_eff=[Flow_time(:,1)
total_productive_time(:,2)./Flow_time(:,2)*100];
average_flow_time_eff=mean(flow_time_eff(:,2));

%Truck and driver Utilization
average_truck_util=mean(Daily_truck_util);
average_driver_util=mean(Daily_driver_util);

truck_util_max=max(truck_util(:,2));
driver_util_max=max(driver_util(:,2));

% Fit trend to SimEvents utilization
%Trucks
Truck_util_sort=sortrows(truck_util,1);
dt=5;%minutes
for j= 1:floor(Truck_util_sort(end,1)/dt)
if j==1
dt_old=0;
end
truck_util_mean(j,:)=mean(Truck_util_sort(Truck_util_sort(:,1)>dt_old &
Truck_util_sort(:,1)<(dt_old+dt),:),1);
dt_old=dt_old+dt;
end

%Drivers
driver_util_sort=sortrows(driver_util,1);
dt=5;%minutes
for j= 1:floor(driver_util_sort(end,1)/dt)
if j==1
dt_old=0;
end
driver_util_mean(j,:)=mean(driver_util_sort(driver_util_sort(:,1)>dt_ol
d & driver_util_sort(:,1)<(dt_old+dt),:),1);
dt_old=dt_old+dt;
end

% Wait time calculations
average_t_OT=mean(t_OT);%average time trucks run after harvest stops
max_field_delay=max(Field_delay(:,2));% max time waiting for a truck
max_pit_delay=max(pit_delay(:,2));% max time waiting to unload

%Mean Delay

```

```

mean_field_delay= mean(Field_delay(Field_delay(:,2)>0,2));%Mean delay,
when there is a delay
mean_pit_delay= mean(pit_delay(pit_delay(:,2)>0,2));%Mean delay, when
there is a delay

%estimate % of loads that experience a delay
percent_field_delay=sum(Field_delay(:,2)>0)/length(Field_delay(:,2))*10
0;
percent_pit_delay=sum(pit_delay(:,2)>0)/length(pit_delay(:,2))*100;

%Fprint
%disp(average_deliveries);disp(2*std_dev);
fprintf('average t_OT %g \n',average_t_OT);
fprintf('Driver util: %g \t Max driver util: %g
\n',average_driver_util,driver_util_max*100);
fprintf('truck util: %g \t Max truck util: %g
\n',average_truck_util,truck_util_max*100);
fprintf('FTE %g \n',average_flow_time_eff);
fprintf('Loads delivered %g plus minus %g \n',average_deliveries,
2*std_dev);
fprintf('Field side delay: Max: %g \t Mean: %g \t Percent delayed: %g
\n',max_field_delay, mean_field_delay,percent_field_delay);
fprintf('Pit delay Max: %g \t Mean: %g \t Percent delayed:
%g\n',max_pit_delay, mean_pit_delay,percent_pit_delay);
%fprintf('%g percent of loads experience a delay at the field edge
\n',percent_field_delay);
%fprintf('%g percent of loads experience a delay at the pit
\n',percent_pit_delay);

%*****Plotting*****

%{%
%loads delivered
figure('Name','Loads_delieverd','Units','inches','Position',[0 0 3.5
3.5],'InvertHardcopy','off','Color',[1 1 1]);
hold on

scatter(loads_delivered(:,1),loads_delivered(:,2),'filled','MarkerFaceC
olor',[0.5 0.5 0.5],'MarkerFaceAlpha',0.2)
stairs(actual(:,1),actual(:,2),'k','LineWidth',2)
legend('Simulation','Actual','Location','Best')
xlabel('Simulation Time (minutes)'); ylabel('Cumulative Deliveries');
a=gca;
a.Title=[]; a.FontWeight='bold'; a.FontSize=10; a.FontName='arial';
export_fig([figpath folder 'loads_delivered_' day1'],'-png', '-r300','-
nocrop')

%Flow time
figure('Name','Flow_time','Units','inches','Position',[0 0 3.5
3.5],'InvertHardcopy','off','Color',[1 1 1]);
hold on
scatter(Flow_time(:,1),Flow_time(:,2),'filled','MarkerFaceColor',[0.5
0.5 0.5],'MarkerFaceAlpha',0.2)
scatter(total_productive_time(:,1),total_productive_time(:,2),'r','fill
ed','MarkerFaceAlpha',0.1)

```

```

xlabel('Load Creation Time (minutes)'); ylabel('Time (minutes)');
legend('Flow time', 'Productive time','Location','Best')
a=gca;
a.Title=[]; a.FontWeight='bold'; a.FontSize=10; a.FontName='arial';
export_fig([figpath folder 'Flow_time_' day1],'-png', '-r300','-
nocrop')

%Flow time eff
figure('Name','Flow_time_eff','Units','inches','Position',[0 0 3.5
3.5], 'InvertHardcopy','off','Color',[1 1 1]);
hold on
scatter(flow_time_eff(:,1),flow_time_eff(:,2), 'filled', 'MarkerFaceColor
',[0.5 0.5 0.5], 'MarkerFaceAlpha',0.2)
ylim([0 100])
xlabel('Load Creation Time (minutes)'); ylabel('Flow Time Efficiency
(%)');
a=gca;
a.Title=[]; a.FontWeight='bold'; a.FontSize=10; a.FontName='arial';
export_fig([figpath folder 'Flow_time_eff_' day1],'-png', '-r300','-
nocrop')

%%{
%Truck utilization 2
figure('Name','Truck Utilization avg','Units','inches','Position',[0 0
3.5 3.5], 'InvertHardcopy','off','Color',[1 1 1]);
hold on
scatter(truck_util(:,1),truck_util(:,2)*100, 'filled', 'MarkerFaceColor',
[0.5 0.5 0.5], 'MarkerFaceAlpha',0.2)
plot(truck_util_mean(1:(end-5),1),truck_util_mean(1:(end-
5),2)*100, 'k', 'LineWidth',2)
ylim([0 100])
xlabel('Simulation Time (minutes)'); ylabel('Truck Utilization (%)');
legend('Simulation', 'Average','Location','Best')
a=gca;
a.Title=[]; a.FontWeight='bold'; a.FontSize=10; a.FontName='arial';
export_fig([figpath folder 'truck_util_avg' day1],'-png', '-r300','-
nocrop')

%driver utilization 2
figure('Name','Driver Utilization avg','Units','inches','Position',[0 0
3.5 3.5], 'InvertHardcopy','off','Color',[1 1 1]);
hold on
scatter(driver_util(:,1),driver_util(:,2)*100, 'filled', 'MarkerFaceColor
',[0.5 0.5 0.5], 'MarkerFaceAlpha',0.2)
plot(driver_util_mean(1:(end-5),1),driver_util_mean(1:(end-
5),2)*100, 'k', 'LineWidth',2)
ylim([0 100])
xlabel('Simulation Time (minutes)'); ylabel('Driver Utilization (%)');
legend('Simulation', 'Average','Location','Best')
a=gca;
a.Title=[]; a.FontWeight='bold'; a.FontSize=10; a.FontName='arial';
export_fig([figpath folder 'driver_util_avg' day1],'-png', '-r300','-
nocrop')
%}

%%{

```

```

%delay at field edge waiting for a truck
figure('Name','Field_Delay','Units','inches','Position',[0 0 3.5
3.5],'InvertHardcopy','off','Color',[1 1 1]);
hold on
scatter(Field_delay(:,1),Field_delay(:,2),'filled','MarkerFaceColor',[0
.5 0.5 0.5],'MarkerFaceAlpha',0.2)
ylim([0, max(ylim)])
xlabel('Load Creation Time (minutes)'); ylabel('Wait Time (minutes)');
a=gca;
a.Title=[]; a.FontWeight='bold'; a.FontSize=10; a.FontName='arial';
export_fig([figpath folder 'field_delay_' day1],'-png', '-r300','-
nocrop')

%Delay at pit waiting to unload
figure('Name','Pit_Delay','Units','inches','Position',[0 0 3.5
3.5],'InvertHardcopy','off','Color',[1 1 1]);
hold on
scatter(pit_delay(:,1),pit_delay(:,2),'filled','MarkerFaceColor',[0.5
0.5 0.5],'MarkerFaceAlpha',0.2)
ylim([0, max(ylim)])
xlabel('Load Creation Time (minutes)'); ylabel('Wait Time (minutes)');
a=gca;
a.Title=[]; a.FontWeight='bold'; a.FontSize=10; a.FontName='arial';
export_fig([figpath folder 'pit_delay_' day1],'-png', '-r300','-
nocrop')
%}
%}

```

Appendix C. Sample Code for Whole Season Simulation

Main Function

```
function [summary]=fun_whole_season_sim(input,weather,figpath)
%*****
% TITLE: Main Function
% AUTHOR: Aaron P. Turner
% DATES: Aug 2018
% DESCRIPTION: Function to call the simulink DES hauling and storage
%model
%simulates harvest until the required amount of grain is harvested
%*****
%Define variables

mdl='Hauling_model_sto_batch_dry.slx';
load_system(mdl);
total_harvest=input.MT;%dry t over season
Hh=input.Hh*60;
Ht=input.Ht*60;
Ncombines=input.Ncombine;
Ncarts=input.Ncart;
summary=table();

%Transport
load_gen_rate(1:100)=input.load_gen_rate;
dt_field_trans(1:100)=input.dt_field_trans;
dt_transport=input.dt_transport;
dt_unload(1:100)=input.dt_unload;
dt_return=dt_transport;
field_buffer=input.Q_field_max;
batch_size=input.batch_size;
dt_inspect=input.dt_inspect;
%}
num_truck=input.Ntruck;%average was 8.6
num_driver=input.Ndriver;%average was 8.6

%Drying and storage
MCi=input.MCi;% initial moisture content

SDC=input.SDC;%Stated dryer capacity
T_rated=input.T_rated;%Rated Dryer temp
T_dry=input.T_dry;%Actual drying temperature
MCoout=input.MCoout;%Can change if needed
wet_cap=input.wet_cap;
load_size(1:100)=input.load_size;% dry tonne
Nstorage=input.Nstorage;
%Define Daily vars

%Moisture content and daily runtime
[MCpred, runtime_all]=get_daily_cond(weather,MCi,input.Hh*60);
```

```

%runtime_all(1:3)=0;%Delay WC till 25%
wet_Q=wet_cap-1;%maximum wet holding cap
wet_bin_initial=inf;%wet bin empty on day 1
i=1;%counter var
%adjusted dryer capacity in dry t/hr
[~,scaled_cap_dry] = Drying_cap_adj(SDC, MCout,MCpred,T_rated,T_dry);
dt_dry_rem=0;%initialize. need it later
wet_carry_prev=0;
%Run daily Simulations until all grain is harvested
while total_harvest>0

    % close all
    %new daily conditions
    runtime=runtime_all(i);%daily harvest time
    dry_rate=scaled_cap_dry(i)/60;%drying rate t/ min

    %Set path dry store or direct to store
    if MCpred(i)>MCout
        Dry=2;
    else
        Dry=1;
    end
    dry_time=load_size/dry_rate;%dry time for dryer server

    %Reduce time for partly dried load at end of previous sim
    if dt_dry_rem(1)>0
        dry_time(1:length(dt_dry_rem))=dt_dry_rem;
    end

    %Run model

    simout=fun_run mdl(num_truck,num_driver,load_gen_rate,dt_field_trans,dt
    _transport,...

    dt_unload,dt_return,field_buffer,dt_inspect,mdl,runtime,batch_size,Dry,
    wet_Q,wet_bin_initial,dry_time,Ht);

    %Check all loads were delivered, if not rerun w/ adjusted time
    if
    length(simout.Loads_in.Data)>length(simout.T_unload_complete.Data)
        %find number of batch elements delivered
        j=length(simout.T_unload_complete.Data);
        %Update runtime to reflect when last load that was delivered
        was
        %actually harvested
        runtime_reduced=simout.Loads_in.Time(j)+1;

        %Rerun

    simout=fun_run mdl(num_truck,num_driver,load_gen_rate,dt_field_trans,dt
    _transport,...

```



```

dt_unload,dt_return,field_buffer,dt_inspect,mdl,runtime_reduced,batch_size,
ize,Dry,wet_Q,wet_bin_initial,dry_time,Ht);
    flag=1;

end

%*****Process data*****

%only update if new crop is harvested
%Returns # of entities in wet holding pit and total time harvest is
%delayed also determines number of loads that entered and left the
%system

%Account for initial loads being given a drytime/mass first in the
%simulation
idx1=floor(length(wet_bin_initial)/batch_size);
%handle updates for when harvest occurs, only drying occurs, and
%when
%nothing occurs

if runtime >0
    [bin_final(i),pit_final(i),delay(i)]=
Daily_sum(simout,field_buffer,runtime,batch_size,figpath,i);

Daily_total_in(i,1)=floor(simout.Loads_in.Data(end)/batch_size);%Truck
loads into the system

Daily_total_in(i,2)=sum(load_size(idx1+1:Daily_total_in(i,1)+idx1));%t
harvested
    Daily_total_out(i,1)=simout.Loads_out.Data(end)/batch_size;
    Daily_total_out(i,2)=sum(load_size(1:Daily_total_out(i,1)));

    total_harvest=total_harvest-Daily_total_in(i,2);
else
    [bin_final(i),pit_final(i),delay(i)]=
Daily_sum(simout,field_buffer,runtime,batch_size,figpath,i);
    Daily_total_in(i,1)=0;
    Daily_total_in(i,2)=0;
    if isempty(simout.Loads_out.Data)
        Daily_total_out(i,1)=0;
        Daily_total_out(i,2)=0;
    else
        Daily_total_out(i,1)=simout.Loads_out.Data(end)/batch_size;

Daily_total_out(i,2)=sum(load_size(1:Daily_total_out(i,1)));
    end
end

%FinalIteration*****

%The final iteration determine how long it took to harvest the
%remaining grain and rerun the simulation with only that runtime
if total_harvest<0

```

```

        target=total_harvest+Daily_total_in(i,2);%remaining at start of
iteration
        j=1;%counter
        %Loop until req. loads are harvested.
        while target>0
            target=target-load_size(j);
            if target>0
                j=j+1;
            end
        end
        %required field unloads to finish the day

        j=j*batch_size;
        runtime=simout.Loads_in.Time(j)+1;
        %Run model

simout=fun_run_mdl(num_truck,num_driver,load_gen_rate,dt_field_trans,dt
_transport,...

dt_unload,dt_return,field_buffer,dt_inspect,mdl,runtime,batch_size,Dry,
wet_Q,wet_bin_initial,dry_time,Ht);

        %Update values w/ rerun for last day

        idx1=length(wet_bin_initial)/batch_size;
        if runtime >0
            [bin_final(i),pit_final(i),delay(i)]=
Daily_sum(simout,field_buffer,runtime,batch_size,figpath,i);

Daily_total_in(i,1)=floor(simout.Loads_in.Data(end)/batch_size);%Truck
loads into the system

Daily_total_in(i,2)=sum(load_size(idx1+1:Daily_total_in(i,1)+idx1));%t
harvested
            Daily_total_out(i,1)=simout.Loads_out.Data(end)/batch_size;

Daily_total_out(i,2)=sum(load_size(1:Daily_total_out(i,1)));

            total_harvest=total_harvest-Daily_total_in(i,2);
        else
            [bin_final(i),pit_final(i),delay(i)]=
Daily_sum(simout,field_buffer,runtime,batch_size,figpath,i);
            Daily_total_in(i,1)=0;
            Daily_total_in(i,2)=0;
            if isempty(simout.Loads_out.Data)
                Daily_total_out(i,1)=0;
                Daily_total_out(i,2)=0;
            else
                Daily_total_out(i,1)=simout.Loads_out.Data(end)/batch_size;

                Daily_total_out(i,2)=sum(load_size(1:Daily_total_out(i,1)));
            end
        end
    end
end

```

```

end
%More daily summary

% table(bin_final',Daily_total_in,Daily_total_out,delay')
% Call function for analysis

[res]=analysis1(simout, runtime, num_truck, num_driver, batch_size, figpath,
i);
T_combine_tot=res.T_combine*Ncombines;
T_carts_tot=res.T_combine*Ncarts+(res.T_carts-res.T_combine)*1;
T_storage_tot=res.T_dryer*Nstorage;
T_driver_tot=res.T_drivers;% Already accounted for
a=table(T_combine_tot, T_carts_tot, T_storage_tot,T_driver_tot);
res=[res, a];

summary=[summary;res];

%Wet bin*****
%Handle wet bin carry over
%setting wet bin to inf sets dt in the model to inf so no entities
%are created

%check if wet bin is used at all.
% %{
if bin_final(i)==0
    wet_carry(i)=bin_final(i);
    wet_carry_prev=wet_carry(i);
    wet_bin_initial=inf;
    dt_dry_rem=0;
else
    dt_dry_rem=[];
    %wet_carry(i)=bin_final(i)+pit_final(i);
    wet_carry(i)=wet_carry_prev+Daily_total_in(i,1)-
Daily_total_out(i,1);
    wet_carry_prev=wet_carry(i);
    %Trick because simulink needs to be same batch structure.
    % wet carry
    %is truck loads. multiply by batches/truck to get correct # of
    %entities generated
    wet_bin_initial=zeros(1,wet_carry(i)*batch_size);
    %wet_bin_initial=zeros(1,wet_carry(i));
    dt_dry_rem(1)=Ht-res.t_end;
    dt_dry_rem(2:wet_carry(i))=dry_time(50:50+wet_carry(i)-2);

end
%}

i=i+1;
end
MCin=MCpred(1:i-1); runtime_act=runtime_all(1:i-1);

%Output Summary
Daily=table(wet_carry',bin_final',Daily_total_in(:,1),Daily_total_in(:,
2),Daily_total_out(:,1),Daily_total_out(:,2),delay',MCin, runtime_act);

```

```

Daily.Properties.VariableNames={'wet_carry','bin_final','loads_in',...
'mass_in','Loads_out','Mass_out','HTL','MCin','runtime'};
summary=[summary Daily];

%Energy Used in drying, base eff. Was 200 BTU/lbH2)
[energy]=Energy_use(summary,T_dry,MCout,2000);

summary=[summary energy];

end
%Function*****

function
[res]=fun_run_mdl(num_truck,num_driver,load_gen_rate,dt_field_trans,dt_
transport,...
dt_unload,dt_return,field_buffer,dt_inspect,mdl,runtime,batch_size,Dry,
wet_Q,wet_bin_initial,dry_time,Ht)

%set model workspace to function and call model
options =
simset('SrcWorkspace','current','ReturnWorkspaceOutputs','on');

res=sim(mdl,[],options);

end

```

Main Function Initialization for Whole Season Validation Conditions

```
*****
% TITLE: Run dry and store simulation of des model
% AUTHOR: Aaron P. Turner
% DATES: June 2018
% DESCRIPTION: Function to call the simulink DES hauling and storage
model
%simulates harvest until the required amount of grain is harvested
*****
***%
%Define variables
clear; clc; close all;
figpath='C:\Users\aptu222\OneDrive - University of Kentucky\Harvest
Logistics\Turner_PhD\Papers\DES_hauling_plus_storage\Figures\sims\';
mdl='Hauling_model_sto_batch_dry.slx';
load_system(mdl);
total_harvest=6959;%dry t over season
Hh=8*60;%8 hrs per day for field work
Ht=24*60;%lenght of simulation
summary=table();
%test case for batch should give same results
%{
%Inputs Average of 2016 corn
%Transport
load_gen_rate(1:1000)=17.2/2;
dt_field_trans(1:1000)=5.76;
dt_transport=11.6;
dt_unload(1:1000)=12.5;
dt_return=dt_transport;
field_buffer=3;
batch_size=2;
dt_inspect=2;
%}

%%{
%Inputs Average of 2016 corn
%Transport
load_gen_rate(1:100)=17.2;
dt_field_trans(1:100)=5.76;
dt_transport=11.6;
dt_unload(1:100)=12.5;
dt_return=dt_transport;
field_buffer=3;
batch_size=1;
dt_inspect=2;
%}
num_truck=8;%average was 8.6
num_driver=8;%average was 8.6

%Drying and storage
Mci=26.7;% initial moisture content
load weather.mat%weather data
SDC=4000;%4000 bu/hr @ 5pt for Sukup 4018
T_rated=220;%Rated Dryer Capacity
```

```

T_dry=140;%Actual drying temperature
MCout=15;%Can change if needed
wet_cap=18;%CHECK approximatly 16.5k bu + .75k in top of dryer????
load_size(1:100)=21.0;% dry tonne

%Define Daily vars

%Moisture content and daily runtime
[MCpred, runtime_all]=get_daily_cond(weather,MCi,Hh);
wet_Q=wet_cap-1;%maximum wet holding cap
wet_bin_initial=inf;%wet bin empty on day 1
i=1;%counter var
%adjusted dryer capacity in dry t/hr
[~,scaled_cap_dry] = Drying_cap_adj(SDC, MCout,MCpred,T_rated,T_dry);
dt_dry_rem=0;%initialize. need it later

%Dummy vars needed to prevent errors for sensitivity portion of the
script
Ncombines=2;
Ncarts=2;
Nstorage=1;
wet_carry_prev=0;
%Run daily Simulations until all grain is harvested
%Same As Main Function from this point on

```

Fieldwork and Moisture Content Estimation

```
function [MCpred, runtime]=get_daily_cond(weather,MCi,Hh)

%*****
%*****
% TITLE: Moisture dry down and field time estimate
% AUTHOR: Aaron P. Turner
% DATES: June 2018
% DESCRIPTION: This functions reads in hourly weather station
observations
% and summerizes daily Temperature and RH values
% Predicts grain dry down from an inital moisture and provides if field
%work occured based on 0.5in rain threshold and no work on Sunday
%20% of rainfall carries over from previous day
%otherwise 8 hours per day
%*****
%beta=0.094;%dry down coeff. determined for the 2016 corn data
beta=0.0812;%based on inbound records not scales
%beta=0.06;%based on inbound records not scales (from Morey)
%beta=0.10;%Just increased to match decrease;
weather_stats=grpstats(weather, 'Date', {'mean',
'min', 'max'}, 'DataVars', ...
{'TempF', 'RH', 'Precipin'});
TempC=(weather_stats.mean_TempF-32)*5/9; % Temperature in deg c

Temp1=grpstats(weather, 'Date', 'sum');
sum_Precipin=Temp1.sum_Precipin;

%Find EMC
%Mod. Henderson. Eqn  $M = ((\ln(1-rh) / (-K * (T+C)))^{(1/N)})$ 
K=0.000086541;
C=49.81;
N=1.8634;
EMC_db=(log(1-weather_stats.mean_RH/100)./(-K*(TempC+C))).^(1/N);
EMC_wb=(100*EMC_db)./(100+EMC_db);%Convert to wb
Temp=table(TempC,sum_Precipin, EMC_db, EMC_wb);
weather_stats=[weather_stats Temp];%Joined data as table

%Determined MC
MCpred(1)=MCi;%initial condition
for i=2:height(weather_stats)
    dt=beta*(MCpred(i-1)-weather_stats.EMC_wb(i));
    if weather_stats.sum_Precipin>0%no change if rain event
        dt=0;
    end
    MCpred(i)=MCpred(i-1)-dt;
end

DayNum=weekday(weather_stats.Date);
Precip_yesterday=0; %assume no rain on day before start of sim
%Determine if work occured
for i=1:height(weather_stats)
```

```

Level_today(i)=Precip_yesterday+weather_stats.sum_Precipin(i);

    if DayNum(i)==1

        runtime(i)=0;
elseif Level_today(i)>0.25%Changed 8/12/18
        runtime(i)=0;
else
        runtime(i)=Hh;

    end

    Precip_yesterday=0.2*Level_today(i);
end
MCpred=MCpred'; Level_today=Level_today'; runtime=runtime';
Temp2=table(Level_today,runtime,MCpred);
weather_stats=[weather_stats, Temp2];
end

```


Energy Use in Drying Estimation

```
function [res]=Energy_use(summary,T_dry,MCout,Base_eff)
%*****
% TITLE: Estimate drying fuel use
% AUTHOR: Aaron P. Turner
% DATES: August 2018
% DESCRIPTION: Use the polynomial fit to multiple simulation runs of
the
% granary model to estimate drying efficiency and energy use
%*****
***%

%function needs summary after DES simulation and drying temperature.
Also
%Base level drying eff @ 10 pts and MC out
%Estimates energy required for grain harvested on a day. Grain could be
%dried in subsequent days
fuel_unit_price=2.0; %$/gallon
electric_unit_price=0.10; %$/kWh
%Model parms.
a0=18053; a10=239; a01=-236;a20=7.92; a11=-7.80; a02=2.10;

%kJ/kgH2O
MCin=summary.MCin;
TempC=(T_dry-32)*5/9;
dry_eff=a0+a10.*MCin+a01.*TempC+a20.*MCin.^2+a11.*MCin.*TempC+a02.*Temp
C.^2;

Base_eff=Base_eff*2.204*1.0551;%Convert to kJ/kgH2O

adj_dry_eff=dry_eff+(Base_eff-6797);%Base from sim output kJ/kgH2O

dry_eff_us=adj_dry_eff/(2.204*1.0551);%convert to BTU/LB

%mass in and MC match by incoming day so has to be evaluated this way
H2O_out=summary.mass_in.*1000.*(100./(100-MCin)-100./(100-
MCout));%kgH2O

LHV=25.3;%LHV for propane MJ /liter
Drying_energy=adj_dry_eff/1000.*H2O_out;%MJ
Fuel_used=Drying_energy./LHV/.93;
Fuel_used_us=Fuel_used*0.26417;
Fuel_cost=Fuel_used_us*fuel_unit_price;
%Convert to kWh, assume 5% electric
Electric_cost=Drying_energy/3.6*.05*electric_unit_price;

%NO dry <15%
for i=1:length(MCin)
if MCin(i)<MCout
adj_dry_eff(i)=0; dry_eff_us(i)=0;Fuel_used(i)=0;
Fuel_used_us(i)=0; Fuel_cost(i)=0; Electric_cost(i)=0;
end
```

```
end
res=table(adj_dry_eff,dry_eff_us,Fuel_used,Fuel_used_us,Fuel_cost,Electric_cost);
end
```

Drying Capacity Adjustment

```
function [scaled_cap_wet,scaled_cap_dry,scaled_cap_wet_bu] =
Drying_cap_adj(rated_cap, MCoout,MCin,T_rated,T_dry)
%*****
% TITLE: Dryer_cap_adj
% AUTHOR: Aaron P. Turner
% DATES: June 2016-2018
% DESCRIPTION: This function adjusts dryer performance based on
incoming moisture, drying temperature and drying mode
%*****

%rated_cap is given dryer capacity @ 220F and 5pts out (20-15) (wet
bph)
%in heat/cool mode
%MC base is the base moisture. 15 or 15.5 % w.b.
%MCin is incoming grain moisture, in %wb
%T_rated=drying temp in deg F
%T_dry=drying temp in deg F
%mode 1= dry cool, 2= full heat,3=dryeration

%Determine adjustment ratios for Moisture and Temperature

Pts=MCin-MCoout;%Pts removed

%Difference between rated and actual drying temp deg C
delT=(T_dry-T_rated)*5/9;

%Regression Coefficients

%Based on Xflow model
a=1.610;
b=.2022;
c=0.006901;
d=1;
f=0.0136;

R_M=a*exp(-1*b*Pts)+c*(MCin.*MCoout)./Pts;%Moisture adjustment
R_T=d+f*delT;%Temperature Adjustment

%Scale capacity
rated_cap=rated_cap/39.368;%Adjust bph to t/hr

rated_cap_dry=rated_cap.*(1-(20)/100);%Adjust to dry t/hr

scaled_cap_dry=rated_cap_dry.*R_M.*R_T;%scale performance dry t/hr

%adjust back to incoming mc (t/hr wet)
scaled_cap_wet=scaled_cap_dry.*100./(100-MCin);
scaled_cap_wet_bu=scaled_cap_wet*39.368; % in wet bph
scaled_cap_dry_bu=scaled_cap_dry*39.368; %dry bhp

end
```

Processes Simulation Data—Flow and Utilization

```
function
[res]=analysis1(simout, runtime, num_truck, num_driver, batch_size, figpath,
day1)
%*****
% TITLE: process and clean simulation output data
% AUTHOR: Aaron P. Turner
% DATES: July 2018
% DESCRIPTION: Function plots entities in process for daily simulation
also
% determines total delay in harvesting due to bottleneck and total
entities. Finds wait time and resource utilization
% in process at end of simulation
%*****

if isempty(simout.Loads_out.Data)
    average_WT_field=0; average_WT_pit=0; average_flow_time=0;
average_flow_time_eff=0;
    percent_delayed_field=0; percent_delayed_pit=0;
    t_OT=0;    t_end=0;
    truck_util_avg=0;    driver_util_avg=0;    dryer_util_avg=0;
    T_combine=0; T_carts=0;T_dryer=0;T_drivers=0;
else

    if isempty(simout.Loads_in.Data)
        average_WT_field=0; average_WT_pit=0; average_flow_time=0;
average_flow_time_eff=0;
        percent_delayed_field=0; percent_delayed_pit=0;
        t_OT=0; truck_util_avg=0;    driver_util_avg=0;
        T_combine=0; T_carts=0;T_drivers=0;
    else
        %These times will be combined w/ number of operators in main
script
        T_combine=simout.Loads_in.Time(end)/60;%combine operation time
        T_carts=simout.T_finish_load.Data(end)/60;%Final load left
field
        %Assumes dryers can leave after they park their last load in
the
        %queue If fewer loads than drivers, assumed driver=loads
delivered
        if length(simout.T_finish_scales.Data)<num_driver
            T_drivers=sum(simout.T_finish_scales.Data);
        else
            T_drivers=sum(simout.T_finish_scales.Data(end-
num_driver+1:end))/60;
        end

        %Summary Loads in Loads out and Wait times
        %%{

        WT_field=[simout.T_start_load.Data (simout.T_start_load.Data-
simout.T_creation.Data)]/60;
        average_WT_field=mean(WT_field(:,2));
    end
end
```

```

percent_delayed_field=sum(WT_field(:,2)>0)/length(WT_field)*100;

    WT_pit=[simout.T_start_unload.Data (simout.T_start_unload.Data-
simout.T_finish_scales.Data)]/60;
    average_WT_pit=mean(WT_pit(:,2));
    percent_delayed_pit=sum(WT_pit(:,2)>0)/length(WT_pit)*100;

    % Productive time transport only
    productive_time=[simout.T_creation.Data...
        (simout.T_finish_load.Data-simout.T_start_load.Data)...
        (simout.T_arrive_storage.Data-simout.T_start_trans.Data)...
        (simout.T_finish_scales.Data-simout.T_start_scales.Data)...
        (simout.T_unload_complete.Data)-
simout.T_start_unload.Data];

    % Productive time
    total_productive_time=[productive_time(:,1)
productive_time(:,2)+productive_time(:,3)+productive_time(:,4)+producti
ve_time(:,5)]/60;

    %Flow time. Time from when load is generated till it is
unloaded.
    Flow_time=[simout.T_creation.Data
(simout.T_unload_complete.Data-simout.T_creation.Data)]/60;

    %Average Flow time.
    average_flow_time=mean(Flow_time(:,2));

    %Flow time efficiency
    flow_time_eff=[Flow_time(:,1)
total_productive_time(:,2)./Flow_time(:,2)*100];
    average_flow_time_eff=mean(flow_time_eff(:,2));

    %Flow time
    %%{
    f=figure('Name','Flow+WT','Units','inches','Position',[0 0 3.54
8],'InvertHardcopy','off','Color',[1 1 1]);
    left_color = [0 0 0];
    right_color = [0 0 0];
    set(f,'defaultAxesColorOrder',[left_color; right_color]);
    subplot(2,1,1)
    hold all
    yyaxis left
    plot(Flow_time(:,1),Flow_time(:,2),'-
o','MarkerEdgeColor',left_color)
    plot(total_productive_time(:,1),total_productive_time(:,2),'-
s','MarkerEdgeColor',left_color)
    ylabel('Time (minutes)');
    ylim([0 inf]);
    yyaxis right
    plot(flow_time_eff(:,1),flow_time_eff(:,2),'--
o','MarkerfaceColor',[0.5 0.5 0.5])

```

```

        xlabel('Load Creation Time (Hours into Simulation)');
ylabel('Time (Hours)');
        %legend('Flow Time', 'Productive Time','FTE','Location','Best')
        l=legend('Flow Time', 'Productive
Time', 'FTE', 'Location', 'southoutside', 'Orientation', 'horizontal');
        l.FontSize=10; l.Position=[0 0.8759 .98 0.19];
        legend('boxoff')
        ylim([0 100]);ylabel('Flow Time Efficiency, FTE (%)')
        a=gca;
        a.Title=[]; a.FontWeight='bold'; a.FontSize=10;
a.FontName='arial';

        subplot(2,1,2)
        hold on

        plot(WT_field(:,1),WT_field(:,2),'-
o','MarkerEdgeColor',left_color)
        plot(WT_pit(:,1),WT_pit(:,2),'-d','MarkerFaceColor',left_color)
        ylim([0, max(ylim)])
        xlabel('Time Departed Queue (Hours into Simulation)');
ylabel('Wait Time (hours)');
        l=legend('Field Side', 'Recieving
Pit', 'Location', 'northoutside', 'Orientation', 'horizontal');
        l.FontSize=10; l.Position=[0 .38 .98 0.19];
        legend('boxoff')
        a=gca;
        a.Title=[]; a.FontWeight='bold'; a.FontSize=10;
a.FontName='arial';
        export_fig([figpath 'Flow+WT' num2str(day1)], '-png', '-r300', '-
nocrop')
        %}

        % *****Resource utilization*****

        %Final time. when all resources return to field. all
        %simout.XXX.Time are the same time. (Not for dryer) And it is
the time stamp when
        %the haul back is complete and the resource is released.
        t_max=simout.T_creation.Time(end);
        t_OT=(t_max-runtime); %Amount of time hauling continues after
harvest stops
        %Truck utilization, account for truck being "utilized" from
first unload
        %Batch order
        batch_order=simout.Batch_order.Data;

        %Truck total time including empty haul back
        res=[simout.T_creation.Data (simout.T_start_load.Time-
simout.T_creation.Data)];
        %Truck_time=[Truck_time; res];
        Truck_total_time=res(batch_order==1,2);

        %Truck utilization, averaged for the day
        truck_util_avg=(sum(Truck_total_time)/num_truck)/t_max*100;

```

```

%Instant util
truck_avail=time_clean2(simout.Truck_avail);
truck_util_inst=[truck_avail.Time (1-
truck_avail.Data/num_truck)*100];

%Driver Utilization
res=[simout.T_creation.Data (simout.T_start_trans.Time-
simout.T_start_trans.Data)];
%Driver_time=[Driver_time; res];
Driver_total_time=res(batch_order==1,2);

%Driver utilization, averaged for the day
driver_util_avg=(sum(Driver_total_time)/num_driver)/t_max*100;

%Instant util
driver_avail=time_clean2(simout.driver_avail);
driver_util_inst=[driver_avail.Time (1-
driver_avail.Data/num_driver)*100];

% %{}
% Trucks
f=figure('Name','Truck_util','Units','inches','Position',[0 0
3.543 3.543],'InvertHardcopy','off','Color',[1 1 1]);
set(f,'defaultAxesColorOrder',[left_color; right_color]);
hold on
stairs(simout.Truck_util.Time/60, simout.Truck_util.Data*100,'-
','LineWidth',1.2,'MarkerEdgeColor',left_color)

scatter(truck_util_inst(:,1)/60, truck_util_inst(:,2), 'o', 'MarkerfaceCol
or', left_color, 'MarkerFaceAlpha', 0.3)
%plot(simout.driver_avail, '-d', 'MarkerEdgeColor', left_color)
ylim([0, 100])
xlabel('Simulation Time (hours)'); ylabel('Utilization(%)');
l=legend('Average',
'Instant', 'Location', 'northoutside', 'Orientation', 'horizontal');
l.FontSize=10; l.Position=[0 0.8759 .98 0.19];
legend('boxoff')
a=gca;
a.Title=[]; a.FontWeight='bold'; a.FontSize=10;
a.FontName='arial';
export_fig([figpath 'Truck_util_' num2str(day1)], '-png', '-
r300', '-nocrop')

hold off
%Driver
f=figure('Name','Driver_util','Units','inches','Position',[0 0
3.543 3.543],'InvertHardcopy','off','Color',[1 1 1]);
set(f,'defaultAxesColorOrder',[left_color; right_color]);
hold on
stairs(simout.driver_util.Time/60,
simout.driver_util.Data*100, '-
','LineWidth',1.2,'MarkerEdgeColor',left_color)

```

```

scatter(driver_util_inst(:,1)/60,driver_util_inst(:,2),'o','MarkerfaceC
olor',left_color,'MarkerFaceAlpha',0.3)
    %plot(simout.driver_avail,'-d','MarkerEdgeColor',left_color)
    ylim([0, 100])
    xlabel('Simulation Time (hours)'); ylabel('Utilization(%)');
    l=legend('Average',
'Instant','Location','northoutside','Orientation','horizontal');
    l.FontSize=10; l.Position=[0 0.8759 .98 0.19];
    legend('boxoff')
    a=gca;
    a.Title=[]; a.FontWeight='bold'; a.FontSize=10;
a.FontName='arial';
    export_fig([figpath 'Driver_util_' num2str(day1)],'-png', '-
r300','-nocrop')
    hold off
    %}

end
%}
%Time dryer was used
T_dryer_used=[simout.T_dry_finish.Data (simout.T_dry_finish.Data-
simout.T_dry_start.Data)];

%Storage facility operator time

if isempty(simout.wet_bin.Data)%error for Wet bin not called below
15%
    T_dryer=simout.T_dry_finish.Data(end)/60;%hrs %should be 0
else
    if simout.wet_bin.Data(end)>0
        T_dryer=24;%hrs
    else
        T_dryer=simout.T_dry_finish.Data(end)/60;%hrs
    end
    %Dryer in use
    dryer_use=time_clean2(simout.Dryer_stat);
end
%Dryer utilization could be 24 hrs/day
dryer_util_avg=sum(T_dryer_used(:,2))/(24*60)*100;
t_end=simout.Loads_out.Time(end);%Time final load left the system

%Dryer
%%{
f=figure('Name','Dryer_util','Units','inches','Position',[0 0 3.543
3.543],'InvertHardcopy','off','Color',[1 1 1]);
left_color = [0 0 0];
right_color = [0 0 0];
set(f,'defaultAxesColorOrder',[left_color; right_color]);
hold on
stairs(simout.Dryer_util.Time/60, simout.Dryer_util.Data*100,'-
','LineWidth',1.2,'MarkerEdgeColor',left_color)

scatter(dryer_use.Time/60,dryer_use.Data*100,'o','MarkerfaceColor',left
_color,'MarkerFaceAlpha',0.3)

```



```

        %plot(simout.driver_avail,'-d','MarkerEdgeColor',left_color)
        ylim([0, 100])
        xlabel('Simulation Time (hours)'); ylabel('Utilization(%)');
        l=legend('Average',
'Instant','Location','northoutside','Orientation','horizontal');
        l.FontSize=10; l.Position=[0 0.8759 .98 0.19];
        legend('boxoff')
        a=gca;
        a.Title=[]; a.FontWeight='bold'; a.FontSize=10; a.FontName='arial';
        export_fig([figpath 'dryer_util_' num2str(day1)],'-png', '-r300','-
nocrop')
        hold off
        %}
end
res=table(average_WT_field,percent_delayed_field,
average_WT_pit,percent_delayed_pit,...
        average_flow_time, average_flow_time_eff,t_OT,t_end,
truck_util_avg,...

driver_util_avg,dryer_util_avg,T_combine,T_carts,T_drivers,T_dryer);

end

```

Processes Simulation Data—Delays and Final Status

```
function
[bin_final,pit_final,total_delay]=Daily_sum(simout,field_buffer,runtime
,batch_size,figpath,day)
%*****
% TITLE: process and clean simulation output data
% AUTHOR: Aaron P. Turner
% DATES: July 2018
% DESCRIPTION: Function plots entities in process for daily simulation
also
% determines total delay in harvesting due to bottleneck and total
entities
% in process at end of simulation
%*****

%Find how long harvest is delayed
%incremental times from when field buffer is full to when an entity
departs
%Counts total missed field work. IF delay lasts past runtime, delay is
only
%Counted to runtime
%8/11/18*****
if max(simout.Field_Q.Data)==field_buffer
    idx=find(simout.Field_Q.Data==field_buffer);%Index when full
    for j=1:length(idx)
        %Only count points during harvest hours
        if simout.Field_Q.Time(idx(j)+1)<runtime %idx(j)<runtime
changed 7/26

            delay(j)=simout.Field_Q.Time(idx(j)+1)-
simout.Field_Q.Time(idx(j));
            else
                delay(j)=runtime-simout.Field_Q.Time(idx(j));
            end

        end
    end
else
    delay=0;
end

%Total of delays
total_delay=sum(delay)/60;%In hours

%Clean Matlab time variable to plot.
%Error handling set to zero if no harvest occurs
if isempty(simout.wet_bin.Data)
    wet_bin_Q=timeseries(0,0);
else
    [wet_bin_Q]=time_clean(simout.wet_bin,simout.Dryer_stat);
end
%on evaluate when harvesting occurs
if runtime>0
```

```

    [pit_Q]=time_clean(simout.Pit_Q,simout.Pit_stat);
    [field_Q]=time_clean2(simout.Field_Q);

else
    pit_Q=timeseries(0,0);
    field_Q=timeseries(0,0);
end

%Entities in process at end of day
bin_final=wet_bin_Q.Data(end);
pit_final=pit_Q.Data(end);
%%{
%Plot*****

figure('Name','day','Units','inches','Position',[0 0 5.5
5],'InvertHardcopy','off','Color',[1 1 1]);
subplot(2,1,1)
plot(simout.Loads_in.Time/60,simout.Loads_in.Data/batch_size,'ko',simou
t.Loads_out.Time(1:batch_size:end)/60,simout.Loads_out.Data(1:batch_siz
e:end)/batch_size,'kx')
l=legend('Loads in', 'Loads out',
'location','Northoutside','Orientation','horizontal');
    l.FontSize=10;
    legend('boxoff')
xlabel('Simulation Time (hours)'); ylabel('Number of Loads');
xlim([0 24]); xticks([2:2:24]);
a=gca;
a.Title=[]; a.FontWeight='bold'; a.FontSize=10; a.FontName='arial';
subplot(2,1,2)
hold all
a=stairs(wet_bin_Q.Time/60,wet_bin_Q.Data,'r-');
a1=stairs(pit_Q.Time/60,pit_Q.Data,'g-');
a2=stairs(field_Q.Time/60,field_Q.Data,'b-');

xlim([0 24]); xticks([2:2:24]);
l=legend('Bins & Dryer', 'Pit','Field
Side','location','Northoutside','Orientation','horizontal');
    l.FontSize=10;
    legend('boxoff')
xlabel('Simulation Time (hours)'); ylabel('Entities In Process');
set([a a1 a2],'lineWidth',1);
a=gca;
a.Title=[]; a.FontWeight='bold'; a.FontSize=10; a.FontName='arial';
hold off

%Uncomment to save figures to file
%export_fig([figpath 'day' num2str(day)],'-png', '-r300','-nocrop')
%}
end

```

Clean Simulink Utilization Output Data

```
function [res]=time_clean(dataset,server)
%*****
% TITLE: Clean simout data
% AUTHOR: Aaron P. Turner
% DATES: June 2018
% DESCRIPTION: Function to get rid of extra points that occur
% at same time step and combine entities at the server and queue.
%*****
***%

%For the Queue
time=unique(dataset.Time);%unique events

%Pick the final value
for i=1:length(time)
    temp=dataset.Data(dataset.Time==time(i));
    data(i)=temp(end);
end

Queue=[time data'];
clear time data
%Add Server status
time=unique(server.Time);%unique events

%Pick the final value
for i=1:length(time)
    temp=server.Data(server.Time==time(i));
    data(i)=temp(end);
end

server=[time data'];

%Create tables, join, then set missing values to previous values to
match
%up time syncing
Queue=array2table(Queue,'VariableNames',{'Time','Queue'});
server=array2table(server,'VariableNames',{'Time','server'});
[joined, ia, ib]=outerjoin(Queue,server);
for j=1:height(joined)
    if ia(j)==ib(j)
        Time2(j) =joined.Time_Queue(j);
        Qtotal(j)=joined.Queue(j)+joined.server(j);
    else
        Time2(j)=max(joined.Time_Queue(j),joined.Time_server(j));
        if ia(j)==0
            joined.Queue(j)=joined.Queue(j-1);
        end
        if ib(j)==0
            joined.server(j)=joined.server(j-1);
        end
        Qtotal(j)=joined.Queue(j)+joined.server(j);
    end
end
```

```
end  
  
res=timeseries(Qtotal',Time2');  
  
end
```

Main Function for Sensitivity Analysis

```
%*****
% TITLE: Sensitivity Analysis
% AUTHOR: Aaron P. Turner
% DATES: Aug 2018
% DESCRIPTION: Function to define the input equipment and conditions
for
%sensitivity analysis
%*****
***%
%Changed line 12 22 28 52 and func call for func_sys_def
tic
clc; clear; close all

load weather.mat% input weather data
Scombine=[2.45,2.71,2.98,3.24,3.50,3.76,4.03,4.29,4.55];%standard +/-
30%
%Scombine=3.5;
dt_transport=[15:5:60];
Final=table();
for j=1:length(Scombine)
    Scombine1=Scombine(j);
    for i=1:length(dt_transport)

        summary=func_sys_def(Scombine1,dt_transport(i),weather);
        days_complete= length(summary.runtime);
        days_work=sum(summary.runtime>0);
        HTL=sum(summary.HTL);%harvest time lost
        Combine_hours=sum(summary.T_combine_tot);% combine machine hours
        Cart_hours=sum(summary.T_carts_tot);%cart operator hours
        Storage_hours=sum(summary.T_storage_tot);%Labor @ storage
        Driver_hours=sum(summary.T_driver_tot);%Driver hours
        Truck_Transport_hours=dt_transport(i)/60*321*2;%Total transport
Hours based on total loads hauled @ transport distance
        Drying_cost=sum(summary.Fuel_cost+summary.Electric_cost);%total
drying cost
        time=dt_transport(i); Speed=Scombine1;

    temp=table(Speed,time,days_complete,days_work,HTL,Combine_hours,Cart_ho
urs,Storage_hours,Driver_hours,Truck_Transport_hours,Drying_cost);
        Final=[Final; temp];
        disp(i)
    end
    disp(j)
end
toc
```

Define System for Sensitivity Analysis

```
function[summary]=func_sys_def(Scombine,dt_transport,weather)
%*****
% TITLE: Define system
% AUTHOR: Aaron P. Turner
% DATES: Aug 2018
% DESCRIPTION: Function to define the input equipment and conditions
for
%sensitivity analysis
%*****

%*****Inputs*****
clear; clc; close all;
figpath='XXX\';
%Field Conditions
Hh=10;% Total time available for harvest hrs/day
Ht=24;% Length of simulation
Area=2000; % Area to harvest in acres
%Area=1000; % Area to harvest in acres
Yield_us=152;% Average yield bu/ac

%Harvester
Ncombine=1; %Number of Combines
%Scombine=3.5;%Combine speed, mph
Nrow=12;%Number of rows
RowSpace=30;%Row Spacing, inches
Vcombine=350;%Hopper capacity, bu
Ef=0.7;%Field efficiency

Scombine=4.366;%Combine speed, mph
%Ef=0.8;
%In-field transportation
Ncart=1;%Number of carts
Vcart=1000;%Volume capacity of carts, bu
batch_size=1;%number of unloads placed on a truck

%On-Road Transportation
load_size=950;%Bu loaded on each grain cart
dt_field_trans=6;% Timeto load a truck
Ntruck=3;%Number of trucks
%Ntruck=2;%Number of trucks
Ndriver=2;%Number of drivers
%dt_transport=20;

dt_transport=40;
%Storage
dt_inspect=4;% Weigh and inspect time
dt_unload=15;%Unload time at receiving pit
%Example GSI bin 21' dia 7 rings
Vbins=9088;%bu capacity
%Vbins=4500;
Nstorage=1;%persons at storage facility
dryer_cap=82;%wet holding on dryer
MCi=28;% initial moisture content on Sept 1
```

```

load weather.mat%weather data
Year=2016;
%Year=2010;
SDC=730;
%SDC=730*2;
T_rated=220;%Rated Dryer Capacity
T_dry=220;%Actual drying temperature
MCoat=15;%Must be this

weather=weather(year(weather.Date)==Year,:);

%Conditions for WC
%{
T_dry=140;
Yield_us=Yield_us*0.87;
%}
%***** Calculations and Units*****

%Field
Area=Area/2.47; %ha
Yield=Yield_us*56/2204*2.47*.85;%Convert to dry t/ha
MT=Yield*Area;% total mass to harvest in dry t

%Combine
w=Nrow*RowSpace/12;%working width,ft
Ca_us=Scombine*w*Ef/8.25;
Cm_us=Ca_us*Yield_us;
w=w/3.28;%in m
Scombine=Scombine*1.61;%kph
Ct=Scombine*w/10;%Area Capacity theoretical ha/h/combine
Ca=Ct*Ef*Ncombine;%Area Capacity actual,ha/h

Cm=Ca*Yield;%Material capacity, dry t/h

%Truck and Field Side interactions
Q_field_max=floor((Ncart*Vcart+Ncombine*Vcombine)/(load_size/batch_size
));%
load_size=load_size*56/2204*.85;%dry t

load_gen_rate=(load_size/Cm*60)/batch_size;

%Wet holding

Vbins=Vbins*1.245/35.3147;%bu^3 to m^3

%Using density from standard and add Packfactor+ standard is @ 13%mc
Bin_cap=Vbins*718/1000*1/(1-.05)*(1-.13);%dry t
%}

dryer_cap=dryer_cap*56/2204*.85;%Change bu to dry t

WH_total=Bin_cap+dryer_cap;

wet_cap=floor(WH_total/load_size);%Wet holding for the model

```



```
%Combine inputs into a table
input=table(Hh, Ht, MT,load_gen_rate,batch_size, Q_field_max,load_size,
...
    dt_field_trans, Ncombine,Ncart,Ntruck, Ndriver,Nstorage,
dt_transport, ...
    dt_inspect, dt_unload, Nstorage, wet_cap,
Mci,SDC,T_dry,T_rated,MCout);

%Run the whole season simulation
[summary]=fun_whole_season_sim(input,weather, figpath);

end
```

Appendix D. Yield Loss Measurement

Field Datasheet

	Wet Weight (g)	Dry weight (g)	Test Weight
Moisture Sample			
Length of Pass (ft)		Mass Harvested:	
Yield (10m row)	Number of Ears	# of Ears Taken	Dry weight (g)
Rep 1			
Rep 2			
Rep 3			
8 row= 16.15' 12 row=10.76ft	Number of Ears	Dry Weight (g)	
Drop loss*			
Ear Loss**			
8 row= 1.35' 12 row=0.90ft	Number of kernel	Dry Weight (g)	
Head kernel loss			
Cylinder***			
Head/Separation****			
Combine speed		Hybrid	
Combine Model		Planting date	
Head Width/Model		Sample ID	
Fan Speed		Replication	
Rotor Speed		Field	
Concave Setting		Date	
Other		Lat/Long	
*Pre harvest loss (whole ears in 30.0 m ² unharvested)			
**Machine+pre harvest (whole ears or eq 3/4 lbs)			
***kernels on cob			
****kernels on ground			
# rows	Header width (ft)	Length for 30m ² (ft)	Length for 2.5m ² (ft)
8	20	16.15	1.35
12	30	10.76	0.90
6	15	21.53	1.79

Appendix E. Supplemental Information for DES Transportation Model

Operating Characteristics

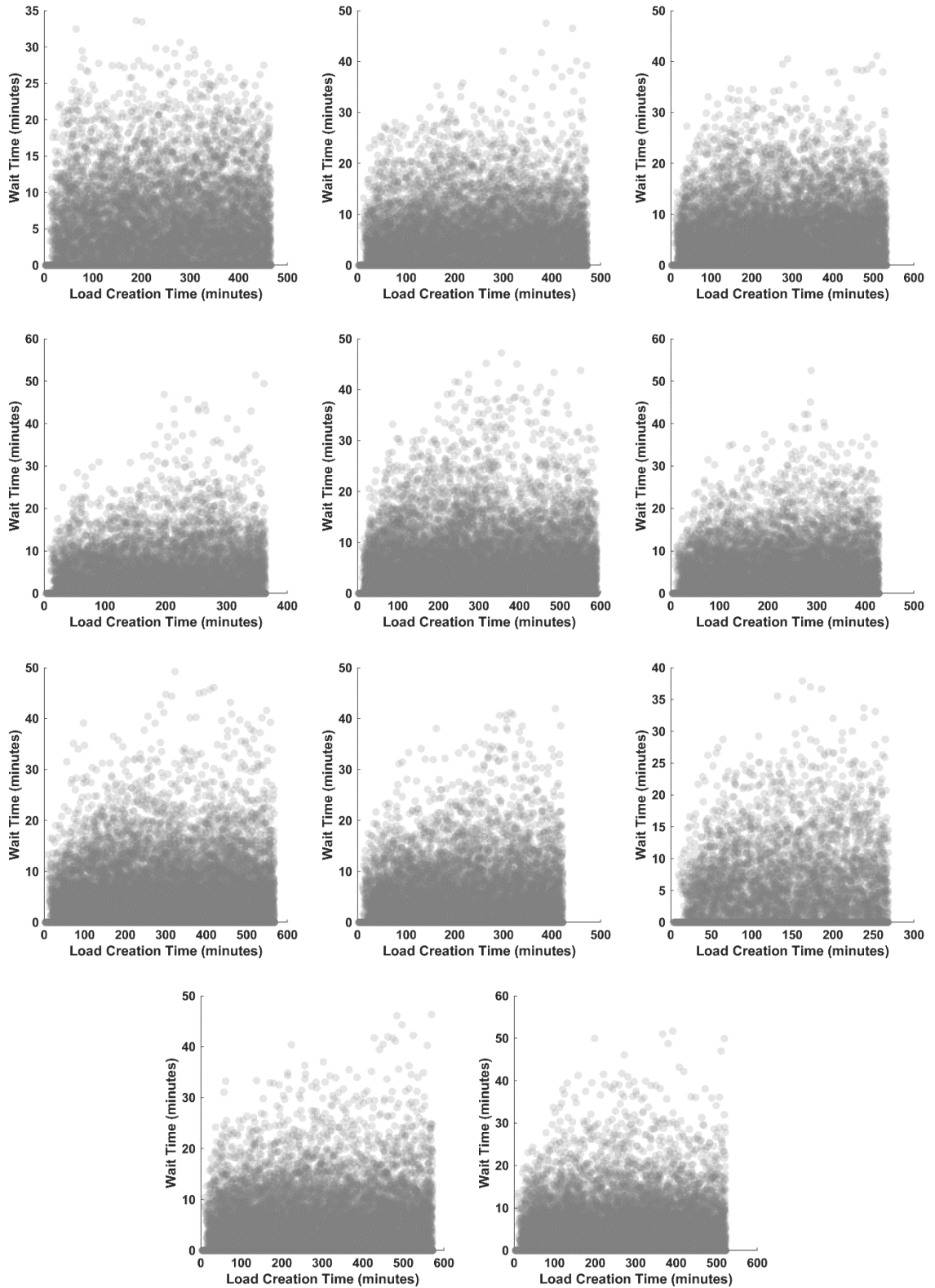
Duration of field work, number of trucks and one way distance for all days

Field Time, Trucks, and Distance

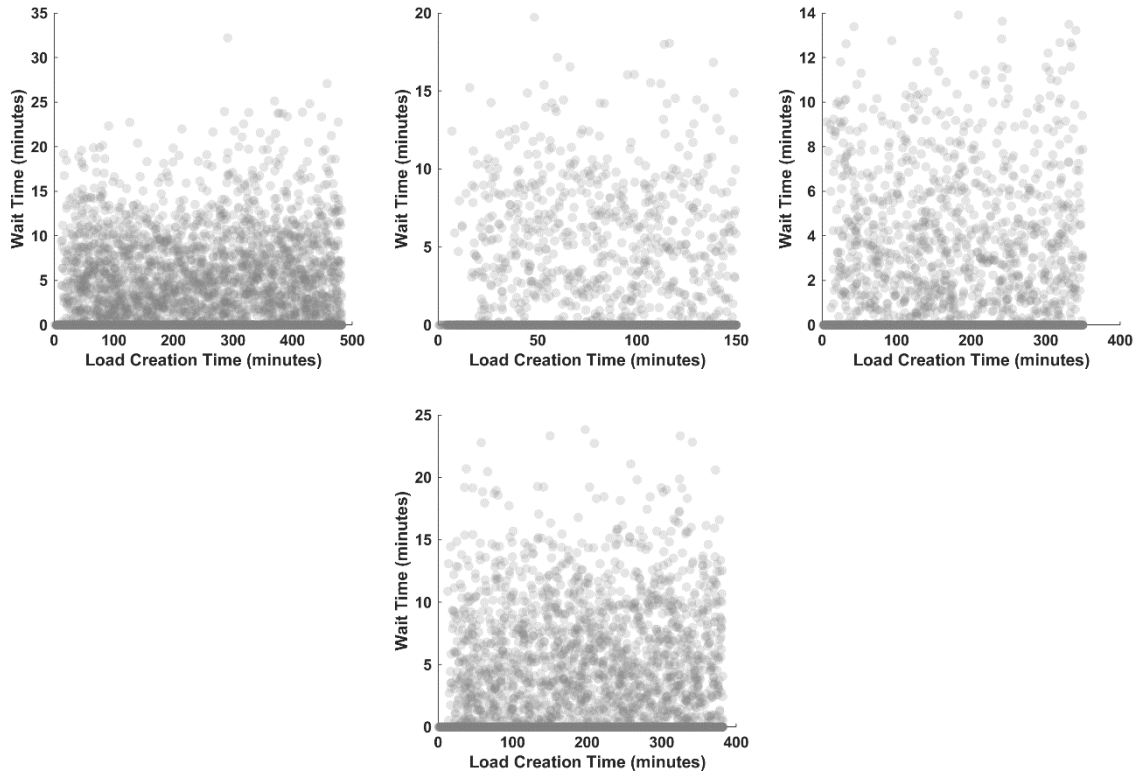
Crop	Fieldwork (minutes)	Number Trucks	One-Way Distance (miles)
Corn	421	5	2.1
Corn	566	11	2.2
Corn	427	10	2.5
Corn	590	6	3.2
Corn	363	7	2.7
Corn	440	10	3.4
Corn	531	9	2.7
Corn	470	9	2.6
Corn	93	3	11.8
Corn	464	8	15.8
Corn	520	10	14.5
Corn	570	11	11.3
Corn	101	1	11.2
Corn	268	7	11.2
Wheat	348	2	2.2
Wheat	149	3	2.2
Wheat	521	3	3.0
Wheat	480	4	2.6
Wheat	379	4	3.4
Wheat	558	6	2.6
Wheat	706	7	3.7
Wheat	619	6	7.1

Pit Wait Times

Example Pit Wait Time for Corn

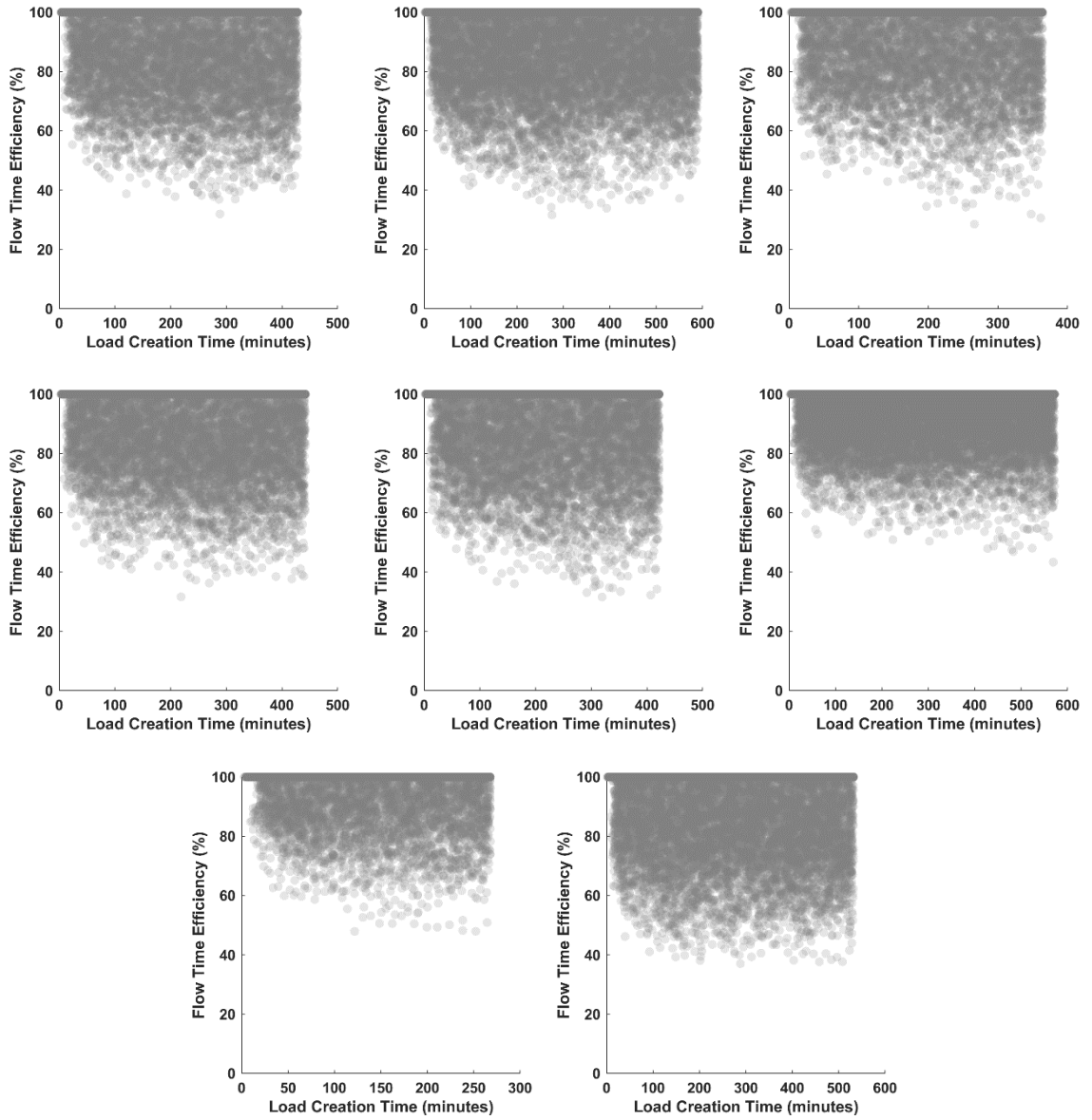


Example Pit Wait Time for Wheat

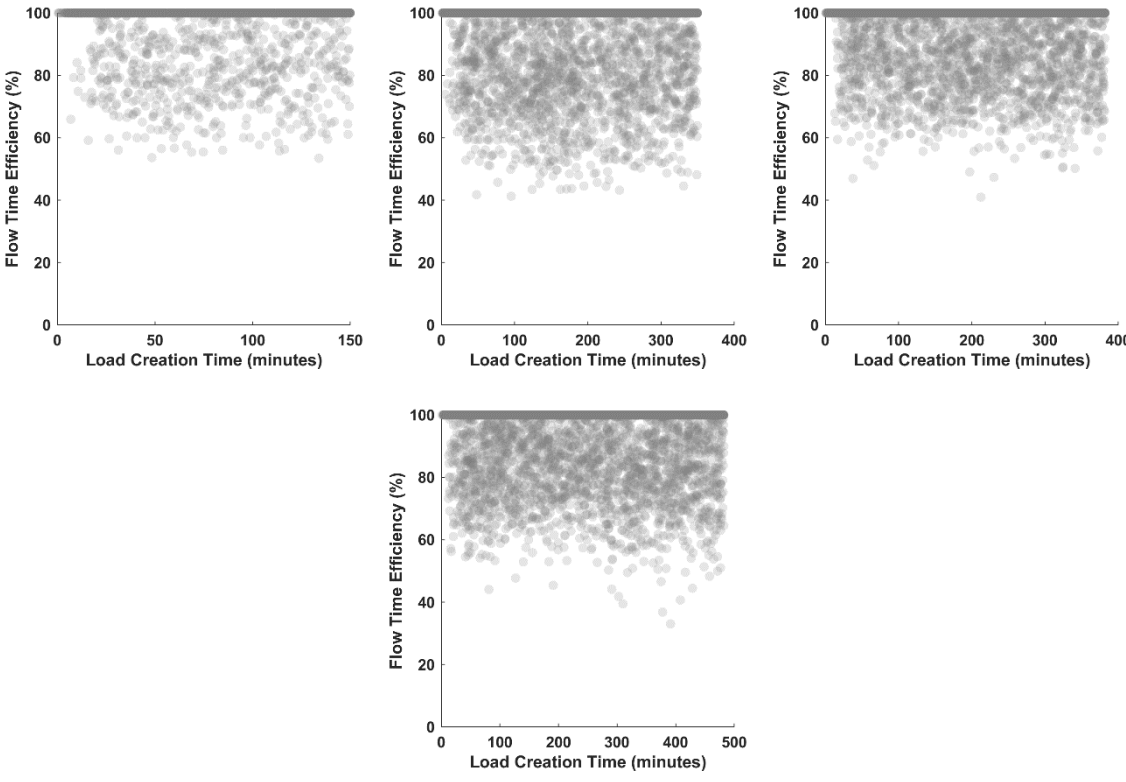


Flow Time Efficiency

Example Flow Time Efficiency-Corn



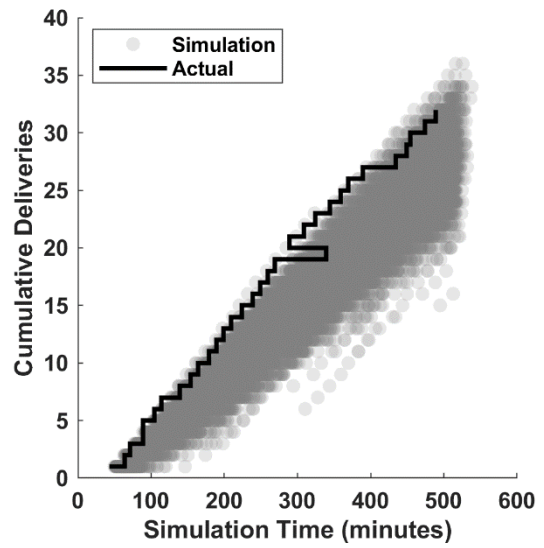
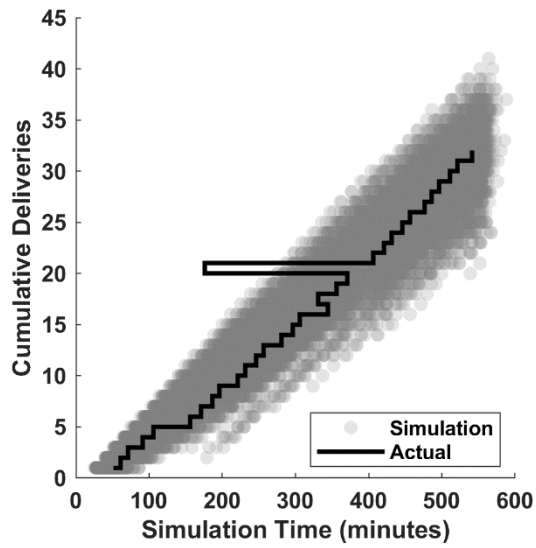
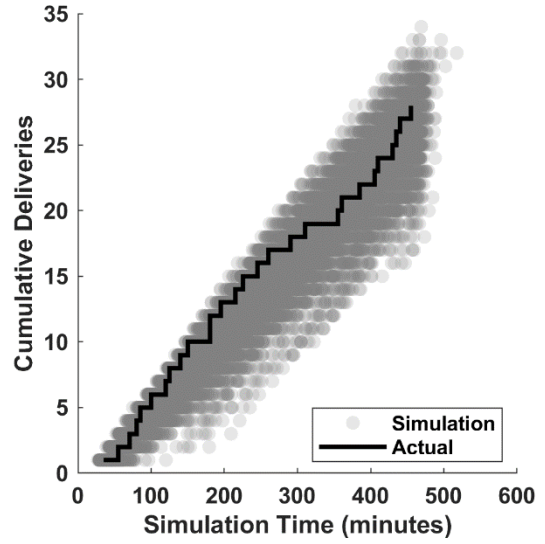
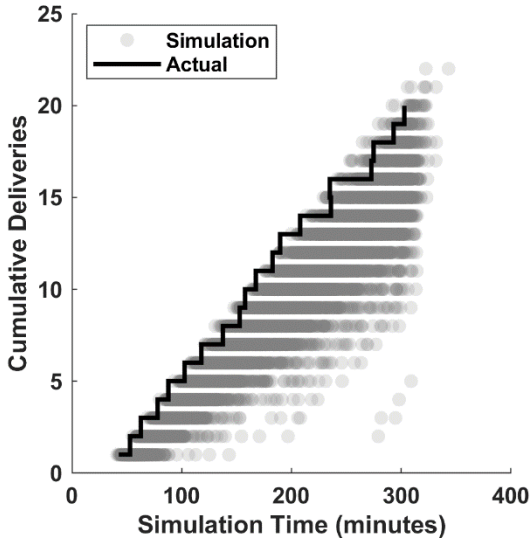
Example Flow Time Efficiency-Wheat

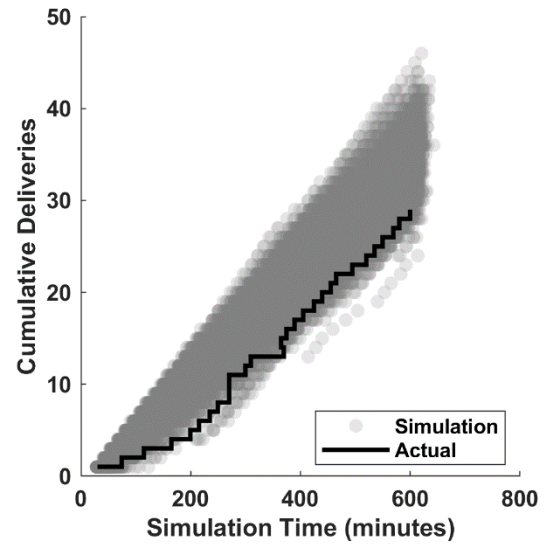
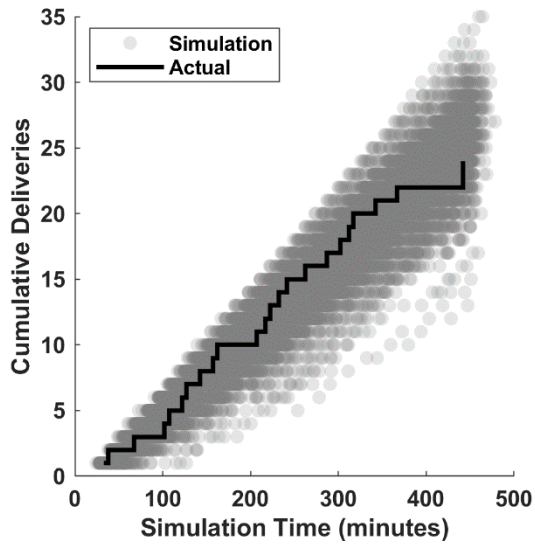
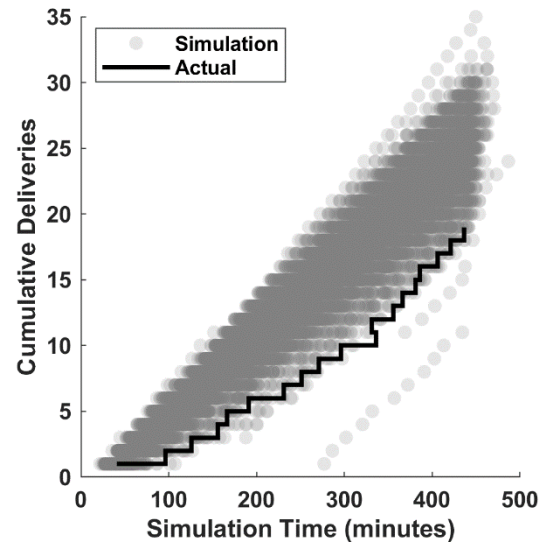
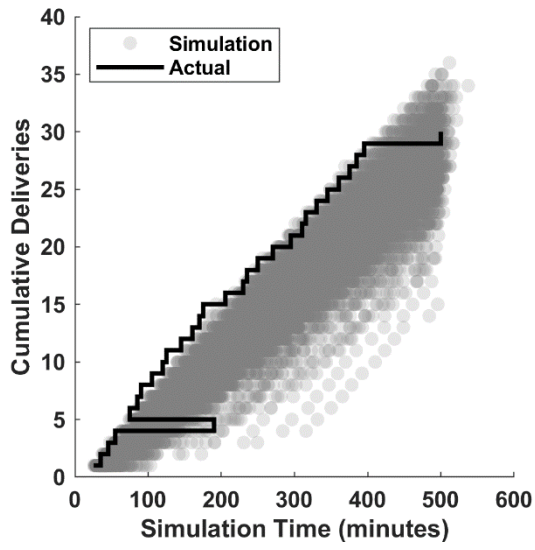


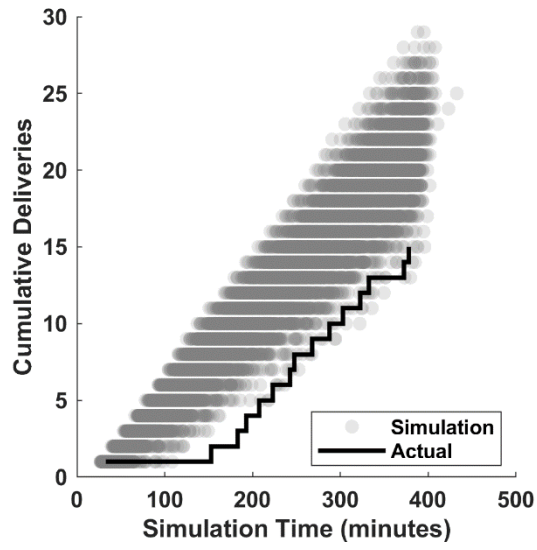
Loads Delivered

Inconsistencies indicate trucks were unloaded out of order they left the field

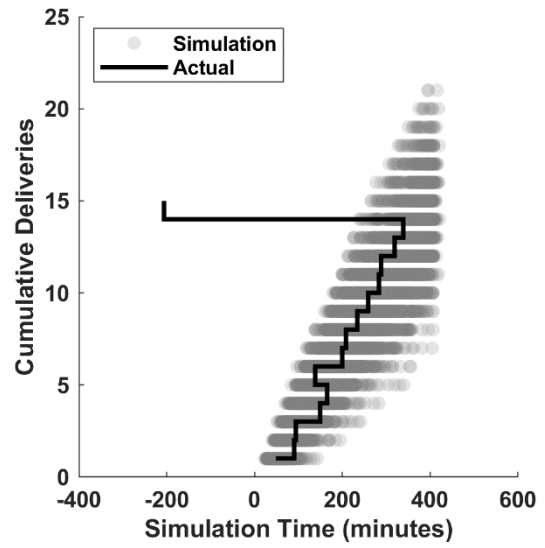
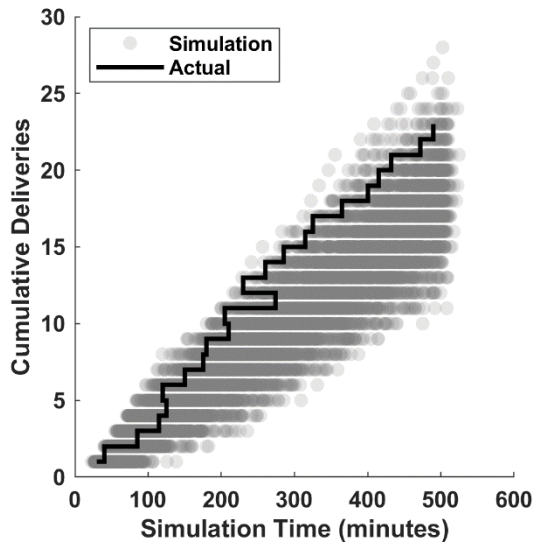
Corn-

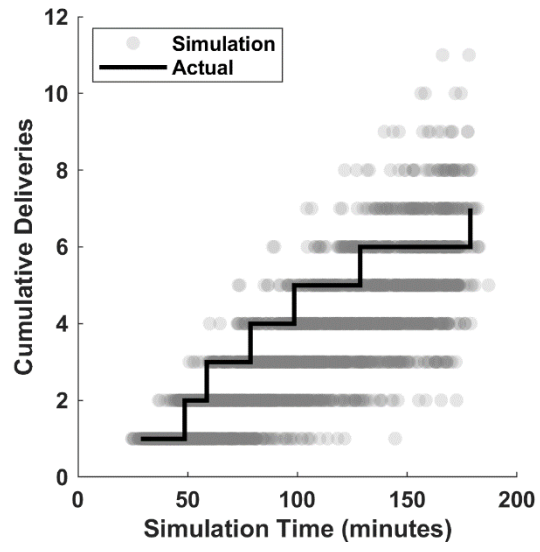






Wheat-

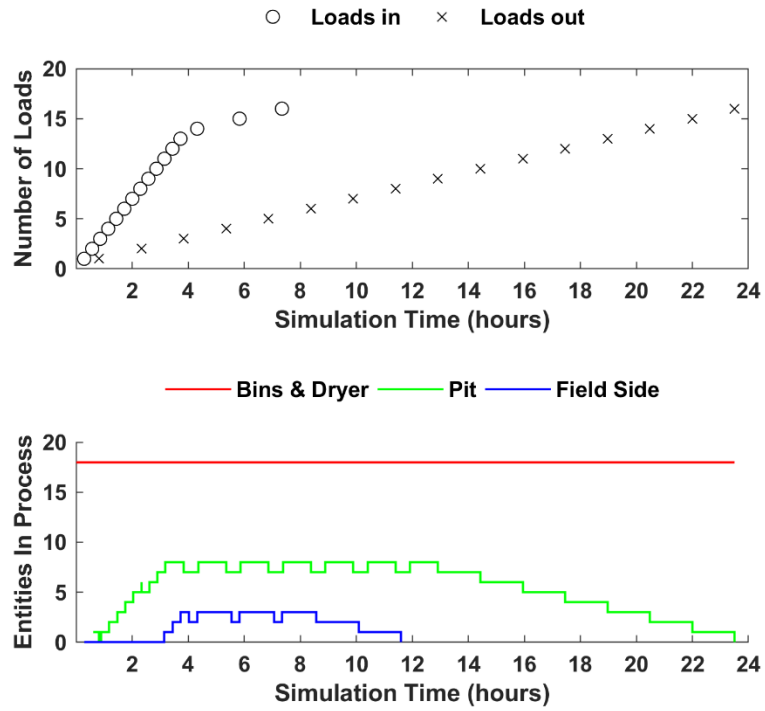




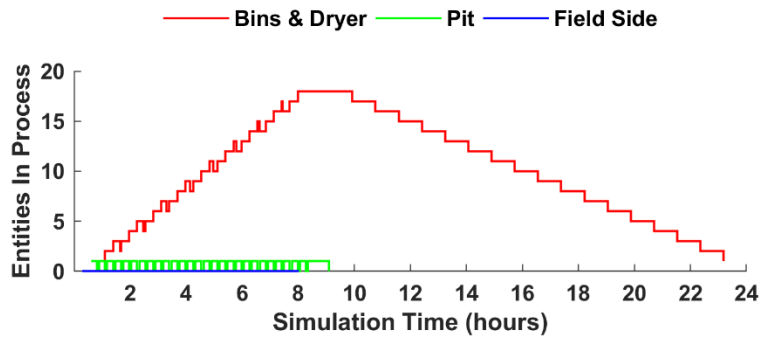
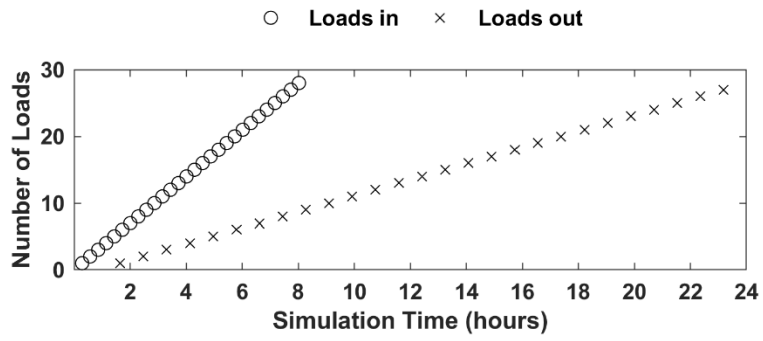
Appendix F. Supplemental Information for Whole Season Application

Daily Simulation Overview

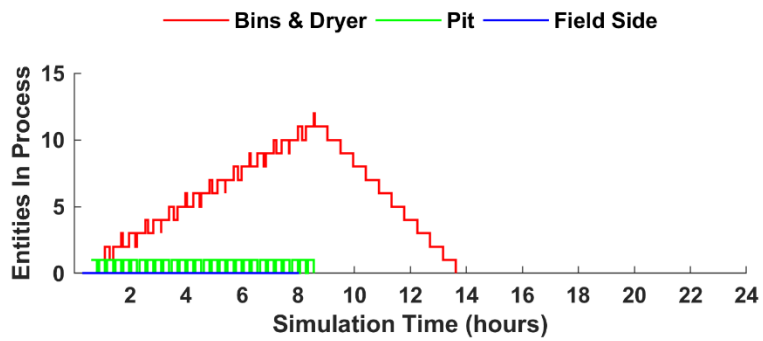
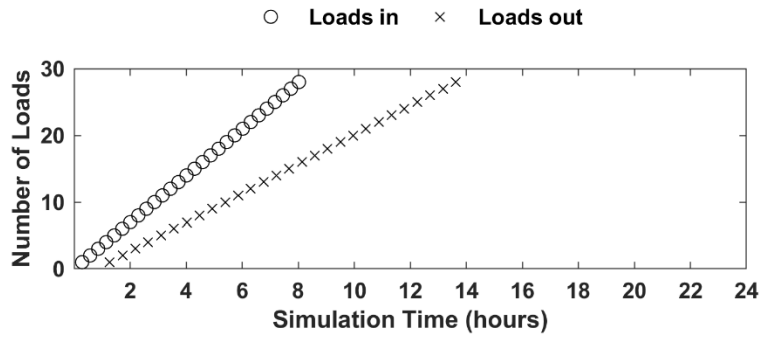
Early Season Example



Mid-Season Example

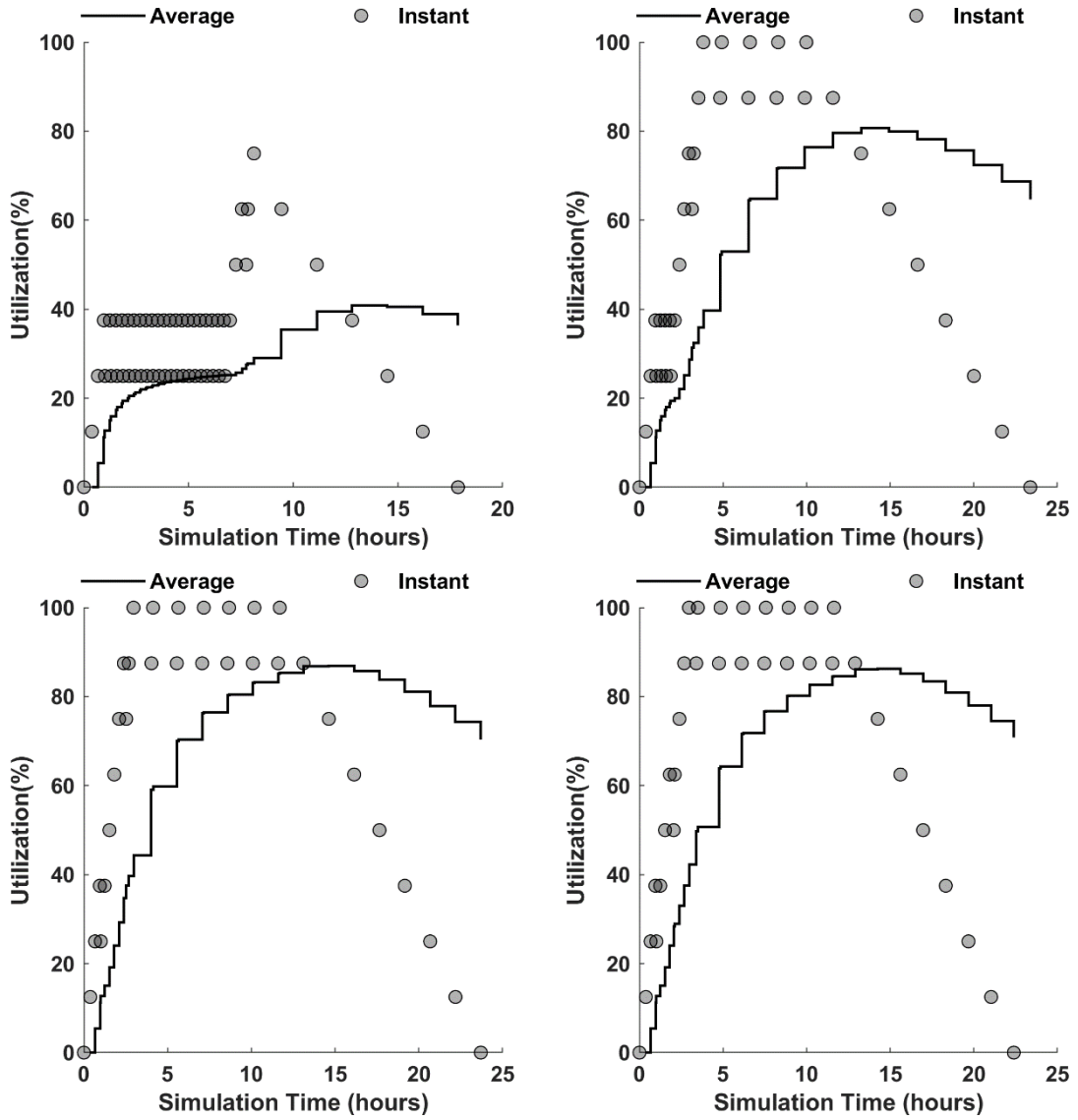


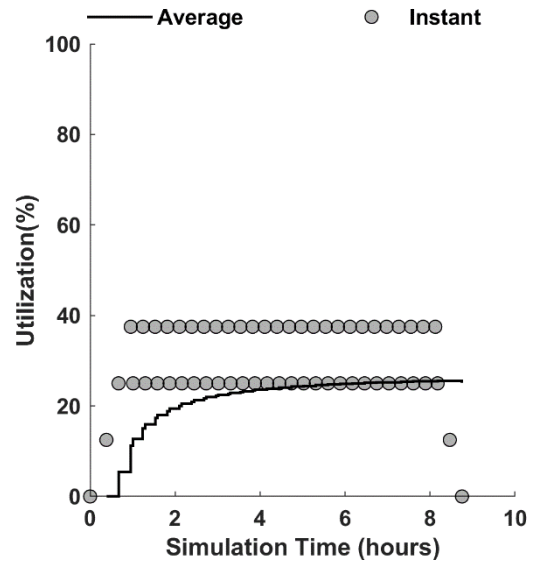
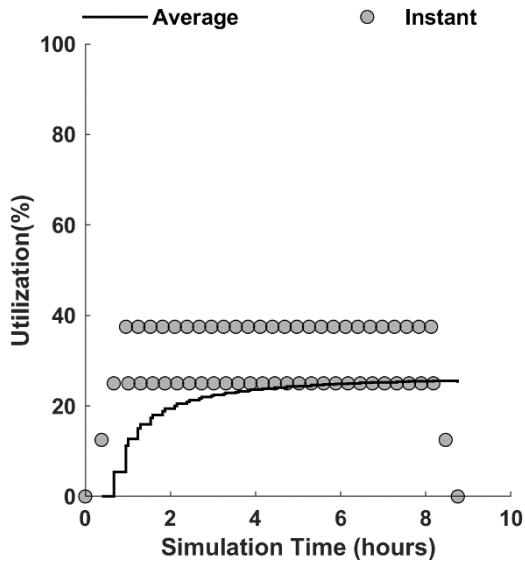
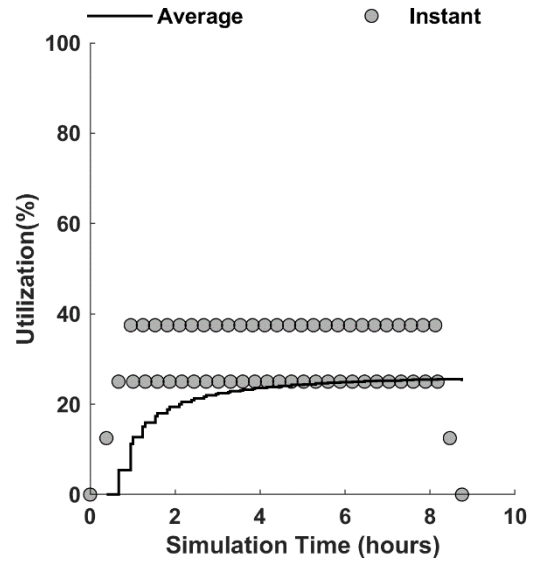
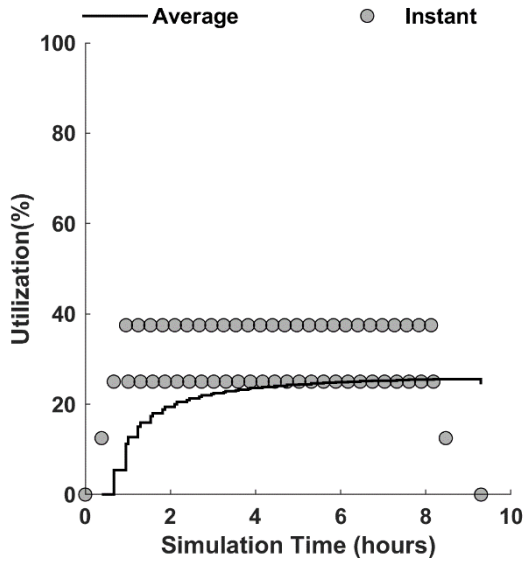
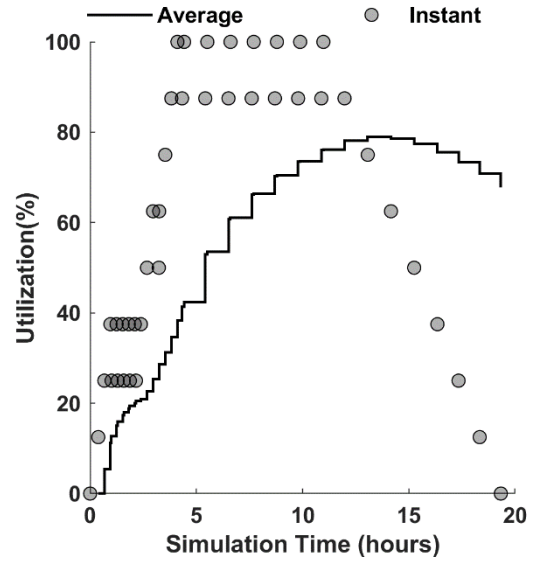
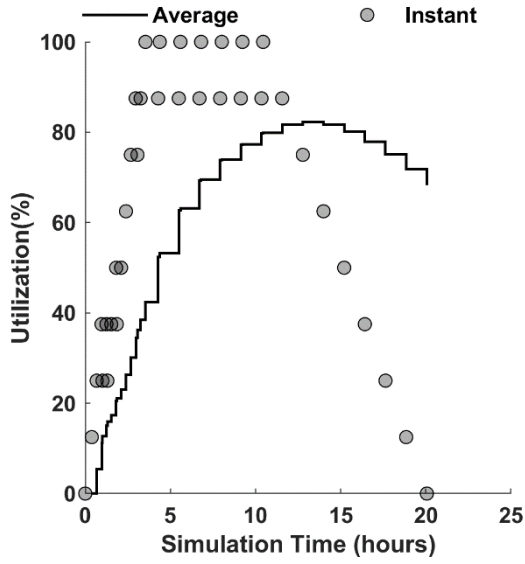
Late Season Example

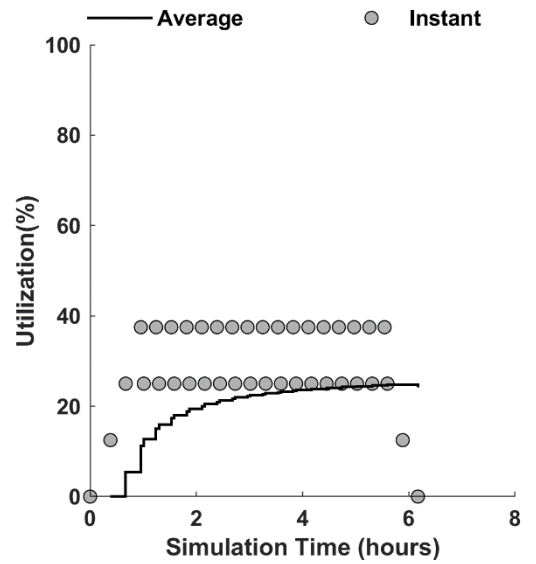
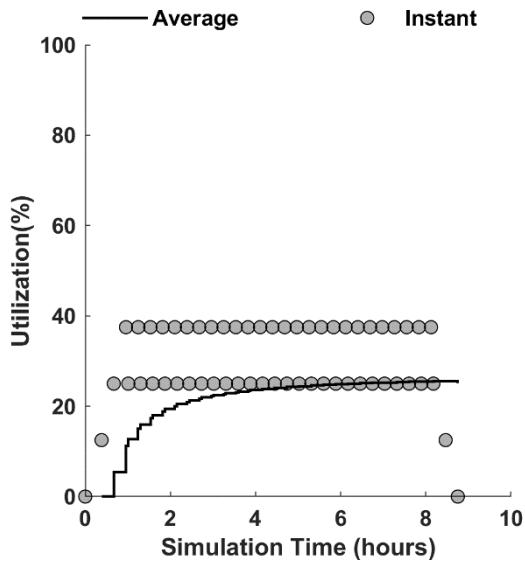
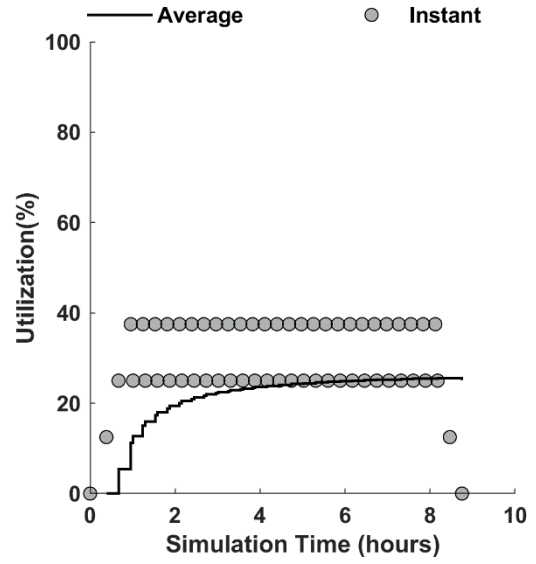
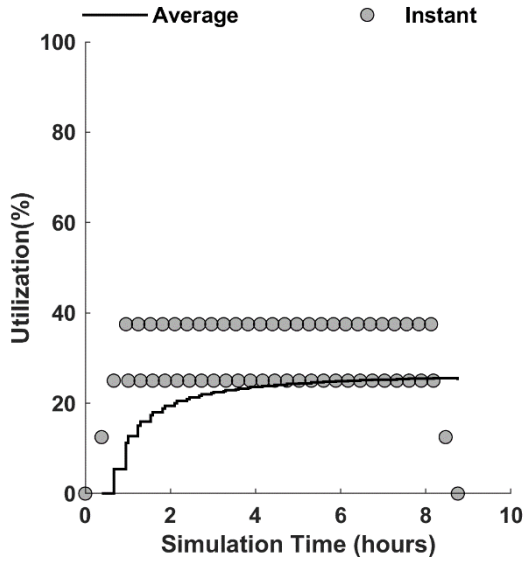


Driver Utilization

Driver resource utilization for all days. Season progresses from left to right, top to bottom

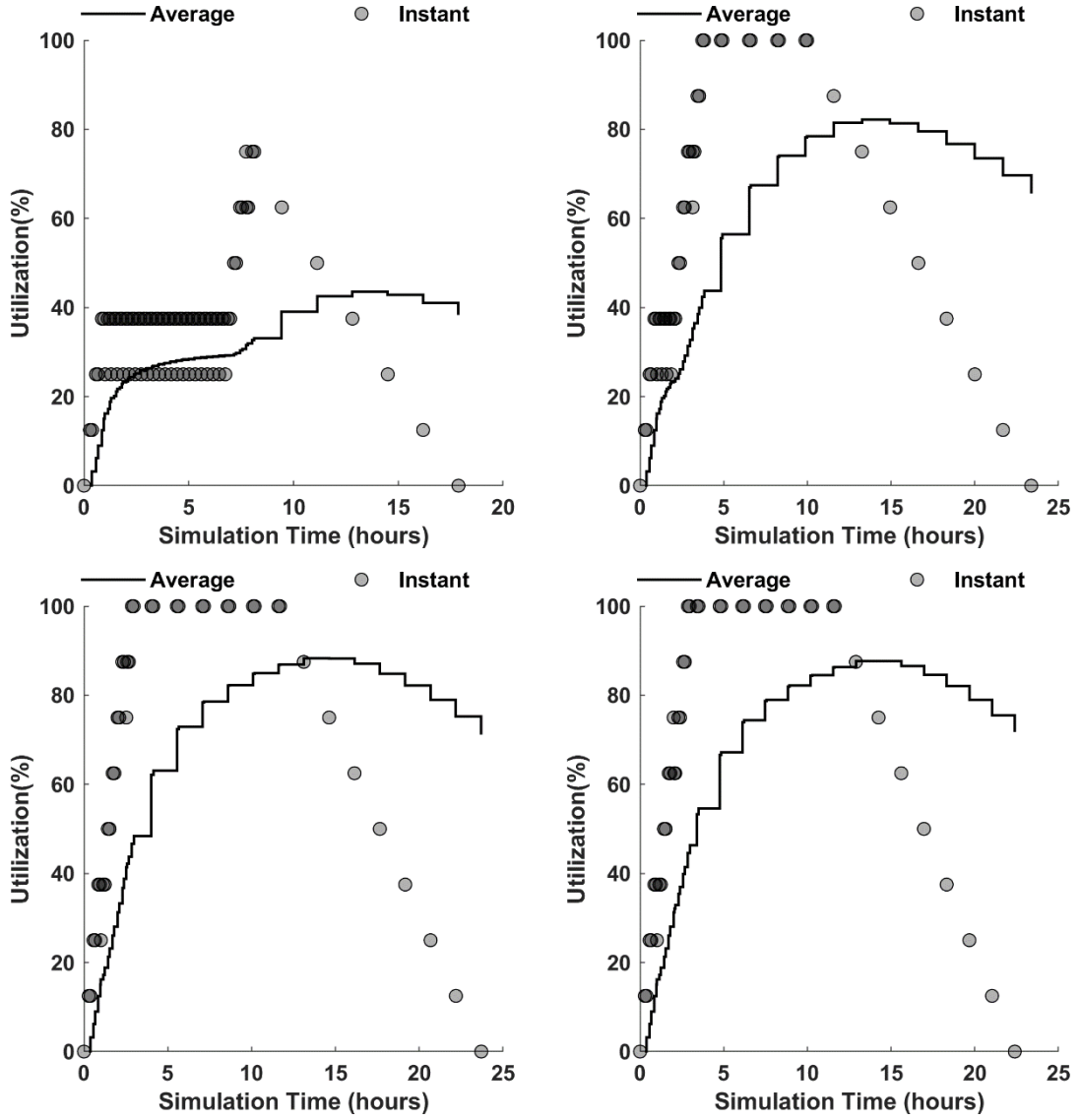


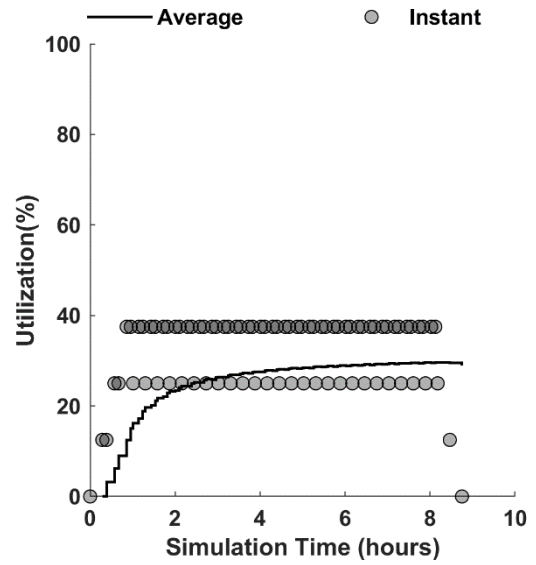
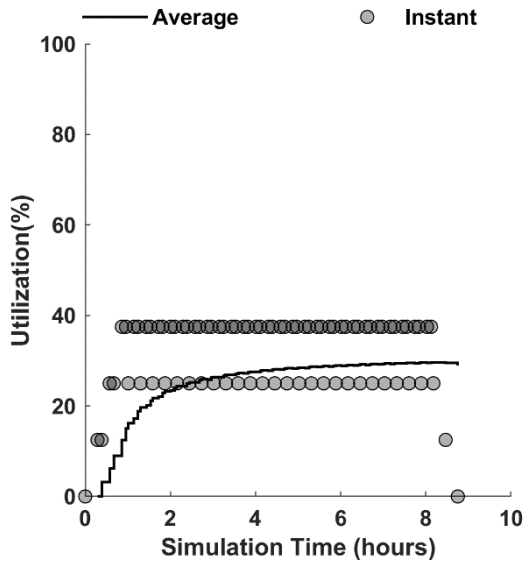
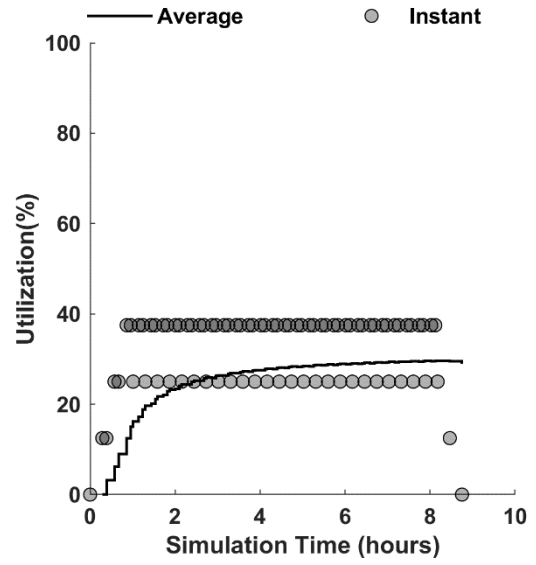
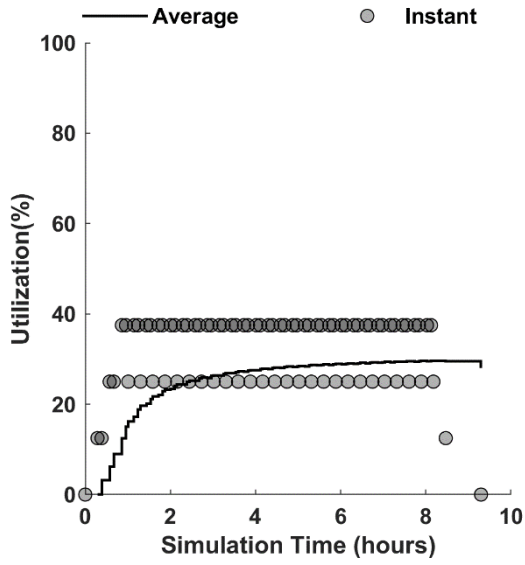
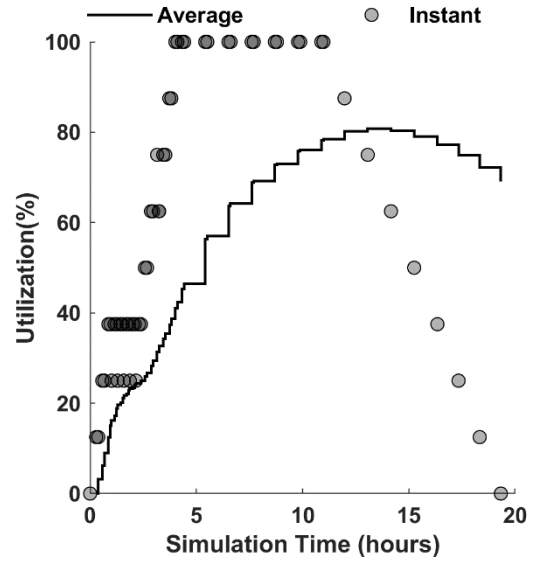
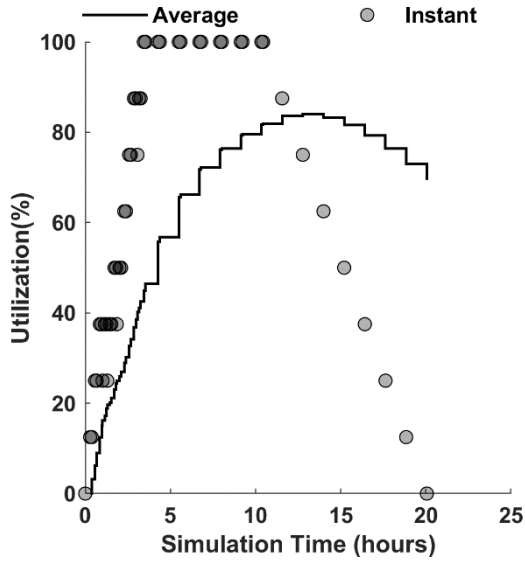


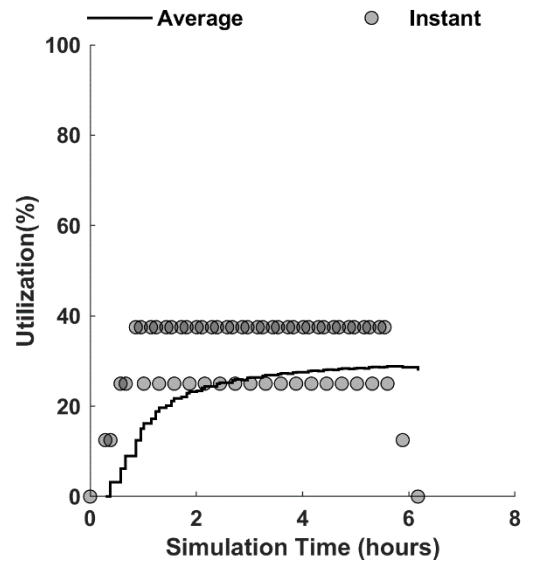
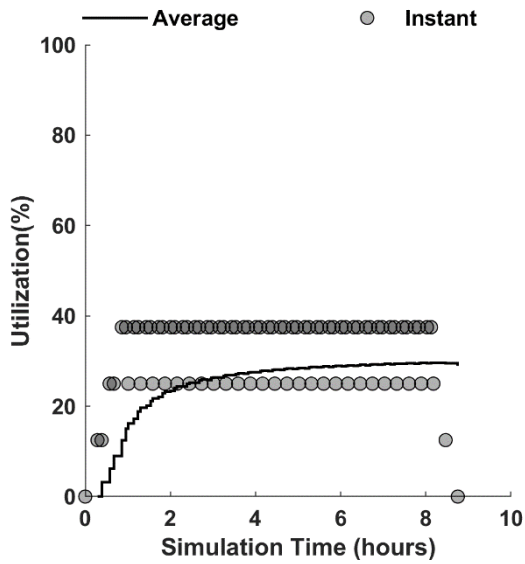
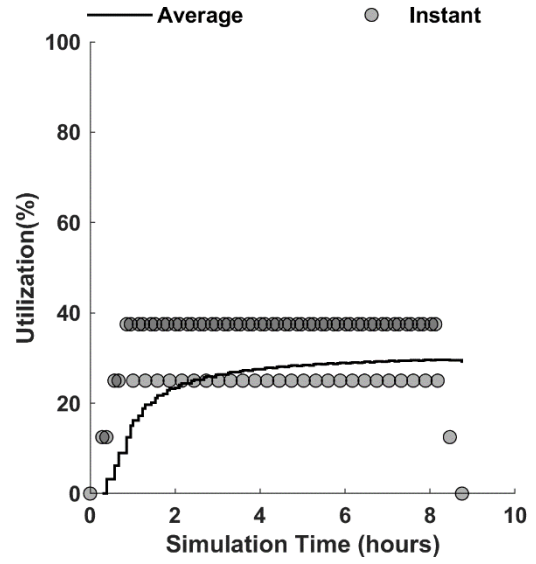
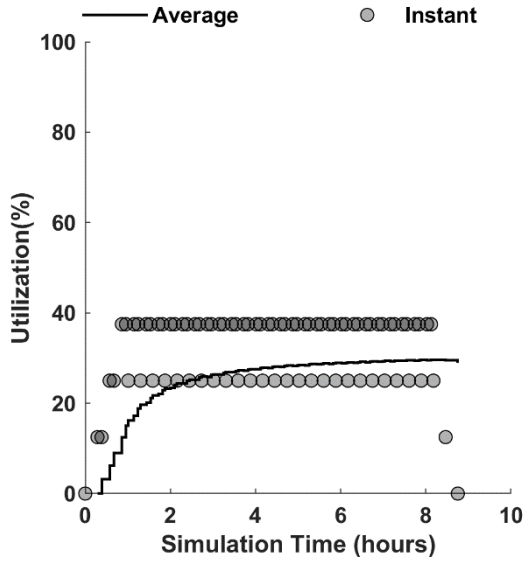


Truck Utilization

Truck resource utilization for all days. Season progresses from left to right, top to bottom

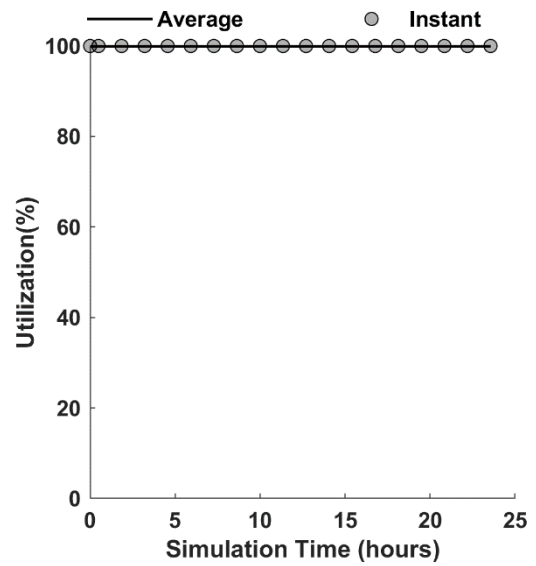
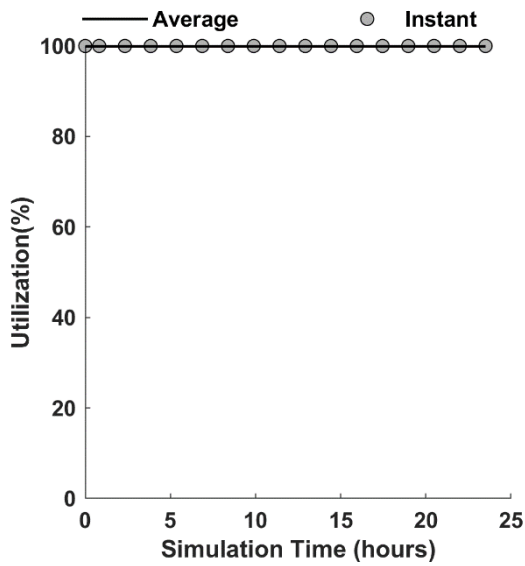
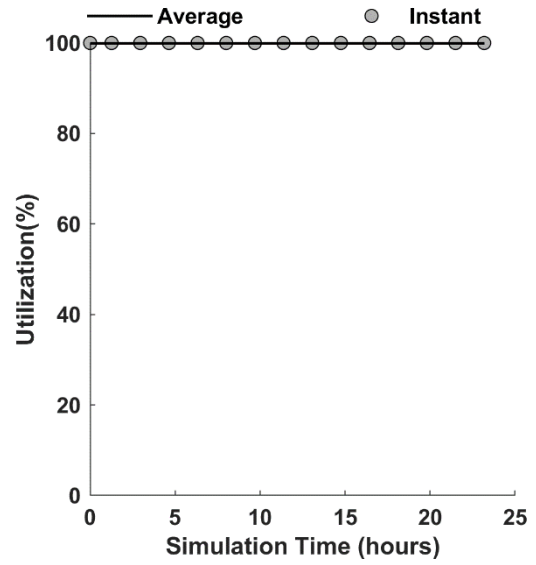
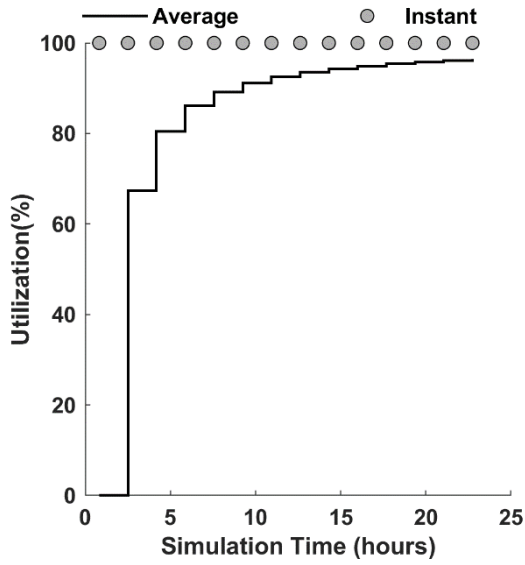


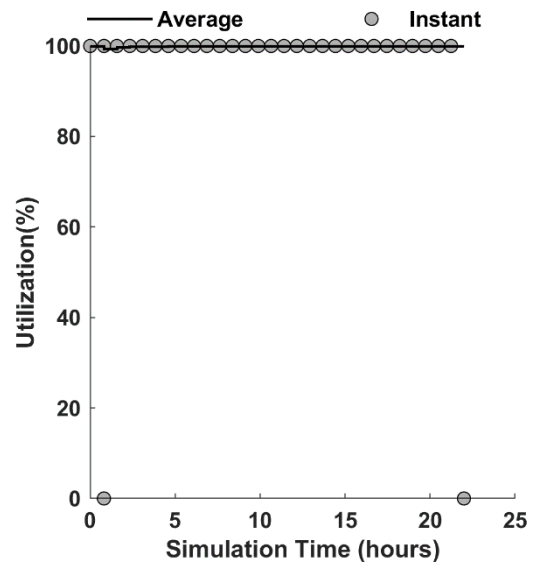
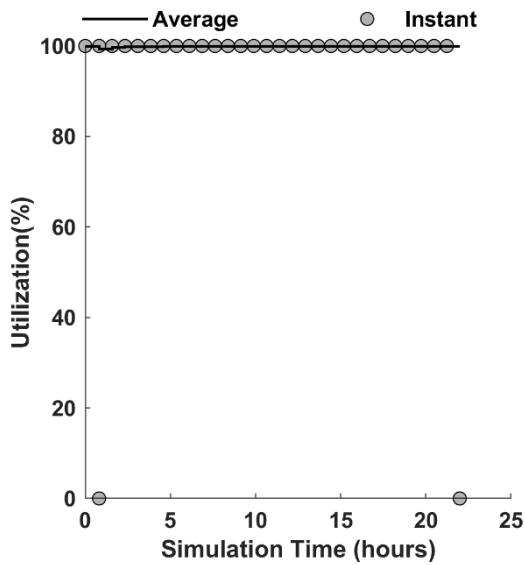
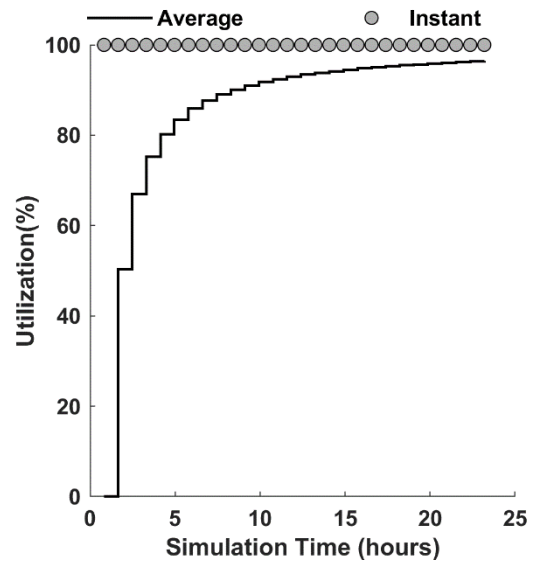
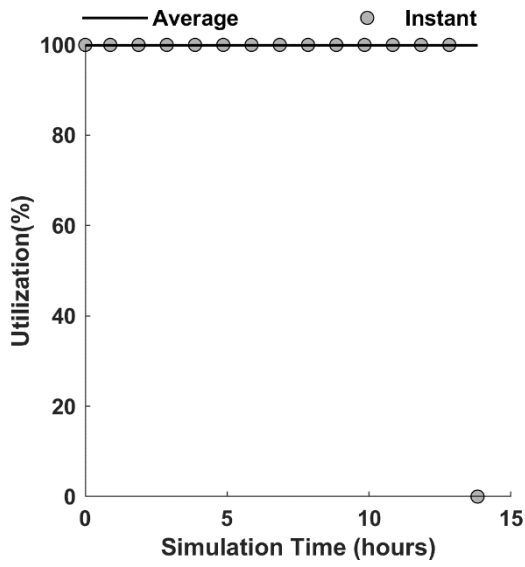
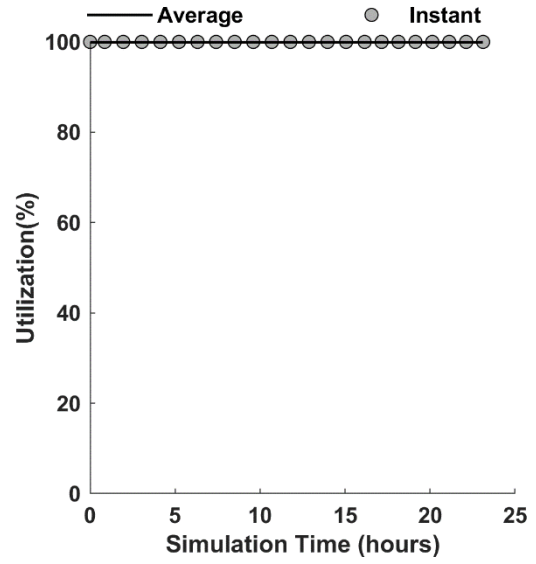
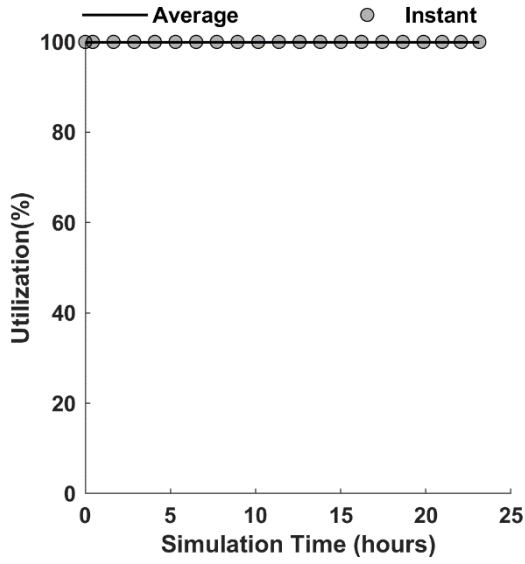


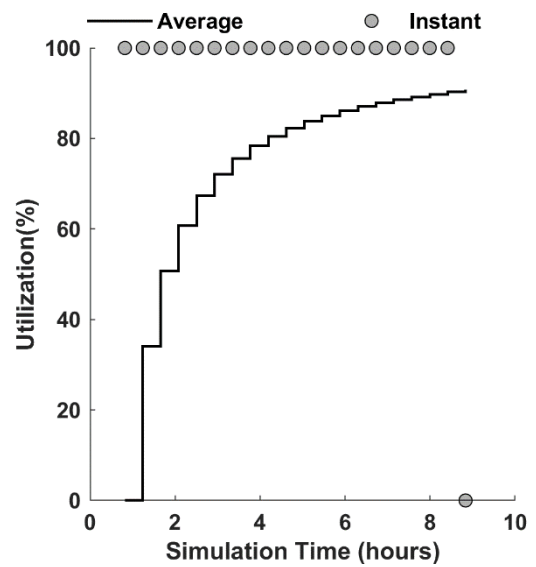
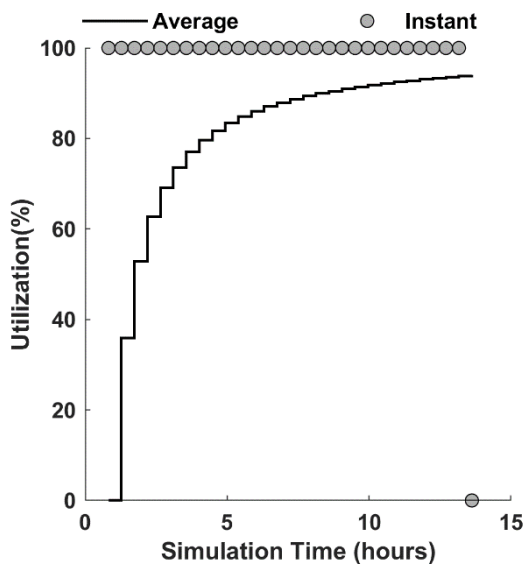
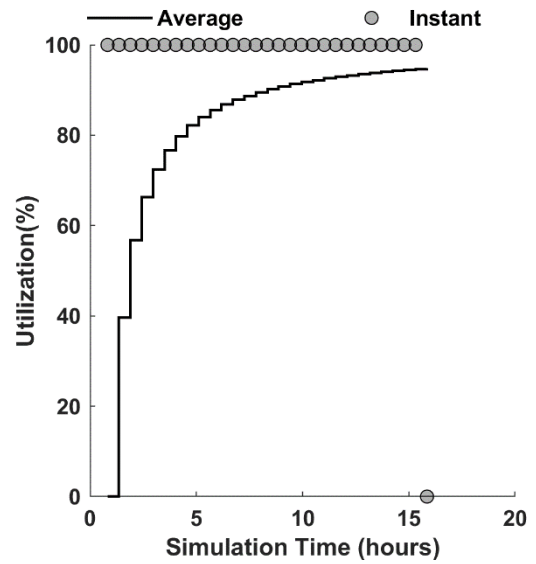
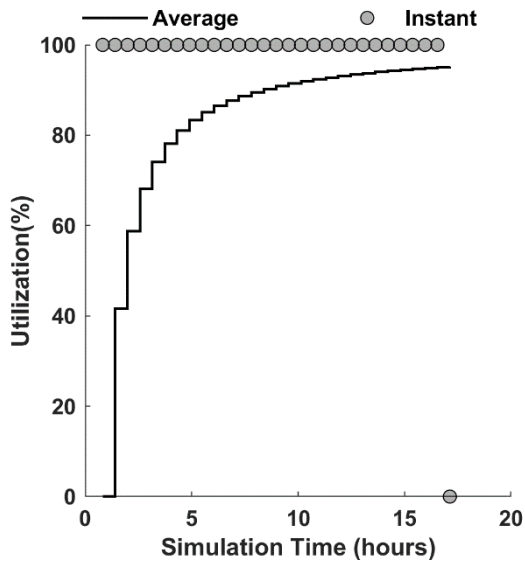
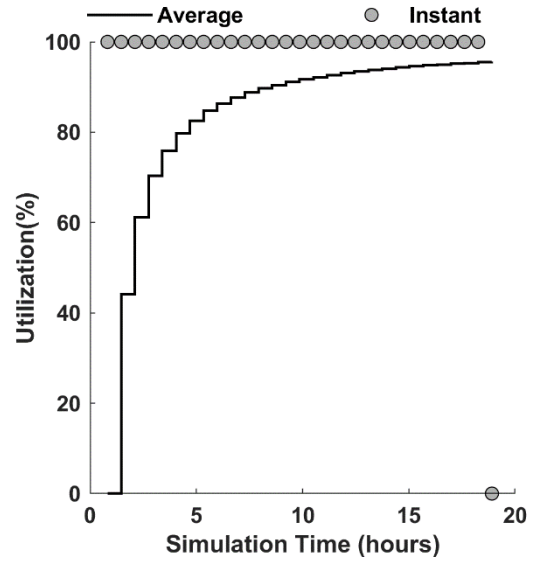
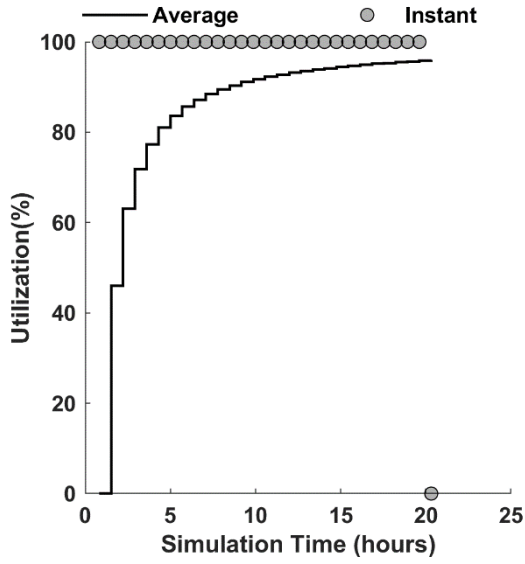


Dryer Utilization

Dryer resource utilization for all days. Season progresses from left to right, top to bottom

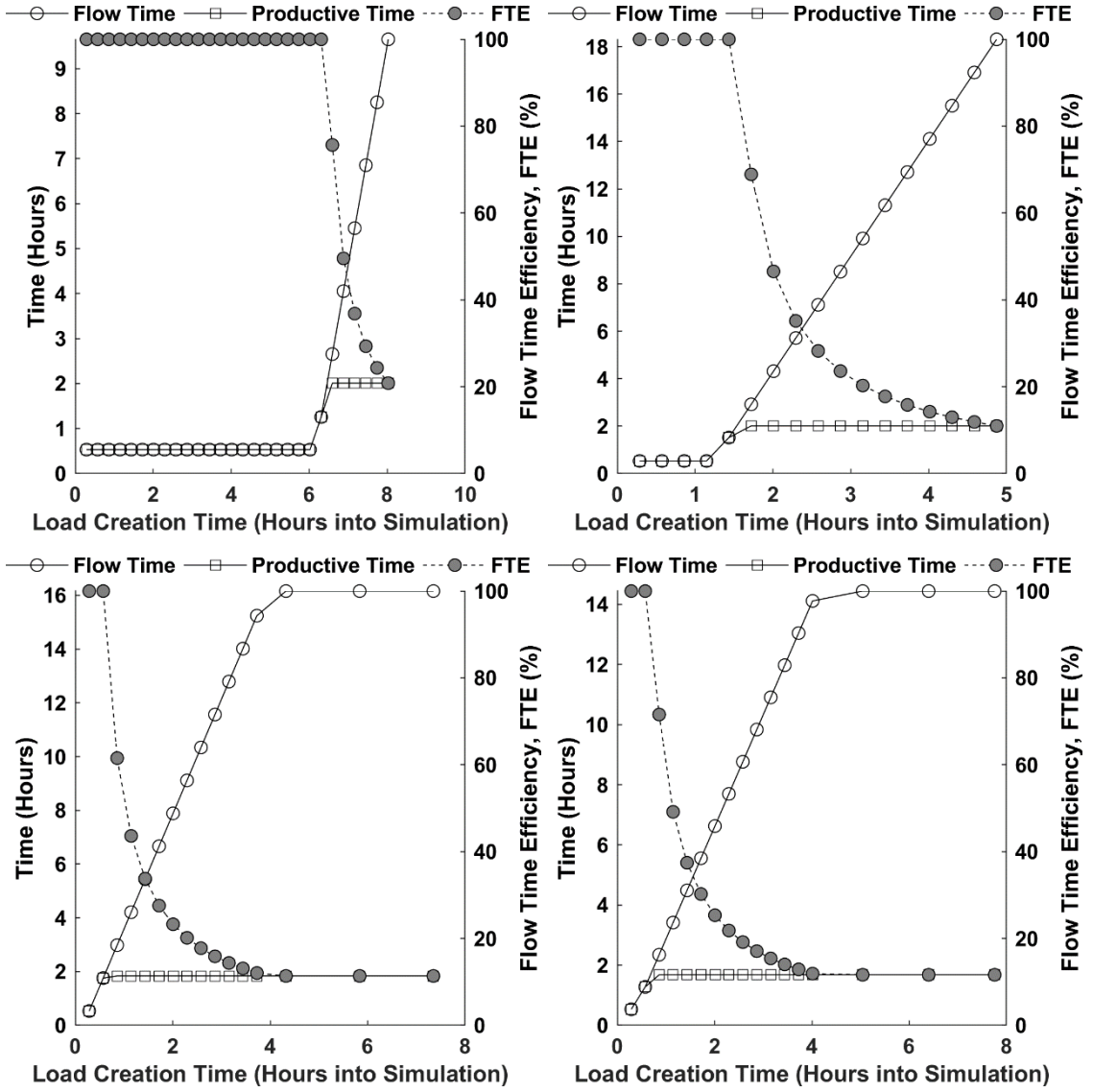


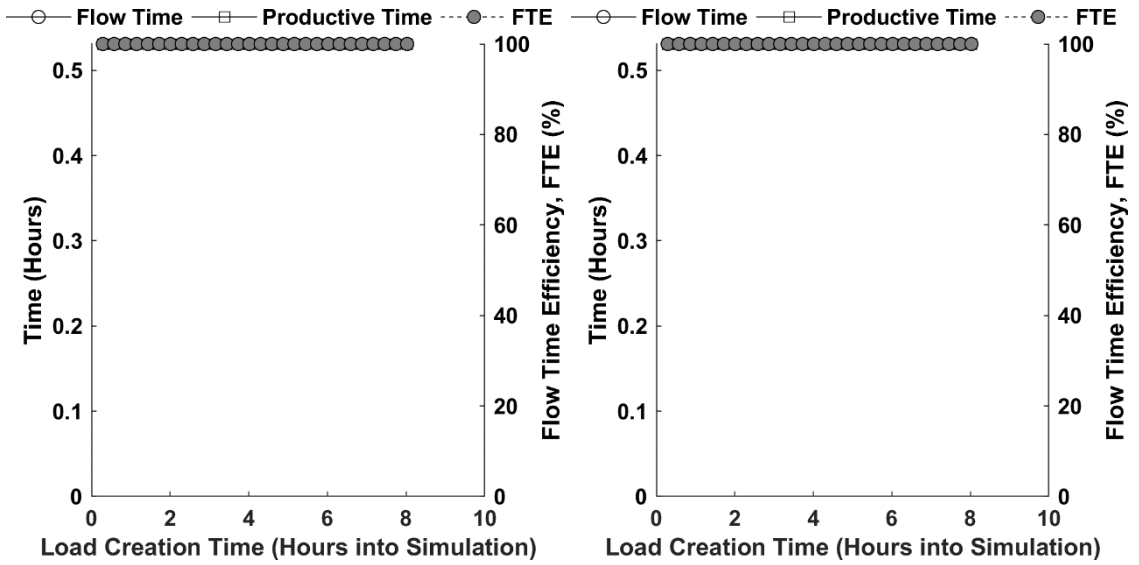
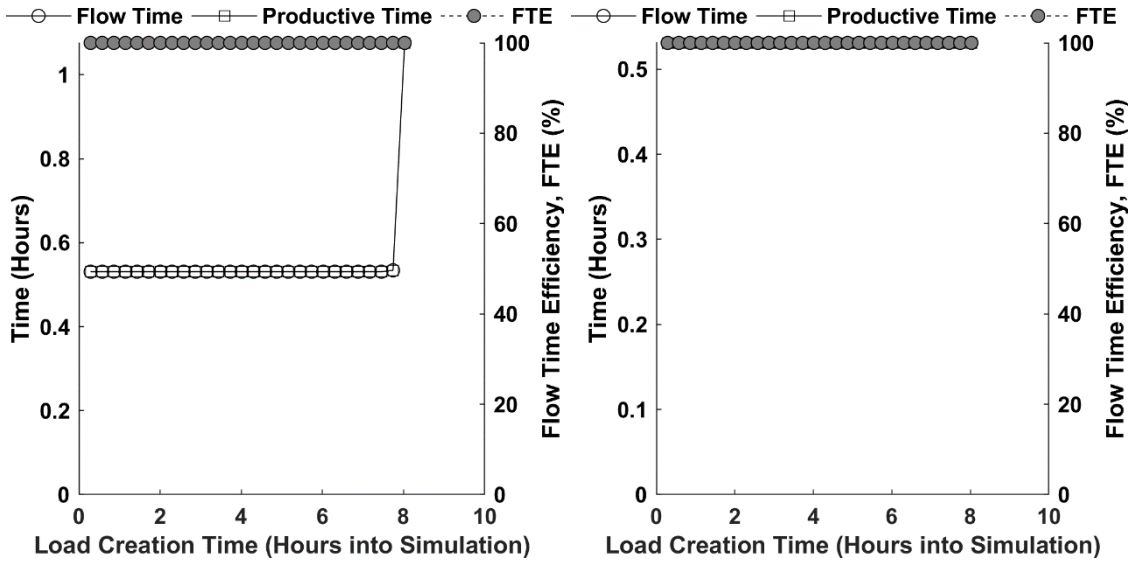
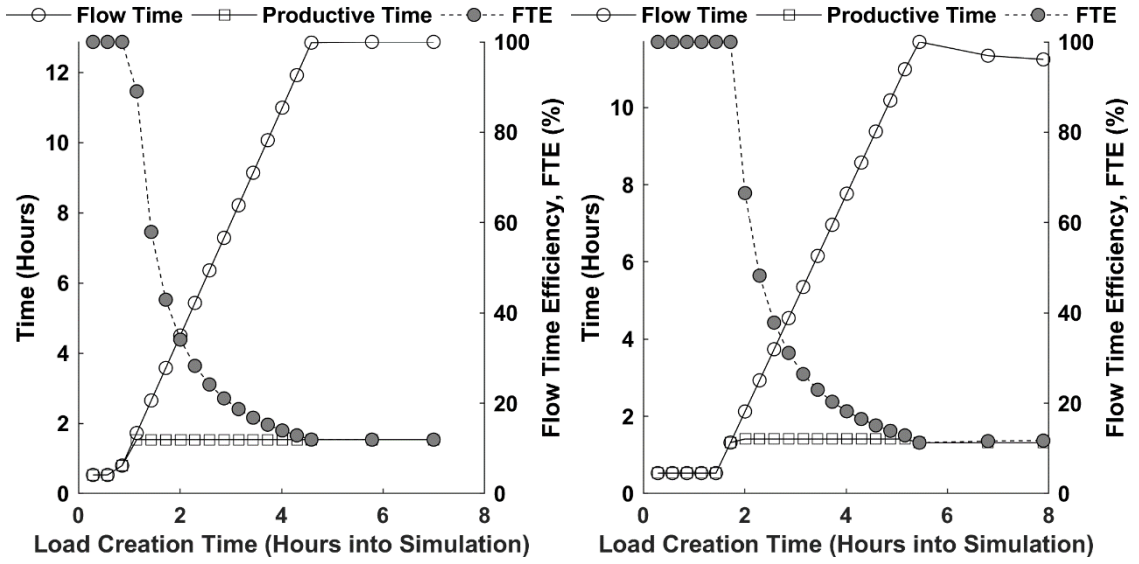


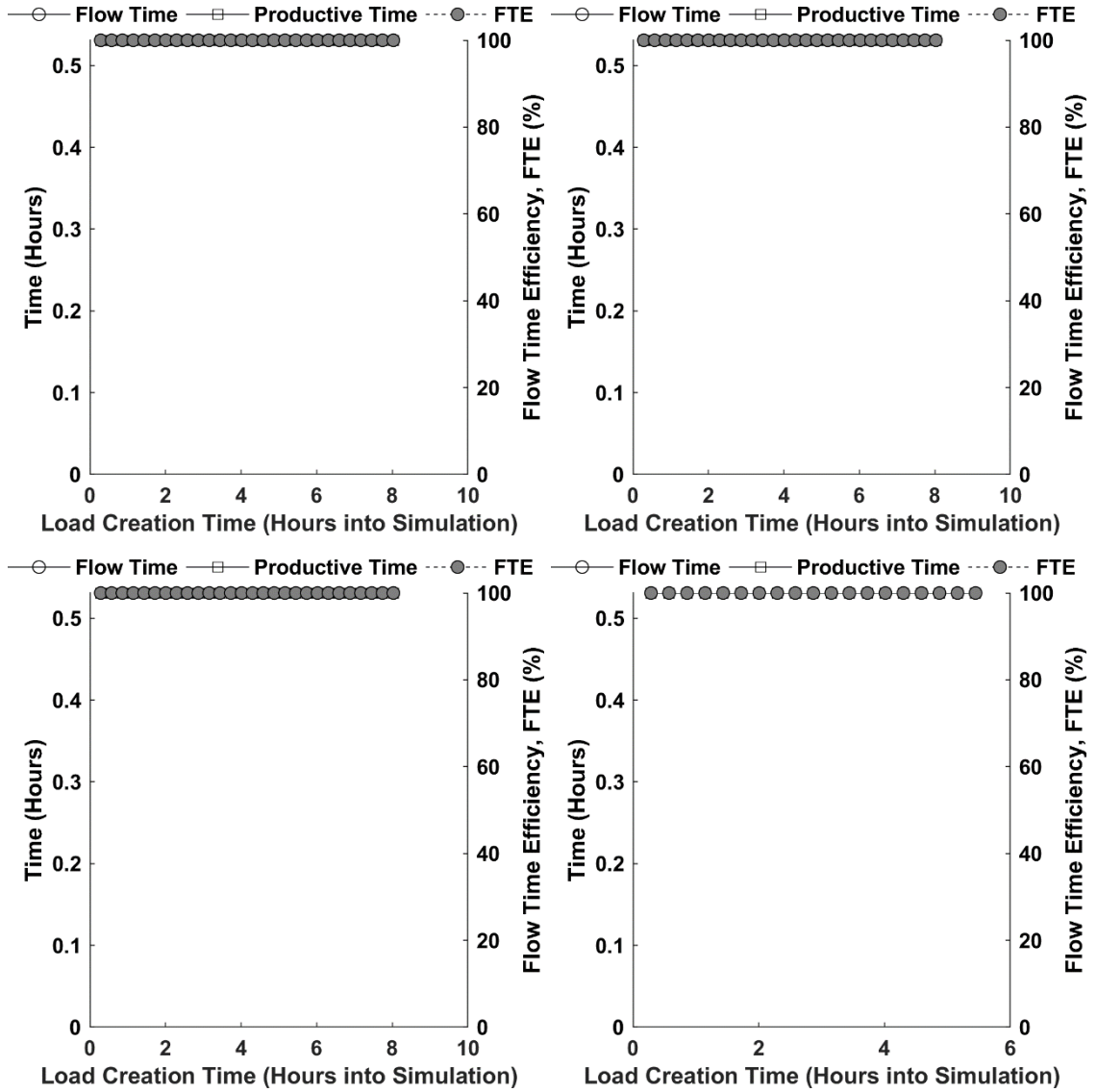


Flow Time

Entity flow time for all days. Season progresses from left to right, top to bottom

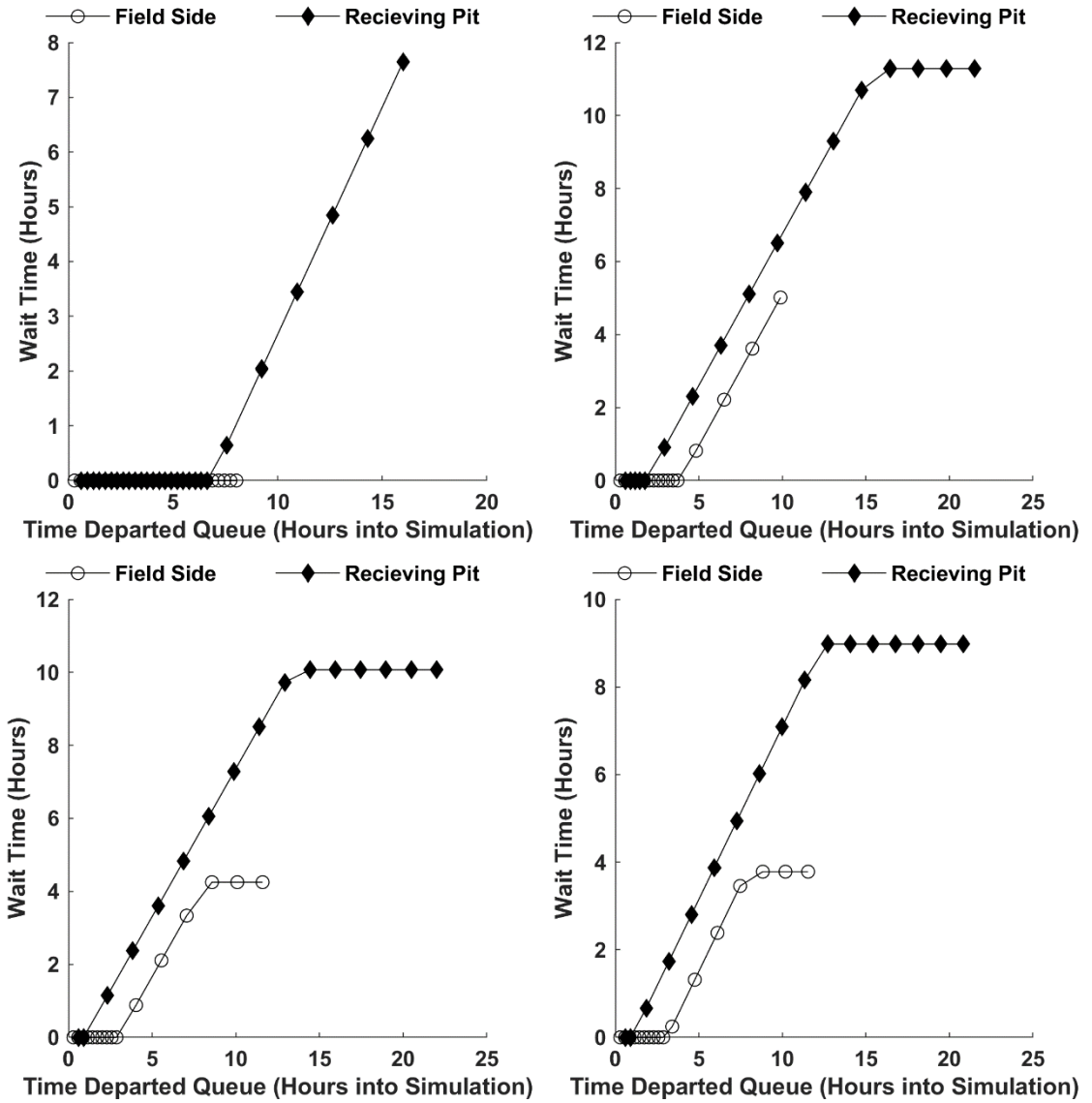


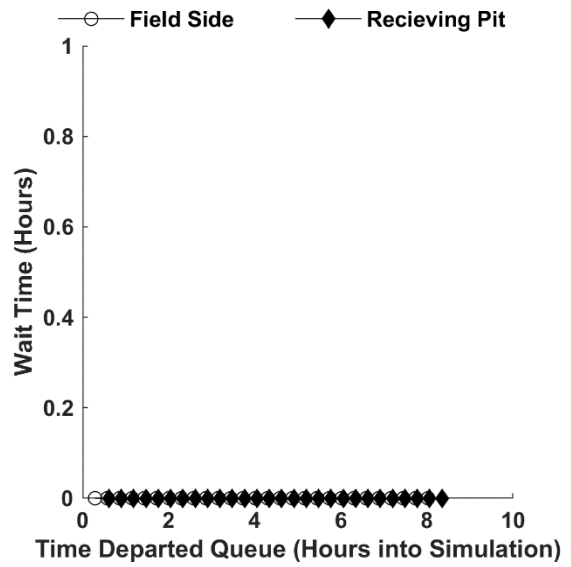
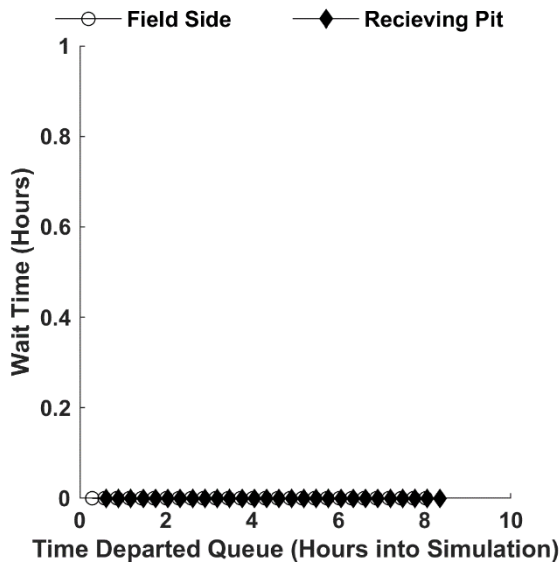
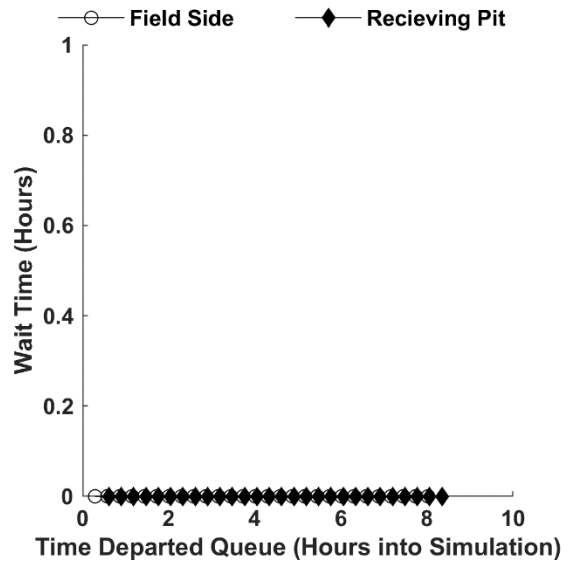
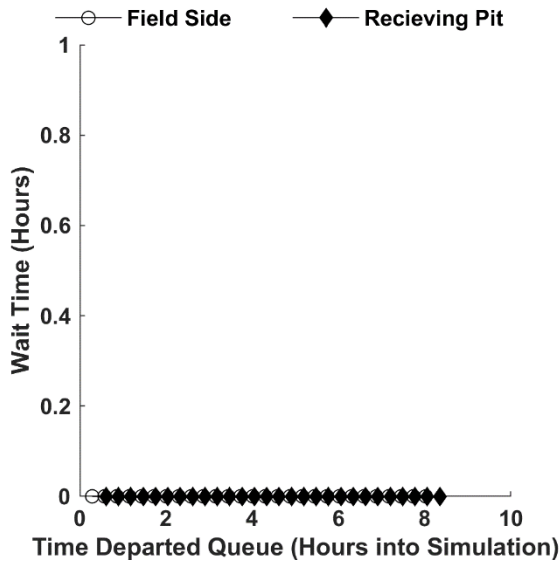
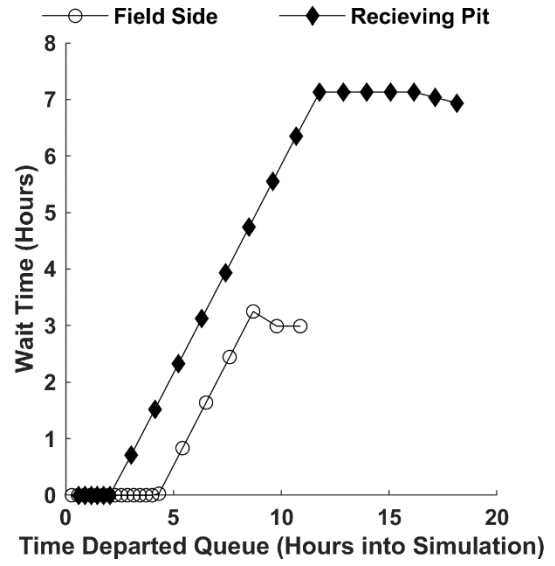
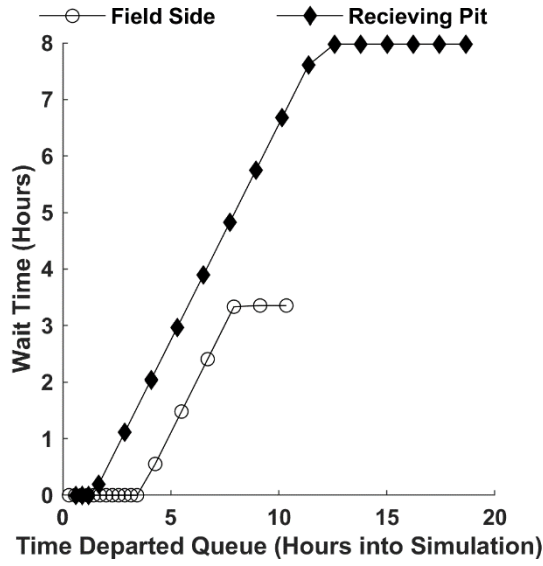


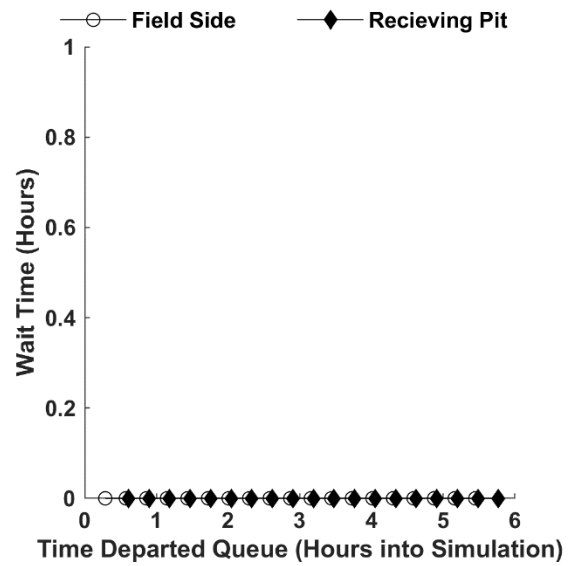
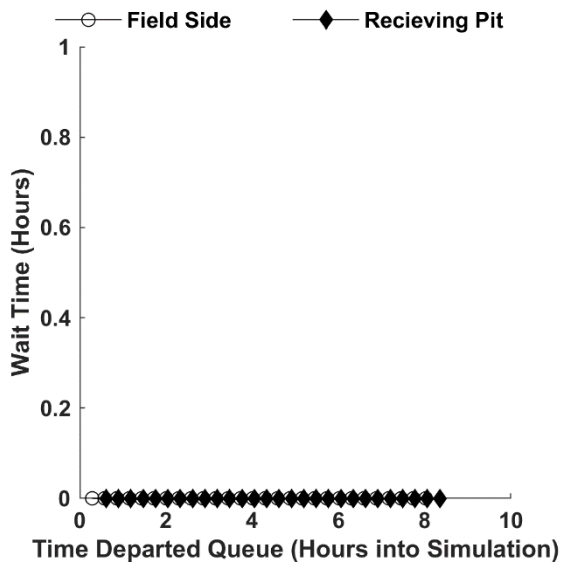
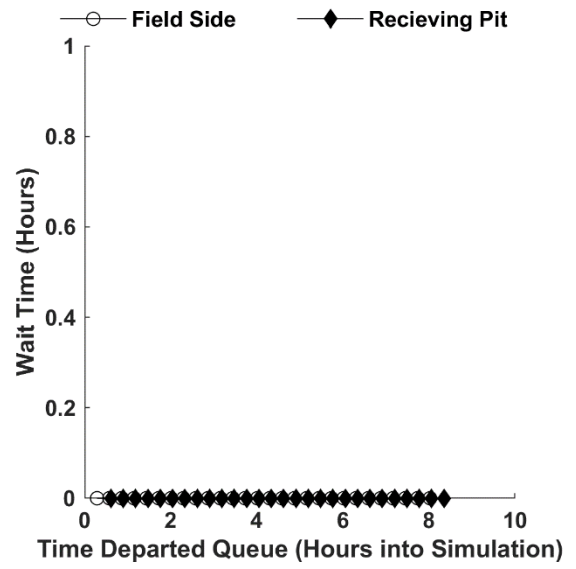
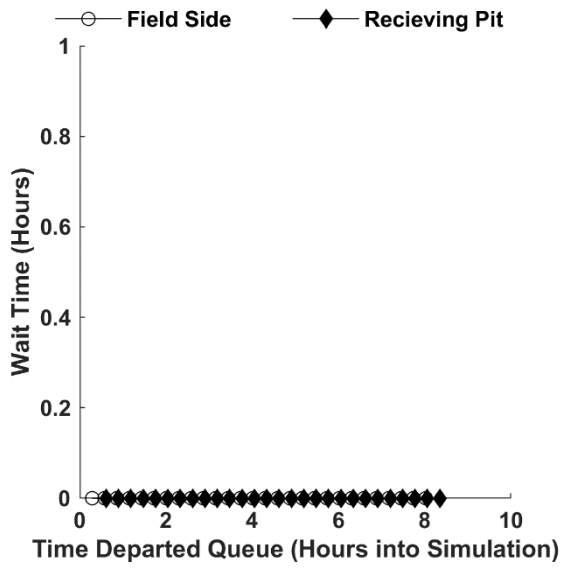


Wait Time

Field and pit wait times for all days. Season progresses from left to right, top to bottom



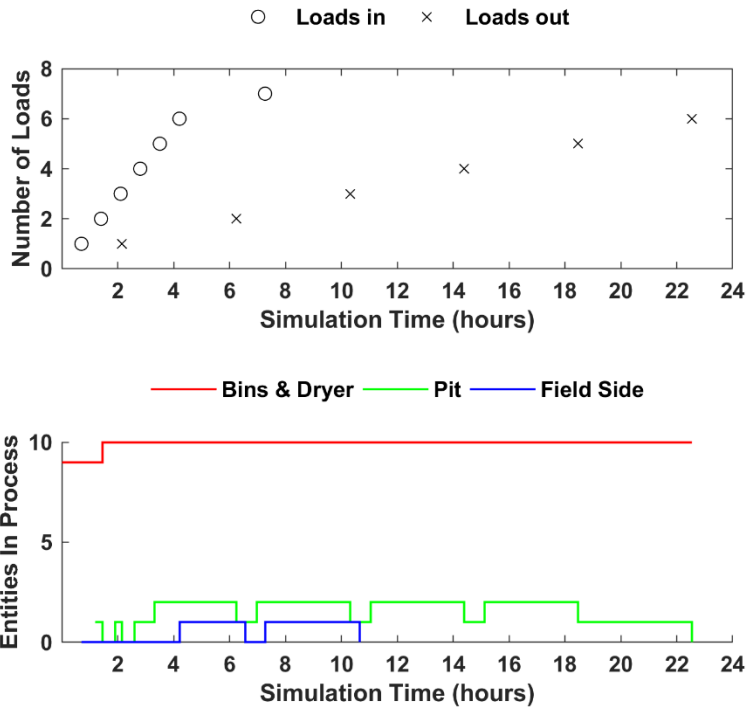




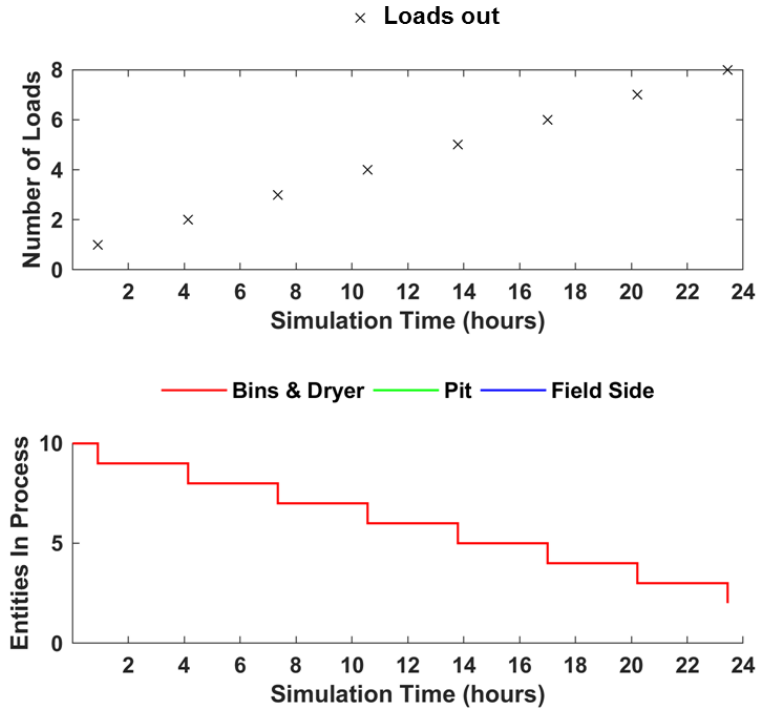
Appendix G. Supplemental Information from Sensitivity Analysis

Daily Simulation Overview

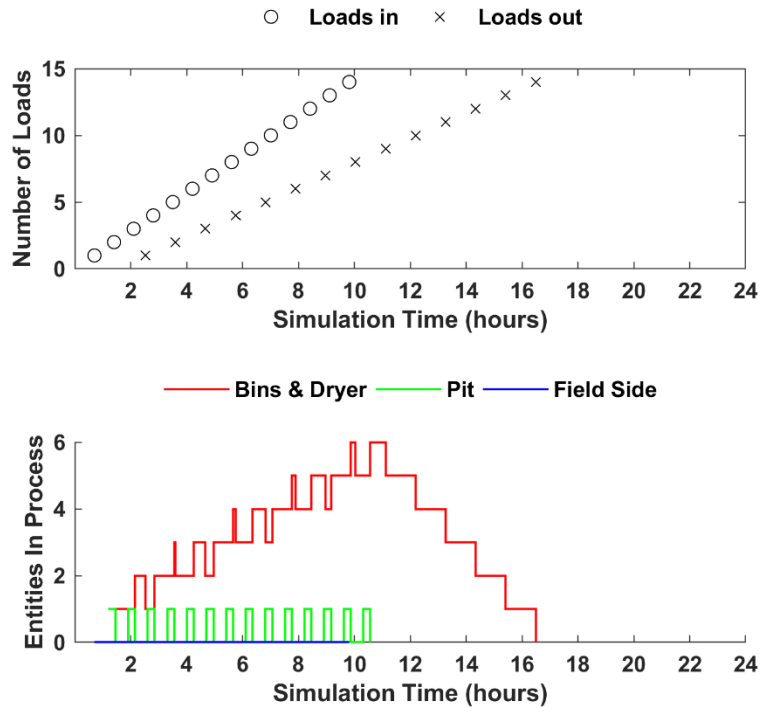
Baseline Configuration Example- Early Season



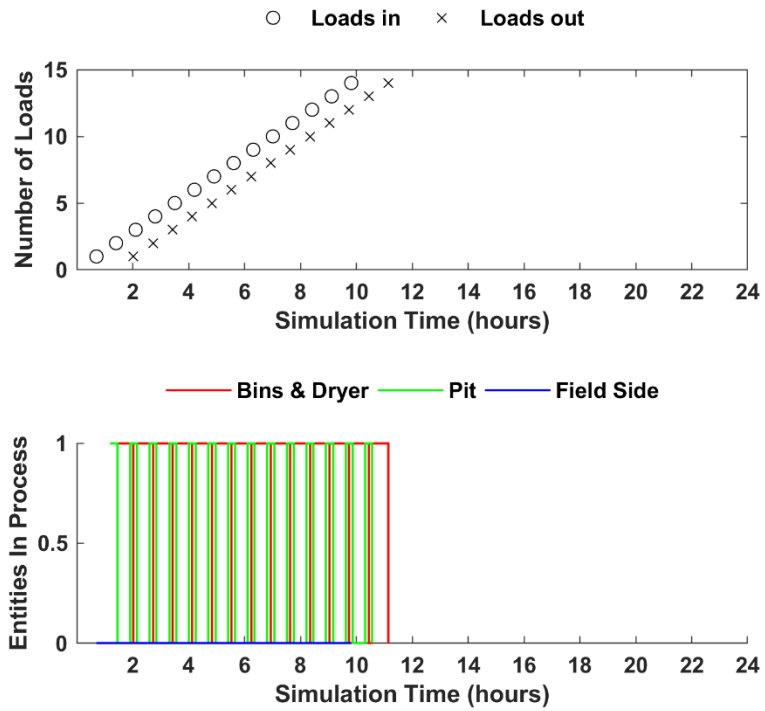
Baseline Configuration Example- No Fieldwork Drying only



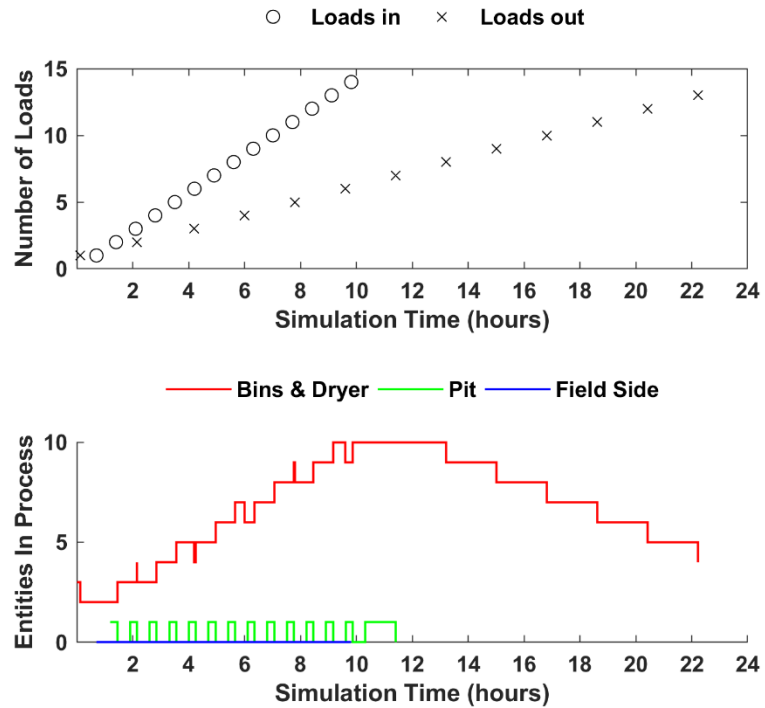
Baseline Configuration Example- Mid-Season



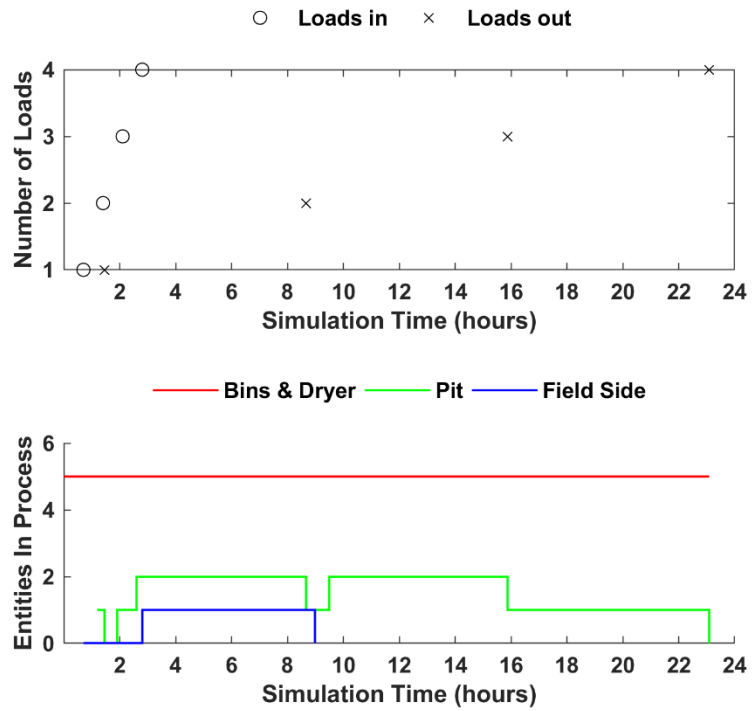
Baseline Configuration Example- Late Season



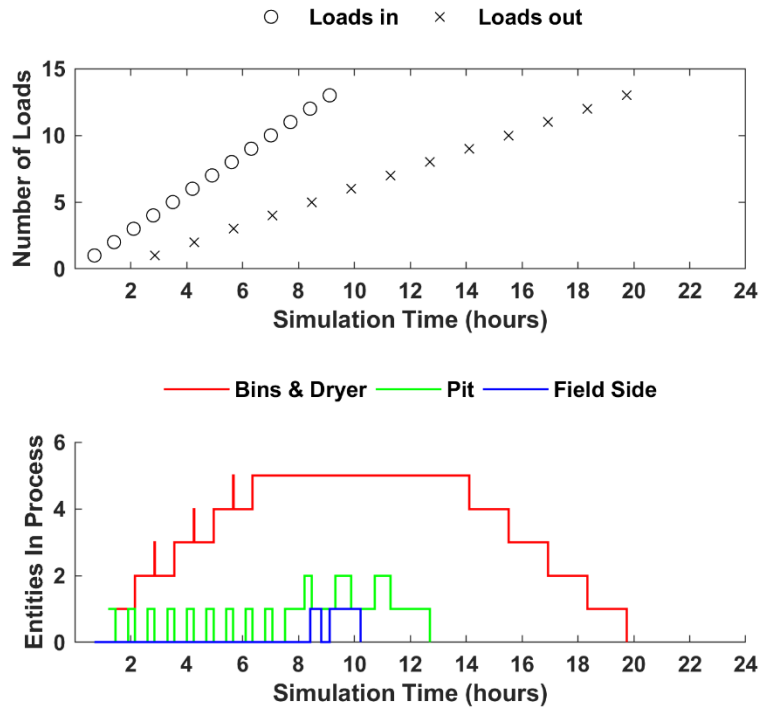
Baseline Configuration with Doubled Dryer Size Example- Early Season



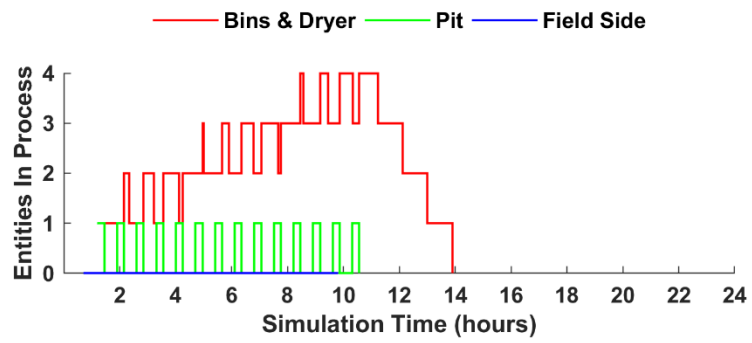
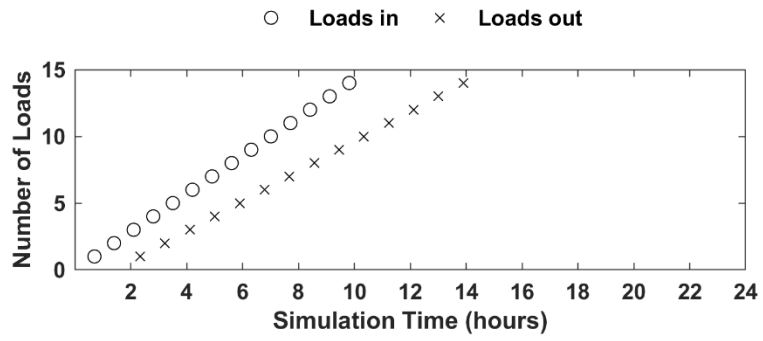
Minimally Equipped Configuration Example- Early Season



Minimally Equipped Configuration Example- Mid-Season

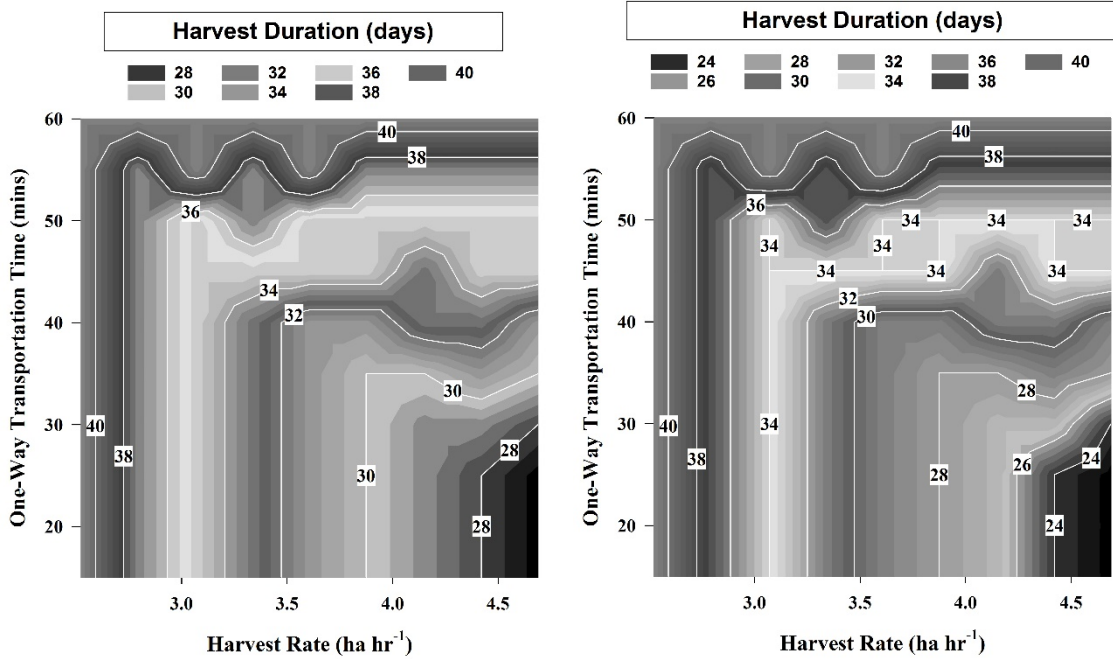


Minimally Equipped Configuration Example- Late Season

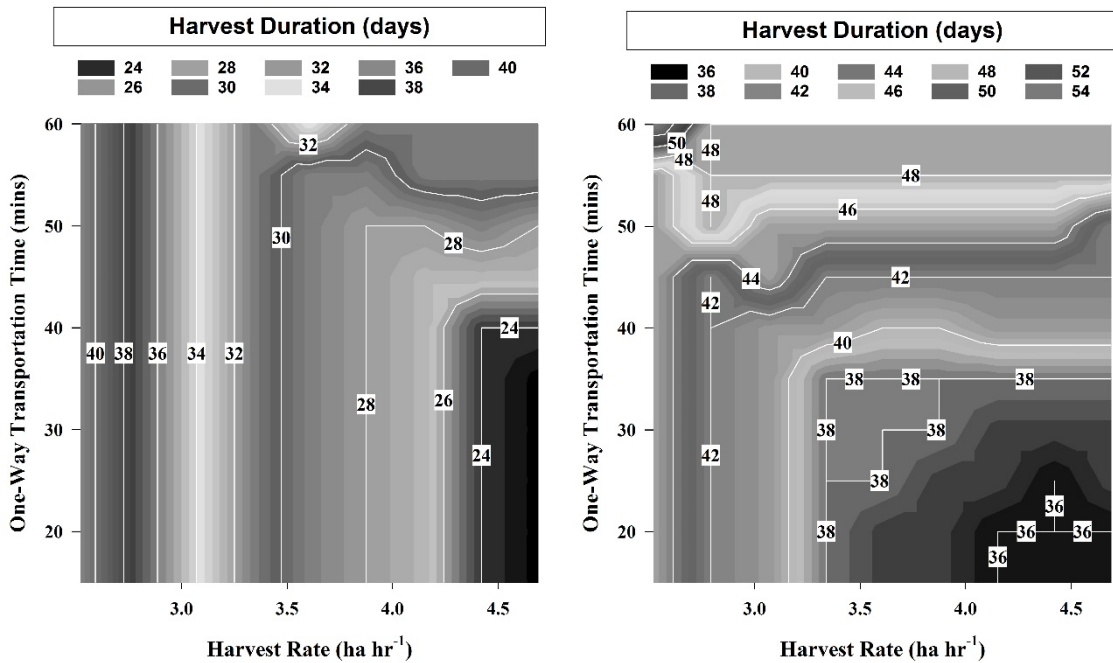


Example Harvest Length from Sensitivity Analysis

Baseline (left) Double Drying Capacity (right)

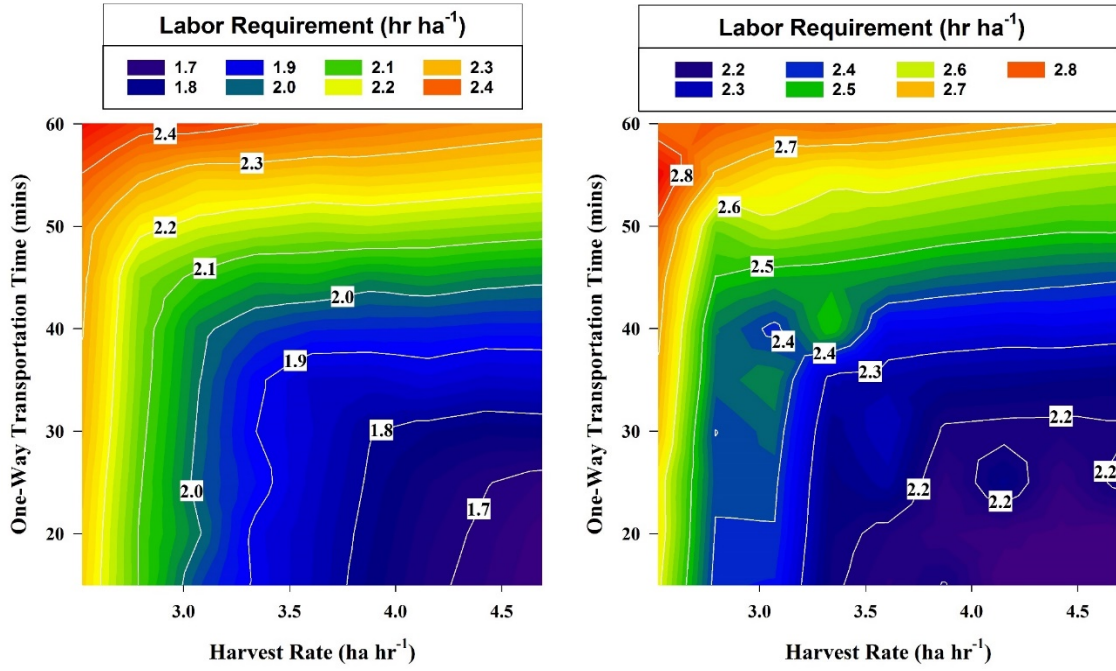


Double Drying Capacity and an Additional Driver (left) Minimally Equipped Configuration (right)



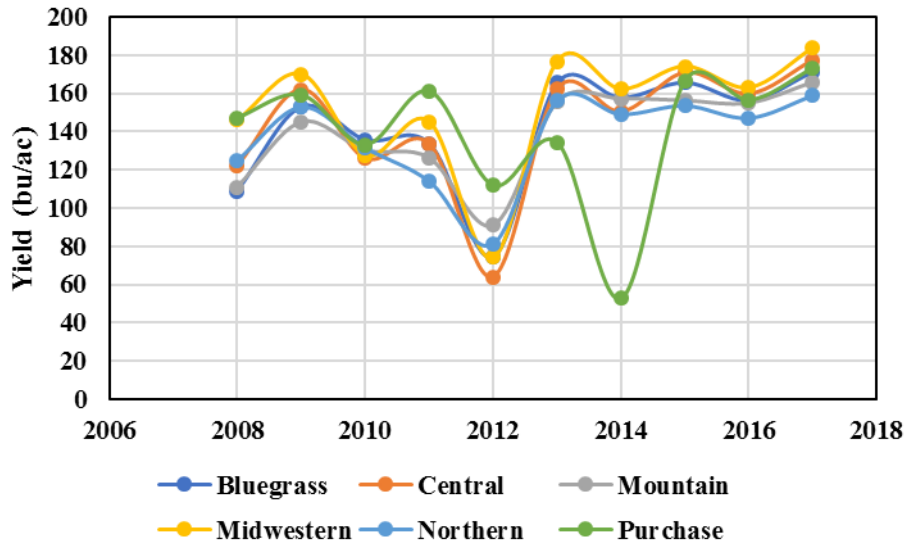
Example Labor Requirements from Sensitivity Analysis

Labor requirement for baseline operation (left) and minimally equipped (right)



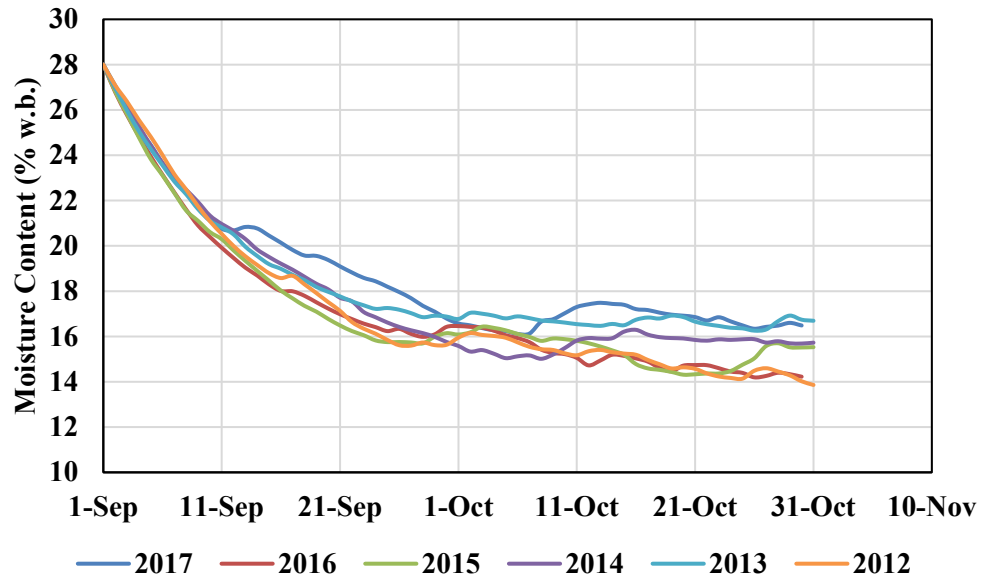
Appendix H. Trends in Weather and Yield

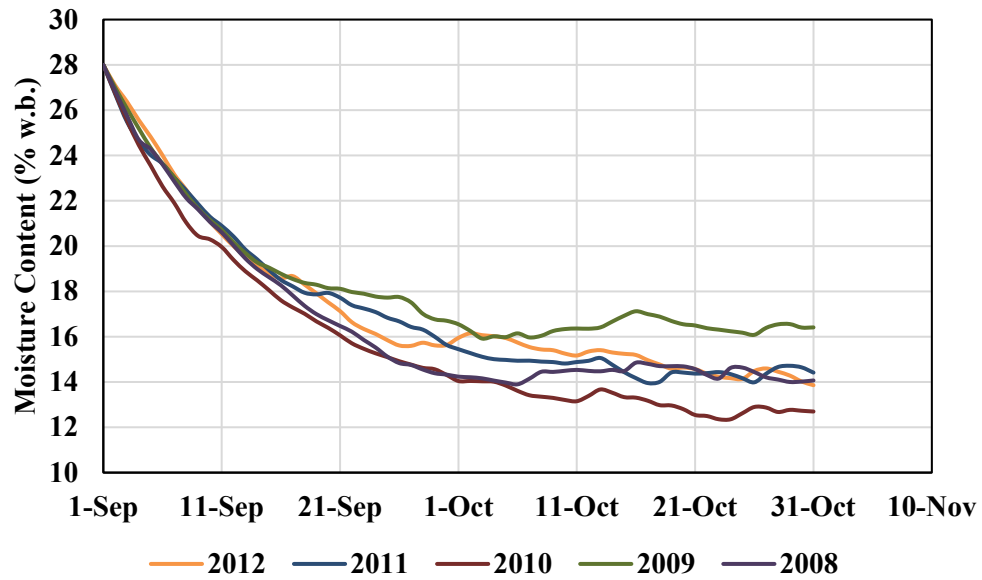
Kentucky Yield Trends 2008-2017



Estimated Corn Field Drying for Bowling Green, KY

Assumed MC=28% on Sept 1





Weather Data for Bowling Green, Ky

Average weather data for Bowling Green, Ky (2008-2017)

Date	Mean Temperature (°C)	Mean RH (%)	Mean EMC (%w.b.)	P Z<0.25in
1-Sep	24.5	72.9	15.1	0.70
2-Sep	24.5	71.0	14.5	0.80
3-Sep	24.3	71.1	14.6	0.80
4-Sep	24.2	70.0	14.3	0.70
5-Sep	22.7	74.7	15.5	0.70
6-Sep	22.2	73.3	15.2	0.80
7-Sep	22.9	70.8	14.6	0.60
8-Sep	22.7	69.6	14.4	0.90
9-Sep	22.5	71.4	14.7	0.90
10-Sep	22.4	73.6	15.2	0.90
11-Sep	21.8	77.0	15.9	0.80
12-Sep	21.3	72.7	15.2	0.80
13-Sep	20.7	69.9	14.9	1.00
14-Sep	20.9	71.4	15.0	1.00
15-Sep	20.7	70.6	14.8	1.00
16-Sep	21.2	71.6	14.9	1.00

17-Sep	20.7	74.5	15.6	0.80
18-Sep	21.8	71.5	14.8	0.90
19-Sep	21.6	72.2	15.1	0.70
20-Sep	22.4	72.3	15.0	0.80
21-Sep	22.3	69.3	14.4	0.80
22-Sep	21.3	66.9	14.1	0.90
23-Sep	20.7	66.9	14.1	0.90
24-Sep	21.1	68.9	14.4	0.90
25-Sep	21.7	68.7	14.4	1.00
26-Sep	20.3	70.9	14.9	0.70
27-Sep	20.2	68.9	14.4	1.00
28-Sep	19.9	66.8	14.2	0.90
29-Sep	18.6	69.9	15.0	0.90
30-Sep	17.8	69.0	15.0	0.90
1-Oct	17.2	68.0	14.7	0.80
2-Oct	16.9	71.0	15.4	0.60
3-Oct	16.4	69.7	15.1	0.80
4-Oct	16.7	68.8	14.8	1.00
5-Oct	18.6	67.1	14.3	1.00
6-Oct	18.2	68.7	14.7	0.60
7-Oct	18.0	68.4	14.6	0.90
8-Oct	17.5	69.8	15.3	0.80
9-Oct	17.5	73.5	15.8	0.70
10-Oct	17.3	72.7	15.7	0.70
11-Oct	16.2	72.5	15.8	1.00
12-Oct	17.8	73.3	15.7	0.90
13-Oct	18.2	76.5	16.2	0.80
14-Oct	17.4	71.3	15.4	0.80
15-Oct	16.7	68.4	15.0	0.80
16-Oct	15.0	68.6	15.3	0.90
17-Oct	14.9	62.5	13.9	0.90
18-Oct	13.8	62.0	13.9	0.90
19-Oct	12.5	66.7	15.0	1.00
20-Oct	13.1	66.9	14.9	0.90
21-Oct	13.6	63.4	14.2	1.00
22-Oct	13.9	62.8	14.0	1.00
23-Oct	14.5	65.1	14.4	0.80
24-Oct	14.2	67.1	14.9	0.80
25-Oct	13.2	67.7	15.0	0.80
26-Oct	14.2	67.5	15.0	0.70

27-Oct	13.4	73.0	16.4	0.60
28-Oct	11.6	70.6	16.0	0.60
29-Oct	10.6	65.8	15.0	1.00
30-Oct	12.5	61.9	14.0	0.90
31-Oct	11.6	63.4	14.4	0.60

REFERENCES

- Abawi, G. Y. (1993). A simulation model of wheat harvesting and drying in northern Australia. *Journal of Agricultural Engineering Research*, 54(2), 141-158.
doi:<http://dx.doi.org/10.1006/jaer.1993.1009>
- Allen, T. T. (2011). *Introduction to discrete event simulation and agent-based modeling: Voting systems, health care, military, and manufacturing*. London, United Kingdom: Springer Science & Business Media.
- Amiama, C., Pereira, J. M., Castro, A., & Bueno, J. (2015). Modelling corn silage harvest logistics for a cost optimization approach. *Computers and Electronics in Agriculture*, 118, 56-65. doi:<http://dx.doi.org/10.1016/j.compag.2015.08.024>
- ASABE Standards (2000). D497.4 agricultural machinery management data. St. Joseph, MI: ASABE.
- ASABE Standards. (2007). D245. 6—Moisture relationship of plant-based agricultural products (pp. 604-638). St. Joseph, MI: ASABE.
- ASABE Standards. (2012). S352.2 Moisture measurement- unground grain and seeds. St. Joseph, MI: ASABE.
- ASABE Standards. (2014). S448.2: Thin-layer drying of agricultural crops. St. Joseph, MI: ASABE.
- ASABE Standards. (2015a). D497. 6Agricultural machinery management data. St. Joseph. MI: ASABE.
- ASABE Standards. (2015b). Ep 496.3Agricultural machinery management. St. Joseph MI: ASABE.
- ASABE Standards. (2015c). S248.3 Construction and rating of equipment for drying farm crops. St. Joseph, MI: ASABE.
- ASABE Standards. (2015d). S495.1 Uniform terminology for agricultural machinery management. St. Joseph, MI: ASABE.
- Audsley, E., & Boyce, D. (1974). A method of minimizing the costs of combine-harvesting and high temperature grain drying. *Journal of Agricultural Engineering Research*, 19(2), 173-188.

- Ayres, G. E., Babcock, C., & Hull, D. O. (1972). *Corn combine field performance in iowa*. Paper presented at the Grain Damage Symposium, The Ohio State University, Columbus, Ohio.
- Babeir, A. S., Colvin, T. S., & Marley, S. J. (1986). Predicting field tractability with a simulation model. *Transactions of the ASAE.*, 29(6). doi:10.13031/2013.30347
- Baptist, R. (1992). Derivation of steady-state herd productivity. *Agricultural Systems*, 39(3), 253-272. doi:[http://dx.doi.org/10.1016/0308-521X\(92\)90099-A](http://dx.doi.org/10.1016/0308-521X(92)90099-A)
- Benock, G., Loewer Jr, O., Bridges, T., & Loewer, D. (1981). Grain flow restrictions in harvesting-delivery-drying systems. *Trans ASAE*, 24(5), 1151-1161.
- Benock, G., Loewer, O., Bridges, T., & Loewer, D. (1981). Grain flow restrictions in harvesting-delivery-drying systems. *Transactions of the ASAE*.
- Benson, E. R., Hansen, A. C., Reid, J. F., Warman, B. L., & Brand, M. A. (2002). *Development of an in-field grain handling simulation in arena. Asabe paper no. 023104*. ASAE, St. Joseph, MI.
- Berruto, R., & Maier, D. E. (2001). Analyzing the receiving operation of different grain types in a single-pit country elevator. *Trans. ASAE*, 44(3), 631-638.
- Bochtis, D. D., Sørensen, C. G., & Busato, P. (2014). Advances in agricultural machinery management: A review. *Biosystems Engineering*, 126, 69-81.
- Bridges, T. C., Loewer, O. J., Walker, J. N., & Overhults, D. G. (1979). A computer model for evaluating corn harvesting, handling, drying and storage systems. *Transactions of the Asae*, 22(3), 618.
- Brooker, D. B., Bakker-Arkema, F. W., & Hall, C. W. (1992). *Drying and storage of grains and oilseeds*: Springer Science & Business Media.
- Buckmaster, D. R., & Hilton, J. W. (2005). Computerized cycle analysis of harvest, transport, and unload systems. *Computers and Electronics in Agriculture*, 47(2), 137-147.
- Busato, P., Berruto, R., & Saunders, C. (2007). Optimal field-bin locations and harvest patterns to improve the combine field capacity: Study with a dynamic simulation model. *Agricultural Engineering International: CIGR Journal*, IX.

- Carpenter, M. L., & Brooker, D. B. (1972). Minimum cost machinery systems for harvesting, drying and storing shelled corn. *Transactions of the ASAE.*, 15(3), 515-0519. doi:<https://doi.org/10.13031/2013.37942>
- Chowdhury, M. H., & Buchele, W. F. (1976). Colorimetric determination of grain damage. *Transactions of the ASAE.*, 19(5), 807-0808. doi:<https://doi.org/10.13031/2013.36122>
- Davis, S., Diegel, S., & Boundy, R. (2007). Transportation energy data book: Edition 26. Oak ridge national laboratory. *ORNL*, 6978.
- De Toro, A. (2005). Influences on timeliness costs and their variability on arable farms. *Biosystems Engineering*, 92(1), 1-13.
- De Toro, A., Gunnarsson, C., Lundin, G., & Jonsson, N. (2012). Cereal harvesting – strategies and costs under variable weather conditions. *Biosystems Engineering*, 111(4), 429-439. doi:<http://dx.doi.org/10.1016/j.biosystemseng.2012.01.010>
- De Toro, A., & Hansson, P. A. (2004). Analysis of field machinery performance based on daily soil workability status using discrete event simulation or on average workday probability. *Agricultural Systems*, 79(1), 109-129. doi:10.1016/s0308-521x(03)00073-8
- Dudenhoeffer, N. E., Luck, B. D., Digman, M. F., & Drewry, J. L. (2017). Simulation of the forage harvest cycle for asset allocation. *Applied Engineering in Agriculture*, 34(2), 327-334.
- Edwards, W. (2014). Estimating the cost for drying corn. *Ag Decision Maker*. Retrieved from <https://www.extension.iastate.edu/agdm/crops/pdf/a2-31.pdf>
- Edwards, W., & Johanns, A. (2012). Wages and benefits for farm employees. *Ag Decision Maker*. Retrieved from <https://www.extension.iastate.edu/agdm/wholefarm/html/c1-60.html>
- Edwards, W., Plastina, A., & Johanns, A. (2016). Grain harvesting equipment and labor in iowa. *Ag Decision Maker*. Retrieved from <https://www.extension.iastate.edu/agdm/crops/pdf/a3-16.pdf>
- Elmore, R. W., & Roeth, F. W. (1999). Corn kernel weight and grain yield stability during post-maturity drydown. *Journal of production agriculture*, 12(2), 300-305.

- Farm Fans Inc. (1999). *Operator's manual c-2130b, c-2140b, c-2160b, c-2175b, and c-21100b grain dryers*. Indianapolis, IN: FFI Corporation.
- Glen, J. J. (1987). Mathematical models in farm planning: A survey. *Operations Research*, 35(5), 641-666.
- Halich, G. (2018). Custom machinery rates applicable to kentucky (2018). *University of Kentucky Cooperative Extension Service*. Retrieved from <https://www.uky.edu/Ag/AgEcon/pubs/customratesKY.pdf>
- Hanna, H. M. (2008). Pm 574 profitable corn harvesting. Retrieved from <https://store.extension.iastate.edu/product/Profitable-Corn-Harvesting>
- Hanna, H. M., Kohl, K., & Haden, D. A. (2002). Machine losses from conventional versus narrow row corn harvest. *Applied Engineering in Agriculture*, 18(4), 405-410.
- Harmon, J. D., Luck, B. D., Shinnars, K. J., Anex, R. P., & Drewry, J. L. (2017). Time-motion analysis of forage harvest: A case study. *Trans ASABE*, 61(2), 483-491.
- Harrigan, T. (2003). Time-motion analysis of corn silage harvest systems. *Applied Engineering in Agriculture*, 19(4), 389-396.
- Hellevang, K. J. (2013). *Ae701 grain drying*. North Dakota State University.
- Holtman, J. B., Pickett, L. K., Armstrong, D., & Connor, L. J. (1973). A systematic approach to simulating corn production systems. *Transactions of the ASAE.*, 16(1), 19-0023.
- Huitink, G. (2001). Mp 437 corn production handbook, 65-72. Retrieved from <https://www.uaex.edu/publications/pdf/mp437/chap8.pdf>
- Hwang, S., Epplin, F. M., Lee, B.-h., & Huhnke, R. (2009). A probabilistic estimate of the frequency of mowing and baling days available in oklahoma USA for the harvest of switchgrass for use in biorefineries. *Biomass and Bioenergy*, 33(8), 1037-1045. doi:<http://dx.doi.org/10.1016/j.biombioe.2009.03.003>
- Isaac, N. E., Quick, G. R., Birrell, S. J., Edwards, W. M., & Coers, B. A. (2006). Combine harvester econometric model with forward speed optimization. *Applied Engineering in Agriculture*, 22(1), 25-31.
- Jackson, J. J. (2015). *Optimal uses of biomass resources in distributed applications*. (PhD), University of Kentucky, Lexington, KY.

- Johnson, W., & Lamp, B. (1966). *Principles, equipment and systems for corn harvesting*. Wooster, OH: Agricultural Consulting Associates, Inc.
- Johnson, W. H., Lamp, B., Henry, J., & Hall, G. (1963). Corn harvesting performance at various dates. *Transactions of the ASAE.*, 6(3), 268-0272.
- Kiker, C., & Lieblich, M. (1986). Financial analysis of on-farm grain drying. *Journal of Agricultural and Applied Economics*, 18(2), 73-84.
- Klinner, W. E., & Biggar, G. W. (1972). Some effects of harvest date and design features of the cutting table on the front losses of combine-harvesters. *Journal of Agricultural Engineering Research*, 17(1), 71-78.
doi:[http://dx.doi.org/10.1016/S0021-8634\(72\)80016-7](http://dx.doi.org/10.1016/S0021-8634(72)80016-7)
- Licht, M., Hurburgh, C., Kots, M., Blake, P., & Hanna, M. (2017). *Is there loss of corn dry matter in the field after maturity?* Paper presented at the 29th Annual Inegrated Crop Managment Conference.
- Liu, Q., & Bakker-Arkema, F. W. (1997). Stochastic modelling of grain drying: Part 2. Model development. *Journal of Agricultural Engineering Research*, 66(4), 275-280. doi:<https://doi.org/10.1006/jaer.1996.0145>
- Loewer, O., Kocher, M., & Solaimanian, J. (1990). An expert system for determining bottlenecks in on-farm grain processing systems. *Applied Engineering in Agriculture*, 6(1), 69-72.
- Loewer, O. J., Benock, G., & Bridges, T. C. (1980). Effect of combine selection and harvesting rate on grain drying and delivery system performance. *Transactions of the ASAE.*, 23(6), 1548-1553.
- Loewer, O. J., Bridges, T. C., & Bucklin, R. A. (1994). *On-farm drying and storage systems*. St. Joseph, MI: ASABE.
- Loewer, O. J., Bridges, T. C., White, G. M., & Overhults, D. G. (1980). The influence of harvesting strategies and economic constraints on the feasibility of farm grain drying and storage facilities. 23(2). doi:10.13031/2013.34605
- Loewer, O. J., Bridges, T. C., White, G. M., & Razor, R. B. (1984). Optimum moisture content to begin harvesting corn as influenced by energy cost. *Transactions of the ASAE.*, 27(2), 362-365.

- Maier, D. E., & Bakker-Arkema, F. W. (2002). *Grain drying systems*. Paper presented at the Proceedings of the 2002 Facility Design Conference of the Grain Elevator & Processing Society, St. Charles, Illinois, USA, July.
- Maier, D. E., & Watkins, A. E. (1998). *Drying of white food corn for quality*. Purdue University.
- Marley, S. J., & Ayres, G. E. (1972). Influence of planting and harvesting dates on corn yield. *Transactions of the ASAE.*, 15(2), 228-231.
doi:<https://doi.org/10.13031/2013.37873>
- Martin, B. A. (2018). *Two essays on whole farm modeling and crop marketing in western kentucky*. (MSc), University of Kentucky, Lexington, KY.
- McGechan, M. B. (1985a). A parametric study of cereal harvesting models i. Critical assessment of measured data on parameter variability. *Journal of Agricultural Engineering Research*, 31(2), 149-158. doi:[http://dx.doi.org/10.1016/0021-8634\(85\)90067-8](http://dx.doi.org/10.1016/0021-8634(85)90067-8)
- McGechan, M. B. (1985b). A parametric study of cereal harvesting models ii. Analysis of sensitivity to parameter variability. *Journal of Agricultural Engineering Research*, 31(2), 159-170.
- McNeill, S., & Montross, M. (2007). Corn harvesting, handling, drying, and storage. Retrieved from <http://www2.ca.uky.edu/agcomm/pubs/id/id139/harvesting.pdf>
- Midwestern Regional Climate Center. (2018). Cli-mate application tools environment sub_daily data(database). Retrieved 6/15/2018
<https://mrcc.illinois.edu/CLIMATE/>
- Montross, M. D., & Maier, D. E. (2000). Simulated performance of conventional high-temperature drying, dryeration, and combination drying of shelled corn with automatic conditioning. *Transactions of the ASAE.*, 43(3), 691.
- Morey, R. V., Cloud, H. A., & Lueschen, W. E. (1976). Practices for the efficient utilization of energy for drying corn. *Transactions of the ASAE.*, 19(1), 151-0155.
- Morey, R. V., Zachariah, G. L., & Peart, R. M. (1971). Optimum policies for corn harvesting. *Transactions of the ASAE.*, 14(5), 787-792.
- MWPS-13. (1987). *Grain drying handling and storage handbook*: Midwest Plan Service, Ames, IA.

- Ng, H., Wilcke, W., Morey, R., Meronuck, R., & Lang, J. (1998). Mechanical damage and corn storability. *Transactions of the ASAE.*, 41(4), 1095-1100.
- Nichols, T. E. (n.d.). *Economics of on-farm corn drying*. NCH-21. North Carolina State University.
- Nielsen, R. L., Brown, G., Wuethrich, k., & Halter, A. (1996). *Kernel dry weight loss during post-maturity drydown intervals in corn*. Purdue University. West Lafayette, IN. Retrieved from <http://www.agry.purdue.edu/ext/corn/research/rpt94-01.htm>
- Parunak, H. V. D., Savit, R., & Riolo, R. L. (1998). *Agent-based modeling vs. Equation-based modeling: A case study and users' guide*. Paper presented at the Multi-agent systems and agent-based simulation.
- Paulsen, M. R., de Sena, D. G., Jr., de Assis de Carvalho Pinto, F., Zandonadi, R. S., Ruffato, S., Gomide Costa, A., . . . Danao, M. G. C. (2014). Measurement of combine losses for corn and soybeans in brazil. *Applied Engineering in Agriculture*, 60(6), 841-855.
- Pierce, R., & Thompson, T. (1981). Energy use and performance related to crossflow dryer design. *Transactions of the ASAE.*, 24(1), 216-0220.
- Plastina, A. (2018). *Ag decision maker-estimated costs of crop productin in iowa*. Iowa State University.
- Radajewski, W., Jolly, P., & Abawi, G. Y. (1987). Optimization of solar grain drying in a continuous flow dryer. *Journal of Agricultural Engineering Research*, 38(2), 127-144.
- Rotz, C. A., & Harrigan, T. M. (2005). Predicting suitable days for field machinery operations in a whole farm simulation. *Applie Engineering in Agriculture*, 21(4). doi:10.13031/2013.18563
- Rotz, C. A., Muhtar, H. A., & Black, J. R. (1983). A multiple crop machinery selection algorithm. *Transactions of the Asae*, 26(6), 1644-1649.
- Rubinstein, R. Y., & Kroese, D. P. (2016). *Simulation and the monte carlo method* (3 ed. Vol. 10). Hoboken, NJ: John Wiley & Sons.

- Silva, L. C., Queiroz, D. M., Flores, R. A., & Melo, E. C. (2012). A simulation toolset for modeling grain storage facilities. *Journal of Stored Products Research*, 48, 30-36. doi:<https://doi.org/10.1016/j.jspr.2011.09.001>
- Søgaard, H. T., & Sørensen, C. G. (2004). A model for optimal selection of machinery sizes within the farm machinery system. *Biosystems Engineering*, 89(1), 13-28.
- Sorensen, C. (2003). Workability and machinery sizing for combine harvesting. *Agricultural Engineering International*, V.
- Sørensen, C. G., & Bochtis, D. D. (2010). Conceptual model of fleet management in agriculture. *Biosystems Engineering*, 105(1), 41-50.
- Spedding, T. A., & Sun, G. Q. (1999). Application of discrete event simulation to the activity based costing of manufacturing systems. *International Journal of Production Economics*, 58(3), 289-301. doi:[https://doi.org/10.1016/S0925-5273\(98\)00204-7](https://doi.org/10.1016/S0925-5273(98)00204-7)
- Sukup. (2016). *Tower dryer owner's operation manual*. Sheffield, IA: Sukup Manufacturing Co.
- Sumner, P. E., & Williams, E. J. (2009). Bulletin 973: Measuring field losses from grain combines. Retrieved from <http://hdl.handle.net/10724/12068>
- Tako, A. A., & Robinson, S. (2012). The application of discrete event simulation and system dynamics in the logistics and supply chain context. *Decision Support Systems*, 52(4), 802-815. doi:<https://doi.org/10.1016/j.dss.2011.11.015>
- Thomison, P. R., Mullen, R. W., Lipps, P. E., Doerge, T., & Geyer, A. B. (2011). Corn response to harvest date as affected by plant population and hybrid. *Agronomy Journal*, 103(6), 1765-1772.
- Thompson, T. L., Peart, M., & Foster, G. H. (1968). Mathematical simulation of corn drying — a new model. *Transactions of the ASAE.*, 11(4), 582. doi:<https://doi.org/10.13031/2013.39473>
- Thompson, T. L., Peart, R. M., Foster, G. H., Loewer, O., & Bridges, T. (1994). Granary. University of Florida.
- Tippayawong, K. Y., Piriyaageera-anan, P., & Chaichak, T. (2013). Reduction in energy consumption and operating cost in a dried corn warehouse using logistics techniques. *Maejo International Journal of Science and Technology*, 7(2), 258.

- Trego, T., & Murray, D. (2010). *An analysis of the operational costs of trucking*. Paper presented at the Transportation Research Board 2010 Annual Meetings, Washington, DC.
- U.S. Energy Information Administration. (2018). Data for petroleum & other liquids. Retrieved from <https://www.eia.gov/petroleum/data.php>
- USDA-NASS. (2017). Quick stats. *Washington, DC*.
- USDA. (2013a). Grain inspection handbook *Book ii, chapter 4 corn*. Washington, DC: Grain Inspection, Packers and Stockyards Administration.
- USDA. (2013b). Grain inspection handbook *Book ii, chapter 1 general information*. Washington, DC: Grain Inspection, Packers and Stockyards Administration.

VITA
Aaron Paul Turner

EDUCATION:

- M.S 2014 Biosystems and Agricultural Engineering
 University of Kentucky, Lexington, KY
- B.S 2010 Engineering Technology (Mechanical)
 New Mexico State University, Las Cruces, NM

PROFESSIONAL EXPERIENCE:

- Engineer Associate University of Kentucky Biosystems & Ag. Engineering Department
(2012-Present)
- Graduate Research Assistant University of Kentucky Biosystems & Ag. Engineering
Department (2010-2012)

REFEREED JOURNAL ARTICLES:

- [1] **Turner, A.P.**, M.P. Sama, L.S. Bryson, and M.D. Montross. 2018. Effect of Pre-processing on the Bulk Compression Behaviour of Switchgrass and Miscanthus. *Biosystems Engineering. In Press.*
- [2] Petingco, M.C., M.E. Casada, R.G. Maghirang, S.A. Thompson, S.G. McNeill, M.D. Montross, and **A.P. Turner**. 2017. Influence of Kernel Shape and Size on the Packing Density and Compressibility of Hard Red Winter Wheat. *Transactions of ASABE*. 61(4):1437-1448.
- [3] Bhadra, R., M.E. Casada, **A.P. Turner**, M.D. Montross, S.A. Thompson, S.G. McNeill, R.G. Maghiran, and J.M. Boac. 2017. Stored Grain Pack Factor Measurements for Soybeans, Sorghum, Oats, Barley, and Wheat. *Transactions of ASABE*. 61(2).
- [4] Hamidisepehr, A. M.P. Sama, **A.P. Turner**, O.O. Wendroth. 2017. A Method for Reflectance Index Wavelength Selection from Moisture Controlled Soil and Crop Residue Samples. *Transactions of ASABE*. 60(5): 1479-1487.
- [5] **Turner, A.P.**, M.D. Montross, J.J. Jackson, N.K. Koeninger, S.G. McNeill, M.E. Casada, J.M. Boac, R. Bhadra, R.G. Maghirang, and S.A. Thompson. 2016. Stored Grain Surface Estimation Using a Low Density Point Cloud. *Appl. Eng. Ag.*, 33(1): 105-112.
- [6] Bhadra, R., M. E. Casada, S. A. Thompson, J. M. Boac, R. G. Maghirang, M. Montross, **A. P. Turner**, and S. McNeill. 2016. Technical Note: Field observed angles of repose for stored grain in U.S. *Appl. Eng. Ag.*, 33(1): 131-137.

- [7] Bhadra, R., M.E. Casada, J.M. Boac, **A.P. Turner**, S.A. Thompson, M.D. Montross, R.G. Maghirang, and S.G. McNeill. 2016. Technical note: Correlating Bulk Density (with Dockage) and Test weight (without Dockage) for Wheat Samples. *Appl. Eng. Ag.* 32(6): 925-930.
- [8] **Turner, A.P.**, M.D. Montross, J.J. Jackson, N.K. Koeninger, S.G. McNeill, M.E. Casada, J.M. Boac, R. Bhadra, R.G. Maghirang, and S.A. Thompson. S.A. 2016. Error Analysis of Stored Grain Inventory Determination. *Transactions of the ASABE.* 59(3): 1061-1072.
- [9] **Turner, A.P.**, M.D. Montross, S.G. McNeill, M.P. Sama, R. Bhadra, J.M. Boac, M.E.. Casada, R.G. Maghirang, and S.A. Thompson. S.A. 2016. Modeling the Compressibility Behavior of Hard Red Wheat Varieties. *Transactions of the ASABE.* 59(3): 1029-1038.
- [10] Sama, M.P., J.T. Evans, **A.P. Turner**, and S.S. Dasika. 2016. As-Applied Estimation of Volumetric Flow Rate from a Single Sprayer Nozzle Series Using Water Sensitive Spray Cards. *Transactions of the ASABE.* 59(3): 861-869.
- [11] Jackson, J.J., **A.P. Turner**, T. Mark, and M.D. Montross. 2016. Densification of Biomass Using a Pilot Scale Flat Ring Roller Pellet Mill. *Fuel Processing Technology* 148:43-9. doi:10.1016/j.fuproc.2016.02.024
- [12] Boac, J. M., R. Bhadra, M.E. Casada, S.A. Thompson, **A.P. Turner**, M.D. Montross, S.G. McNeill, and R.G. Maghirang. 2015. Stored Grain Pack Factors for Wheat: Comparison of Three Methods to Field Measurements. *Transactions of the ASABE* 58(4): 1089-1101. doi:10.13031/trans.58.10898
- [13] Bhadra, R., **A.P. Turner**, M.E. Casada, M.D. Montross, S.A. Thompson, J.M. Boac, S.G. McNeill, and R.G. Maghirang. 2015. Pack Factor Measurements for Corn in Grain Storage Bins. *Transactions of the ASABE* 58(3): 879-890. doi: 10.13031/trans.58.11033

PROFESSIONAL SKILLS:

Machinery management, Programming (MATLAB, Basic and Sauer-Danfoss Plus+1), Data acquisition, Instrumentation, Basic CAN network design, GIS (ArcGIS, QGIS, CartoDB), Lean principles, Computer-aided design (SolidWorks, Autodesk Inventor), Biomass harvest, and Energy assessments.

NON-REFEREED CONFERENCE PRESENTATIONS AND ABSTRACTS:

- [1] **Turner A.P.**, M.D. Montross, J. Dvorak, M.P. Sama, B. Martin, T. Mark. 2018. Variability in Yield and Harvest Losses Versus Moisture in KY. E-poster presented at ASABE Agricultural Equipment Technology Meeting in Louisville, KY.

- [2] **Turner A.P.**, M.D. Montross, M.P. Sama, J. Dvorak, T. Mark, B. Martin. 2017. Grain Harvest Cycle Analysis Based on Precision Agriculture Data. Presented by M.D. Montross at ASABE Annual International Meeting in Spokane, WA.
- [3] Petingco, M.C., R. Bhadra, M.E. Casada, R.G. Maghirang, M.D. Montross, S.A. Thompson, S.G. McNeill, and **A.P. Turner**. 2017. Influence of kernel shape and size distribution on wheat compaction in storage. Poster presented at ASABE Annual International Meeting in Spokane, WA.
- [4] Casada M.E., **A.P. Turner**. 2017. Determining Time, Aeration, and Loading Cycle Effects on Grain Packing. Presented at NC-213 annual meeting in Kansas City, MO.
- [5] **Turner A.P.**, M.D. Montross, J. Dvorak, M.P. Sama, B. Martin, T. Mark. 2017. Analysis of Grain Transportation Records to Determine Equipment Performance. E-poster presented at ASABE Agricultural Equipment Technology Meeting in Louisville, KY.
- [6] **Turner A.P.**, M.D. Montross, J. Dvorak, M.P. Sama. 2016. Tracking Grain Trucks using a Fleet Management System. Presented at ASABE Annual International Meeting in Orlando, FL.
- [7] Benedict, E.K., M.P. Sama, **A.P. Turner**. 2016. As-Applied Estimation of Volumetric Flow Rate Distribution from a Spray Nozzle Using Liquid Mass on a Target. Poster presented at ASABE Annual International Meeting in Orlando, FL.
- [8] **Turner A.P.**, M.D. Montross, S.G. McNeill, N.K. Koeninger, S. Thompson, M. Casada, J.M. Boac, and R. Bhadra. 2015. Modeling the Compressibility Behavior of Hard Red Wheat Varieties. ASABE Annual International Meeting, New Orleans, LA.
- [9] Montross, M.D., **A.P. Turner**, N.K. Koeninger, and J.J. Jackson. 2015. Energy Crop Production on Reclaimed Mine Land, Marginal Agriculture Land, and Prime Agriculture Land in Kentucky. ASABE Annual International Meeting, New Orleans, LA.
- [10] Sama M. P., J.T. Evans, and **A.P. Turner**. 2015. As-Applied Estimation of Volumetric Flow Rate on a Single Sprayer Nozzle Series Using Water Sensitive Spray Cards. ASABE Annual International Meeting, New Orleans, LA.
- [11] Koeninger N.K., M.D. Montross, C.T. Agouridis, **A.P. Turner**, and J.J. Jackson. 2015. Determining Soil Erosion with Varying Corn Stover Cover Factors. ASABE Annual International Meeting, New Orleans, LA.
- [12] Jackson J.J., M.D. Montross M.D., **A.P. Turner**, and N.K. Koeninger. 2015. Composition and Enzymatic Hydrolysis of Biomass Pretreated with Alkaline Hydrogen Peroxide Spray. ASABE Annual International Meeting, New Orleans, LA.
- [13] **Turner A.P.**, M.D. Montross, and N.K. Koeninger. 2014 Mechanical Properties of Radially Compressed Miscanthus and Switchgrass. ASABE Annual International Meeting, Montreal, QC.

- [14] Schiavone D., Montross M., **Turner A.**, Jackson J. 2014. Bale Moisture Measurement via Time-Domain Reflectometry. Poster presented at ASABE Annual International Meeting in Montreal, QC.
- [15] Koeninger N., M. Montross, C. Agouridis, and **A.P. Turner**. 2014. Impact of Varying Cover Factors on Soil Erosion Due to Biomass Removal. ASABE Annual International Meeting, Montreal, QC.
- [16] **Turner, A.P.** M.D. Montross, C. Rodrigues, D. Schiavone, J.J. Jackson, S. McNeill, J. Boac, R. Bhadra, S.A. Thompson, M. Casda, and R. Maghriang. 2013. Field Measurement of Packing in Stored Grain. ASABE Annual International Meeting, Kansas City, MO.
- [17] **Turner, A.P.**, M.D. Montross, W.C. Adams, C., Foster, and D. Lewis. 2012 Single Pass Grain and Biomass Harvest for Wheat and Corn in Western Kentucky. ASABE Annual International Meeting, Dallas, TX.

OUTREACH/SERVICE:

- [1] Member BAE Departmental Research and Graduate Studies Committee, 2016-present.
- [2] Farm energy assessments for GOAP (Governor's Office of Agricultural Policy) On-Farm Energy Program, 2015-present. Perform site visits, evaluate renewable and energy efficient projects in terms of energy savings and payback, and develop decision aids to evaluate projects.
- [3] Graduate Student Advisor to UK Wildcat Pulling Team, 2014-present. Primary involvement through assisting students with their design, instrumentation, data collection, and controls for ASABE's International Quarter Scale Tractor Student Design Competition.
- [4] National Farm Machinery Show (NFMS)-BAE Exhibit, 2012-2013, 2017. NFMS showcases a variety of agricultural equipment products and services. Presented department research related to biomass/bioenergy, energy efficiency, and grain storage to attendees.
- [5] BAE Graduate Recruitment Weekend, 2012-2014, 2016. Annual department recruitment event. Led department and area tours for potential graduate students.
- [6] Morehead State Bioenergy Field Day. 2012. Displayed mobile pelleting unit and biobutanol display.
- [7] E-day (Engineer's Day), University of Kentucky, 2012-2013. Presented department research related to biomass/bioenergy and grain storage to attendees.
- [8] ASABE Annual International Meeting. 2011. Student volunteer. Set up for job fair and silent auction.

CERTIFICATIONS

- [1] Fundamentals of Engineering (2009)
- [2] Certified SolidWorks Associate (2009)

AWARDS:

- [1] New Faces of ASABE (2018)
- [2] ASABE Superior Paper Award (2017)
- [3] Gamma Sigma Delta Outstanding PhD. Student (2016)